BIOTECHNOLOGICAL TOOLS TO STUDY TOMATO FRUIT QUALITY UNDER STRESS CONDITIONS

Rosalba De Stefano

Dottorato in Scienze Biotecnologiche XXV ciclo
Indirizzo Biotecnologie per le Produzioni Vegetali
Università di Napoli Federico II

Dottorato in Scienze Biotecnologiche XXV ciclo
Indirizzo Biotecnologie per le Produzioni Vegetali
Università di Napoli Federico II

BIOTECHNOLOGICAL TOOLS TO STUDY TOMATO FRUIT QUALITY UNDER STRESS CONDITIONS

Rosalba De Stefano

Dottoranda: Rosalba De Stefano

Relatore: Prof.ssa Amalia Barone

Correlatore: Dott. Antonio Di Matteo

Coordinatore: Prof. Giovanni Sannia

Alla mia famiglia e ai miei fedeli amici

INDEX

Summary

The studies carried out during my Ph.D thesis focused on the identification of genetic mechanisms which regulate tomato fruit quality traits under abiotic (water deficit) and biotic (*Botrytis cinerea*) stress conditions. Specifically the work was developed through two lines of research with certain objectives:

1) Identification of candidate genes controlling tomato fruit quality in response to water deficit, through microarray tools and the use of an Introgression line (IL9-2-5)
2) The study of shelf life and *Botrytis cinerea* resistance of transgenic tomatoes enriched in flavonoids

In the first part of study the selected approach consisted to study the peculiar behavior of the genotype IL9-2-5, an introgression line of the cultivated *Solanum lycopersicum* with a 9 cM introgression from the wild species *Solanum pennellii*. This introgressed segment gives fruits with high soluble solids amount and previous experiments, performed in laboratory where I worked, highlighted its superior performances under water stress. This was confirmed in the present thesis. In particular, the Blum index (parameter that allows to evaluate yield of a cultivated plant under drought stress) evidenced a lower yield losses under 50% water treatment in IL9-2-5 compared with M82, in both two tolerance tests. In addition, phenotipic data for fruit quality highlighted very low changes in firmness, soluble solids and nutrient content underlining more stability under water deficit in IL9-2-5 compared with M82, in the first tolerance test. Among phenotypic data, a stability in AsA content in IL9-2-5 under 50% water treatment was noteworthy, while in M82 was evident its dramatic decrease. Also transcriptomic data were in line with the hypothesis of a more stability of the IL9-2-5, specifically its comparison between the two water treatments in microarray analysis highlighted the low fold changes of transcripts, indeed only 5 probes differentially expressed were retrieved. On the contrary, the elevated amount of TCs showing differential expression in M82 under 50% water treatment (204) indicated an activation/repression of a lots of genes involved in defense mechanisms towards abiotic stress. The correlation data (by CoExpression Tool) made possible to establish a relation among AsA metabolism, carbohydrate metabolism and water stress. This part of work allowed to identify IL9-2-5 as a genotype to use in breeding programs to obtain fruit with good quality traits (in particular soluble solids and vitamin C amount, both important for tomato processing industry) reducing water consumption.

In the second part of study, transgenic tomatoes, accumulating different flavonoid compounds, were tested to have extended shelf life and enhanced pathogen resistance to *Botrytis cinerea*. Comprehensively all the transgenic lines investigated were very interesting as healthy foods, but only purple and indigo tomatoes (both accumulating anthocyanins) showed 2-fold longer shelf life and increased resistance to the opportunistic pathogen tested, compared with red tomato. On the other hand, orange tomato (which accumulates flavonols) had longer shelf life compared with red tomato but shorter than purple and indigo tomatoes. In addition, orange tomato showed no resistance to *Botrytis cinerea*. Our data suggest that high antioxidant capacity of anthocyanins reduces the increase in reactive oxygen species, better than flavonols during late ripening stages, and scavenges H_2O_2 (and probably other ROS too), produced by *Botrytis c.* during infection, better than flavonols, stopped

necrosis damns. This part of work allowed to identify all transgenic lines investigated, not only interesting as healthy foods, but also interesting to enhance fruit shelf life, but just purple and indigo to enhance also resistance to *Botrytis cinerea*.

Riassunto

Il pomodoro *(Solanum lycopersicum)* rappresenta una delle colture ortive più importanti al mondo, che, a seconda della destinazione commerciale, viene utilizzato sia come prodotto fresco che come prodotto trasformato per la produzione di pelati, concentrati e succhi. L'interesse nel costituire varietà con resa, taglia, forma e proprietà organolettiche migliorate è stato da sempre l'obiettivo dei tradizionali programmi di *breeding* nel pomodoro. In particolare, negli ultimi anni l'attenzione dei *breeder* è stata rivolta al miglioramento delle caratteristiche organolettiche (incremento in solidi solubili, maggiore consistenza del frutto, maggiore *shelf life* ecc.) e della qualità nutrizionale (incremento di vitamine, flavonoidi, carotenoidi ecc.). Infatti, i progressi della biologia molecolare e lo sviluppo di più efficienti strumenti d'ingegneria metabolica hanno promosso studi in grado di migliorare le conoscenze in pomodoro dei pathway metabolici coinvolti nella sintesi di molecole ad attività antiossidante e di altri composti benefici per la salute.

Talvolta la sua produttività può essere ampiamente compromessa da avversità sia di origine ambientale che biotica. La comprensione delle basi genetiche dell'adattamento alle avversità ambientali, caratteri quantitativi (QTL), sta riscuotendo sempre maggiore interesse da parte della comunità scientifica, considerando le previsioni riguardo un aumento delle temperature e una minore disponibilità di risorse idriche. A tal proposito le scienze biologiche e agronomiche stanno cercando di individuare soluzioni al fine di mantenere un'elevata efficienza di produzione della coltura del pomodoro in condizioni di siccità. Poco è stato ancora fatto riguardo la caratterizzazione fisiologica e genetica di varietà di pomodoro tolleranti allo stress, contrariamente all'enorme mole di dati sviluppati in *Arabidopsis*, mais, riso e frumento. In particolare il problema principale dei caratteri quantitativi, come la tolleranza a stress idrico, è capire quali e quanti geni sono implicati nella manifestazione del particolare fenotipo di interesse (circa 2000 geni). Altri problemi correlati allo studio di tale fenotipo sono la presenza simultanea di altri stress abiotici e la messa a punto di un protocollo standard da utilizzare per l'analisi della tolleranza.

Nel presente lavoro di tesi la prima parte del lavoro si è incentrata sull'identificazione di geni candidati per il controllo della qualità del frutto in risposta a due trattamenti idrici, ossia restituzione rispettivamente del 100% e 50% dell'acqua persa. In particolare sono state realizzate due prove per valutare la tolleranza a tale stress in due anni diversi (2010 e 2011) e in due località differenti (Bari e Portici) in condizioni semi-controllate. L'inizio del trattamento è stato fatto coincidere con il momento in cui il 50% dei frutti aveva mostrato allegazione al primo palco. Le analisi fenotipiche sono state effettuate sui frutti allo stadio rosso maturo. In particolare è stata valutata la resa produttiva sia totale che commerciabile e di queste sono stati calcolati, in base all'Indice di Blum, le perdite in produzione totale e commerciabile di entrambi gli anni. Inoltre sono state valutate caratteristiche qualitative legate alla commerciabilità del frutto, quali solidi solubili totali accumulati nel frutto e consistenza della bacca, nonché accumulo di composti ad attività benefica per la salute umana quali Acido Ascorbico (AsA), fenoli e carotenoidi. Particolare rilievo è stato dato allo studio trascrittomico atto alla comprensione dei meccanismi genetici che regolano

l'accumulo di AsA nel frutto, anch'esso avente eredità di tipo quantitativo (controllato da più geni e dipendenti dall'ambiente), in risposta al trattamento del 50% di acqua persa. Tale studio è stato condotto su una linea di introgressione, IL9-2-5, contenente un segmento di 9 cM proveniente dalla specie selvatica *Solanum pennellii,* nel background di M82, la varietà commerciale. In questo genotipo sono stati già identificati 3 QTL relativi all'AsA, mostranti effetti epistatici e non additivi. Sulla prima regione è stato localizzato un gene candidato per una monodeidroascorbato reduttasi, enzima coinvolto del riciclo dell'AsA; sulla seconda regione vi è un QTL che controlla lo sviluppo semi-determinato della pianta, portando ad uno sviluppo maggiore del numero di foglie, con conseguente maggiore accumulo di fotosintetati disponibili per organi sink come il frutto, e quindi con maggiore disponibilità di zuccheri per la biosintesi di AsA; sullala terza regione è presente il gene dell'invertasi apoplastica *Lin5* recante una mutazione polimorfica (SNP) nella regione CDS, la quale conduce ad una maggiore attività enzimatica dell'invertasi, che ha la funzione di scindere il saccarosio proveniente dal floema mantenendo favorevole il gradiente di tale disaccaride. Quindi è quella regione corrispondente ad un maggiore accumulo di solidi solubili totali.
Le IL sono particolarmente adatte a studiare caratteri complessi (QTL) come la tolleranza alla carenza idrica e la qualità del frutto, dato che le variazioni fenotipiche osservate possono essere direttamente associate al segmento introgresso nella singola IL. Inoltre considerando la stabilità genetica di dette linee, gli esperimenti possono essere riprodotti facilmente anche da gruppi di ricerca indipendenti, in aree geografiche e climatiche differenti. La relazione tra stress idrico e quantità di AsA presente nelle cellule è stata già ampiamente documentata; in particolare l'elevato stress ossidativo che si genera a seguito dello stress idrico viene annientato dall'elevato potenziale antiossidante dell' AsA. Inoltre esso svolge un'importante funzione nella fotosintesi, agendo nella reazione della perossidasi di Mehler insieme all'ascorbato perossidasi nel regolare lo stato redox dei trasportatori fotosintetici di elettroni e come cofattore per la violaxantina de-epossidasi l'enzima coinvolto nella foto protezione mediata dal ciclo delle xantofille.
Precedenti esperimenti condotti nel laboratorio dove ho lavorato per questa prima parte della tesi hanno messo in evidenza particolari differenze nell'architettura della radice della IL9-2-5 e specificamente lo sviluppo lineare sia delle radici principali che di quelle avventizie, nonché nel numero di queste ultime. Presumibilmente queste differenze nella struttura della radice spiegano in parte la migliore performance della IL9-2-5 sottoposta a stress idrico, manifestato in una minore perdita produttiva rispetto ad M82. Inoltre i dati fenotipici mettono in evidenza una maggiore stabilità dei caratteri analizzati quali accumulo di solidi solubili, consistenza del frutto e accumulo di nutrienti quali AsA, fenoli e carotenoidi. Particolarmente interessante è stata l'osservazione di elevata stabilità dell'AsA nella linea di introgressione rispetto ad M82 dove il suo crollo è elevato.
Le analisi trascrittomiche, che sono state effettuate solo sul materiale proveniente dalla prova del primo anno, confermano l'ipotesi di una maggiore stabilità della IL9-2-5 sottoposta a stress, come dimostrano anche i dati microarray dei trascritti che sono differenzialmente espressi nella linea di introgressione nel trattamento al 50% rispetto a quello al 100% (5 *probes*)*,* sottolineando un basso *Fold Change* di trascritti. Al contrario l'elevato ammontare dei trascritti aventi espressione differenziale in M82 al trattamento 50% rispetto a quello al 100% (204 *probes*) indica una serie di "aggiustamenti" atti a fronteggiare lo stress. Infatti, tra i trascritti analizzati si evidenziano molti geni putativamente coinvolti nei meccanismi di difesa a stress quali

salt tolerance protein, universal stress protein family protein, anthocyanidin synthase, peptidyl-prolyl cis-trans isomerase-like 3, peptidylprolyl isomerase, proline-rich cell wall, cyclophilin, dnaj heat shock n-terminal domain-containing protein, dehydration responsive element-binding protein 1 e *dehydration-responsive family protein.*
Considerando la poca informazione proveniente dai singoli confronti tra i due trattamenti nei due genotipi per spiegare la maggiore stabilità fenotipica della linea d'introgressione, è stata effettuata un'analisi ANOVA a due livelli di classificazione nella quale i due fattori presi in esame sono stati genotipo e trattamento. Tale approccio ha permesso di mettere in evidenza tutti i trascritti mostranti espressione differenziale nei due genotipi in risposta al trattamento idrico. Infatti tale analisi ha permesso di individuare 504 trascritti mostranti interazione *genotipo x trattamento* permettendoci di analizzare specifici trascritti, che alla base delle conoscenze presenti in letteratura, ci sono sembrati idonei a spiegare la migliore performance della IL9-2-5 sottoposta a stress idrico.
Inoltre, considerando il polimorfismo per l'invertasi apoplastica *Lin5* presente nella linea di introgressione che porta ad un maggiore accumulo di carboidrati nel frutto rispetto ad M82, nel presente studio è stata posta particolare attenzione a quei trascritti coinvolti nel metabolismo dei carboidrati. I dati provenienti dall'analisi di correlazione di 97 trascritti, alcuni provenienti dalla lista delle 504 *probes* mostranti interazione *genotipo x trattamento*, altri identificati in base a conoscenze di letteratura, quali trasportatori di saccarosio e di monosaccaridi, hanno permesso di identificare un network con interazioni tra trascritti coinvolti nella biosintesi dell'AsA, trascritti coinvolti nel metabolismo dei carboidrati e trascritti coinvolti nella risposta a stress. Particolarmente interessante è la correlazione tra una *GDP-mannose pyrophosphorylase*, un'enzima chiave nella biosintesi di AsA e un trasportatore di saccarosio *LeSUT2*, una *water channel protein* e una a *photoassimilate-responsive protein*. Il trascritto corrispondente alla *GDP-mannose pyrophosphorylase* è stato saggiato anche mediante qRT-PCR confermando i dati microarray di una forte *down expression* in M82 e un lieve cambiamento in IL9-2-5. Anche il trascritto codificante una *photoassimilate-responsive protein* all'analisi qRT-PCR mostrava una forte sotto-espressione mentre in IL9-2-5 il cambiamento di espressione era molto basso confermando anche in questo caso il dato microarray. Un altro trascritto con comportamento particolarmente interessante dall' analisi microarray è stato anche un *proline transporter,* che mostrava una *over expression* in M82 sottoposto a stress idrico rispetto al controllo, mentre risultava praticamente invariato in IL9-2-5 sottoposto a trattamento idrico. Quindi, in conclusione questi dati hanno permesso di confermare l' IL9-2-5 come genotipo tollerante a stress idrico in due anni e due posti diversi, mostrando una minore perdita produttiva e una maggiore stabilità nei caratterii qualitativi del frutto. Non molto è attualmente noto riguardo la caratterizzazione fisiologica e genetica di varietà di pomodoro tolleranti a stress idrico, rispetto alla mole di dati forniti per riso, mais e frumento. Quindi allo scopo di identificare particolari geni da trasferire a varietà coltivate, che conferiscono da un lato tolleranza a stress idrico e dall'altro pregevoli caratteri qualitativi, il presente lavoro di tesi ha posto un tassello importante in tale direzione.
La seconda parte del lavoro ha riguardato un importante aspetto legato alla qualità del frutto, ossia la sua *shelf-life* dopo la raccolta. Nel concetto di *shelf life* è incluso anche la presenza di patogeni che potrebbero inficiarne la conservabilità; in particolare nel pomodoro un patogeno che reca molte perdite produttive durante la fase di conservazione è *Botrytis cinerea*, patogeno necrotrofo, causa della cosiddetta "muffa grigia", difficile da combattere per il suo ampio "arsenale" di fattori di virulenza

complementari. Il suo controllo è molto importante nella fase di post-raccolta, in quanto contribuisce in modo cospicuo alla *shelf-life* del frutto.
Tra i composti ad attività benefica sulla salute dell'uomo, presenti nel frutto, vi sono i flavonoidi, che sono un'importante risorsa di antiossidanti idrofilici. Essi sono importanti poiché sono stati dimostrati avere effetti positivi contro malattie coronariche, alcuni tipi di cancro, l'ossidazione dei lipidi a bassa densità e riduzione dei rischi primari che inducono all'arteriosclerosi. Nei laboratori della professoressa Cathie Martin del JIC di Norwich, dove è stata svolta questa parte dell'attività di ricerca, precedentemente sono state ottenute linee transgeniche di pomodoro, sia nel background di MicroTom (avente piccola pezzatura) che MoneyMaker (avente grande pezzatura). Esse accumulano elevate quantità di antocianine (pomodoro porpora), specifici flavonoli (pomodoro arancione) e l'ibrido tra le due linee accumulava sia flavonoli che antocianine (pomodoro indaco). In prove sperimentali di conservabilità in condizioni di sterilità controllate il pomodoro porpora ha dimostrato il doppio del tempo richiesto per diventare morbido e inedibile, rispetto al *wild type* (pomodoro rosso). Inoltre, tali frutti hanno mostrato anche più resistenza all'attacco del patogeno necrotrofo *Botrytis cinerea*. Per comprendere i meccanismi coinvolti in queste osservazioni le tre linee transgeniche e il *wild type* sono stati sottoposti a prove comparative parallele di conservabilità e test di resistenza a *Botrytis cinerea.* Per il test di conservabilità i frutti sono stati raccolti a 15 giorni dallo stato *breaker* (B+15), per i pomodori trasformati nel background di MicroTom, e dopo 1 settimana (B+1W) per quelli nel background di MoneyMaker. Per quanto riguarda i pomodori di piccola pezzatura la prova ha messo in evidenza che dopo circa tre settimane i frutti *wild type* già non erano più edibili, mentre le linee transgeniche conservavano ancora a lungo la conservabilità; in particolare, dopo 5 settimane dall'inizio della prova il pomodoro arancione cominciava a presentare i primi sintomi di non edibilità, mentre le altre due linee transgeniche conservavano edibilità oltre le 9 settimane dopo l'inizio del test. Per i pomodori a grande pezzatura, già dopo una settimana dall'inizio della prova il *wild type* mostrava i primi segni di non edibilità, mentre il pomodoro arancione mostrava i primi segni di non edibilità dopo circa 13 giorni dall'inizio del test; anche in questo caso la conservabilità delle due linee che accumulavano antocianine (pomodori porpora e indaco) era maggiore conservando edibilità fino a 28 giorni dall'inizio del test. Il secondo step è stato il monitoraggio dell'espressione di alcuni dei geni correlati alla maturazione del frutto mediante qRT-PCR, utilizzando RNA da differenti stadi (da verde maturo a B+64d). I geni che sono stati analizzati sono stati: *Polygalacturonase 2, β-Galactosidase* e *Phytoene synthase.*
L'espressione del gene codificante la *Polygalacturonase 2* mostrava un picco di espressione nello stadio B+3 nel genotipo *wild type*, mentre l'espressione risultava essere minore fino allo stadio B+14 per i tre genotipi transgenici e tra di essi la più bassa espressione era mantenuta dal pomodoro porpora. L'espressione del gene codificante la *β-Galactosidase* per tutti i genotipi mostrava un picco di espressione nello stadio B+3, tranne che per il pomodoro porpora il cui picco di espressione era spostato allo stadio B+7 pur mantenendosi sempre basso rispetto agli altri genotipi analizzati. L'espressione del gene codificante la *Phytoene synthase* (la cui espressione aumenta durante la maturazione) per i pomodori *wild type* e indaco mostrava un picco di espressione allo stadio B+3, con quella del *wild type* di circa il doppio rispetto al pomodoro indaco. Per quanto riguarda gli altri due genotipi (pomodoro arancione e porpora) il picco di espressione si presentava nello stadio B+7 con valori nel pomodoro porpora di circa la metà rispetto a quello arancione.

Successivamente sono stati effettuati saggi di attività enzimatica, durante i diversi stadi di maturazione del frutto (negli stessi stadi dell'esperimento precedente), di due enzimi coinvolti nella degradazione della parete cellulare, poligalatturonasi (PG) e β-glucosidasi (TBG) (solo nei pomodori di piccola pezzatura) per i quali è nota un' attività nella maturazione del frutto. L'attività enzimatica si è mostrata significativamente inferiore nel pericarpo dei frutti del pomodoro porpora paragonati al *wild type* per entrambi gli enzimi saggiati. Per gli altri due genotipi non è stato possibile saggiarne l'attività enzimatica per problematiche tecniche legate al saggio colorimetrico. Successivamente è stata valutata l'attività antiossidante totale mediante saggio TEAC (Trolox Equivalente Antioxidant Capacity) sulla frazione idrosolubile e liposolublile del frutto, effettuato in diversi stadi da MG a B+10W per i pomodori trasformati nel background di MicroTom. I risultati hanno mostrato un'elevata attività antiossidante per tutte e tre le linee transgeniche parallelamente all'accumulo di flavonoidi nel frutto, mentre nel pomodro rosso essa rimaneva circa 5 volte inferiore, conservando un andamento piuttosto stabile durante la maturazione. L'attività antiossidante si è conservata alta per tutte linee transgeniche fino allo stadio B+8W, quando difatti vi è stato un repentino abbassamento di tale attività, mentre è rimasta decisamente più elevata per le altre linee transgeniche. Per quanto riguarda le linee transgeniche trasformate nel background di MoneyMaker l'attività antiossidante è stata condotta solamente ad uno stadio di maturazione, ossia B+10d, mostrando un' attività antiossidante maggiore nel pomodoro porpora rispetto a quello arancione.
E' stata poi monitorata la resistenza dei frutti all'infezione di *Botrytis cinerea*, utilizzando frutti raccolti dopo due settimane dallo stadio *breaker* per le linee trasformate nel background di MicroTom sia mediante ferita che mediante spray. Dopo due giorni dall'inoculazione mediante ferita, i frutti del pomodoro *wild type* ed arancione mostravano un significativo incremento dell'area danneggiata, mentre il diametro delle lesioni rimaneva molto piccolo per entrambe le linee accumulanti antocianine. Dopo 3 giorni dall'inoculo il diametro della parte danneggiata nei frutti del *wild type* e arancione raggiungeva tre volte il diametro della lesione dei pomodori porpora e indaco, indicando che questi ultimi hanno una maggiore resistenza allo sviluppo e al progredire dell'infezione da *Botrytis cinerea*. In aggiunta è stato effettuato un test quantitativo delle biomassa del fungo mediante qRT-PCR con primer amplificanti il gene della cutinasi di fungo su frutti di pomodori infettati con *Botrytis cinerea*. Anche questo test ha confermato che la biomassa fungina nei genotipi *wild type* e arancione risultava essere di circa quattro volte maggiore rispetto a quella sviluppatasi nel pomodoro porpora e indaco. Al fine di indagare i meccanismi di azione dei diversi composti rispetto alla crescita del fungo sono stati effettuati saggi di attività di crescita del fungo *in vitro*, lasciando crescere il fungo su substrato con aggiunta di estratti provenienti da pomodoro *wild type*, porpora e arancione, ma non è stata notata interferenza di nessuno di questi estratti con la crescita del fungo, lasciando supporre che il meccanismo di interazione si esplicava solo *in vivo* avendo bisogno della cellula vegetale vivente. Infatti, è stato ipotizzato che la resistenza dei pomodori accumulanti antocianine era dovuta all'attivià specifica delle antocianine nell'inibire la formazione di perossido d'idrogeno, che fa parte di una serie di reazioni del "*burst* ossidativo" che mette in atto *Botrytis cinerea* nell'innescare necrosi. Tale meccanismo di reazione è stato confermato dall' utilizzo di un saggio colorimetrico mediante 3,3'-Diaminobenzidine, che colora specificamente perossido d'idrogeno. In tale saggio infatti è stato messo in evidenza nel pomodoro porpora una circoscrizione dello sviluppo di perossido d'idrogeno, che

rimane limitato alla regione di infezione, mentre nel pomodoro rosso ed arancione l'aria di diffusione del perossido d'idrogeno era molto ampia. Sommariamente i dati ottenuti hanno messo in evidenza una maggiore conservabilità nelle linee transgeniche, che per i pomodori che accumulano antocianine risultava essere maggiore, e una resistenza al fungo necrotrofo presente solo nei pomodori porpora e indaco, ipotizzando un coinvolgimento specifico delle antocianine nel contrastare lo sviluppo di ROS messo in atto dai meccanismi di infezione del fungo, che invece non avviene per i flavonoli accumulati nel pomodoro arancione.
Il presente lavoro di tesi ha messo in evidenza l'utilità di due diversi approcci biotecnologici nello studio della qualità del frutto in relazione a stress idrico e ad attacco del patogeno necrotrofo *Botrytis cinerea.* Il primo approccio ha avvalorato l'utilizzo della tecnologia microarray in combinazione con l'impiego di linee di introgressione nello studio di caratteri ad eredità quantitativa (tolleranza a stress idrico e accumulo di AsA), che hanno quindi la problematica di coinvolgere molti geni che interagiscono tra di loro e che sono influenzati dall'ambiente. Nel secondo caso è stata avvalorata l'elevata potenzialità dell'utilizzo dell'ingegneria genetica nello studio di specifici pathway metabolici e in particolare della funzione di specifici composti coinvolti nella determinazione di qualità del frutto che lo rendono più o meno commerciabile (maggiore conservabilità e maggiore resistenza a *Botrytis cinerea*).

1. Introduction

Tomato is an herbaceous dicotyledon plant that belongs to the family Solanaceae, which is one of the most important families of angiosperms and contains many of the commonly cultivated plants, including potato tomato, pepper, eggplant, petunia, and tobacco. It is the 3rd most economically important crop family, exceeded only by grasses and legumes, and the most valuable in terms of vegetable crops (Hoeven et al. 2002). The tomato genus *Lycopersicon* is one of the smallest genera in Solanaceae, though the centerpiece in the family for genetic and molecular research. The cultivated tomato was originally named *Solanum lycopersicum* by Linnaeus (Linnaeus, 1753). In 1754, Miller separated tomatoes and designated the genus *Lycopersicon* and the species *esculentum* for the cultivated tomato (Miller, 1754). The genus *Lycopersicon* was initially distinguished from the genus *Solanum* by its distinct characteristics of anthers and leaves. Recently, based on molecular analysis a new taxonomic classification of tomato has been suggested and the cultivated tomato have been renamed *Solanum lycopersicum*.

Tomato originated in western South America, and domestication is thought to have occurred in Central America. The cultivated tomato is widely grown around the world and constitutes a major agricultural industry. Globally agricultural area allocated for its cultivation reaches 4.6 millions of hectares and its total production is evaluated about 5 millions of tons (statistical data FAO, 2010) in Europe. Worldwide, it is the third largest produced commodity (FAOSTAT 2010; http://faostat.fao.org) and unquestionably the most popular garden crop. There are more varieties of tomato sold worldwide than any other vegetable. Major tomato producing countries in descending orders include China, USA, India, Turkey, Egypt, and Italy (http://faostat.fao.org) (Fig. 1.1). In addition to tomatoes that are eaten directly as raw vegetable or added to other food items, a variety of processed products such as paste, whole peeled tomatoes, diced products, and various forms of juice, sauces, and soups have gained significant acceptance. Tomato fruit represents a very important component of Mediterranean diet containing antioxidants such as ascorbic acid (AA), b-carotene, lycopene, lutein, and zeaxanthin (Daood et al., 1990; Proteggente et al., 2002; Visioli et al., 2004). The Mediterranean diet, rich in plant-derived foods, has been associated with lower risk of certain cancers (Trichopoulou et al., 2003) and cardiovascular disease (Estruch et al., 2006).

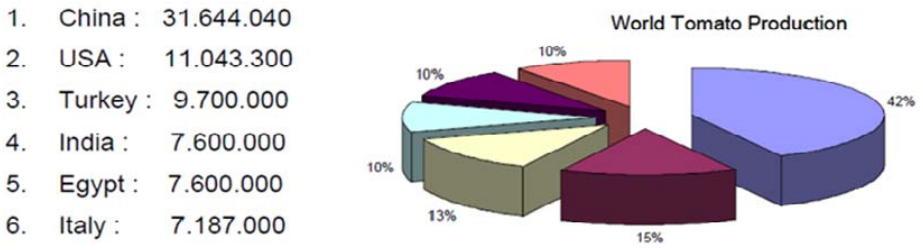

Figure 1.1 World tomato production distribution. Major tomato producing countries in the world (http://faostat.fao.org).

1.2 Tomato genomic resources

The tomato genoma (*Solanum lycopersicum*) sequencing started in 2004 by an international consortium of 10 countries (Mueller *et al*., 2009). Initially the approach was to sequence only the euchromatic sequence using a BAC-by-BAC approach (http://www.sgn.cornell.edu/help/about/tomato sequencing .pl.). In 2009, a whole-genome shotgun approach was initiated that, in conjunction with other data, yielded high quality assemblies. The Tomato Sequencing Project is part of the larger "International Solanaceae Genome Project (SOL): Systems Approach to Diversity and Adaptation" initiative. Launched in 2003, this project has set ambitious research goals for the following 10 years, including physical, evolutionary, and functional genomics of the family Solanaceae (Muller *et al.,* 2005);(http://www.sgn.cornell.edu/solanaceae project/index.pl). At the same time, other studies are being conducted in tomato, including efforts to expand EST database of tomato. The TIGR Tomato Gene Index (LeGI) is a collection of virtual tentative consensus (TC) sequences constructed by clustering and assembling 213,974 ESTs and 2,043 ETs (release 11) generated in several laboratories, including the TIGR Institute, Cornell University, and the Boyce Thompson Institute (Barone *et al*., 2009). The advent of genomics has brought a real increase to the generation of data, knowledge and tools that can be applied to breeding; molecular markers and linkage maps allowed to find associations between markers and phenotypes. With the advance of tomato genome sequences and genomic tools, the genetic control of plant growth and development is expected to be better understood. Identification of candidate genes for important traits and knowledge of functional nucleotide polymorphisms within genes might lead the breeders to identify useful alleles in the wild germplasm and to create novel genotypes by introgressing and pyramiding favorable alleles. In addition, plant breeders might consider manipulating transcription and regulation factors in the genome to generate a pool of new trait variation. Tomato is also an excellent model system for both basic and applied plant research. It is a diploid species with a rather small genome (0.95 pg/1C, 950 Mbp), lacks of gene duplications, has a manageable asexual propagation and whole plant regeneration, and accounts for availability of a wide number of mutants. Furthermore, it is ease to cultivation, has a short life cycle, high selfing, fertility and homozygosity. Members of *Solanum* are easily transformed genetically, and transgenic tomatoes are routinely produced using co-cultivation with *Agrobacterium tumefaciens*. Tomato was the first food crop in the U.S. for which a genetically engineered variety was marketed and also for which a disease resistance gene was positional cloned (Fooland, 2007). Tomato is also a model for fruit development with a lot of data available at physiological and genetic levels. The plant lends itself to studies on fruit architecture, ripening and all aspects of fruit quality. Particularly, many efforts have been addressed to improve both organoleptic and nutritional quality in tomato fruit (Levin *et al.*, 2004). Strategies to achieve the goal focused mainly on transgenic approaches and on characterization of mutant or quantitative trait loci (QTL) with pronounced effects on such traits. The problem about quantitative genetic traits is to understand how many genes are involved in a specific phenotype. In particular, the –omics technologies could help to solve the complex traits in major genes (and link higher performing genotypes to polymorphic QTLs). This may allow monitoring quality associated superior allelic combinations in assisted breeding programs, despite QTLs show low heredity and high environmental interaction. Many –omics approaches used in tomato for dissecting genetic determinants of fruit quality have

focused on ripening processes because of the high magnitude of metabolic modifications they imply (Alba *et al.*, 2005). In fact, ripening confers desirable flavour, colour, and texture, increases fruit pathogen susceptibility, imparts numerous quality and nutritional characteristics including fiber content and composition, lipid metabolism and antioxidant composition. The ability to understand key control points in global ripening regulation and biosynthesis of health promoting molecules, such as carotenoid, flavonoid, vitamin C, and flavour volatiles, will allow the manipulation of nutrition and quality characteristics associated with ripening.

1.3 Fruit quality traits

Breeding aims in tomato have gone through four phases: breeding for yield in the 1970s, for shelf life in the 1980s, for taste in the 1990s and for nutritional quality in the last few years. Recently, recovery of these quality phenotypes in food crops has benefited from renewed research activity, a trend driven both by the efforts of public health agencies and consumers to obtain the so known “functional foods”. So the challenge is to introduce specific genes into elite production varieties through breeding, preserving their performance attributes.

Fruit quality comprises features that might belong to two different categories: 1. Marketable features 2. Nutrient content. The former involves physico-chemical features which affect taste (sweetness and acidity) and aroma, but also fruit texture and shelf life, and are influenced by genotypic differences, mineral nutrition, ripening stage at harvesting and storage conditions during post-harvesting, The latter regards nutritional properties, including both water-soluble and fat-soluble antioxidants, like lycopene, Ascorbic Acid (AsA), carotenoids, polyphenols (caffeic acids, flavonoids, clorogenic acid) and so on. On average in 100 g of fresh tomato there are 95% of water, 3% of sugars (glucose and fructose), 0.2 % of fats, 0.9% of proteins and 1.2% of fiber. Both the nutritional and the sensorial attributes are built throughout the successive phases of fruit development corresponding to cell division, cell expansion, and ripening. While the fruit ripening process is obviously important (Giovannoni, 2001), there are also increasing evidences that support the key role of early fruit development for the acquisition of several fruit quality traits, including the accumulation of sugars and organic acids, the determination of cell wall and texture characteristics, and the cuticle biosynthesis (Carrari et al., 2006; Chaı¨b et al., 2007; Mintz-Oron et al., 2008). During fruit development, these processes mainly take place during the cell expansion phase, which supports fruit growth by allowing a large increase in fruit cell volume linked with membrane and cell wall synthesis and the concomitant accumulation of water, mineral ions, and metabolites in the vacuoles, thereby giving its fleshy characteristics to the fruit.

1.3.1 Fruit shelf life

The purpose of obtaining maximum profit increasing tomato fruit production will succeed only if it is supplemented with similar efforts to minimize the post-harvest losses and enhance fruit shelf life. Post-harvest losses of fruits and vegetables are a very big problem, and in developing countries account for almost 50% of the crops produced. The softening, that accompanies ripening of fruits, exacerbates damage during shipping and handling, and plays a major role in determining the cost of tomatoes, because it has a direct impact on palatability, consumer acceptability, shelf life, and post harvest disease/pathogen resistance (Vicente, et al., 2007). Generally, reductions in fruit firmness due to softening are accompanied by increased expression of cell wall–degrading enzymes acting upon proteins and carbohydrates

(Fry et al., 2004). Consumers demand products with a perfect degree of ripening and with good organoleptic quality. Most of the changes take place during fruit ripening, mainly associated with fruit softening which affects transport, storage, shelf life and pathogen resistance (Brummell & Harpster, 2001). However, despite many efforts to suppress expression of cell wall–degrading enzymes, experiments have not yet provided the insight needed to genetically engineer fruits whose softening can be adequately controlled (Giovannoni et al., 1989, Saladie et al., 2007). This may be due to the presence of functionally redundant components of a complicated metabolic network involved in fruit softening. It also suggests that the suppression of enzymes acting on cellulose, hemicellulose, and pectin is not sufficient to prevent softening (Tieman et al., 1992; Giovannoni et al., 2004). Because the improvement in fruit shelf life achieved so far is not adequate, the identification of new targets influencing fruit softening is required. Fruit ripening is a complex developmentally regulated network of processes and events encompassing alterations in gene expression and chemical and physiological changes. The textural, metabolic, organoleptic, and nutritional properties of ripening tomato fruit have been investigated, and the concurrent increase in susceptibility to fungi that accompanies fruit ripening is mentioned frequently (Giovannoni, 2001, 2004, 2007; Alba et al., 2005). Crucial to determining shelf life is also the influence of opportunistic pathogens, because ripe fleshy fruit is more susceptible to disease and decomposition than unripe green fruit (Prusky, 1996). Among the processes that occur during ripening, the disassembly of cell walls as fruits soften is crucial for susceptibility (Cantu et al., 2008a). *Botrytis cinerea* is a very significant opportunistic tomato pathogen with a broad host range. It is notoriously aggressive on fleshy fruit, and its interaction with tomato fruit is a model pathosystem to investigate necrotrophic microorganisms (Powell et al., 2000). During *B. cinerea* infections of plant tissues, cell wall-degrading enzymes are secreted by the fungus. Although some of these enzymes are required for virulence (Kars et al., 2005), the fungus fails to infect ripe fruit in the absence of endogenous fruit cell wall disassembly (Cantu et al., 2008). Cantu and co-workers (Cantu et al., 2009) showed that whether the fungus is able to invade and grow on fruit depends on the activation of some of the pathways involved in fruit ripening, and it can induce these pathways in unripe fruit, suggesting that the pathogen itself can initiate the induction of susceptibility by exploiting endogenous developmental programs.

1.3.3 Nutrient content

For the very huge amount in antioxidant, tomato fruit represents an important contribution to human feeding. Antioxidants have important beneficial effects on health and human wellbeing. Indeed, a lots of epidemiological studies highlighted the importance of eating fruits and vegetables, to prevent cardiovascular diseases and some form of cancers (Renaud et al., 1998; Temple, 2000). Recently, some works (Franceschi et al., 1994; Giovannucci et al., 1995) deal with the importance to consume products originated from tomatoes (sauces, pizza, ketchup) and the same tomatoes with inversely correlation of risk to arise cancers at digestive system and prostate. Other experimental studies show that lycopene is an important carotenoid, has antioxidant activity (Levy et al., 1995) and interferes with tumor cells (Clinton, 1998). Other important nutrients present in vegetables are vitamin E, vitamin C (AsA), retinoic acid and other, carotenoids, polyphenols like hydroxytyrosol in oliv oil, resveratrol in red wine, quercitic and genistein in soy and catechin in tè, that have an inhibitory effect on cancer and so are useful in chemoprevention (Thomasset et al.

2007). Nowadays, improving fruit quality is one of main objectives of tomato breeding programs. Because tomatoes are so important for human diet there is an increased interest to get high antioxidant levels both by traditional breeding and new biotechnological tools.

1.3.3.1 Ascorbic acid (AsA)

Ascorbic acid, generally known as vitamin C, is a weak acid and water-soluble sugar, structurally related to glucose. It is stable enough in acid solution, but less compared with other vitamins and is very sensitive to light, heat and air, factors which stimulate its oxidation. Anyway, its biological role as antioxidant molecule is of primary importance in the living world. This property is due to its ability to give one electron, transforming in monodehydroascorbic acid (MDHA) that is very unstable and to give another electron producing dehydroascorbic acid (DHA), which might be reduced by glutathione-dependent dehydroascorbate reductase (DHAR), to regenerate AsA.
For its water-soluble nature AsA is not accumulated and its surplus is eliminated daily by the organism. Humans are not able to synthesize AsA so they have the necessity to regularly take it by food or supplements. This inability is consequence of a mutation in gene coding for the terminal enzyme of AsA biosynthesis (Sato & Udenfriend, 1978). The recommended intake was established at 45 milligrams per day by the World Health Organization. Vitamin C is a cofactor in at least eight enzymatic reactions including several collagen synthesis reactions that, when dysfunctional, cause the most severe symptoms of scurvy. In animals, these reactions are especially important in wound-healing and in preventing bleeding from capillaries. Ascorbate may also act as an antioxidant against oxidative stress. In addition, it contributes to metabolism of some amino acids (phenylalanine and tyrosine) necessary for hormone formation; it converts inactive folic acid to active folinic acid takes a role in calcium and iron metabolism; it protects a lots of molecules (thiamine, riboflavin, folic acid and so on) against oxidation by stabilizing them. Regarding human health, AsA is involved in reduction of degenerative diseases (Gey, 1998) and in reinforcement of lymphocytes activity and immune system (Padayatty et al., 2003).
The best natural sources of Vitamin C are fruits and vegetables, and among these, the Kakadu plum and the camu camu fruit contain the highest concentration of this vitamin. It is also present in some cuts of meat, especially liver. Among vegetables also red tomato is a good source of vitamin and obviously it depends on the variety, soil condition, climate where it grows, storage conditions, and method of preparation. Generally its value was estimated in 14 mg per 100 g (http://ndb.nal.usda.gov/ndb/foods/show/3207). Anyway vitamin C is the most widely nutritional supplement and is available in a variety of forms, including tablets, drink mixes, crystals in capsules or naked crystals. The scientific international organisms suggest review of demands of AsA daily intake considering also its bioavailability (Food and Nutrition Board, Institute of Medicin, Washington DC, NAS 1997). In order to follow these criteria it will be desirable to increase it in food thus improving diet to direct benefit for consumers.
The AsA biosynthetic pathway has been localized to the cytosol except for the final step. Early evidence from radiolabelling studies indicated that the biosynthesis pathway in plants was different from that in animals and then it was supposed that ascorbate is synthesized in plant by oxidation of L-galactose. In plants, the major ascorbic acid biosynthesis pathway namely the Smirnoff-Wheeler pathway, was identified (Wheeler et al., 1998) and its involves activated forms of the sugars GDP

D-Mannose, GDP L-Galactose, and L-Galactose before L-galactono-1,4-lactone is finally derived and converted to L-ascorbic acid (Fig.1.2). Recent experimental evidences demonstrate the existence of alternative biosynthetic pathways in plant (Valpuesta & Botella, 2004). In one of these, AsA might be synthesized from D-galacturonic acid that comes from pectins degradation (Di Matteo et al. 2010). According to another pathway (similar to the animal one) AsA synthesis starts with GDP-D-mannose, which through L-gulose formation, L-gulonic and than L-gulone-1-4-lactone gives AsA. Finally, also myo-inositol might be precursor through the formation of D-glucuronic acid, D-gulonic acid and L-gulone-1-4-lactone. In this pathway the epimerization of GDP-D-mannose to GDP-L-galactose is considered the limiting reaction (Wheeler et al., 1998). A recycling pathway also exists for ascorbic acid: because of its role as an antioxidant, reduced ascorbate is oxidised into an unstable radical (monodehydroascorbate), which disproportionates into ascorbate and dehydroascorbate, the latter representing the second oxidised form. Dehydroascorbate is also unstable and rapidly degrades so the ascorbate pool can be depleted if the oxidised forms are not recovered by two reductases: monodehydroascorbate reductase (MDHAR) and dehydroascorbate reductase (DHAR) (Noctor and Foyer, 1998; Smirnoff and Wheeler, 2000). Modulation of DHAR activity may control the levels of ascorbate in tissues. It is well known that ascorbate content is influenced by light and varies during plants development (during senescence, germination, fruit ripening and so on) and under stress conditions; this suggests that there are finely regulated mechanisms that control ascorbate pool size.
Ascorbic acid is an essential compound also for plants, having a primary role as an antioxidant, preventing oxidative stress as well as playing a role in plant development and hormone signaling (Pastori et al., 2003), the activation of the cell cycle (Potters et al., 2002), and possibly cell wall loosening during cell expansion or fruit ripening (Fry, 1998). It has proposed functions in photosynthesis as an enzyme cofactor (including synthesis of ethylene, gibberellins and anthocyanins) and in control of cell growth. It has a major role in photosynthesis, corroborated by the evidenced hypersensitivity of some vtc *Arabidopsis thaliana* mutants to ozone and UV-B radiation (Conklin et al., 200). The rapid response of ascorbate peroxidase expression to photo-oxidative stress, and the properties of transgenic plants with altered ascorbate peroxidase activity support an important antioxidative role for ascorbate. The control of ROS cellular level (which increases during abiotic and biotic stresses but also normal cellular reactions) is possible by combined action of a network of antioxidant within AsA has a leading role because is able to remove directly a lots of reactive species (singlet oxygen, superoxide and hydroxyl radical), through multiple mechanisms (Padh, 1990). AsA redox state depends, in part, by ascorbate quantity content in tissues and the AsA peroxidases (APXs) are the main AsA consumers in cell.

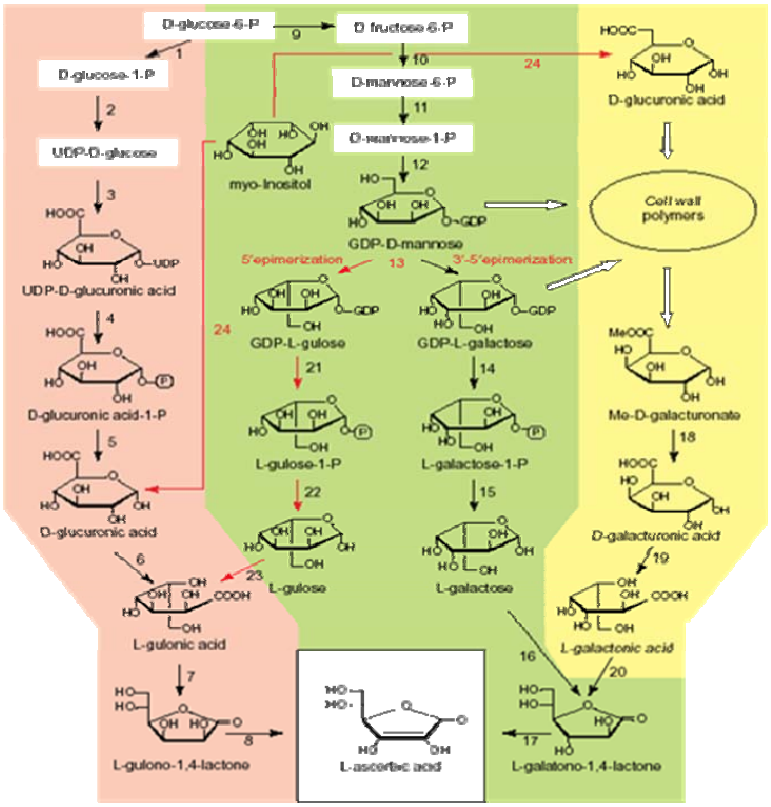

Figure 1.2. Biosyntetic pathways for AsA production (Valpuesta and Botella, 2004)

1.3.3.2 Phenolic compounds

Phenolic compounds represent one of the main classes of secondary metabolites, which includes a broad spectrum of substances very heterogeneous, but all characterized by the presence of an aromatic ring with one or more hydroxyl substituent. In some situations hydroxyl group might be covered by O-methylation or other kind of substitutions; in addition some compounds have other functional groups that influence their physico-chemical properties. Although a high number of phenolic compounds were found in animals, the presence of a phenolic fraction is a peculiar feature of plant tissue. Phenols are important in fruits and vegetables: they contribute to colour and taste. In particular sour taste is associated to phenolic acids, astringency to tannins and bitter to naringenin and neohesperedin; colour to anthocyanins and their particular reactions of co-pigmentation. The wide spectrum of these molecules allows a huge variety of functions; for examples flavonoids give protections against UV radiation, anthocyanins are the main pigments of flowers, salicylic acid is important in the reactions plant-microorganism, lignins are the mail component in cell wall allowing mechanical resistance to plants and impermeability to vascular tissues and so on.

Flavonoids are widespread throughout the plant kingdom, from mosses to angiosperms (Koes et al., 1994). More than 6,000 different flavonoids have already been described in the scientific literature, and the number is continuously rising. Key to all of them is their basic molecular structure that is centered on a C-15 molecular skeleton (the flavan nucleus) comprising two aromatic rings with six carbon atoms (rings A and B) interconnected by a heterocycle containing three carbon atoms (ring C). Flavonoids are very important for plants' life because they play key roles in the

recruitment of pollinators and seed dispersers, in signaling between plants and microbes, in male fertility of some species, in defense (as antimicrobial agents and feeding deterrents), and in UV protection.
In the past decade it has become more and more evident that the composition of secondary metabolites greatly influences the quality and health potential of food and food products. Flavonoids represent an important source of hydrophilic dietary antioxidants. Generally, foods rich in both soluble and membrane-associated antioxidants are considered to offer the best protection against disease (Yeum, K.J. et al., 2004). Flavonoids are important since they have been suggested to protect against oxidative stress, coronary heart disease, certain cancers, and other age related diseases (Kuo, 1997; Yang et al., 2001; Ross & Kasum, 2002). A diet rich in flavonoids reduces the primary risk factor for artherosclerosis and related diseases (Brouillard et al., 1997; Hannum, 2004). It has been suggested that an increase in the daily intake of certain flavonoids could lead to between 7 and 31% reduction in the incidence of all cancers and between 30 and 40% reduction in deaths from coronary heart disease (Hertog et al., 1993; Soobrattee et al., 2006). Plant polyphenolics have synergistic effects on health; the anti-bacterial activities of flavonoids are enhanced when they are administered in combination (Arima et al., 2002), and quercetin and kaempferol inhibit cancer cell proliferation synergistically (Ackland et al., 2005) so that combinations of flavonoids, which are present naturally in fruit and vegetables, are more effective in preventing disease than individual flavonoids.
In recent years, considerable efforts have been directed at elucidating the flavonoid biosynthetic pathway (fig. 1.3) at the molecular genetic level. Two classes of genes can be distinguished within the flavonoid pathway:(I) the structural genes encoding enzymes that directly participate in the formation of flavonoids, and (II) regulatory genes that control the expression of the structural genes. The precursors of the synthesis of most flavonoids are malonyl-CoA and p-coumaroyl-CoA, which are derived from carbohydrate metabolism and phenylpropanoid pathway, respectively (Forkmann and Heller, 1999). The biosynthesis of flavonoids is initiated by the enzymatic step catalysed by chalcone synthase (CHS), resulting in the yellow coloured chalcone. The pathway proceeds with several enzymatic steps to other classes of flavonoids, such as flavanones, dihydroflavonols and finally to the anthocyanins, the major water-soluble pigments in flowers and fruits. Other flavonoid classes (i.e. isoflavones, aurones, flavones, proanthocyanidins and flavonols) represent side branches of the flavonoid pathway and are derived from intermediates in anthocyanin formation. Another step, downstream in the main pathway towards anthocyanins, can convert the dihydroflavonols (DHK, DHQ, DHM) into flavonols by the enzyme flavonol synthase (FLS). The structural genes encoding the enzymes involved in flavonoid formation are predominantly regulated at the level of transcription (Weisshaar and Jenkins, 1998). The transcriptional regulation of the first enzyme in the flavonoid-specific part of phenylpropanoid biosynthesis, chalcone synthase (CHS), has been investigated in detail in Arabidopsis. Within an operationally defined minimal AtCHS promoter, three different cis-acting elements have been identified (Hartmann et al., 2005): an ACGT containing element (ACE), a MYB recognition element (MRE), and the response element (RRE). MYB proteins are characterized by a highly-conserved DNA-binding domain that generally consists of up to four imperfect amino acid sequence repeats (R) of about 52 amino acids, each forming three α–helices. The third helix of each repeat is the ‘‘recognition helix’’ that makes direct contact with DNA and intercalates in the major groove. In Arabidopsis thaliana, 126 MYB genes of the R2R3 type have been described

(Stracke et al., 2001; GenBank accession no. AF469468 for At3g60460), but only limited functional information is available for the majority of plant MYB genes. The functional data available indicate that MYB transcription factors are involved in a wide array of cellular processes such as development (Oppenheimer et al., 1991), signal transduction (Urao et al., 1993), plant disease resistance (Daniel et al., 1999), cell division (Hirayama and Shinozaki, 1996), and secondary metabolism (Dubos et al., 2010).

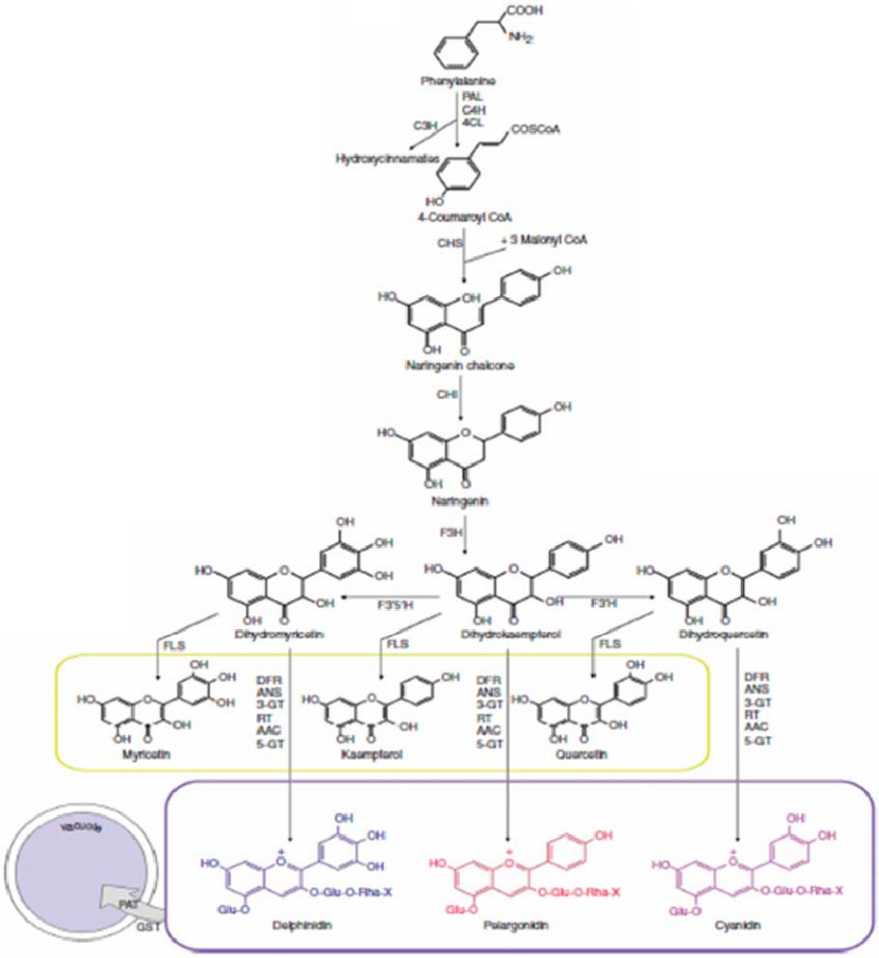

Figure 1.3 - Schematic representation of the anthocyanin biosynthetic pathway. **Yellow box**: flavonols; **purple box**, anthocyanins; PAL, phenylalanine ammonia lyase, 4CL, 4-coumarate:coenzyme A ligase; C4H, cinnamate 4-hydroxylase, C3H, 4-coumarate 3-hydroxylase, CHS, chalcone synthase; CHI, chalcone isomerase; F3H, flavanone-3-hydroxylase; F3'H, flavonoid-3'-hydroxylase, F3'5'H, flavonoid-3'5'-hydroxylase, FLS, flavonol synthase, DFR, dihydroflavonol reductase; ANS, anthocyanidin synthase, 3-GT, flavonoid 3-O-glucosyltransferase; RT, flavonoid 3-O-glucoside-rhamnosyltransferase AAC, anthocyanin acyltransferase; 5-GT, flavonoid-5-glucosyltransferase; GST, glutathione S-transferase; PAT, putative anthocyanin transporter. PAT and GST may be involved in transport of anthocyanins into the vacuole (purple circle). X, acyl group on the 3-glucoside moiety of the anthocyanin. (Butelli et al., 2008)

1.4 Abiotic and Biotic stress

When plants are subjected to unfavourable growing conditions, they are considered to be under stress. Stresses can affect plant growth, plant survival and crop yields. Since plants are sessile organisms they are unable to escape adverse environmental conditions, and thus have developed strategies to adapt to changing environmental conditions. Plant cells have evolved signaling pathways to perceive and integrate different signals from the environment and respond by modulating the expression of appropriate genes. Drought, heat, cold and salinity are among the major **abiotic**

stresses that adversely affect plant growth and productivity. In general, abiotic stress causes a series of morphological, physiological, biochemical and molecular changes that affect plant growth, development and productivity and they are often interrelated; these conditions singularly or in combination induce cellular damage. **Biotic Stresses** occur as a result of damages caused by other living organisms, such as bacteria, viruses, fungi, parasites, insects, weeds, and cultivated or native plants. Pathogen general attack strategies are: necrotrophy, in which plant cells are killed; biotrophy, in which plant cells remain alive; hemibiotrophy, in which the pathogen initially keeps cells alive but kills them at later stages of infection.

1.4.1 Water stress

The physiological responses of crop plants to water stress are very complex and generally cause a reduction in growth and a decline in productivity. Water scarcity results in cellular dehydration at the cytological level, which causes concentration of solutes, changes in cell volume and shape of the plasma membrane, decreasing the gradient of internal water, loss of turgor and of membrane integrity and protein denaturation. The tolerance to water stress is the result of the coordination of physiological and biochemical changes at cellular and molecular levels, such as the synthesis of abscisic acid (ABA), the accumulation of various osmolytes and proteins with a role in repair and protection, in synergy with an efficient antioxidant system (Cushman and Bonhert, 2000). The term “drought tolerance” of a cultivated plant should be referred as its capacity to obtain an appreciable yield rather than its capacity to survive at limited water conditions. The efforts of breeder to improve plant drought tolerance are hard due to its quantitative genetic control and poor knowledge of physiology of production at limited water conditions. The main problem is to understand which and how many genes are involved in the complex response (about 2000 estimated genes). Also is difficult to set-up a common protocol to assess drought tolerance (phenological stage to give stress, the stress intensity and duration). Although water stress has been well documented in other types of plants such as *Arabidopsis*, rice, beans, maize, sorghum and potato, little information are available in tomato. Some wild tomato species display a great variety of interesting phenotypes for drought tolerance and can be crossed with the cultivated tomato. *S. pennellii* LA716 is one of them. A collection of 50 introgression lines (ILs), which covers the entire genome of their donor parent *S. pennellii* in the background of the cultivated species *S. lycopersicum* M82 was previously generated (Eshed et al, 1992; Eshed and Zamir, 1994). This genetic resources, together with the currently expanding tomato research platforms, such as genome sequencing and microarray applications, could facilitate research toward a better understanding of drought-tolerance mechanisms in tomato.

1.4.2 *Botrytis cinerea*

Botrytis cinerea, a necrotrophic pathogen, causes serious damage, in particular to post-harvest conditions. The disease is manifested by necrotic areas, caused by plant hypersensitive response, with extensive fungal growth, giving the characteristic appearance of grey mould. Because of its necrotrophic lifestyle, the fungus depends essentially on its ability to kill host cells before colonizing the plant. Von Tiedemann (1997) showed that *Botrytis cinerea* induces a big oxidative burst and that the virulence of the fungal isolates was related positively with the intensity of this oxidative burst. There is evidence that *Botrytis* may even requires the hypersensitive response of its host plant to achieve full pathogenicity (Govrin and Levine 2000).

Free radical scavengers present in plant cells and enzymes like catalase and peroxidise, are able to protect against the cytotoxicity of ROS. Anthocyanin levels have been associated with resistance to *Botrytis* in grape, and may reduce post-harvest spoilage of fruits in general by *Botrytis* (Iriti et al., 2004). The *Botrytis* attach is a significant problem also during fruit ripening, which is characterized by processes that modify texture and flavour but also by a dramatic increase in susceptibility to necrotrophic pathogen. Disassembly of the major structural polysaccharides of the cell wall (CW) is a significant process associated with ripening and contributes to fruit softening. In tomato, polygalacturonase (PG) and expansin (Exp) are among the CW proteins that cooperatively participate in ripening-associated CW disassembly. Simultaneous transgenic suppression of LePG and LeExp1 was shown to reduce the susceptibility of ripening fruit to *Botrytis cinerea* (Cantu et al., 2007). Fruit ripening is characterized by a dramatic increase in susceptibility to necrotrophic pathogens, resulting in large economic losses of perishable horticultural products. CW metabolism of many edible fruit has been studied extensively in the context of ripening, but the contribution of ripening-associated CW disassembly to pathogen susceptibility has not been experimentally defined. It is generally assumed that self-disassembly of the fruit wall contributes to susceptibility because many of the fruit cell wall degrading enzymes involved in ripening are also produced by the invading pathogens and secreted into fruit tissues.

1.5 Aim of the work

The general objective of this thesis was to study genetic mechanisms of regulation of tomato fruit quality traits under abiotic (water deficit) and biotic (*Botrytis cinerea*) stress conditions. Specific objectives were:

1. Identification of candidate genes, controlling tomato fruit quality in response to water deficit, through microarray tool and the use of an Introgression line (IL9-2-5)
2. The study of shelf life and *Botrytis cinerea* resistance of transgenic tomatoes enriched in flavonoids

In the first case, the selected approach consisted of:

- Investigation of fruit quality traits in one Introgression Line compared with control genotype (cultivated variety) under water stress.
- Selection of candidate genes involved in the control of Ascorbic acid content, and of water deficiency response.
- Understanding molecular networks activated in the two genotypes to elucidate the basis of phenotypic differences observed

In the second case, the selected approach consisted of:

- Screening of transgenic tomatoes accumulating flavonoids for exthended shelf life and enhanced *Botrytis cinerea* resistance
- Determination of antioxidant capacity of water-soluble extracts from transgenic lines during ripening and during fungus infection

Chapter 1. Identification of candidate genes involved in tomato fruit quality under water stress

1. Materials and Methods

1.1. Plant material

Tomato genotypes M82 and IL9-2-5 were supplied by Tomato Genetics Resource Center (TGRC) (http://tgrc.ucdavis.edu/). *Solanum lycopersicum* cv M82 (accession LA3475), and IL9-2-5 (accession LA4082) underwent two comparative trials, respectively in at the University of Bari in 2010 and at the University of Naples (Portici) in 2011, during which three plant-replica were grown in semi-controlled environments, under different treatments of water supplementation Treatments were randomly assigned to plants according to a split-plot design with the water restitution as main factor and the replication of the washtub within the same water treatment as sub-factor. In particular the water treatments consisted in two levels of water restitutions that were 100% and 50% of water lost respect field capacity. Treatments were applied when 50% of the plants showed fruit set on the first differentiated flower truss. Fruits were harvested at red ripe stage, weighted and used for soluble solids (°brix) evaluation. Fruits were cut longitudinally, seeds, columella, placenta and locular tissues were removed, while flesh and epidermis were stored in liquid Nitrogen. Frozen tissues were grounded using a WARING blander and finally stored at -80 °C for further analyses.

Moisture at field capacity (FC) was estimated using the following equation according to Pedotransfert di Rawl and Brakensiek (1985):

FC = 0.3486 - 0.0018 * % sand+ 0.0039 * % clay + 0.0228 * % organic substance/ /0.67 - 0.0738 * bulk density,

Water lost from each washtube was calculated as

{FC-[(FW-DW)/DW]}*(Vol*d)+l

where

- **FC** is the soil moisture at field capacity
- **FW** is the fresh weight of soil measured before irrigation
- **DW** is the dry weight of soil measured after drying in oven at 105°C for 12 h
- **Vol** is the soil volume in washtubs
- **d** is the soil density
- **l** is the water lost in 24 h

1.2. Yield evaluation

To estimate yield losses, under 50% of water treatment for the two genotypes a Blum index (Blum, 2005) was used, applying the following formula for each genotype:

$(x_2-x_1)/x_1$ in which:

- $\mathbf{x_1}$ is the yield at 100% of water treatment
- $\mathbf{x_2}$ is the yield at 50% of water treatment

1.3 Phenotypic analysis

Fruit texture was assayed at red-ripe stage by using a T.R. TURIONI penetrometer measuring the force required to push a plunger tip of 32 mm into fruit. Fruits from each plants were evaluated by 10-15 measurements.

Fruits were squeezed out and **total soluble solids** (°brix) content of the resulting juice was measured using a portable refractometer ATC-1 Atago. Within each plant 10-20 fruits were assayed on average.

1.3.1 Ascorbic acid (AsA) quantification

AsA levels were measured using the procedure described by Kampfenkel et al. (1995) and modified according to Di Matteo' s protocol (Di Matteo et al., 2010). Frozen tissue (250 mg) was placed in a 1.5-mL tube with a bead and 200 µL of ice-cold 6% trichloroacetic acid (TCA) (Sigma), and was homogenized for two time at 50 Hz in a TissueLyzer (Qiagen) for 1 min. Samples were then incubated on ice for 10 min and centrifuged for 25 min at 25,000 × g at 4°C. 6% TCA was added to the supernatant up to a total volume of 500 µL, and samples centrifuged as above for 10 min. Two different assays were performed one to evaluate reduced form and the other for tot AsA. The absorbance was read at 525 nm using water as reference with a UV spectrophotometer (Beckman DU-640). For tot AsA 20 µL of sample were placed in three wells for three replicates. To reduce oxidized form 20 µL of DTT 5 mM (diluted in 0.4 M Phosphate buffer, pH 7.4) were added. Samples were incubated for 20 min at 37 °C. 10 µL of N-ethyl maleimide (0.5% v/v NEM) were added to the reaction that subsequently was mixed and kept for 1 min at room temperature. Then 80 µL of color reaction were added to each sample after that they were incubated for 40 min at 37 °C

The solution of color reaction was obtained by adding 2.75 part os A solution and 1 of B solution. A and B solutions are so composed A solution: 31% Orthophosforic Acid, 4.6% v/v TCA, 0.6% v/v ferric chloride; B solution: 4% 2,2-dipyridyl (diluted in 70% ethanol)

For reduced AsA 20 µL of sample were placed in three wells for three replicates. 20 µL of phosphate buffer at pH 7,4 and 10 µL of water were added to each sample. Subsequently 80 µL of color reaction (composed as previously described) were added to samples and incubated for 40 min at 37 °C.

The Tot and reduced AsA concentrations were expressed as mg*100/g fresh weight. according to the standard curves designed over a dynamic range between 0 and 100 nmol AsA. The equation for Tot AsA is : y(Abs)= 0,0118x - 0,0222; for reduced AsA is: y(Abs)= 0,0115x - 0,023.

1.3.2 Total phenols quantification

The amount of total phenols was determined according to Folin- Ciocalteu's procedure (Singleton and Rossi, 1965). 1 ml of 60% methanol was added to 250 mg of ground tissue in a 1.5 ml tube with a bead. Samples were homogenized twice in a Tissue Lyzer (Qiagen) at 50 Hz for 1 min. Extracts were placed on ice 3 min in the dark and vortexed. The extraction was transferred in a 15 ml tube and volume brought to 5 ml with 60% methanol. Samples were centrifuged at 3000 g for 5 min. 62.5 µl of the supernatant, 62.5 µl of Folin-Ciocalteu's reagent (Sigma), and 250 µl of H_2O were incubated for 6 min. After addition of 625 ml of 7.5% sodium carbonate and 500 ml of H_2O, samples were incubated for 90 min at room temperature in the dark. Absorbance was measured at 760 nm. The total phenolics concentration was expressed in terms of µg of gallic acid equivalents mg-1 of fresh weight, based on a gallic acid standard curve designed over a dynamic range 0 to 125. Abs 760nm = (0.0234 x µg gallic ac.) – 0.0776 (R2 = 0.995).

1.3.3 Carotenoids quantification

Carotenoids and chlorophylls a and b content in ripe fruits were estimated by Hartmut et al.' s protocol (1983). All the steps were performed at 4°C and in dark. 100 mg of tissue already smashed in liquid nitrogen were mixed by mortar and pestle with 96% ethanol containing 0.3 mg mL-1 of $CaCO_3$,. Then the samples were centrifuged at

13.000 g for 5 min at 4°C. Carotenoids (Car) content was measured at 470 nm and chlorophyll a (Ca) and b (Cb) at 665 and 649 nm, respectively; their concentrations were calculated according to the following equations:
Ca (µg) = 13.95 x A_{665} - 6.88 x A_{649}
Cb (µg) = 24.96 x A_{649} - 7.32 x A_{665}
Car (µg) = (1000 A_{470} -2.05 x Ca - 114.8 Cb)/245

1.3.4 Glutathione quantification

To detect Glutathione concentration a Glutathione Detection Kit (BioVision) was used following a single protocol to evaluate at the same time reduced (GSH), oxidized (GSSG) and total glutathione.
The assay was performed according to BioVision's procedure (www.biovison.com). Standard Curve was performed adding 10 µl of the 20 µg/µl standard GSH stock to 990 µl of Assay Buffer to generate a 0.2 µg/µl working standard solution, and then adding 0, 2, 4, 6, 8, 10 µl to a 96-well plate to generate 0.4, 0.8, 1.2, 1.6, 2.0 µg/well GSH, and bring the volume to 90 µl with Assay Buffer.

1.3.5 Statistical analysis of phenotypic data

Evaluated phenotypic data were analyzed by a parametric test and statistical analysis was performed using SPSS (Statistical Package for Social Sciences) 17.0 for Windows (evaluation version release 17.0.0). To compare the different behavior of genotypes versus different water treatments was used Student's t test coupled with 10000 bootstrapping resampling; the genotypes effect and their interaction with treatments was evaluated using a Univariate ANOVA.

1.4 Transcriptomic analysis

1.4.1 RNA isolation

Total RNA was extracted from frozen, homogenized and powdered tomato fruit tissue stored at -80°C according to Griffiths and coworkers' protocol (1999). 4 g of powdered sample were added to 12 mL of Extraction Buffer (Solution A; tab. 1.1) and to 15 mL of phenol/chloroform (1:1) (Solution B; tab. 1.1) in Oakridge tubes. Then they were vigorously mixed and centrifuged at 10.000 rpm 15 min at room temperature. Supernatant was taken off and put in a clean Oakridge tube and added to 15 mL of phenol/chloroform (1:1) (Solution B). Tubes were mixed again and centrifuged at 10.000 rpm 15 min at room temperature. 11 mL of supernatant were put in clean tube and nucleic acids were taken down for 1 h at -20°C by adding 27.5 mL of 100% cold ethanol and 1.1 mL of 3 M sodium acetate (pH 6.0). After, samples were centrifuged at 10.000 rpm 15 min at 4 °C. Pellet was washed by 15 mL of 70% ethanol and then it was dissolved in 2 mL of 2X Extraction Buffer of cetyltrimethylammonium bromide (CTAB) (Solution C; tab. 1.1). So, nucleic acids were taken down again by adding 4 mL of CTAB Precipitation Buffer (Solution D; tab. 1.1) and centrifuged at 10.000 rpm 30 min at room temperature. Pellet was dissolved in 400 µL of 1.4 M NaCl, and than 1 mL of 100% cold ethanol was added and precipitated again at -20°C over-night. The day after, samples were centrifuged at max speed for 10 min at 4 °C. Pellet was washed in 1 mL of 70% ethanol and dissolved in 400 µL of water-DEPC and incubated at 50 °C for 5 min. 400 µL of phenol/chloroform (Solution B) were added, vortexed and centrifuged for 15 min. Aqueous phase was transferred in clean tube and the treatment repeated. Nucleic acids precipitated overnight at -20 °C by adding 1 Vol of 3 M sodium acetate (pH 6.0)

and 3 Vol of 100% cold ethanol. Samples were washed with 1 mL of 70% ethanol and pellet dissolved in 180 µL of water-DEPC, added 20 µL of RQ1 DNase Reaction Buffer (Solution E; tab. 1.1) and 1 µL of RQ1 DNase (Promega) and then incubated at 37°C for 30 min. RNA concentration and purity was evaluated by Nanophotometer (Implein) and its integrity by Nano Bioanalyzer AGILENT 2100 with nano chip 6000.

1.4.2 Synthesis of antisense RNA

Total RNA (1 µg) was used as a template to synthesize antisense RNA (aRNA) by KIT KREATECH ULS™ RNA ampULSe: Amplification and Labelling Kit for Combimatrix arrays (Kreatrech) marked with fluorescent ULS-dye Cy5. In the first step the cDNA was synthesized. In one 1.5-mL RNase-free tube was added: 10 µL of 1 µg of mRNA, 1 µL of T7-Oligo(dT) Primer and Water-DEPC to 12 µL. Mix was incubated at 70°C for 10 min and than on ice for 1 min, so centrifuged briefly to collect all the content. After 2 µL of 10X First-Strand buffer, 4 µL of dNTPs mix, 1 µL of RNase Inhibitor and 1 µL of Array Script were added together with water RNase free up to 20 µL. Samples were briefly centrifuged and incubated at 42°C for 2 h. For cDNA synthesis it was added: 63 µL Water-DEPC, 10 µL 10X Second-Strand buffer, 4 µL of dNTPs mix, 2 µL DNA Polymerasi I, 1 µL RNasi H and water RNase free up to 100 µL. Samples were incubated at 16°C for 2h and then put on ice. To isolate cDNA, 250 µL of Binding Buffer were added to the samples and mix was put directly in Filter Cartridge wash tube. Samples were centrifuged at 10.000 g at room temperature for 1 min and supernatant was removed. cDNA was washed with 500 µL of Wash Buffer and than centrifuged two times at 10.000 g for 1 min at room temperature. To elute cDNA 10 µL of Nuclease-free pre-heated water were added and incubation was performed for 2 min at room temperature. After, samples were centrifuged at 10.000 g for 1.5 min at room temperature to collect purified cDNA. To get aRNA, in vitro transcription was performed at room temperature adding: 16 µL Double-stranded cDNA in Nuclease-free water, 16 µL T7 dNTP mix (75 mM), 4 µL T7 10X Reaction Buffer, 4 µL T7 Enzyme Mix and Nuclease-free water to 40 µL. Samples were incubated at 37°C for 14h. To stop the reaction, 100 µL Nuclease-free water were added. To isolate aRNA 350 µL of aRNA Binding Buffer and 250 µL of 100% ethanol were added. Each sample was loaded in aRNA Filter Cartridge tube and centrifuged for 1 min at 10.000 g. Supernatant was removed and 650 µL of Wash Buffer were added to the samples and centrifuged at 10.000 g for 1 min. Supernatant was removed and 650 µL of 80% ethanol were added, samples were so centrifuged and supernatant removed again. To dry filters, samples were centrifuged for 1 min at 10.000 g and filters were transferred in a new tube, and 100 µL of Nuclease-free pre-heated water were added and mixes were incubated at room temperature for 2 min, then centrifuged at 10.000 g for 2 min. 5 µg of aRNA were labeled by ULS-Dye Cy5. To isolate aRNA linked to the colorant the Kreatech protocol by KREA pure column was used.

Table 1.1 – Composition of the solutions used for total RNA extraction

RNA Extraction Buffer (A Solution)	**2X CTAB Extraction Buffer (C Solution)**
6% (w/v) 4-aminosalicylic acid	1.4 M NaCl
1% (w/v) 1,5-naphthalenedisulfonic acid	2% (w/v) CTAB
50mM Tris-HCL pH 8.3	0.1 M Tris-HCL pH 8.0
5% (w/v) Phenol Solution	20 mM EDTA pH 8.0
Phenol Solution	**CTAB Precipitation Buffer (D Solution)**
100 g Crystal Phenol	1% CTAB (w/v)
14 mL m-cresol	50 mM Tris-HCL pH 8.0
0.1 g 8 idrossi-chinolin	10 mM EDTA pH 8.0
30 mL DEPC Water	**10X RQ1 DNasi Reaction Buffer (E Solution)**
Phenol/Chloroform Solution (B Solution)	400 mM Tris-HCL pH 8.0
500 g Crystal Phenol	100 mM MgSO4
0.5 g 8 idrossi-chinolin	10 mM CaCl2
500 mL Chloroform	
20 mL isoamyl alcohol	
200 mL 100mM Tris-HCL pH 8.0	

1.4.3 Chip design and synthesis

Chip TomatoArray1.0 was synthesized on CombiMatrix plataform at "Piattaforma di Genomica Funzionale della Facoltà di Scienze Matematiche Fisiche e Naturali" of Università di Verona. This chip had 90k silicon electrodes that support 20.200 DNA probes synthesized *in situ* with 4 replicates, each one casually spread in the array to evaluate variability of the experiment. Each probe was composed of oligonucleotides, made up of 35 oligomers, designed to be specific for the different Tentative Consensus (TC) that come out from TIGR *S. lycopersicum* Gene Index Release 11.0 (June 21, 2006). As negative control, 9 oligonucleotidic sequences provided by Combimatrix were utilized. Prehybridization, RNA fragmentation, hybridization with 3 µg of labeled and fragmented aRNA and posthybridization washes were performed according to CombiMatrix protocols PTL020_00_90K_Hyb_Imaging.pdf. Three replicates of hybridization were done for each genotype (M82, IL 9-2-5 from 2010 experiment) for the two water treatments 50-100% for a total of six replicates for genotype. In particular, each replicate was done using RNA isolated from fruits that come from a single plant. After hybridization and washing, the microarray was dipped in imaging solution, covered with LifterSlip™, and then scanned using a Perkin Elmer ScanArray 4000XL and the accompanying acquisition software (ScanArray Express Microarray Analysis System v4.0). The resulting TIFF images were processed to extract raw data using the CombiMatrix Microarray Imager Software v5.8.0 copy@right 2001, Quick Start Guide or the User's Manual Microarray Imager, available on web https://webapps.combimatrix.com. Signal probe medians and standard deviations were imported into the SPSS software, and normalization was achieved by correcting each probe median based on the ratio between the median of the array and the average median of arrays. Following data normalization and quality control were log transformed (base 2). Finally, probe signals with a variability coefficient higher than 0.5 as well as spikes and factory probes were filtered out. Also, probes with signal intensities in the upper most and lower most 10% of values were deleted. Automatic high-throughput annotation, gene ontology

mapping and categorization of TCs showing differential transcription signals were got through bioinformatic tools of Blast2Go (http://www.blast2go.org/).

1.4.4 Statistical analysis and bioinformatic procedure

The signal differentially expressed were identified using t-test module of software TMEV (TIGR Multiple Experiment Viewer) version 4.4.0 (http://www.tigr.org/software/tm4/ - Saeed et al., 2003). In particular to compare transcriptional profile of IL 9-2-5 with M82 control a significance threshold of $P < 0.01$ was chosen (Tusher et al., 2001). To analyze the co-regulation among signals differentially expressed a hierarchical clustering was generated, utilizing Pearson correlation. Tentative Consensus sequences that showed a different expression were utilized as input for Blast2GO (http://blast2go.bioinfo.cipf.es/ - Conesa et al., 2005) to provide automatic high-throughput annotation, gene ontology mapping and categorization of TCs showing differential transcription signals. Sequences whose annotation was not automatically provided through similarity matching in the NCBI's non-redundant NR database were processed manually using the similarity search tools FASTA33 http://www.ebi.ac.uk/Tools/ fasta33/index.html and/or SGN BLAST http://sgn.cornell.edu/tools/blast/. In each case, an expectation value threshold of 10 was used. To improve statistical power, to identify patterns of similar expression in microarray, instead of being limited to 'up' or 'down' under some treatments, but identified as being 'up' or 'down' across many transcripts, it was used the software CoExpression tool, setting a threshold of 70% and using a Pearson correlation.

1.4.5 Experimental validation by qRT-PCR

TCs expression profiles of genes considered to be key control points for AsA accumulation in tomato fruit in response to drought stress were validated by real-time quantitative RT-PCR in a 7900HT Fast Real-Time PCR System (Applied Biosystems). Amplification was performed in 12.5-µL reaction volumes using a Power SYBR® Green PCR Master Mix (Applied Biosystems). Relative quantification was achieved by the ΔΔCt method (Livak KJ, et al. 2001). Primer pairs were designated using software Primer Express version 2.0. The primer pair sequences are listed in table 1.2. Primer pairs were validated using a standard curve over a dilution range 1-10-3 ($R2 > 0.98$; slope close to -3.3). For each TCs three biological replicates for treatments were considered and for each experiment three technical replicates were performed. As calibrator was used M82 at 100% water treatment and as internal control endogenous gene Elongation Factor 1 (*EF1*).

Table 1.2 – Primer pairs used to perform qRT-PCR analysis.

Code	Sequence	Annotation
id_7532 Fw id_7532 Rv	5‘-GCTTCTGGATCAGTCTGCAGC-3‘ 5‘-CTGGAGCCATGTACCCAACTGT-3‘	receptor-like protein kinase
id_1090 Fw id_1090 Rv	5‘-GCTGGAGAAGGAGTATATTTGCCA-3‘ 5‘-TCAATCATTGCGCGGTGT-3‘	Photoassimilate- responsive protein
id_6940 Fw id_6940 Rv	5‘GCCACCGATGTCTCCTGCT-3‘ 5‘TGTTCGCTTTGTTCTGCCAC-3‘	zinc finger transcription factor-like protein
id_14033 Fw id_14033 Rv	5‘AGCAAAAGGGCACTGCCA-3‘ 5‘CTTAATGTGAGTGTCCAAGAAGAGATCT-3‘	GDP-mannose pyrophosphorylase
id_10977 Fw id_10977 Rv	5‘GATCAAGCGCGTTAAAGCAAC-3‘ 5‘AGGCATCATCCGATTCATCAG-3‘	granule-bound starch synthasechloroplastic amyloplasticame
id_17088 Fw id_17088 Rv	5'CACAATTCATCATCACCGCAA3' 5'CACAATTCATCATCACCGCAA3'	vtc2-like protein
id_16469 _Fw id_16469 _Rv	5‘-CACTCTCTTGGCAGTTCTATGG -3‘ 5‘-CAAGAAATCCCCAAAATGGA -3‘	Monodehydro Ascorbate Reductase
id_10714_Fw id_10714_Rv	5‘-GGTGTCACCAAAACCCAATACA -3‘ 5‘- GAGTGGACCCATTGCCA -3‘	Monodehydro Ascorbate Reductase
id_14628_Fw id_14628_Rv	5‘- GGTACAAGGAAAACGGCATTGA -3‘ 5‘- GGTTATGGTTTCACCGGTTGC -3‘	Probable monodehydroascorbate reductase, cytoplasmic isoform 2
id_20204_Fw id_20204_Rv	5‘-CACAACTCTATTCAAAGGGCAAG-3‘ 5‘- TGTTTTGAAGAACGCATCTGTC-3‘	Monodehydro Ascorbate Reductase
id_20205_Fw id_20205_Rv	5‘- TCGAGGTGGCTCTTGGACAC -3‘ 5‘- TCAAGCTTTCAGGCACACTCC -3‘	Dehydroascorbate reductase
id_20206_Fw id_20206_Rv	5‘- CCCCAAGTTTGTTGCTTTCC -3‘ 5‘- CTCTGTTCCATCACCGGAGTC-3‘	Dehydroascorbate reductase
id_20207_Fw id_20207_Rv	5‘- CGATGCCAAAGCACCATTTT -3‘ 5‘- GGGTGCTCGAACTTCGTGG -3‘	Dehydroascorbate reductase

2. Results

2.1. Evaluation of genotypes under water deficit

The genotypes IL9-2-5 and M82 were grown for two years and in two different places under semi-controlled conditions and two levels of water-loss restitution. The two treatments consisted of supplying water at the field capacity (100 %) and at half of the field capacity (50%). In the first trial at the University of Bari (year 2010) the water consumption was 1200 mc/ha for 100% water treatment and 500 mc/ha for 50% water treatment (Fig. 2.1). In the second experiment at the University of Naples (Portici, year 2011) water consumption were 2554 mc/ha and 1654 mc/ha for 100% and for 50% treatments respectively (Fig. 2.2).

2.1.1. Evaluation of fruit yield

Table 2.1 reports the average values of marketable and total production from the two experiments, separated for genotypes (M82 and IL9-2-5) and treatments (100% and 50%). In particular, as for **Marketable fruits**, in the first experiment M82 produced 1.25 kg/plant in 100% treatment and 0.49 kg/plant in 50% treatment, while IL9-2-5 produced 1.28 kg/plant in 100% treatment and 0.73 kg/plant in 50% treatment. In the second experiment, M82 produced 0.76 kg/plant at 100% treatment and 0.47 kg/plant in 50% treatment, while IL9-2-5 produced 0.73 kg/plant in 100% treatment and 0.55 Kg/plant in 50% treatment. Regarding the **Total Production**, in the first

experiment M82 produced 1.38 Kg/plant in 100% treatment and 0.52 Kg/plant in 50% treatment, while IL9-2-5 produced 1.29 Kg/plant in 100% treatment and 0.77 Kg/ plant in 50% treatment.

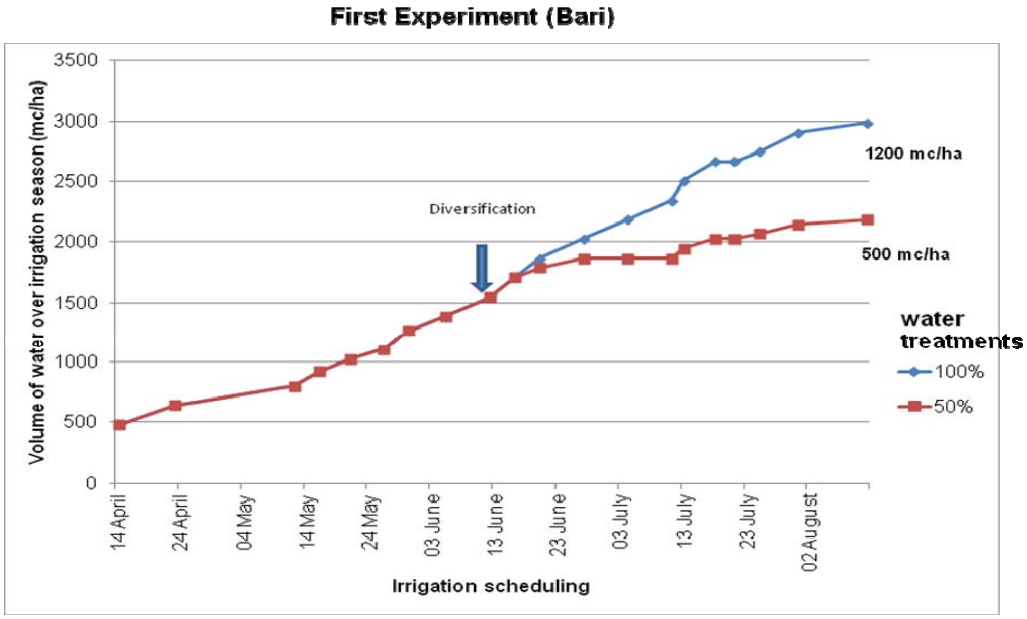

Figure 2.1- Water consumption trend during the first experiment The diversification point corresponds to the time when 100% and 50% treatments were differentiated. 1200 and 500 mc/ha are the volumes of water lost at 100% and 50% water treatments, respectively.

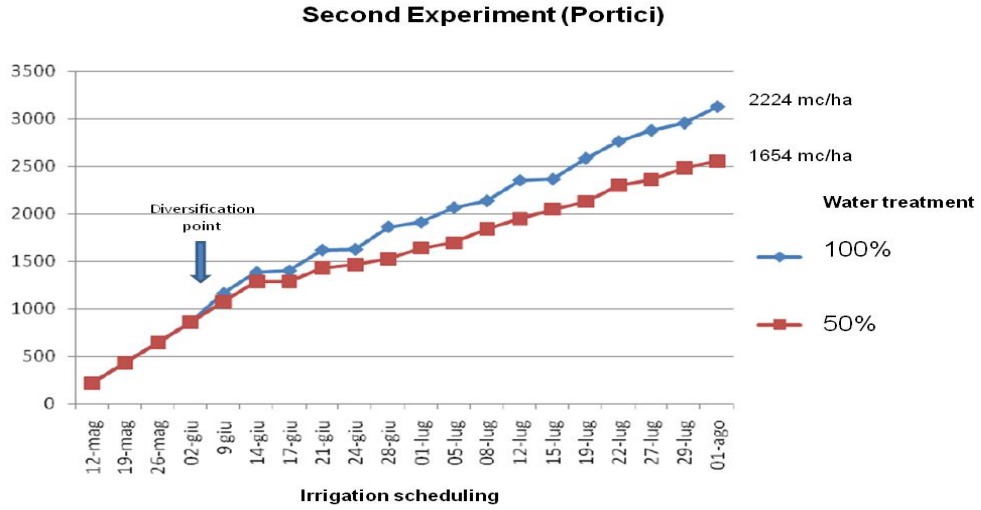

Figure 2.2- Water consumption trend during the second experiment. The diversification point corresponds to the time when 100% and 50% treatments were differentiated. 2224 and 1654 mc/ha are the volumes of water lost at 100% and 50% of water treatments, respectively.

In the second experiment, M82 produced 0.79 Kg/plant in 100% treatment and 0.54 Kg/plant in 50% treatment, while IL9-2-5 produced 0.87 Kg/plant in 100% treatment and 0.79 Kg/plant in 50% treatment. Yield losses, both for M82 and IL9-2-5 at 50% treatment, are statistically significant for the two trials. In the first experiment, the higher yield performance of IL9-2-5 is statistically significant, both for marketable and

total yield, while in the second experiment it is significant only for total yield. Tolerance of genotypes under water stress was evaluated according to **Blum Index** for the two trials, considering both marketable and total fruit yield (tab. 2.2). In particular, in the first experiment for M82 an average Blum index of 63.99 for marketable yield and 63.61 for total yield were observed. IL9-2-5 showed an average value of 39.11 for marketable yield and 44.42 for total yield. In the second experiment the average value of Blum Index was 52.24 for M82 marketable yield and 51.89 for total yield, for IL9-2-5 it was 46.52 for marketable yield and 20.73 for total yield. The values obtained for both marketable and total yield are statistically different between the two genotypes in the first experiment, while in the second experiment the difference was significant only for total yield.

Table 2.1- Average and Standard Error for yield traits recorded for M82 and IL9-2-5 at 100% and 50% of water supply in the first and second experiment.

	Yield		**Marketable fruits (kg)**		**Total fruits (kg)**	
Trial	**Treatment**	**Genotype**	Average	SE	Average	SE
First experiment	100%	M82	1.25	0.2	1.38	0.2
		IL9-2-5	1.28	0.15	1.29	0.2
	50%	M82	0.49§	0.15	0.52§	0.18
		IL9-2-5	0.73*§	0.04	0.77*§	0.01
Second experiment	100%	M82	0.76	0.06	0.79	0.05
		IL9-2-5	0.73	0.2	0.87	0.26
	50%	M82	0.47§	0.1	0.54§	0.07
		IL9-2-5	0.55§	0.01	0.79*§	0.09

Differences were statistically validated by Student's t test coupled with 10000 bootstrapping resampling

*: significant differences within treatments and between genotypes

§: significant differences within genotypes and between treatments

Table 2.2- Blum Index for M82 and IL9-2-5 genotypes at 50% of water supply compared with control in the first and second experiment

Yield		Marketable (kg)		Total (kg)	
Trial	Genotype	Average	SE	Average	SE
First experiment	M82	63.99	11.76	63.61	13.20
	IL9-2-5	39.11*	3.09	44.42*	0.45
Second experiment	M82	52.24	18.43	51.89	10.38
	IL9-2-5	46.52	14.70	20.73*	6.31

Differences were statistically validated by Student's t test coupled with 10000 bootstrapping resampling

*: significant differences within treatments and between genotypes

2.1.2. Evaluation of fruit quality

2.1.2.1 Physical and chemical properties

As for **Fruit texture** (Fig. 2.3 and 2.4), in the first experiment, it was 18.94 $N*mm^{-2}$ for M82 and 25.3 for IL9-2-5 $N*mm^{-2}$ at 100% treatment. At 50% treatment M82 showed a value of 29.76 $N*mm^{-2}$, while IL9-2-5 a value of 25.44 $N*mm^{-2}$. At 50% treatment the differences between genotypes are statistically significant and only M82 shows significant differences between water treatments. In the second experiment, M82 at 100% treatment showed an average texture of 22.3 $N*mm^{-2}$, while IL9-2-5 a value of 32.11 $N*mm^{-2}$. At 50% treatment M82 had a value of 32.71 $N*mm^{-2}$, while IL9-2-5 a value of 29.55 $N*mm^{-2}$. Comprehensively under 100% of water treatment, M82 fruits were softer than IL9-2-5 fruits, by contrast 50% water treatment, M82 fruit became harder than IL9-2-5, these differences are statistically significant. Regarding the average of **Soluble Solids** (Fig. 2.3 and 2.4), in the first experiment, at 100% treatment M82 showed a value of 4 °brix, while for IL9-2-5 it was 4.95°brix. At 50% of water treatment M82 showed a value of 6.2 °brix and IL9-2-5 of 5.95 °brix. The difference observed at 50% treatment is statistically significant between genotypes. In the second experiment, the average of soluble solids content at 100% treatment was 6.10 for M82 and 7.9 °brix for IL9-2-5. At 50% of water treatment M82 showed a value of 7.9 and IL9-2-5 of 8.5 °brix. The differences are statistically significant between genotypes both at 100% and 50% treatments.

2.1.2.2 Nutritional properties

Data regarding evaluation of nutritional properties on fruits obtained from the two experiments are reported in Fig. 2.3 and 2.4. In the first experiment, **AsA** concentration per dry weight (DW) was 1.73 $mg*g^{-1}$ for M82 and 1.62 $mg*g^{-1}$ for IL9-2-5 at 100% treatment, while at 50% treatment it was 0.70 mg g^{-1} for M82 and 1.43

mg*g^{-1} for IL9-2-5. Regarding Tot AsA concentration per DW, at 100% treatment M82 showed a value of 2.01 mg*g^{-1} and 1.94 mg g^{-1} for IL9-2-5, while at 50% treatment it was 1.42 mg*g^{-1} for M82 and 1.54 mg*g^{-1} for IL9-2-5. At 50% treatment the difference in Tot AsA concentration between M82 and IL9-2-5 was statistically significant, and also for M82 it was significant between 100% and 50% treatments. In the second experiment, AsA concentration per DW at 100% treatment was 0.69 mg g^{-1} for M82 and 0.51 mg g^{-1} for IL9-2-5, while at 50% treatment it was 0.64 mg g^{-1} for M82 and 0.93 mg g^{-1} for IL9-2-5. Tot AsA concentration per DW at 100% treatment was 0.78 mg g^{-1} for M82 and 0.65 mg g^{-1} for IL9-2-5, while at 50% treatment, it was 0.83 mg g^{-1} for M82 1.03 mg g^{-1} for IL9-2-5. The difference in AsA concentration was significant between two treatments for IL9-2-5. Differences in both AsA and Tot AsA concentration were statistically significant between the two genotypes within 50% treatment. Tot AsA concentration was statistically significant between 100% and 50% treatments only for IL9-2-5. In the first experiment, **Total Phenols** concentration per DW at 100% treatment was 40.77 µg GAE*mg^{-1} for M82 and 34.38 µg GAE*mg^{-1} for IL9-2-5, while at 50% treatment it was 30.57 for M82 and 30.17 for IL9-2-5. The difference in total phenols concentration was statistically significant in M82 between 100% and 50% treatments. In the second experiment, total phenols concentration per DW at 100% treatment was 184.08 µg GAE*mg^{-1} for M82 and 135.77 µg GAE*mg^{-1} for IL9-2-5, while at 50% treatment it was 170.90 µg GAE*mg^{-1} for M82 and 223.19 µg GAE*mg^{-1} for IL9-2-5. Differences in total phenols concentration were statistically significant for IL9-2-5 between 100% and 50% treatments. The difference in total phenols concentration was statistically significant between the two genotypes within 50% treatment.

In the first experiment **Carotenoids** concentration per DW at 100% treatment was 156.22 µg*g^{-1} for M82 and 110.81 µg*g^{-1} for IL9-2-5. At 50% treatment was 125 µg*g^{-1} for M82 and 96.19 µg*g^{-1} for IL9-2-5. Differences between genotypes were significant both at 100% and 50% treatment. In the second experiment, carotenoids concentration per DW at 100% treatment was 138.5 µg g^{-1} for M82 and 160.2 µg g^{-1} for IL9-2-5, while at 50% treatment it was 225 µg*g^{-1} for M82 and 213.9 µg*g^{-1} for IL9-2-5.

Total Glutathione concentration was evaluated only in the first experiment. At 100% treatment M82 had a value of 114.81 µg*g^{-1} per DW and 89.16 µg*g^{-1} for IL9-2-5. At 50% treatment M82 had a value of 75.85 µg*g^{-1} and 75.85 µg*g^{-1} for IL9-2-5 showed statistically significant difference only in M82 between 100% and 50% treatment.

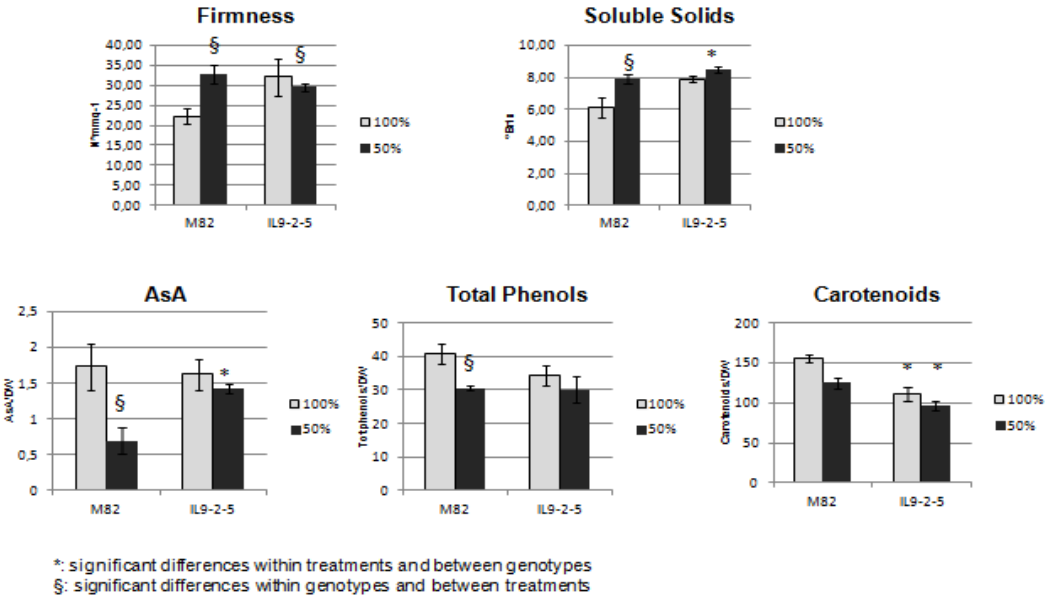

Figure 2.3 - Fruit qualitative trait in M82 and IL9-2-5 at different levels of water supply in the first experiment.

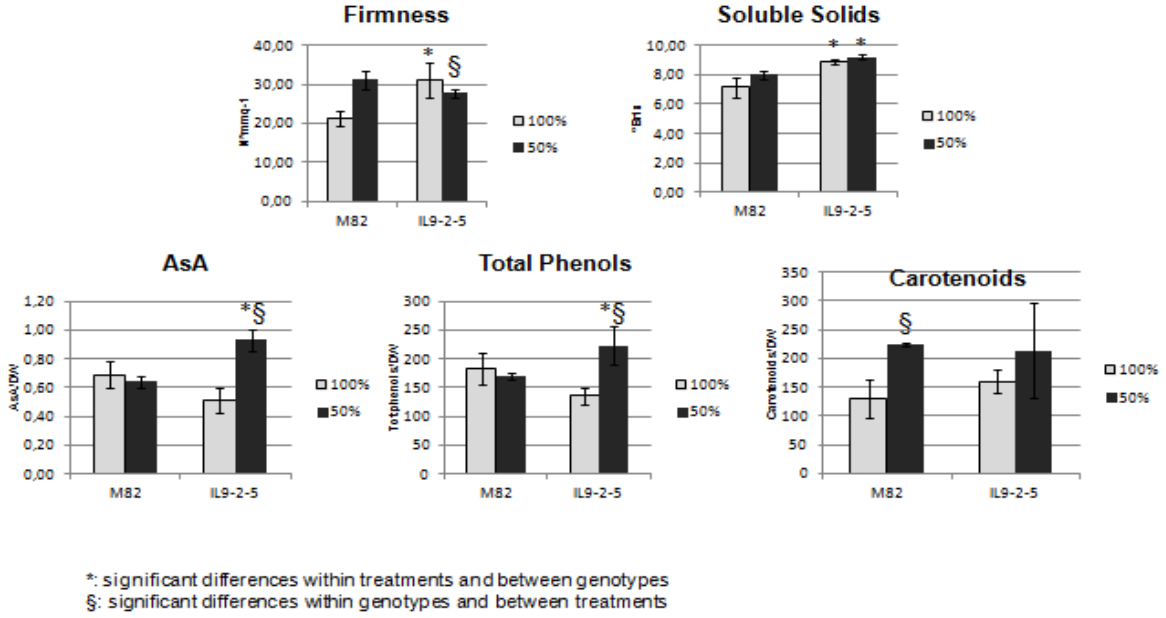

Figure 2.4 - Fruit qualitative traits in M82 and IL9-2-5 grown at different levels of water supply in the second experiment

2.2 Microarray Analysis

In order to investigate the molecular network controlling fruit quality-related processes in response to water deficit, a transcriptomic analysis was performed on a 90k Combimatrix TomatArray 1.0 comparing red-ripe fruit from IL9-2-5 and M82 at two different water treatments. Comparing the gene expression in M82 between water treatments by Student's t test resulted in 204 probes with significant different expression, 64 of which were up-regulated and 140 down-regulated. In figure 2.5 a schematic representation of the 204 probes with significant variation is showed. They were categorized into 8 groups of Fold Change ranging between values -3 and 2.

Among these TCs, a subgroup of genes was identified, which are involved putatively in different processes:

1. Six are involved in AsA pool size, and are phosphoglycerate mutase, glyceraldehyde-3-phosphate dehydrogenase , vtc2-like protein, succinyl--ligase alpha subunit , udp-glucose dehydrogenase and photoassimilate-responsive protein par-1b-like protein.
2. Nine are Involved in defense mechanisms towards abiotic stress, and are salt tolerance protein, universal stress protein family protein, anthocyanidin synthase, peptidyl-prolyl cis-trans isomerase-like 3, peptidylprolyl isomerase and Cyclophilin, dnaj heat shock n-terminal domain-containing protein, dehydration responsive element-binding protein 1, dehydration-responsive family protein.

On the other hand, in case of IL9-2-5, the comparison between the two water treatments by Student's t test only retrieved 5 probes differentially expressed (tab. 2.3), of which 3 were up-regulated and 2 down-regulated, underlining low fold changes. This would imply that the IL9-2-5 phenotype is more stable to water deficit than the M82 one, thus supporting the higher tolerance of IL9-2-5 to reduced water restitutions.
Comprehensively, the comparative transcriptomic analysis of fruit allowed the identification of 544 transcripts (2,69% of total transcripts on the chip) showing significant interaction *genotype x treatment* at the ANOVA test (supplementary tab. 1), thus evidencing different regulation patterns in M82 and IL9-2-5 in response to water treatments. These genes might justify the different variation of M82 and IL9-2-5 in their performances when water restitution to field capacity was reduced. In particular, within the set of mRNAs differently responding to water deficit (Supplemetary tab. 1.1), a sub-set of transcripts implicated in AsA biosynthesis, stress response and carbohydrate metabolism were identified (tab. 2.4). All these mRNAs were hypothesized as relevant for explaining variations in fruit quality traits observed in the two studied genotypes.
To highlight the different expression pattern of these TCs in M82 and IL 9-2-5 in relation to different water treatments a graphic representation was provided in fig. 2.6. Within each genotype changes in the expression of TCs was presented as fold change (FC) of the expression in fruit treated with 50% of water restitution compared to the fruit treated with the 100% one. TCs selected were categorized into three groups according to the different processes in which they are putatively involved: A) AsA biosynthesis, B) stress response C) carbohydrate metabolism (fig 2.6).
Both TCs included in AsA biosynthesis, GDP-mannose pyrophosphorylase Id_14033 and vtc2-like protein showed down regulation in M82, while in IL9-2-5 the fold variation is very low. As for the group of transcripts involved in stress response, most of them (dehydration responsive element-binding protein 1 id_15504, multiple stress-responsive zinc-finger protein isap1 id_16729, non-specific lipid transfer protein id_4506 and proline transporter id_18536) showed lower fold variation in IL9-2-5 over application of water deficit compared to M82. The remaining TCs (water channel protein id_7450 and chloroplastic quinine-oxidoreductase id_9787) showed an opposite pattern of expression between the two genotypes. Finally, most of transcripts included in group C exhibited higher variation in M82 in response to water deficit. In particular, mRNAs annotated as chloroplast protein cp12 (id_11656), mevalonate diphosphate decarboxylase (id_6835), hexokinase 2 (id_13169),

fructose-bisphosphatase precursor (id_11902) and 1-deoxy-d-xylulose 5-phosphate synthase (id_18608) showed strong up-regulation in M82 upon water deficit but did not exhibited appreciable variation in their mRNA abundance in IL9-2-5 when the reduction in water restitution was applied.

Table 2.3 - Statistical and annotation details of 5 probes showing differential hybridization signals between the two water treatments in IL9-2-5, at a Student's t test model (P < 0.01).The automatic BLAST annotation of TC sequences was performed by the BLAST2GO software suite.

Code	Annotation	adj p value	Fold Change
id_5173	nadh dehydrogenase subunit d	0.008	0.553
id_380	NA	0.009	0.440
id_6775	Lipase	0.005	-0.252
id_11910	mitochondrial elongation factor tu	0.008	-0.451
id_19256	oxidoreductase of zinc-binding dehydrogenase family	0.008	0.548

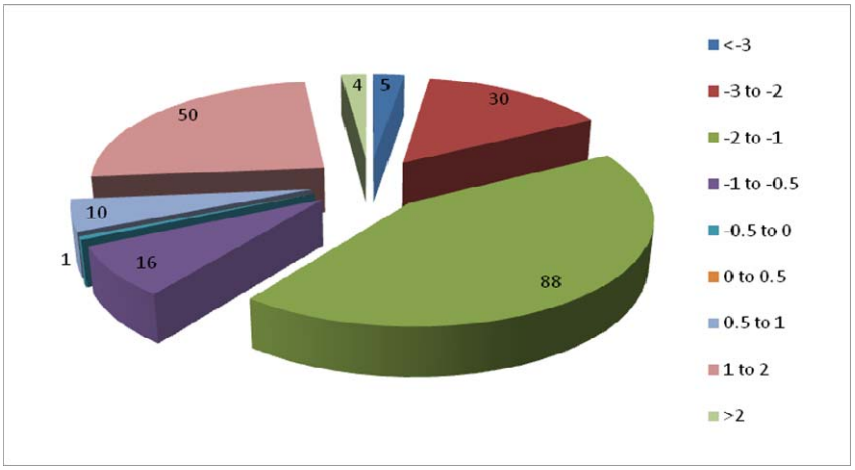

Figure 2.5 – Microarray analysis. Distribution of 204 probes with significant variation (Student's T test,P<0.01) in the mRNA level of M82 between the two treatments. Based on Fold change values probes were categorized into 8 groups and the number of probes included in each group is presented.

Table 2.4 – Selected TCs, showing significant interaction *genotype x treatment* at ANOVA test, in M82 and IL9-2-5 genotypes at 100% and 50% water supply, in microarray analysis, categorized in three groups (A, B and C). FC is the Fold change of each genotype at 50% compared with its 100% water supply.

A	**AsA biosynthesis**	**FC M82 50% vs. M82 100%**	**FC IL9-2-5 50% vs. IL9-2-5 100%**
id_14033	mannose-1-phosphate guanyltransferase	-1,352	0,299
id_17088	vtc2-like protein	-1,585	-0,128
B	**Stress response**	**FC M82 50% vs. M82 100%**	**FC IL9-2-5 50% vs. IL9-2-5 100%**
id_15504	dehydration responsive element-binding protein 1	-2,110	0,015
id_16729	multiple stress-responsive zinc-finger protein isap1	-1,799	0,171
id_7450	water channel protein	-1,910	0,966
id_4506	non-specific lipid transfer protein	1,207	0,147
id_9787	chloroplastic quinone-oxidoreductase	1,222	-0,529
id_18536	proline transporter	1,395	-0,030
C	**Carbohydrate metabolism**	**FC M82 50% vs. M82 100%**	**FC IL9-2-5 50% vs. IL9-2-5 100%**
id_1781	udp-glucose dehydrogenase	-2,463	-0,649
id_11656	chloroplast protein cp12	-3,424	-0,169
id_6835	mevalonate diphosphate decarboxylase	-2,228	0,255
id_13169	hexokinase 2	1,402	-0,172
id_11902	fructose-bisphosphatase precursor	1,429	-0,010
id_9556	pyruvate kinase isozymechloroplastic flags: precursor	1,603	-0,581
id_8791	nadh-ubiquinone oxireductase	1,605	-0,486
id_18608	1-deoxy-d-xylulose 5-phosphate synthase	2,333	0,040
id_2862	cellulose synthase-likeglycosyltransferase family 2	-1,026	0,459
id_14033	mannose-1-phosphate guanyltransferase	-1,352	0,299
id_17015	udp-galactose 4-epimerase-like protein	1,015	-0,531
id_6089	2-oxoglutarate-dependent dioxygenase	1,028	-0,347
id_2059	galactose kinase	1,359	-0,222
id_7532	receptor-like protein kinase INRPK1a	-2,478	-0,305
id_1090	photoassimilate-responsive protein	-2,167	-0,068
id_6940	zinc finger transcription factor-like protein	-1,054	1,422
id_10977	granule-bound starch synthasechloroplastic amyloplasticame	-0,915	0,186

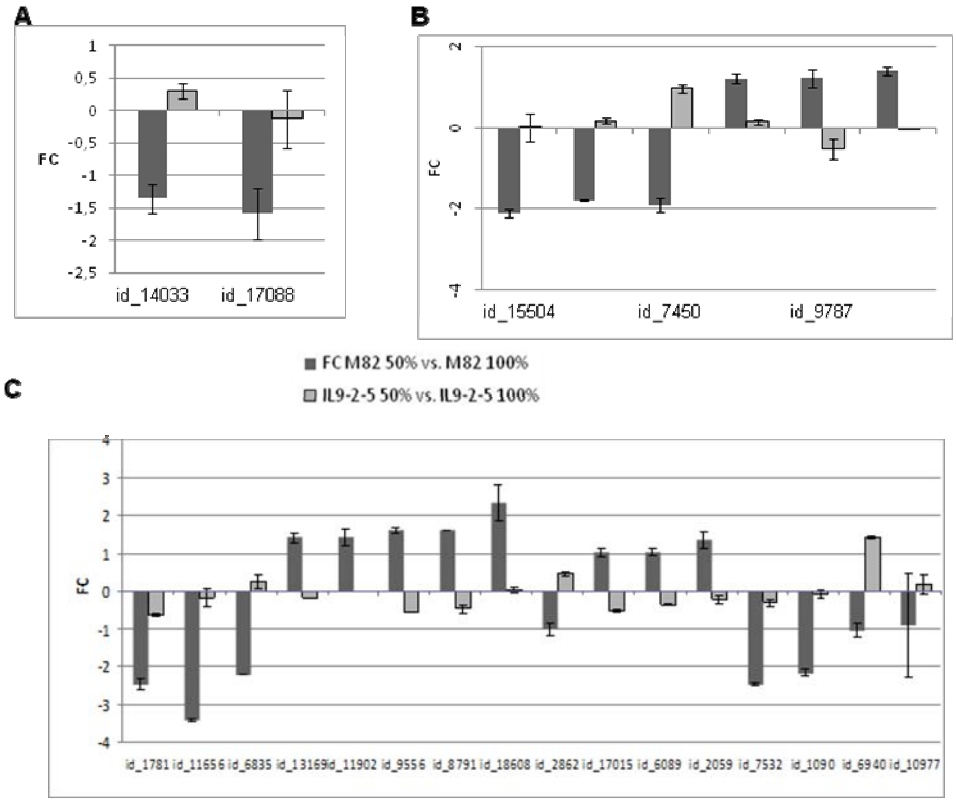

Figure 2.6 – Differential response to reduced water supply in M82 and IL9-2-5 of mRNAs selected from probes showing significant interaction *genotype x treatment* at microarray analysis: A. involved in AsA biosynthesis B. involved in stress response C. involved in carbohydrate metabolism. For id identification see table 3.6.

2.3 qRT-PCR analysis

Some mRNAs involved in AsA recycling, which were missed by the microarray analysis during the data processing, were investigated by qRT-PCR. They were 4 monodehydroascorbate reductase (MDHAR) and 3 dehydroascorbate reductase (DHAR) transcripts. In addition, the expression level of some mRNAs included in the group of TCs selected from the microarray analysis (see tab. 2.4) was validated by qRT-PCR. They include a receptor like kinase, a photoassimilate-responsive protein, a zinc finger transcription factor-like protein, a GDP-mannose pyrophosphorylase, a granule-bound starch synthase and a vtc-2 like protein.

Results are summarized in figure 2.7. The receptor like kinase (id_7532) showed an expression profile by qRT-PCR analysis that did not confirm microarray data. As for the photoassimilate-responsive protein (id_1090), the qRT-PCR analysis confirmed a down-regulation in M82 while in IL9-2-5 the level of mRNA increased upon water deficit. For vtc-2 like protein (id_17088) qRT-PCR analysis did not confirm microarray data.

As for AsA recycling genes, MDHAR1 (id_20104) in M82 showed strong up-regulation, while in IL9-2-5 its change in the expression level was not significant. In addition, MDAHR2 (id_16469) showed up-regulation in both genotypes, MDAHR3 (id_10714) did not show differences between genotypes and MDAHR4 (id_14628) exibited down-regulation only in IL9-2-5. The 3 DHAR showed similar trend of expression with up-regulation in M82 and down-regulation in IL 9-2-5.

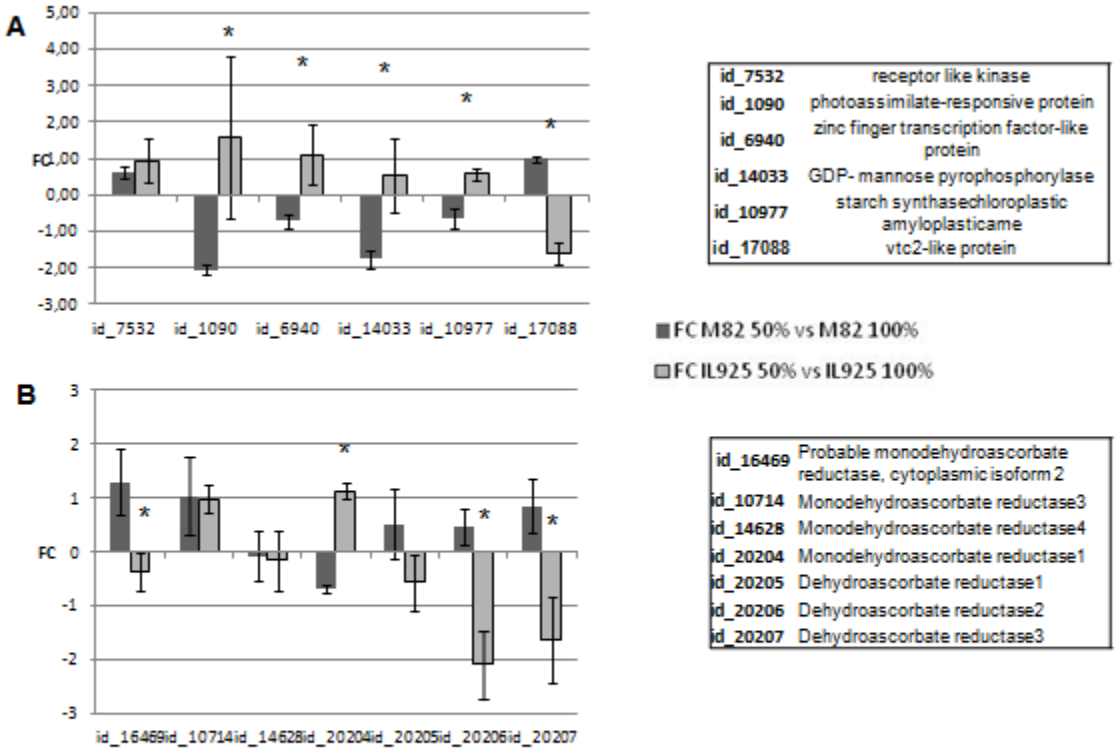

*: Significant differences at Student's T test

Figure 2.7- qPCR expression analysis of mRNAs putativly relevant for AsA and carbohydrate metabolism in response to water deficit. **A.** mRNAs selected from microarray analysis **B.** mRNAs involved in AsA recycling but missing across microarray data processing. Asterisk indicates significant differences between M82 and IL9-2-5 at Student's t test coupled with bootstrap re-sampling of 1000 sample ($P<0.05$).

2.4 Correlation analysis

Given that AsA fruit content was differently affected by water deficit between M82 and IL9-2-5 and variations in its levels were associated to dramatic change in the expression of genes related to carbohydrate metabolism and stress response, key co-regulative mechanisms governing the modulation of fruit quality in response to water deficit were investigated. To do this a subset of 97 TCs (tab 2.5) was selected, including transcripts related to AsA metabolism and their family members identified by similarity across the tomato genome, transcripts related to AsA recycling, transcripts putatively involved in the carbohydrate metabolism and stress response, some sucrose and hexose transporters. Within this subset, microarray normalized expression signals were used to undertake a co-regulation analysis by using the CoExpression Tool software with a 70% Pearson threshold and a bootstrap procedure. Results were drawn in figure 2.8. In this diagram, transcripts are indicated as nodes and a line bridging two nodes identifies a Pearson correlation higher than 0.70 between them. Noteworthy, a transcript annotated as GDP-mannose pyrophosphorylase, key function in AsA biosynthesis, correlated with a sucrose transporter LeSUT2, with a putative water channel protein and with a photoassimilate-responsive protein involved in carbohydrate accumulation in response to biotic stress (Herbers et al., 1995). The GDP-mannose pyrophosphorylase also evidenced correlation with a 1-deoxy-d-xylulose 5-phosphate synthase, which is involved in the mevalonate-independent isopentenyl pyrophosphate pathway. The networking also highlighted correlations between a vtc2

mRNA and a monosaccharide transporter, LeHT1, which is also linked to the photoassimilate-responsive protein. Another vtc2 transcript correlated with an hexokinase 2, a regulatory enzyme involved in the first step of glycolysis, like a DHAR did.

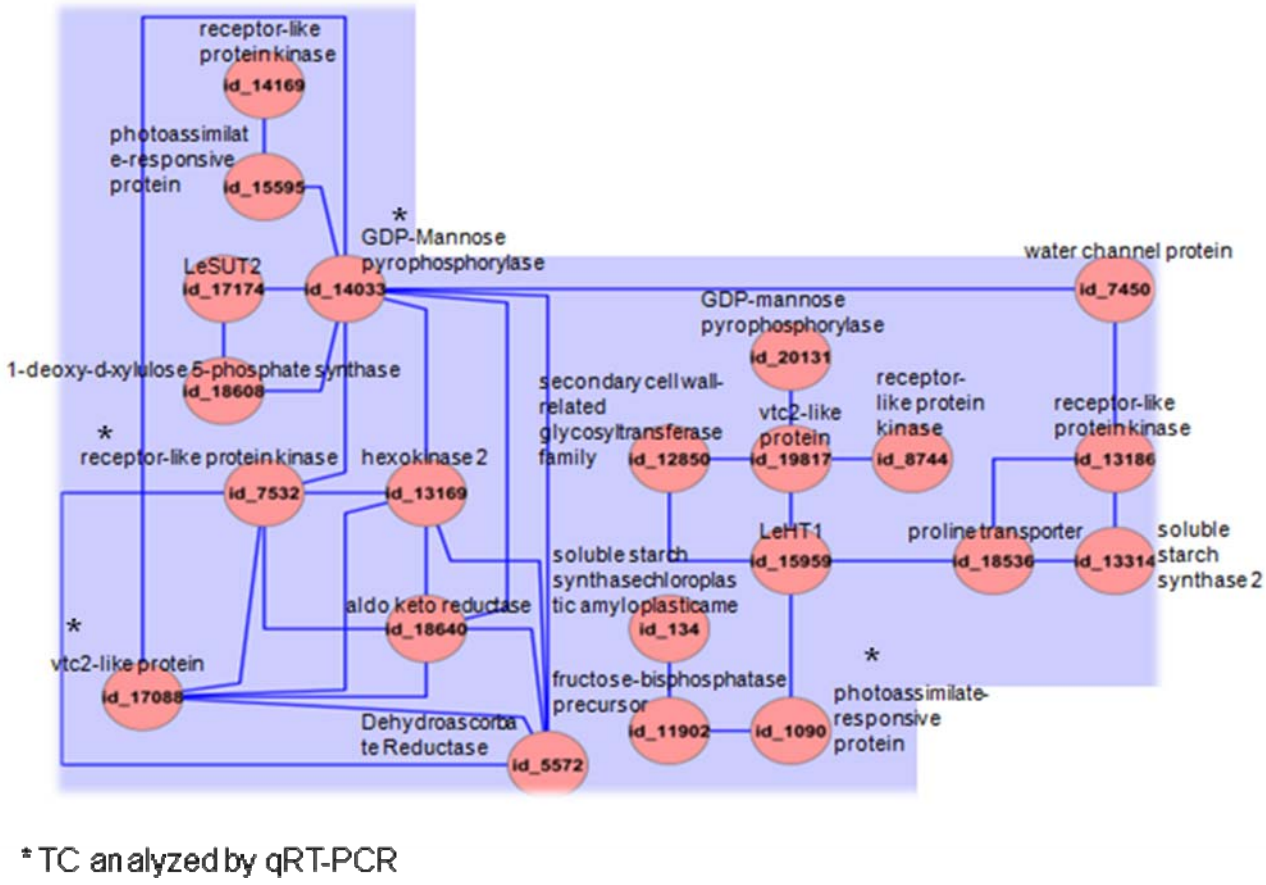

Figure 2.8 – Co-regulated expression of mRNAs involved in AsA and carbohydrate metabolism in response to water deficit. Analysis was performed using CoExpression Tool with 0.07 Pearson correlation threshold and bootstrap re-sampling.

Table 2.5 - List of TCs selected for co-regulation analysis by the CoExpression Tool software. Transcripts are grouped in three categories: **A**. AsA metabolic process, **B.** stress response, **C.** carbohydrate metabolism. Asterisk highlights transcripts also validated by qRT-PCR.

A

AsA metabolic process	Code
Dehydroascorbate Reductase	id_2059*
	id_19876*
	id_1016*
	id_5572
GDP-mannose pyrophosphorylase	id_18316
	id_9732
	id_20131
	id_8637
	id_14033
	id_9233
vtc2-like protein	id_20196
	id_19817*
aldo keto reductase	id_20203
	id_15490
	id_2428
	id_7471

B

Stress response	Code
dehydration responsive element-binding protein 1	id_15504
multiple stress-responsive zinc-finger protein isap1	id_16729
water channel protein	id_7450
aldehyde dehydrogenase	id_11952
non-specific lipid transfer protein	id_4506
chloroplastic quinone-oxidoreductase	id_9787
proline transporter	id_18536
elicitor-inducible cytochrome p450	id_19814
atp phosphoribosyl transferase	id_7833
	id_13012
receptor-like protein kinase	id_13186
	id_7532 *
	id_17057
	id_15490
	id_2428
	id_7471
	id_5553
	id_11423
	id_14169
	id_17438
	id_18130
	id_8744
	id_10857
zinc finger transcription factor-like protein	id_6940*
	id_18316
	id_1992
	id_13999
	id_6970
	id_17018
	id_1045
	id_18316*
	id_1992

C

Charbohydrate metabolism	Code
LeHT1	id_11820
	id_15959
LeHT2	id_3226
L3HT3	id_15959
LeSUT1	id_4927
LeSUT2	id_17174
LeSUT4	id_7966
Lin 8	id_20201
Lin 6	id_20202
cellulose synthase-likeglycosyltransferase family 2	id_2862
secondary cell wall-related glycosyltransferase family 47	id_12850
udp-galactose 4-epimerase-like protein	id_1775
2-oxoglutarate-dependent dioxygenase	id_17015
	id_6089
galactose kinase	id_15943
hexokinase 2	id_5553
mfs family transporter: sugar (sialic acid)	id_11423
phosphate transporter	id_14169
	id_17438
	id_18130
	id_8744
	id_10857
udp-galactose 4-epimerase-like protein	id_7826
	id_1090
sugar transporter family protein	id_11559
udp-glucose dehydrogenase	id_6940
chloroplast protein cp12	id_18316
mevalonate diphosphate decarboxylase	id_1992
fructose-bisphosphatase precursor	id_13999
	id_6970
photosystem ii reaction center w protein	id_17018
pyruvate kinase isozymechloroplastic flags: precursor	id_1045
nadh-ubiquinone oxireductase	id_18316
1-deoxy-d-xylulose 5-phosphate synthase	id_1992
soluble starch synthasechloroplastic amyloplasticame	id_18076 *
	id_134
starch synthase iic precursor	id_10977
starch synthase iia	id_2388
	id_1775
starch synthase iv	id_17064
starch synthase iii	id_4736
soluble starch synthase 2	id_18543
granule bound starch synthase i	id_13314
	id_18076
photoassimilate-responsive protein par-1b-like protein	id_15595
	id_7826 *
	id_1090
cellulose synthase-likeglycosyltransferase family 2	id_11559
secondary cell wall-related glycosyltransferase family 47	id_2862

3. Discussion

AsA pool size in plant cells depends on tightly regulated processes such as AsA synthesis, recycling, degradation, and transport that, combined with the existence of multiple biosynthesis pathways, make its regulation difficult to engineer. In recent

years, AsA level in tomato has mostly been engineered by overexpression of enzymes involved in its biosynthesis, such as overexpression of D-galacturonic acid reductase in *A. thaliana* (Agius et al., 2003), GDP-D-mannose 3,5-epimerase in tomato (Gilbert et al., 2009). Genetic engineering of AsA in tomato has also been achieved by overexpression of monodehydroascorbate reductase (MDHAR) (Eltayeb et al. 2007) and dehydroascorbate reductase (DHAR) (Chen et al. 2003) genes and antisense expression of an ascorbate oxidase gene (Pignocchi et al., 2003). AsA regulation has also been studied by QTL analysis and the development of molecular markers to identify novel genes associated with high AsA levels (Ishikawa et al., 2006). AsA content lends itself to QTL analysis as it is a character exhibiting quantitative variation, which is controlled by several genes, more or less influenced by the environment. As matter of fact, wild tomato accessions are rich in ascorbic acid, that is going lost in commercial varieties, containing up to 5 times more AsA. Dissection of wild genetic variability associated to AsA QTLs has become possible as introgression lines (ILs) become available. A QTL for tomato fruit AsA content (Stevens et al. 2007a) has been fine mapped in IL9-2-5 within a region of approximately 0.3 cM. Stevens and co-workers (2008) demonstrated that the QTL 9-2-5 from S. pennellii includes three regions. The first region had an overall positive effect on tomato fruit ascorbic acid content, and a MDHAR candidate gene mapped in this region. The second region includes a gene/s controlling plant weight and is associated with a semi-determinate, rather than determinate, growth leading to increased leaf numbers and plant weight. The self-pruning (*sp)* gene is a candidate gene for controlling plant weight and may modulate the strength of the photosynthetic vegetative source, thus contributing to increase AsA level; in this second part there is also a portion that may exert a negative influence on the ascorbic acid content. The third region, localized between the two previously described, showed an increasing effect on fruit AsA content and includes a Brix-9-2-5 locus encoding a fruit apoplastic invertase Lin5, whose wild allele showed an increased enzymatic activity (Baxter et al., 2005). Lin5 is a cell wall invertase that cleaves sucrose in glucose and fructose, and is exclusively expressed in flower (mainly ovary but also petal and stamen) and in young fruit (Godt and Roitsch, 1997; Fridman and Zamir, 2003). Its increasing effect on the fruit AsA could be argued because an increase in fruit sugar level could increase fruit AsA pool, considering that AsA synthesis pathway starts from glucose. IL9-2-5, indeed, was already identified as an introgression producing fruit with high soluble solids content (°Brix). This would be promising for tomato industry beacuse fruit with high soluble solids requires less processing energy to generate pastes of the appropriate consistency for consumer tastes and major total soluble solids give also more sweetness and therefore the addition of less sugar during processing is required (Baxter et al., 2005).

Results presented in this thesis confirmed that IL9-2-5 also performed higher tolerance under water deficit compared to the parental variety M82. In particular, experimental trials carried out in semi-controlled conditions in two different areas of Southern Italy (Bari and Portici), replicated over two consecutive summer seasons, allowed to comprehensively record a lower reduction in yield and AsA level in IL9-2-5. In fact, IL9-2-5 showed a lower Blum index for total yield and marketable yield than M82, that is a lower yield losses under 50% water treatment. In addition, previous studies carried out on the same IL evidenced differences in the architecture of the root system (Maria Vasco' s PhD thesis). In particular, IL9-2-5 roots showed a higher linear development in both total root system and first order adventitious roots, respect to M82. Also, the total root mass was higher in IL9-2-5 compared to M82.The

association in IL9-2-5 of the higher tolerance to water deficit with an higher root system development allowed to argue that the exploration of an higher soil surface might enable an increased efficiency in water extraction ability.
Fruit phenotyping for quality traits highlighted, particularly for the first experiment, very low changes in firmness, soluble solids and nutrient content in IL9-2-5 compared to M82, also underlining a higher phenotypic stability in this IL under water deficit. Noteworthy, within the first experiment, fruit AsA level underwent a dramatic reduction in M82 under the 50% water treatment while in IL9-2-5 it did not exhibit significant changes. At the same time, within the second experiment, M82 stably maintained its AsA level in the fruit while IL9-2-5 showed an important increase in AsA level (0.69 and 0.93 $mg*g^{-1}$ of DW respectively in 100% and 50% treatments), thus confirming a relevant environmental effect on this quality trait (Toor et al., 2006). Comprehensively, both trials confirmed the higher performances in AsA fruit level of IL9-2-5 under the 50% water treatment. Physiological processes controlling the effect of water stress on AsA level in plants has been extensively investigated. Water stress results in the depletion of the AsA pool and triggers ABA-induced stomatal closure (Leung and Giraudat, 1998; Pastori and Foyer, 2002). Such closure limits CO2 assimilation and increases the concentration of NADPH as a consequence of a reduction in Calvin cycle activity. Under normal growth conditions, photoactivated chlorophyll transfers its excitation energy to the photosynthetic reaction centers, but under stomatal closure in a water-stressed leaf, in which NADP is limiting, the excitation energy of the photoactivated chlorophyll is transferred to triplet oxygen and excites it to the singlet form. Consequently, water stress increases the production of activated oxygen species (Bowler et al., 1992).
Results of our transcriptomic analysis support the hypothesis of lower amplitude response to water deficit in IL9-2-5, possibly accounted by a reduced sensing of the deficit, thus leading to a more stable phenotype. In fact, when we compared the transcriptome of IL9-2-5 under 50% water treatment with the one under 100% treatment, only 5 probes exhibited significant changes in the expression (tab. 3.3) and their variations in the expression showed low intensities. On the contrary, M82 exhibited a higher amplitude transcriptional response to water deficit implicating changes in the expression of 204 TCs including genes involved in defense mechanisms towards abiotic stress such as salt tolerance protein, universal stress protein family protein, anthocyanidin synthase, peptidyl-prolyl cis-trans isomerase-like 3, peptidylprolyl isomerase, proline-rich cell wall, cyclophilin, dnaj heat shock n-terminal domain-containing protein, dehydration responsive element-binding protein 1 and dehydration-responsive family protein. Our hypothesis is also supported by the up-regulation of a proline transporter (table 3.4), which has been involved in the response to water stress (Yoshiba et al., 1997), in M82 (FC= 1.39), while in IL9-2-5 no significant change in the expression was recorded upon water deficit.
Given that a polymorphism in the CDS of the apoplastic invertase gene has been involved as major determinant of the phenotypic variation in IL9-2-5 (Baxter et al., 2005) with an effect on the invertase activity in the fruit columella and on the carbohydrate content in the fruit, in our study we paid particular attention to the responding pattern to water deficit of mRNAs involved in carbohydrate metabolism. Overall, the co-regulation-based networking (fig. 2.8) highlighted many relations between AsA genes and genes involved in carbohydrate metabolism and stress response explaining variations in fruit quality upon water deficit in the two tomato lines. Particularly interesting were correlations among a transcript annotated as GDP-mannose pyrophosphorylase, key function in AsA biosynthesis (Conklin et al., 1999),

with a sucrose transporter LeSUT2, a putative water channel protein and a photoassimilate-responsive protein involved in carbohydrate accumulation in response to biotic stress (Herbers et al., 1995). The GDP-mannose pyrophosphorylase mRNA showed a significant interaction *genotype x treatment* at the ANOVA test (supplementary tab. 1) in microarray analysis. Validation of its transcription pattern by qRT-PCR confirmed a dramatic down-regulation in M82 under 50% treatment, while an increasing trend was observed in IL9-2-5. This would, at least in part, account for the higher level of AsA in IL9-2-5 under water deficit. Similarly, the transcript coding for a photoassimilate-responsive protein par-1b-like protein showed a dramatic decrease in its expression in M82 under 50% of water stress, while a very low increase in IL9-2-5 was recorded. Herbers and co-workers (1995) demonstrated that the induction of par-1 mRNA may be mediated by an increase in soluble sugars in the plant cells and by a pathogenesis interaction. Pierpoint et al. (1981) and Ohashi and Matsuoka (1985) reported the induction of PR proteins under mannitol-induced osmotic stress. Viruses have been described to cause severe perturbations in carbohydrate metabolism in leaves leading to the accumulation of starch and/or soluble sugars. Sturm and Chrispeels (1990) found that bacterial infections caused rapid induction of extracellular invertase. Probably glucose and fructose might trigger the induction response. Thus, as already suggested by Jang and Sheen (1994), there might be a common mechanism of sugar sensing in the repression of photosynthetic genes and the activation of stress pathogenesis-related genes. Thus, the repression of this gene in M82 under water deficit might reflect the inhibition of photosynthesis resulting from stress.

In IL9-2-5, the reduced severity in sensing the lower water supply could likely affect photosynthetic activity in leaves, sugar transport from source to sink organ and respiration pathways. This might explain the up-regulation, at the microarray analysis, of a hexokinase-2 in M82 under water stress, while very little variations were observed in IL9-2-5. This gene has a dual-function both catalytic and regulatory and a role in repression of photosintetic genes was reported (Xiao et al., 2000). Similarly, a chloroplast protein cp12 was strongly down-regulated in M82 according to microarray data under water stress, while in IL9-2-5 did not. This is a regulatory peptite lacking enzymatic activity, changing conformation depending on redox state of glyceraldehyde-3-phosphate dehydrogenase which removes hydrogen from NADPH to make glyceraldehyde-3-phosphate in glycolytic breakdown (Marri et al., 2005). The repression in M82 of these genes suggests an increased flux in Calvin cycle, thus an increase in the respiration rate. This is also confirmed by the up-regulation in M82 under water deficit of TCs involved in the respiration pathway such as a pyruvate kinase and a NADH-ubiquinone oxireductase. These mechanisms would account for energy dissipation upon stress response.

Changes of gene expression under drought stress cause a series of physiological and biochemical alterations. Photosynthesis, one of the primary biosynthetic pathways, is significantly affected by drought stress, which restricts the normal function of other metabolic pathways, such as nitrogen fixation (Chaves et al., 2009). The respiration pathway, which breaks complex molecules into simple compounds to provide the energy required for plant development, is accelerated under drought stress (Haupt-Herting et al., 2001). Protection systems such as the antioxidation pathway, which can reinforce plant cells to form reactive oxygen species scavengers, are also affected by drought stress (Apel and Hirt, 2004). Among others, AsA has a major role in photosynthesis, acting in the Mehler peroxidase reaction with ascorbate peroxidase to regulate the redox state of photosynthetic electron carriers and as a

cofactor for violaxanthin de-epoxidase, the enzyme involved in xanthophylls cycle-mediated photoprotection. A modified root architecture and development in the IL9-2-5 might enhance the water uptake efficiency thus enabling root system to supply water to the plant even with permanent water deficit. Unlike M82, in IL9-2-5 the higher rate of water uptake would avoid plant to face with an even heavier response to water deficit thus keeping unmodified photo-assimilation and transport to sink organs of photo-assimilates, also helped by polarization of sucrose to fruit by a higher invertase activity in the columella provided by the wild protein encoded in the introgression 9-2-5. These differential response to water deficit would ensure in the IL9-2-5 fruit under water deficit a higher level of carbohydrate and this would make unnecessary the mobilization of the overall carbohydrates pool to cope with the stress response. This hypothesis is supported by the relevant number of genes involved in carbohydrate metabolism which exhibited lower changes in the mRNA level in IL9-2-5 than M82. Also, the lower energy dissipation from carbohydrate and the less affected photoassimilation would guarantee in the IL9-2-5 fruit under water deficit an higher availability of carbohydrate monomers for AsA biosynthesis, otherwise inhibited in M82 through the key controller GDP-mannose pyrophosphorylase. The co-localization in the wild introgression 9-2-5 of a QTL for tolerance to water deficit will enable strategies to breed tomato for enhanced tolerance to water deficit by transferring the same introgression in the genomic background of high yielding commercial varieties. Currently, backcrossing schemes assisted by molecular markers using IL9-2-5 as donor parental line are in progress. Also, this study allowed the identification of mechanisms controlling AsA level in tomato fruit and within these mechanisms underlined many candidate genes to be exploited for engineering nutritional quality of tomato fruit. Among these the gene encoding for the photoassimilate-responsive protein appear to be promising. Looking for superior alleles of this genes within biodiversity collections to transfer by sexual hybridization in commercial material and over-expression by genetic transformation might represents targeted strategies for attempting fruit AsA level engineering. In this case, the increased activity of this gene would activate higher carbohydrate accumulations providing monosaccharide extra-pool for AsA biosynthesis. Similarly, the GDP-mannose pyrophosphorylase gene could be target of genetic engineering strategies for increasing fruit quality in tomato. As in general, results of this PhD thesis highlighted that genetic mechanisms affecting the balance between fruit carbohydrate metabolism and transport and response to water deficit coul be exploited for engineering fruit quality.

Chapter 2. Shelf life and *Botrytis cinerea* resistance of tomatoes enriched in flavonoids

1. Materials and methods

1.1 Plant material

Plant material used for the experiments consisted of wild type (WT) tomatoes of MicroTom (*Solanum lycopersicum*) and MoneyMaker (*Lycopersicon esculentum*), and transgenic lines of *Del/Ros1* and *AtMYB12* in both MicroTom and MoneyMaker backgrounds and Indigo (*Del/Ros, AtMYB12*) only in MicroTom background, produced in the Department of Metabolic Biology of the John Innes Centre where I was hosted. In *Del/Ros1* lines, the *Delila (Del)* and *Rosea1 (Ros1)* genes encoding transcription factors that regulate anthocyanin biosynthesis in flowers of *Antirrhinum majus* were expressed, specifically in tomato fruits, by using the fruit-specific E8 promoter (Butelli et al., 2008) (fig. 1.1). AtMYB12, a flavonol-specific transcriptional activator of *Arabidopsis thaliana* (Mehrtens et al.,2005), was expressed in tomato fruit, leading to the accumulation of high levels of flavonols in the fruit (Luo J et al., 2008) (fig. 1). The Indigo line, derived from a cross between Del/Ros1N and AtMYB12 lines, which accumulates both high anthocyanin and high flavonol levels in the fruit. Seeds were sown on 0.8% MS medium before transfer to soil after 1 week. Kanamicin 100mg/L was used to select the transgenic seedlings before to transplant in pots containing soil and compost. Sample fruits were collected at different time points of ripening from Mature Green (MG)/Breaker (B) stages.

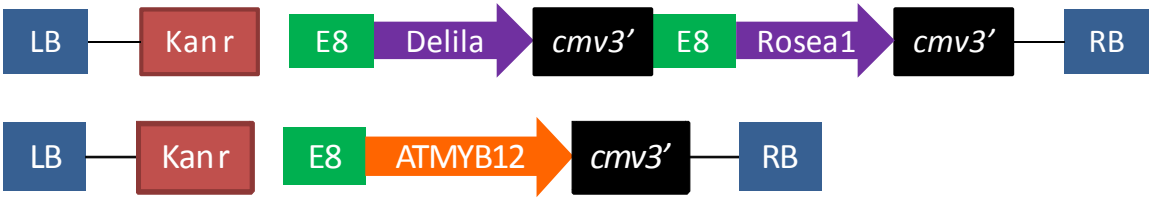

Figure 1.1. Map of T-DNA region of the binary vector used for transformation to get purple and orange tomatoes. LB, left T-DNA border region; RB, right T-DNA border region; Kanr, nptII gene conferring kanamycin resistance under the control of the nos promoter; cmv3, terminator region of cauliflower mosaic virus.

1.2 Storage test

1.2.1 Ripening test

WT, Del/Ros1 N , AtMYB12 and Indigo MicroTom fruits were harvested at 14 days after breaker. All fruits were sterilized in 10% bleach for 10 minutes, followed by rinsing three times in sterilized water. After washing, fruits were left to air dry in a fume hood. 10 fruits were put into one sterilized glass jar and keep at 18°C in dark. Every week, the total weight of 10 fruits was measured and the softening and shrivelling of fruits were calculated. The softening was calculated by manual touch and the shriveling by visual inspection. Every time, after measurement, fruits were transferred to a new sterilized jar. For Del/Ros, AtMYB12 in MoneyMaker background and WT, a shelf life test was performed at the same conditions described above, replacing glass jars with plastic boxes and putting 1 tomato for box.

1.3. Botrytis cinerea infection

In order to perform Botrytis cinerea tests, WT, Del/Ros1 N, AtMYB12 and Indigo fruits in MicroTom background were harvested 14 days after breaker stage. WT, Del/Ros1 N, AtMYB12 in MoneyMaker background were harvested 7 days after breaker stage. Fruits were sterilized in 10% bleach for 10 min, followed by rinsing three times in sterilized water and allowing to air dry. For infection by puncture, the fruits were wounded by a 1.5 mm diameter hole (1mm depth) using a sterilized 200uL tip. For infection by spray intact fruits were used. Botrytis cinerea (B05.10) was grown on MEYAA Medium (normal MEA medium plus extra yeast extract and agar) at 20°C for 10-14 days. Spore suspensions were collected from the medium with 14 ml of 0.05% Tween 80 in sterile water. The number of the spores was determined using a haemocytometer and resuspended in sterile distilled water at the concentration of 107 spores per mL. Spores were stored at 4°C in the dark for a maximum of 14 days. For inoculation, the fungal culture was diluted with ¼ PDB culture into 5×104 spores/mL and pre-inoculated for one and a half hour to activate the pathogen. 5uL fungal culture was added to each wound. All fruits were incubated at 20°C, in high humidity. Lesion diameter was measured at 24, 48 and 72 hours after inoculation. For spraying tests, cultures of Botrytis were diluted to 2.5×105 spores/mL. Intact fruits were sprayed thoroughly with spores, three times in the fume cabinet and kept at 20°C, in high humidity. Infection symptoms were observed at 3dpi, 4dpi and 5dpi.

Botrytis cinerea in vitro growth tests were performed on PDA plates. In combination with PDA, 50% tomato juice from WT (MoneyMaker), Del/Ros or AtMYB12 tomatoes (in MoneyMaker background) was used. For a negative control, PDA with 15mg/mL Triademinol was used. Botrytis B05.10 was grown on PDA plates first for three days. Around 5mm of Mycelium's diameter was cut from this initial plate and placed into the centre of the testing plates. Mycelium circle diameter was measured daily. 100mg/L streptomycin and ampicillin were added to all the plates to inhibit competing bacterial and fungal growth. In order to test the activity of compounds in the different juices against Botrytis cinerea Microtom fruits and Arabidopsis thaliana (ecotype Columbia) leaves were used for infection tests. For fruit infection, the fruit was wounded and the spores were diluted in different juices to give a concentration of 5x105/mL and each day for five days, 10 µL of Del/Ros1 N, Del/Ros C (a line that accumulates lower quantities of anthocyanins, Butelli et al., 2008), AtMYB12 and WT juices were added. As a negative control water was added. For the infection of Arabidopsis leaves the same protocol was used.

To extract DNA for Botrytis c. quantification, the injured portion of the infected fruit was cut out and dried under vacuum at low temperature for 24 hours. The tissue was smashed with a Tissue Lyser for 5 min at maximum speed. DNA was extracted using a Quiagen kit and quantitative PCR was performed using primers for fungus cutinase to detect Botrytis cinerea spread in the different fruits. In order to demonstrate the specific activity of anthocyanin versus B. cinerea, some commercial lines (Brioso and Carousel, bought in the market) were used to perform a Botrytis c. infection, as described previously (5uL 5*10^4 spores/mL in 90% juice or in ¼ PDB for control), and each day for five days were added 10 ul of Del/Ros1 N, Del/Ros C (a line that accumulate lower quantities of anthocyanin) and MicroTom juices.

1.4 qRT-PCR

For RNA isolation, three fruits (biological replicates), for each time point (Mature Green, Breaker, B+3, B+7, B+14, B+28, B+42), were homogenized and mixed under liquid N2 to prepare one biological repeat. Three biological repeats were analysed. RNA extraction was performed using the commercial Qiagen RNeasy Plant Mini kit and RNA concentration was estimated using PicoDrop µL Spectrophotometer release V2.07. RNA extraction and cDNA synthesis were conducted as described by Luo et al., 2008. All qRT-PCR were performed using a Bio-Rad CFX96TM Real Time PCR machine for 2 min at 95°C and then 40 cycles consisting of 20 sec at 95°C, 20 sec at 60°C and 30 sec at 72°C, followed by 65°C to 95°C melting curve detection. All quantifications were normalized by Ubiquitin 3 (X58253). Quantitative real-time were performed using gene-specific primers as shown in table 1.1.

Table 1.1 - Primers designed for qRT-PCR respectively ubiquitin (Endogenous control), polygalacturonase 2a, βgalactosidase 4, phytoene stnthase, cellulase1**.**

Gene	GB No.	Seq (5'-3)	Product size
LeUBI	X58253	LeUBI_RT_F: GCCAAAGAAGATCAAGCACA LeUBI_RT_R: TCAGCATTAGGGCACTCCTT	114bp
LePG-2a	A15981	LePG2a_RT_F: TTGTGGTCCAGGTCATGGTA LePG2a_RT_R: TTTCGGCACCGATAATTTTG	107bp
LeTBG4	AF020390	LeTBG4_RT_F: CTTGGCGAAACAGAAATGGT LeTBG4_RT_R: ACCTCGAACCCATTCAACAG	100bp
LePSY	DQ335097	LePSY_RT_F: TGTTGGAGAAGATGCCAGAA LePSY_RT_R: TTTATCGGTCACCCTTCCAG	106bp
LeCel1	U13054	LeCel1_RT_F: AGCCTCATCACTCCCTTCAA LeCel1_RT_R:GCACCGACATGTGTGTTAGG	111bp

1.5 Analysis of cell wall degrading enzymes

MicroTom WT, Del/Ros1 N, AtMYB12 and Indigo tomatoes were washed, deprived of seeds and homogenized in liquid nitrogen in a mortar. For each time point (MG, B, B+3, B+7, B+14, B+28, B+42) three biological repeats were analysed.

Three grams of the homogenized sample were extracted with 3 mL of sodium acetate buffer (50 mM, pH 5.5, 1M NaCl, 10 g/L polyvinyl-polypyrrolidone; PVPP)

under agitation for 2h at 4°C, centrifuged at 1000 x g for 10 min and the supernatant collected. The supernatant then was dialyzed (Visking tube, diameter 8/32, Scientific Instruments Centre Ltd, UK) against sodium acetate buffer (50 mM, pH 5.0) overnight at 4°C, and the dialyzed samples were used to determine both polygalacturonase and β-galactosidase enzyme activities. All the steps during the extract preparation were carried out at 0-4°C. PG activity was measured in a mixture containing 50 mM sodium acetate buffer pH 5.0, 0.15% (w/v) polygalacturonic acid, and 1 mL of enzyme extract, in a total volume of 3 mL. The mixture was incubated at 37°C, aliquots of 300 µL were taken at different times, mixed with 1mL Borate buffer pH 9 and 200 µL 1% 2-cyanoacetamide (Sigma-Aldrich). To stop the reaction, the mixture was immersed into a boiling bath for 10 min. Samples were cooled down to room temperature and the OD at 276 nm was measured. Results were expressed as delta OD in 1 sec under the assay conditions per kilogram of fresh fruit. β-Galactosidase (TBG) extraction was done as described for PG. The reaction mixture consisted of 0.5 ml of 0.1 M citrate (pH 4.0), 0.4 mL of 0.1% BSA, 0.1 mL of enzyme extract, and 0.5 ml of 10 mM p-nitrophenyl-β-galactoside. After 15 min at 37°C, the reactions were terminated by the addition of 2 mL of 0.4 M sodium carbonate, and the liberated p-nitrophenol was measured at 420 nm with Hewlett-Packard 8453 Diode Array spectrophotometer (HP, Waldbronn, Germany). Results were expressed as delta OD in 1s under the assay conditions per kilogram of fresh fruit.

1.6 Trolox Equivalent Antioxidant Capacity (TEAC)

The TEAC assay is based on the ability of antioxidant molecules to quench the long-lived ABTS (2,2'-azinobis 3-ethylbenzthiazoline-6-sulfonate, Sigma-Aldrich) radical cation, a blue-green chromophore with characteristic absorption at 734 nm, compared with that of trolox (6-hydroxy-2.5,7,8 tetramethylchroman- 2-carboxylic acid, Fluka), a water-soluble vitamin E analog. A stable stock solution of ABTS•+ was produced by reacting a 7 mmol/L aqueous solution of ABTS with 2.45 mmol/L potassium persulfate (final concentration) in water and allowing the mixture to stand in the dark at room temperature for 12–16 h before use. Before starting the assay an ABTS•+ working solution was obtained by the dilution in ethanol of the stock solution to an absorbance of 0.70 ± 0.02 AU at 734 nm, verified by a Hewlett-Packard 8453 Diode Array spectrophotometer (HP, Waldbronn, Germany), and used as the mobile phase in a flow-injection system, according to Pellegrini and coworkers' protocol (Pellegrini et al., 2003). 5 mmol L-1 stock solution of Trolox was prepared in ethanol and stored at -20 °C for a maximum of 6 months. The stock solution of Trolox was diluted daily in ethanol at different concentrations to obtain working solutions for building the dose-response curve. After addition of 1.0 mL of diluted ABTS solution (A734nm 0.700±0.020) to 10 uL of antioxidant compound or Trolox standards (final concentration 0–15 uM) in ethanol the absorbance reading was taken at 30°C exactly 1 min after initial mixing. Fruits were washed, deprived of seeds and homogenized under nitrogen in a mortar. One gram of the homogenized sample was extracted with 4 mL of water under agitation for 20 min at room temperature, centrifuged at 1000 x g for 10 min and the supernatant collected. The extraction was repeated with 2 mL of water and the two supernatants were combined. The pulp residue was re extracted by the addition of 4 mL of acetone under agitation for 20 min at room temperature, centrifuged at 1000 x g for 10 min and the supernatant collected. The extraction was repeated with 2 mL of acetone and the two supernatants were combined. 5 uL of tomato extracts, both in water and acetone, were immediately analyzed for their

antioxidant capacity. Results were expressed as TEAC in mmol of trolox per kg of fresh weight.

1.7 Malondialdehyde (MDA) detection

Fresh fruits (2.5 g) of wild type Del/Ros1 N, AtMYB12 and Indigo in MicroTom genetic background were washed, deprived of seeds and ground in 10 mL of 10 mM sodium phosphate buffer, pH 7.2 using sand at room temperature, and then centrifuged at 2000 g for 10 min. A sample of the supernatant (0.1 mL) was added to tube containing 0.4 mL of distilled water, 0.25 ml of 20% (w/w) trichloroacetic acid, and 0.5 mL of 10 mM thiobarbituric acid. A control was run for each sample in which thiobarbituric acid was replaced by an equal volume of distilled water. Samples were heated in a boiling water bath for 45 min and then centrifuged for 10 min at 2000 x g to remove haziness. The cleared samples were allowed to equilibrate at room temperature before the absorption at 532 nm was measured. The concentration of malondialdehyde (MDA) was calculated using its extinction coefficient of 156 mmol cm-1, which means that the absorbance of 1mmol/L MDA at 532 nm in a light path of 1 cm is 156.

1.8 Hydrogen peroxide detection by 3,3'-diaminobenzidine (DAB) staining

Detection of hydrogen peroxide was performed using DAB (Sigma), as described by Thordal-Christensen et al. 1997. This compound forms an insoluble polymer in the presence of H202 and peroxidase activity, so that H2O2 can be localised in tissues by DAB staining. To prepare DAB solution, DAB-HCl (Sigma D-5637) was prepared at 5 mg/mL in water – and the pH was adjusted to 3.8 with 1 M KOH. This DAB solution was used to infiltrate excised fruit pericarp via the transpiration stream by immersing cut petioles three times (1 min each) in a vacuum machine. Successively samples were kept at RT in the dark overnight. To remove anthocyanins and carotenoids from the fruits, the fruits were soaked in absolute ethanol dark for approximately 2 days. Hydrogen peroxide detection was performed using a stereoscope Digital camera Coolpix S 220 provided of a filter KL 1500 LCD.

1.9 Metabolite analysis

Freeze-dried samples of MicroTom, Del/Ros1 N, AtMYB12 and Indigo from ripe fruits were weighed (in triplicate) in order to have 25 g of sample and extracted in 2 ml of 70% Ethanol and 50 mg/L of Phenyl α-D-glucopyranoside as an Internal Standard, Sigma P6626, vortexed thoroughly and heated at 70oC to 80oC for 15 minutes in a sonicator bath. After this, the samples were centrifuged at speed setting No 4 in the Sorvall RTB6000B bench top centrifuge for 10 min. The supernatant was poured into a fresh screw-capped tube and evaporeted under vacuum using the Buchler vortex-Evaporator at 40 C for 1 hour. For derivatizing to the polar phase, 100 µL of Methoxyamine hydrochloride (Pierce Chemical) was added and heated for 90 min at 30oC with continous stirring. After this step 10 µL of N-Methyl-N-trimethylsiltrifluoroacetamide (Pierce Chemical) was added and heated at 37 oC for 30 min. Before analysis the samples were left at room temperature for 2 hours and afterwards were transferred to Gas Chromatography (GC) vials for analysis by GC-MS. A ZB5-ht column was used with the standard profiling method for the GC-MS. This is a non-polar capillary column and the separation should work on standard range of HP5, DB5, ZB5 and the high temperature versions of the ZB5.

2. Results

2.1 Storage test

MicroTom background

Figure 2.1 shows the results by three curves A. for drying process, B. for softening, and C. for lost of weight. The ripening test showed that AtMYB12 fruits had extended shelf life compared to WT fruits. Indeed in WT drying process of fruit was very sudden compared with the other genotypes analyzed, and the time to have 50% of the fruit shriveled or softened was shifted by 14 days after the start of shelf life test (14 d). Del/Ros 1 N fruit showed the greatest extension of shelf life and comprehensively drying process was quite gradual during the storage and it started later (21d) than other genotypes. Also for softening process (fig. 2.1 B) and fresh weight loss (fig. 2.1 C) genotypes showed the same behavior like for drying one. The figure 2.3 shows the longer shelf life in Del/Ros 1 N and Indigo tomatoes, 84 days after the beginning of storage test fruits appeared still edible.

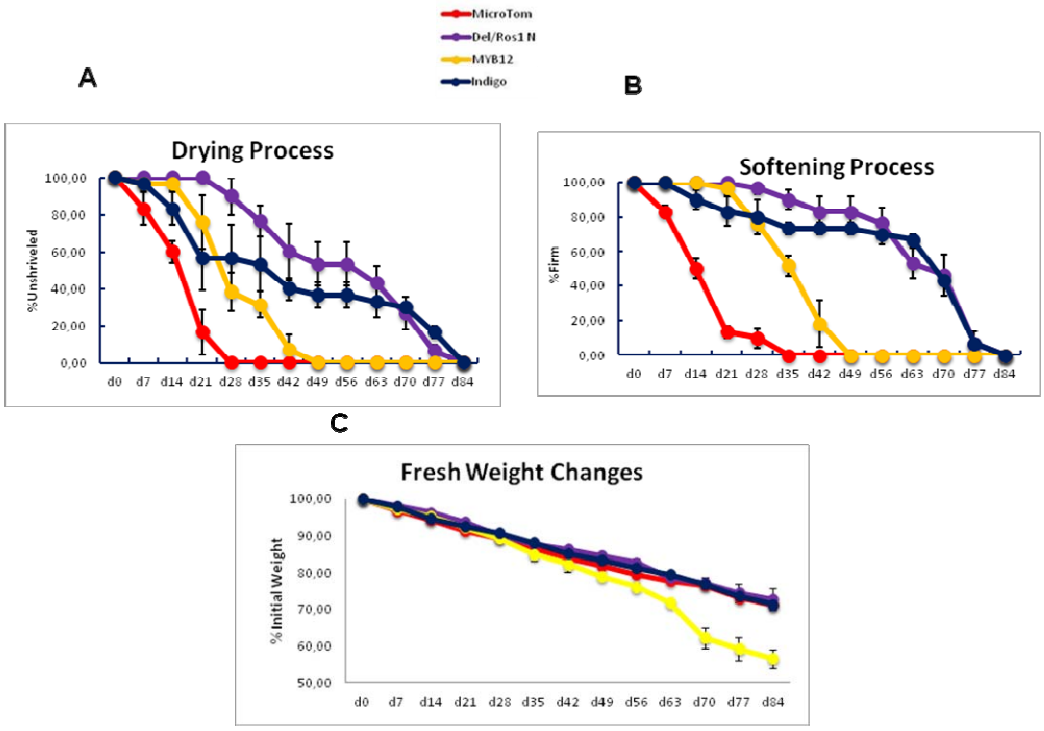

Figure 2.2 - **A.** Drying process, **B.** Softening and **C.** Fresh weight loss of MicroTom, Del/Ros1, AtMyb12 and Indigo tomatoes in storage test. The Percentages of unshrivelled, softened and fresh weight fruits were calculated within every ten fruits in the same jar. Average values were calculated for four individual jars and error bars indicate the standard errors of mean.

Figure 2.3 - Pictures of Storage test for MicroTom and the three transgenic genotypes in MicroTom background analyzed at three different time point (28, 56 and 84 days after beginning of the test.

MoneyMaker background

The same parameters, to determine shelf life, were used also in MoneyMaker background, AtMYB12 fruit showed longer shelf life compared with WT, but not longer than Del/Ros (fig. 2.4 The graph of drying (fig. 2.4 A) showed for WT fruit a sudden shrivelling from the beginning of storage test, while for AtMYB12 fruit shrivelling started after 10d. In Del/Ros fruits the first shrivelling signs appeared after 21d and differently with the other genotypes the drying process was very gradual also in MoneyMaker background. Fig. 2.5 shows the longer shelf life of Del/Ros fruits, which appeared still edible 56 days after the beginning of the test.

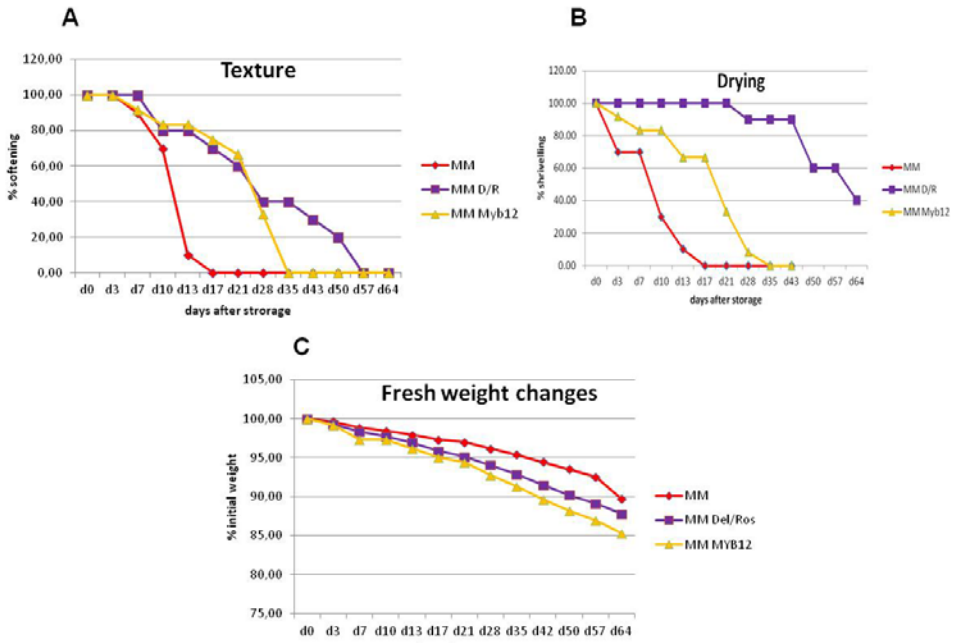

Figure 2.4 - A. Drying process, **B.** Softening and **C.** Fresh weight loss of MoneyMaker, Del/Ros1 and AtMyb in MoneyMaker background in storage test. The Percentages of unshrivelled, softened and fresh weight fruits were calculated within every ten fruits in the same jar. Average values were calculated for four individual jars and error bars indicate the standard errors of mean.

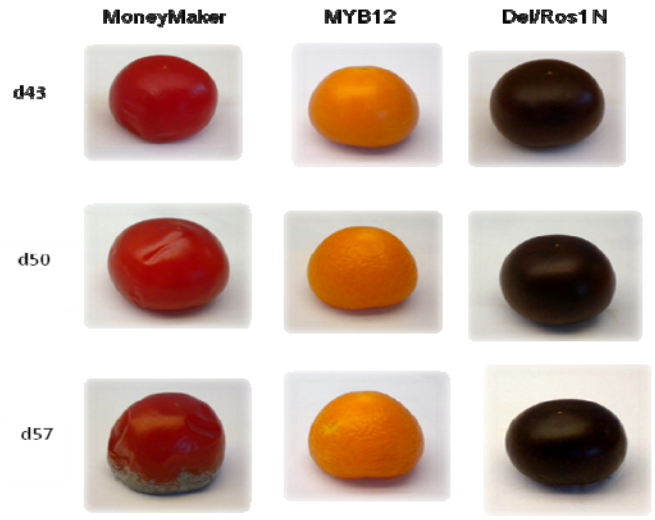

Figure 2.5 - Pictures of Storage test for MoneyMaker and the two transgenic genotypes in MoneyMaker background analyzed at three different time point (43, 50 and 57 days after beginning of the test.

2.2 Expression of ripening-related genes involved in cell wall modification

To better characterize the ripening of purple tomato, WT and Del/Ros1 N fruits were sampled, at different ripening stages to check the expression of ripening related genes encoding enzymes and their activities. Obvious suppression of transcript levels of genes encoding enzymes involved in cell wall degradation were found during the ripening of purple tomatoes. qRT-PCR data are shown in Fig. 10, in which reduced expression of polygalacturonase (SlPG2a) (fig. 2.6 A) and β-galactosidase (SlTBG4) (fig. 2.6 B) cell wall-degrading genes in Del/Ros 1 N fruit compared with all the other genotypes is clear. The expression of Phytoene Synthase (SlPSY) (fig. 2.6 C), that is up-regulated during fruit ripening (Corona et al., 1996), had a peak of expression shifted later to B+7 for Del/Ros1 N fruit compared to the other genotypes. SlPG2a gene expression had a peak for all the genotypes, except for Indigo, at B+3. The expression of this gene followed the order from the highest to the lowest: WT, AtMYB12, Del/Ros 1 N and Indigo showing that high flavonoids reduced expression of this gene. After B+3 stage, the expression of SlPG2a was very low for all the genotypes.

As fig. 2.6 B shows, SlTBG4 gene expression had a peak at B+3 for WT and Indigo genotypes while for Del/Ros1 N fruit it was very low during all the ripening stages. For AtMYB12 fruit after B+7 there was a gradual increase of SlTBG4 expression with the highest expression at B+28.

For SlPSY gene expression (fig. 2.6 C) WT and Indigo fruits had a peak of expression at B+3, while for AtMYB12 and Del/Ros1N fruit maximal expression was shifted to the B+7 stage.

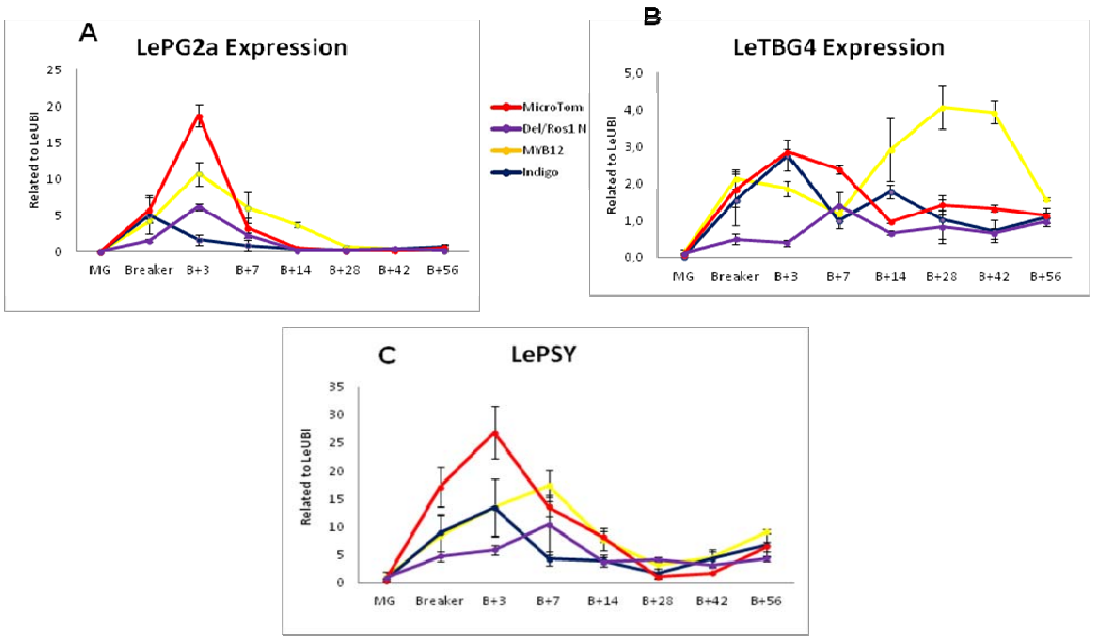

Figure 2.6- Levels of tran script of ripening related genes. **A.** Polygalacturonase 2a, **B.** β Galactosidase and **C.** Pytohene synthase) during ripening in MicroTom and the other three transgenic genotypes in MicroTom background.

2.3 Analysis of cell wall degrading enzyme activities in MicroTom background

Measurement of the total activities of polygalacturonase and β-galactosidase in tomato extracts at different ripening stages confirmed that their activities were reduced significantly in purple fruit compared with wild type MicroTom fruits. In particular for Del/Ros 1 N fruit polygalacturonase activity is very low for all the stages monitored (till B+14) (fig. 2.7 A), while β-galactosidase activity increased during the ripening, showing a peak at B+14 (fig. 2.7 B). Unfortunately enzymatic data for Indigo and AtMYB12 lines are not usable for lack of reliability, probably for interference problems due to flavonols in the colorimetric assay.

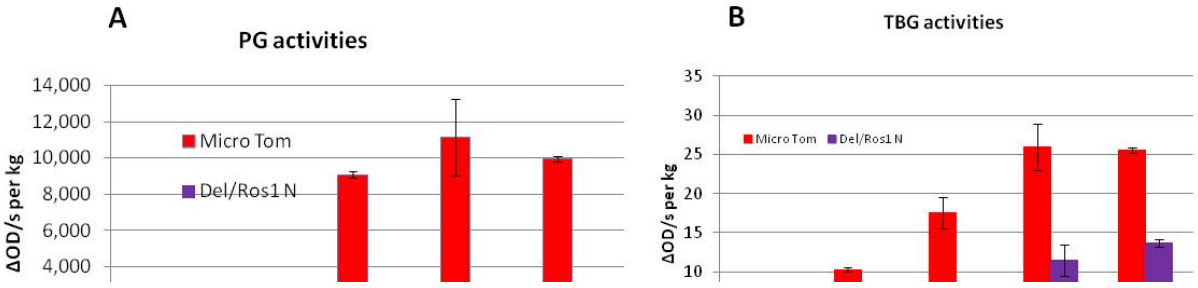

Figure 2.7 - A. (Polygalacturonase) **PG** activities during ripening stages. B, **TBG** (β Galactosidase) activities during ripening stages of the enzymatic assay for MicroTom and Del/Ros1 N tomatoes.

2.4 TEAC assay

MicroTom background

The antioxidant capacity of both water and acetone tomato extract was tested for all genotypes from MG to B+10 W stages (Fig. 2.8). Acetone extracts showed no differences in antioxidant capacity among the genotypes. In contrast, water extracts showed very high levels of antioxidants in all the transgenic lines, that increased for all of them during fruit ripening (following flavonoid accumulation in the fruit) increasing from B+2W stage, at which it reached a maximum value (around 10), in fruit. In contrast, for WT genotypes it remained low (around 2) during all ripening stages. At the B+6W stage AtMYB12 showed a sudden decrease in hydrophilic antioxidant capacity of almost 2 points and reached its lowest value at B+8W. On the contrary for purple and indigo tomatoes, hydrophilic antioxidant capacity retained relatively high, constant values during the later stages of ripening.

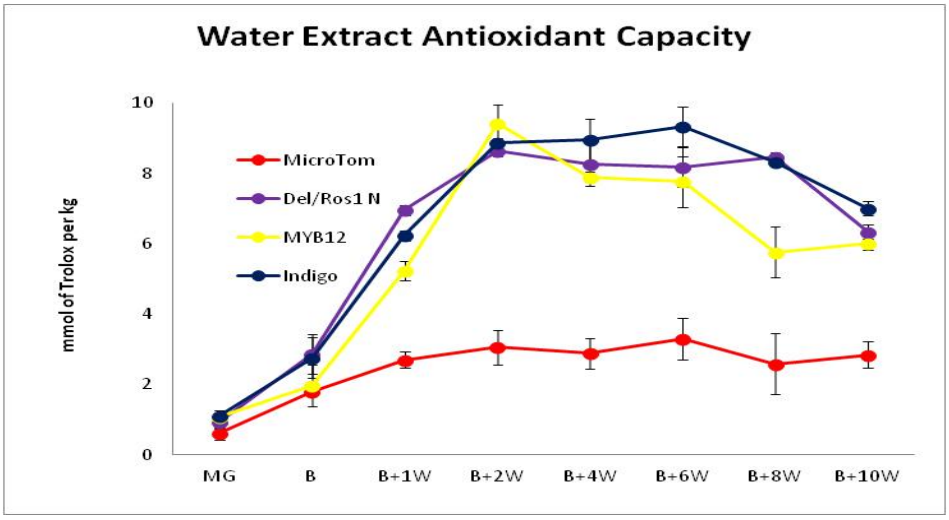

Figure 2.8 - TEAC assay of water extract calculated during ripening for MicroTom and the other three transgenic genotypes. MG= mature green, B= breaker, W= week.

Money Maker background

The antioxidant capacity was tested for both water and acetone extracts, in the MM background, but at a single, ripening stage at B+10 d. As in the MicroTom background, the antioxidant capacity of the acetone extracts was the same for all genotypes. Compared with WT tomato, purple and orange tomatoes showed higher values for hydrophilic antioxidant capacity, but as the histograms showed in Fig. 2.9 the AtMYB12 tomato in MM background had a lower value (around 3.5) compared with the Del/Ros tomato in the MM background that has value around 5.

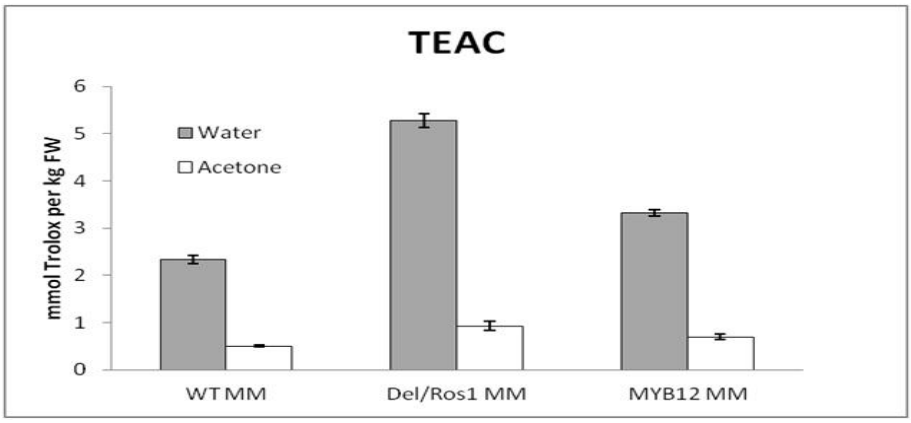

Figure 2.9 - TEAC assay of water extract calculated during ripening for MoneyMaker and the other two transgenic genotypes at B+10 days stage.

2.5 MDA assay

Malondialdehyde (MDA) is a by-product of lipid peroxidation and can be used to measure damage resulting from oxidative stress during tissue senescence (Dhindsa, R. S. et al., 1981). MDA levels in WT fruits increased during ripening, 1 week after Breaker (B+1W). In contrast, in all transgenic lines also over B+4W ripening stage, MDA levels remained low, with values around 15, compared with WT with values around 25 for same stage (fig. 2.10). From B+6W MDA values started to increase, in particular for orange tomatoes, and at B+8W MDA values for transgenic lines were still lower (around 25) compared to wild type (around 35).

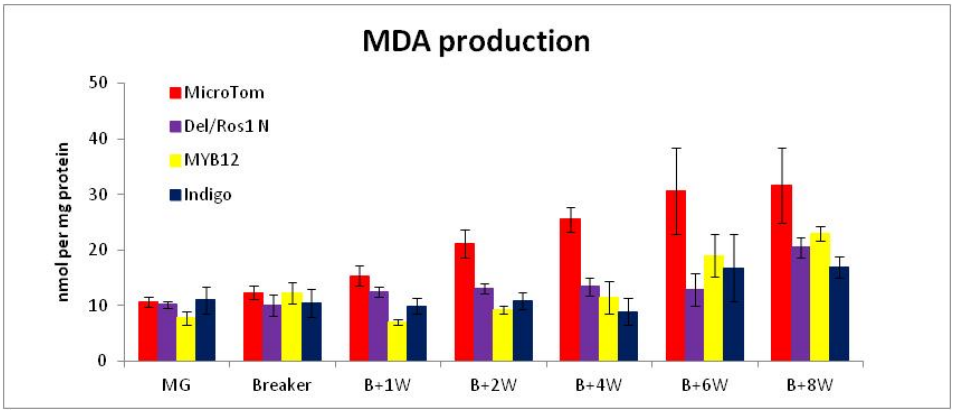

Figure 2.10 - MDA assay during ripening for MicroTom and the other three transgenic genotypes. MG= mature green, B= breaker, W= week.

2.6 *Botrytis cinerea* test

2.6.1 *Botrytis cinerea* inoculation

Botrytis cinerea infection by wounding was performed following the ripening stage week by week from MG to B+8W, monitoring the lesion sizes 3 days post inoculation (dpi). The diameter of the lesions did not increase significantly one day post inoculation in any of the fruits analyzed, suggesting that the fungus needs about 24 hours to germinate following inoculation. From two days post-inoculation, however, WT and AtMYB12 fruits showed greater spread of the damaged areas than in

Del/Ros1 N fruit in which the lesion sizes remained small. After three days, the size of the lesions in purple tomatoes were significantly smaller (up to 3 times) than those on red and orange fruits, indicating that *Del/Ros1* N fruit exhibit marked resistance to the development of lesions following necrotrophic infection (fig. 2.11B). A correlation between fruit ripening and increased susceptibility was observed in MicroTom and AtMYB12 inoculated with *Botrytis cinerea,* as was also observed by Cantu and coworkers showing that susceptibility of tomato fruit to nectrophic pathogens increases during ripening (Cantu, D. et al., 2008). However, in purple fruit, susceptibility to *B. cinerea* did not increase after breaker stage, when the production of anthocyanins was induced (Fig. 15A).
Total tomato and *Botrytis* DNA, from this experiment, was extracted for quantitative PCR to measure the amount of fungus present. This test involved amplification of a cutinase gene from the fungus using specific primers, that revealed that there was significantly more *Botrytis* growing on WT and AtMYB12 tomato fruits compared to *Del/Ros1* N fruit, three days post inoculation (fig. 2.11C).
For *Botrytis cinerea* infection by spray inoculation, fruits were divided into three different categories: the **resistant** group which had no infection on the fruits, the **partial resistant** group which had lesions on the surface but the lesions didn't spread later and the **susceptible** group which had spreading lesions (fig. 2.12). After five days, there were more resistant *Del/Ros1* N fruits than MicroTom and AtMYB12 fruits and the percentage of partial resistant and susceptible fruits was lower in *Del/Ros1* N fruits (fig. 2.12). The purple tomato had lower opportunistic infection and the expansion of lesions was suppressed.
Enhanced resistance to *Botrytis cinerea* infection by wound tests is associated with Del/Ros transgene and was also observed in purple fruit introgressed into the MoneyMaker genetic background compared with WT and AtMYB12. Interestingly AtMYB12 fruit showed lower resistance to *Botrytis* compared with WT MoneyMaker inoculated by wounding, and quantitative PCR results confirmed this observation, showing greater amount of the fungal DNA in AtMyb12-infected fruit compared to WT-infected fruit. Inoculations by spraying were not performed, because of difficulties with their implementation.

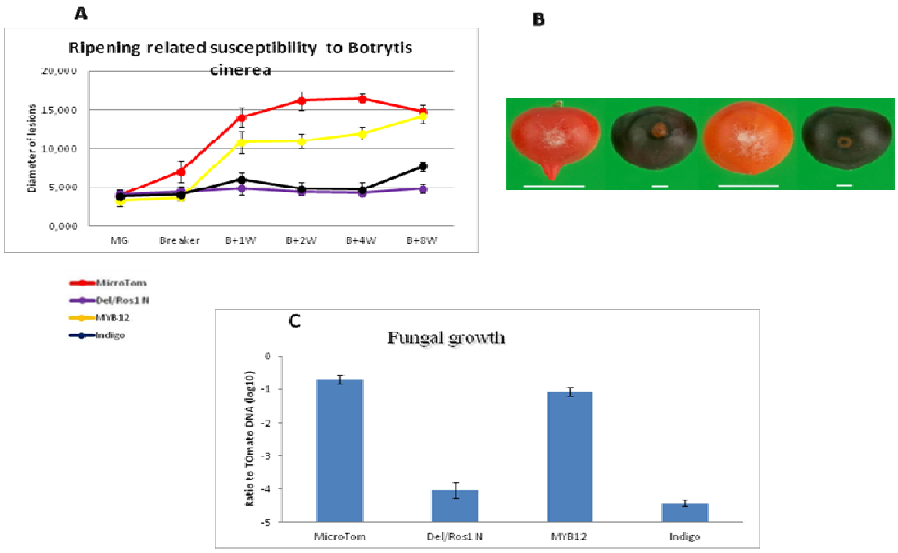

Figure 2.11 – *Botrytis cinerea* susceptibility (by puncture). **A.** Trend susceptibility during ripening for MicroTom and the other three transgenic genotypes. **B.** Pictures of the different susceptibility of genotypes to fungus infection. **C.** qPCR of fungus cutinase at 3dpi related to tomato actin.

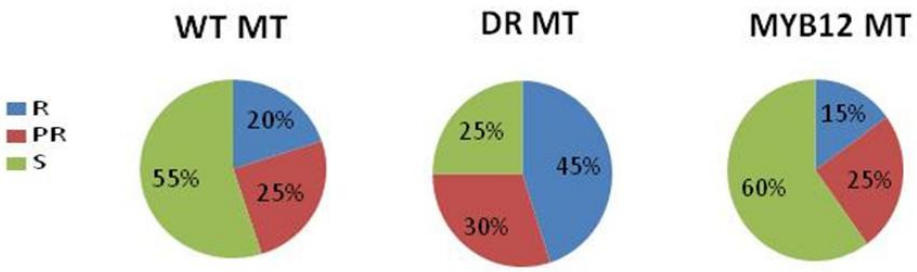

Figure 2.12 – *Botrytis cinerea* susceptibility (by spray). Fruits are separated in three groups according to the seriousness of the symptoms in resistant (R), partial resistant (PR) and susceptible (S).

2.6.2 TEAC assay after infection

Antioxidant activity was monitored for all the genotypes in the MicroTom background after 3dpi of infection by wounding . To perform the test, one half of the fruit was infected and half was used as a control involving just wounding the fruit, using a sterilized 200 µL tip.

For both WT and ATMYB12 the antioxidant activity decrease of the infected portions compared with untreated part, while for Del/Ros 1 N fruits no differences in antioxidant activity was observed between infected and wounded portions (fig. 2.13).

For WT and Del/Ros1N genotypes the total antioxidant capacity after Botrytis cinerea infection by spray was monitored from 1 to 5 dpi (fig. 2.14). In Del/Ros 1N there was an increased antioxidant activity of the water soluble fraction during the the infection while for WT there was a gradual drop between 1 and 4 dpi, after which at 5 dpi there was a very small increase of approximately 0.2 points.

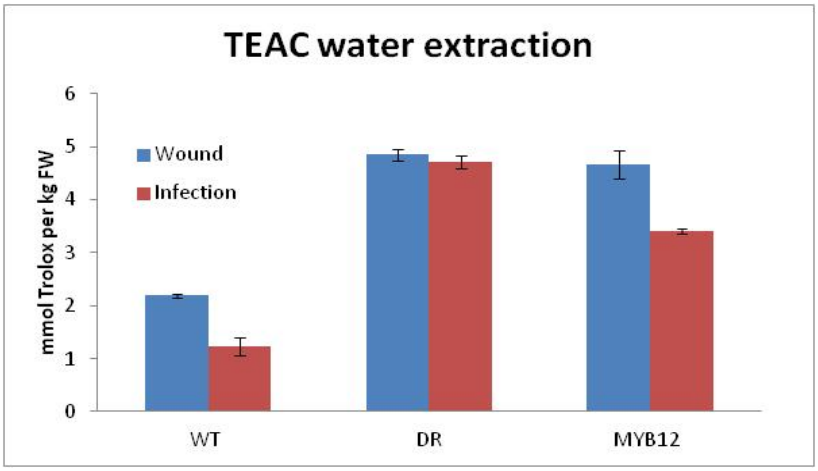

Figure 2.13. TEAC assay after 3dpi of Botrytis infection by puncture (infection in red) compared with same fruit just wounded in blue.

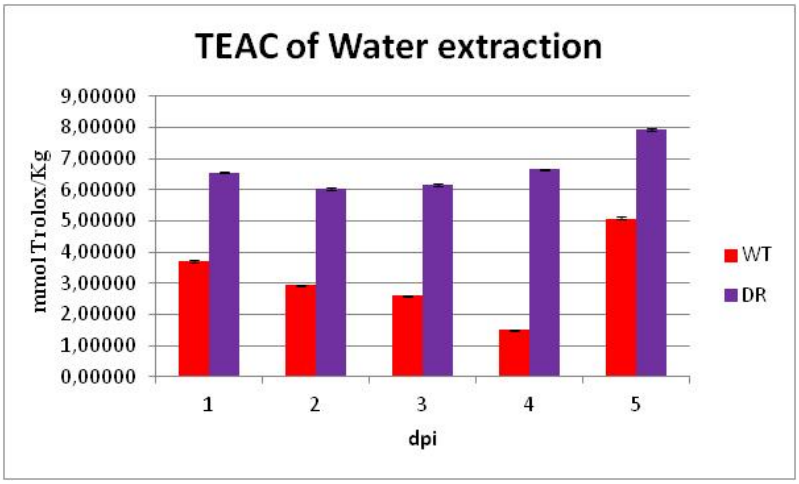

Figure 2.14. TEAC assay during *Botrytis cinerea* infection by spray of MicroTom (WT) and Del/Ros1N (DR)

2.6.3 *Botrytis cinerea* growth on different fruit juices

Botrytis cinerea was grown on agar plates supplemented with fruit juices from WT, Del/Ros and AtMYB12 fruit in MM background. None of the juice extracts directly inhibited the growth of the fungus 3 days after inoculation (fig. 2.15). However, when we supplemented Botrytis spores on commercial red tomatoes (Caurosel and Brioso variety), every 24 hours with 10 µL juice (or water for control) extracted from WT, Del/Ros1 N and Del/Ros1 C in MT background, it was clear that with purple tomato juice infection symptoms were reduced significantly compared to supplementation of spores with WT juice or water in both commercial variety (fig. 2.16 A and B). A similar experiment was performed inoculating the fungus onto Arabidopsis thaliana variety Columbia (Col) leaves and onto a transgenic line that accumulates anthocyanin (Pap1) (D. Rowan et al., 2008) in its leaves. Inoculations were supplemented with juices coming from all the genotypes in the MM background. The results showed that WT and AtMYB12 tomato juices had no effect on Botrytis growth, while Del/Ros1 N juice inhibits it (fig. 2.17).

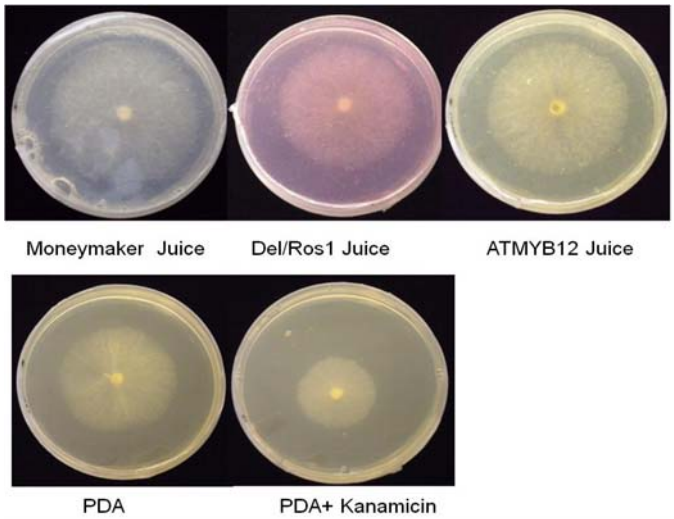

Figure 2.15 - Addition of juice from MoneyMaker, Del/Ros and AtMYB 12 tomatoes to the growth medium had no effect on growth of *B.cinerea*. As positive control PDA medium and negative control PDA with kanamicin 10 mg/L were used. Pictures were taken three days after inoculation.

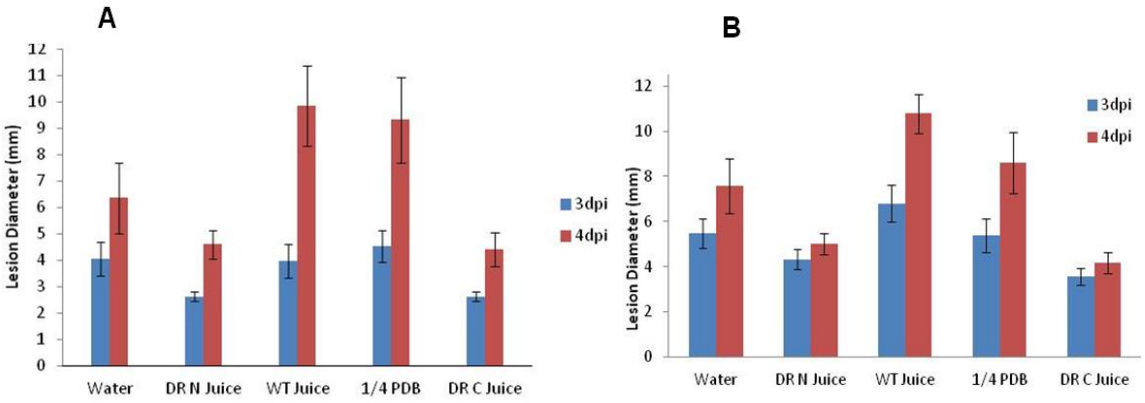

Figure 2.16 - Botryitis infection on **A)** Carousel and **B)** Brioso tomato variety from Sainsbury's market. Treatment: *Botrytis c.* B05.10, 5uL 10^4/mL. Supplement with 10 µL juice (or water) every 24hours. Lesions were evaluated at 3 and 4 dpi (days after inoculation).

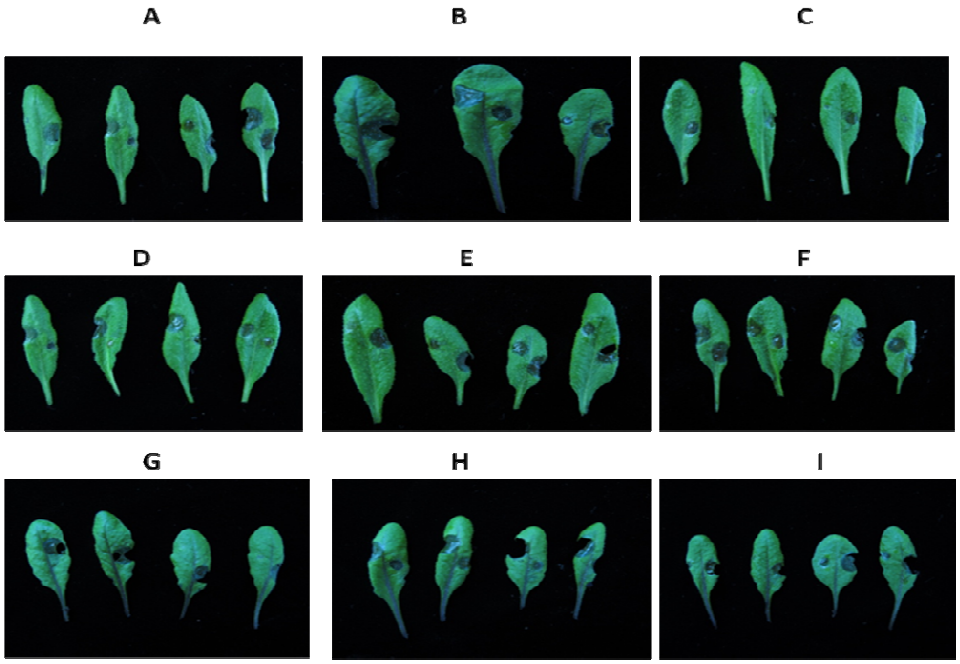

Figure 2.17 - *Arabidopsis thaliana* leaves inoculated with *Botrytis cinerea* with different juices /PDB. **A)** 2dpi PDB/WT, WT/DRN, DRN/MYB12, WT/MYb12. **B)** PAP1 2dpi PDB/WT, WT/DRN, PDB/DRN.**C)** Col 2dpi PDB/WT. **D)** Col 2dpi WT/DR. **E)** Col 2dpi DRN/MYB12. **F)** Col 2dpi WT/MYB12. **G)** PAP1 2dpi PDB/WT. **H)** PAP1 2dpi WT/DR N. **I)** PAP1 2dpi PDB/DR N

2.7 3,3'-Diaminobenzidine (DAB) staining

The staining of infected fruits with 3,3'-Diaminobenzidine which detects hydrogen peroxide showed that, between 24-48 hpi, lesions on WT (fig. 2.18 A) and AtMYB12 (fig. 2.18 C) fruits resulting from fungus infection, stained with DAB, suggesting that H_2O_2 spread quickly while on *Del/Ros1* (fig. 2.18 B) fruits the DAB-stained lesion size remained smaller, suggesting that in purple tomato ROS induction was restricted to the inoculation site and there was no spread of ROS through the healthy tissue.

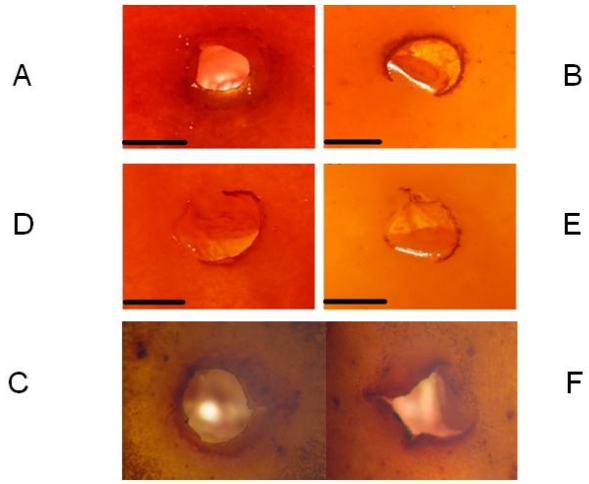

Figure 2.18 - 3,3'-Diaminobenzidine staining of hydrogen peroxide produced between 24 after *Botrytis c.* inoculation site from A to C, WT (A) , Del/Ros1 N (B) and AtMYB12 (C) infected fruits. Wound only from D to F, WT (D), Del/Ros1 N (E) and AtMYB12 (F) not infected fruits.

2.8 Metabolite extraction

Metabolites were measured in the different tomato fruit. According to the study of the statistical significance of these data, calculating P value by T test for the analysis of the differences between transgenic lines and WT. It was interesting to notice was that AtMYB12 fruit has a metabolite profile distinct from those of the other genotypes. In particular the amount of sugars such as glucose and mannose showed very interesting differences between genotypes. For glucose the values were 1.39%, 2.56%, 0.47% and 0.76%, for the mannose the values were 2.04%, 3.68% 1.1%, 1.12% (these values are an average of 3 replicates) respectively for WT, AtMYB12, Del/Ros1 N and Indigo (table 2.1). Furthermore a test of statistical significance was performed between AtMYB12 and all the other genotypes to assess the metabolites that showed very big differences in their amount in the different lines, such as Glycine, 1,4-Butanediamine, D Glucose, D Ribose, Myo-inositol and Sucrose.

Table 2.1 - HPLC results for metabolite content in MicroTom (WT), AtMyb12 (MYB), Del/Ros1N (DR) and Indigo (IND) genotypes. Significance was evaluated according to T Test

Compound	Content				Significance P<0.5			Ratio versus Wild type		
	WT	MYB	DR	IND	MYB	DR	IND	MYB	DR	IND
Alanine	0,61	1,76	0,00	0,26	**	**	**	2,91	0,00	0,44
Serine	0,67	3,47	2,04	2,20	***	*	***	5,19	3,05	3,30
Phosphate	2,59	14,50	8,17	9,31	***	*	***	5,61	3,16	3,60
Glycine	0,00	0,44	0,00	0,00	***					
Malic acid	2,49	3,04	3,61	3,77	*	**	***	1,22	1,45	1,51
Aspartic acid -B	2,13	4,82	3,89	3,74	**		***	2,26	1,83	1,76
Propanoic acid	3,95	1,84	2,03	2,94	***	*	**	0,47	0,51	0,74
Glutamine	12,23	17,88	10,95	18,09	***		***	1,46	0,90	1,48
Phenylalanine	0,52	0,76	0,47	0,78	***		***	1,45	0,90	1,49
Asparagine	1,10	2,68	1,49	1,79	**		***	2,45	1,36	1,63
1,4-Butanediamine	0,83	1,37	0,55	0,40	**		***	1,65	0,66	0,48
Glutamine	0,60	2,71	1,86	3,26	**		**	4,48	3,07	5,39
Idonic acid	0,43	2,42	1,62	2,71	**		**	5,58	3,73	6,25
D-Fructose	0,81	0,00	0,00	0,58	**	**	*	0,00	0,00	0,71
1,2,3-Propanetricarboxylic acid	13,62	7,91	11,24	15,08	***		**	0,58	0,83	1,11
d-Ribose	13,06	3,41	14,01	8,12	***		***	0,26	1,07	0,62
.beta.-D-Glucopyranose	2,51	0,00	2,15	1,59	**		*	0,00	0,86	0,63
D-Glucose, 2,3,4,5,6-pentakis-O-(trimet	9,92	0,86	9,06	5,36	***		***	0,09	0,91	0,54
Ascorbic acid	0,87	3,50	1,86	0,68			**	4,04	2,15	0,78
.beta.-D-Glucopyranose	3,52	0,00	3,09	2,57	**		*	0,00	0,88	0,73
Ribonic acid	2,24	0,00	1,96	1,65	**		*	0,00	0,88	0,74
.beta.-D-Glucopyranose	0,29	0,00	0,29	0,00	***		***	0,00	1,03	0,00
.alpha.-D-Galactofuranose	0,40	0,00	0,00	0,37	***	***		0,00	0,00	0,93
Myo-Inositol	0,58	0,00	0,68	0,62	***	*	**	0,00	1,17	1,07
Glucose	1,39	2,56	0,47	0,76	**		**	1,84	0,34	0,55
Mannose	2,04	3,68	1,16	1,12	**	**	***	1,80	0,57	0,55
.alpha.-D-Xylopyranose	0,62	1,09	0,63	0,48	**		**	1,76	1,01	0,77
Neoergosterone semicarbazone	0,00	0,88	0,00	0,00	**					
2-O-Glycerol-.alpha.-d-galactopyranoside	0,00	3,75	0,89	0,39	**		*			
Sucrose	2,33	0,98	1,42	1,36	***	**	***	0,42	0,61	0,58

3. Discussion

The combination of traits determining commercial quality including shelf life (and susceptibility to Botrytis cinerea) with those for nutritional quality involving the presence of bioactive compounds for health promotion and disease prevention, contributes to increasing the value of the tomato crop. Nowadays the control of fruit ripening is of strategic importance because excessive softening limits shelf life. The postharvest losses of fruits and vegetables in developing countries account for almost 50% of production. Modern techniques involve the harvesting of green tomatoes, gassing them with ethylene to initiate and synchronise ripening, and storage at low temperature to decrease ripening during all the steps until their marketing (E. Baldwin et al., 2010). The effects of these techniques have been to reduce flavour quality. Many attempts have been made in transgenic tomato to extend tomato shelf life by different means (Centeno et al., 2011; Mehta et al., 2002; Meli et al., 2010; Nambeesan et al., 2010), but they have had very limited success. In shelf life, an important role is played by the necrotrophic pathogen, Botrytis cinerea, that causes serious damage, in particular in post-harvest conditions, in apparently healthy crops. This fungus causes serious losses in more than 200 crop species

worldwide, because it is difficult to control because of its huge variety of modes of attack, its diverse hosts as inoculum sources, and its abilities to survive as mycelia and/or conidia for extended periods, and as sclerotia in crop debris. For these reasons the use of any single control measure is unlikely to succeed.

Food quality is becoming a very important aspect for the consumers, and the consumption of "functional food", containing significant amounts of bioactive components, may provide health benefits beyond basic nutrition and play important roles in the prevention of chronic diseases (Rui Hai Liu, 2003). The regular consumption of fruit and vegetables is promoted because a lot of scientific study has shown that their consumption is associated with reduced risks of cancer, cardiovascular disease, stroke, Alzheimer disease, cataracts, and some of the functional declines associated with aging (C. Martin et al., 2011), and prevention is a more effective strategy than the treatment of chronic diseases. In 2007, the Oxford Health Alliance published a Grand Challenge document (Daar et al., 2007) offering a general summary of the reorientation of policies and priorities needed to prevent premature deaths from chronic disease. Research on plants has a very important role to play in leading the identification of those metabolites that promote health and reduce the risk of chronic disease, and tomato is a very important tool for researchers. Indeed it is considered a model plant species for a group of economically important crops, such as potato, pepper, eggplant, since it exhibits a reduced genomic size (950 Mb), a short generation time, and has routine transformation technologies (Barone A. et al., 2009). These features make tomato an ideal species for theoretical studies and practical applications in the genomics field, suitable to increase fruit quality, to understand both metabolic pathways involved in improving health-beneficial compounds and fleshy fruit development and ripening.

In the Department of Metabolic Biology of John Innes Centre (JIC), where I worked for this project, it was observed, while growing the transgenic genotype Del/Ros1 N (rich in anthocyanins) in the MicroTom background, that fruit had an improved shelf life compared to MT wild type fruit. Two factors, fruit softening during over-ripening and pathogen infection, principally determine shelf life. This was visually tested both on the vine and during postharvest storage, in addition to a reduced level of opportunistic fungal infection of fruit. The PhD student Yang Zhang of the JIC and I confirmed scientifically this evidence by appropriate experiments in purple tomatoes, and including also orange (high flavonol) and indigo (high anthocyanin and high flavonol) tomatoes.

The aim of the work described in this chapter was to understand if the extended shelf life and resistance to Botrytis cinerea of the purple tomatoes may result from a specific activity of anthocyanins, or from the undefined activities of the Delila and Rosea1 transcription factors. So to find out whether high flavonol orange fruit have extended shelf life and enhanced pathogen resistance, similar to purple tomatoes, I tested, in addition to purple tomatoes and wild type, the high flavonol, orange fruit, engineered by expression of AtMYB12 specifically in fruit (Luo et al., 2008) and the fruit of the Indigo line, with both high anthocyanins and high flavonols, derived from a cross between the Del/Ros1 line and the AtMYB12 line. The study carried out in this chapter showed that AtMYB12 fruit have extended shelf-life compared with WT, but their shelf life is less than purple and indigo fruits. For AtMYB12 fruit there was no resistance to Botrytis cinerea, and in the Money Maker background, the resistance of AtMYB12 fruit was worse than WT.

Indeed from the storage test we observed that for both drying and softening processes, the parameters commonly used to determine shelf life (Najib E., et al. 2009), for AtMYB12 fruits showed slower over-ripening compared with WT, but this was not as slow as for purple and indigo tomatoes. The same was confirmed in the MM background attesting that the shelf life can be extended by high flavonoid accumulation, regardless of genetic background. To assess this, we measured the suppression of genes expressed at late ripening stages by qRT-PCR analysis in fruits from all the genotypes, in the MicroTom background, harvested at different time points of ripening. Two important genes involved in cell wall degradation and associated with fruit softening, polygalacturonase (SlPG2a) and β-galactosidase (SlTBG4), showed substantial suppression in purple fruit during ripening. The AtMYB12 genotype showed a gradual increase of SlTBG4 expression after B+7 , confirming a delay in ripening compared with WT, but not as big a delay as in purple fruit. This evidence is corroborated by Smith and collegues's work in which they suppressed the transcript TBG4 during tomato fruit ripening, by expression of an antisense tomato cDNA and noticed that these lines were firmer than control fruit and they had the lowest exo-galactanase levels and the highest wall galactosyl content during the early stages of ripening, implicating an involvement of this gene product in cell wall modification which leads to fruit softening. The comparison between the peak for SlPG2a expression in AtMYB12 and Del/Ros1N genotypes is for all at the B+3 stage suggesting that the expression of this gene is not as important as the previous one in determining the difference in shelf life between these two transgenic lines.

Measurement of the total activities of polygalacturonase and β-galactosidase enzymes in tomato extracts at different ripening stages confirmed their significantly reduced activities in purple fruit compared to WT, but it was difficult to perform these in AtMYB12 and indigo fruits probably because of the presence of high levels of flavonols in these two lines interfered with the enzyme assays.

We suggest that the significant elevation in levels of the antioxidants in fruits achieved by inducing anthocyanin biosynthesis in purple and indigo tomatoes and also of flavonols in orange tomatoes, may reduce the tissue-damaging activity of reactive oxygen species (ROS) that occurs during fruit ripening and is ultimately responsible for the marked decrease in softening observed in these fruits compared to wild type fruit. Indeed our data for TEAC assays show that hydrophilic antioxidant capacity is very high for all the transgenic genotypes up to the stage B+24 d, at which point, AtMYB12 fruit showed a sudden decrease, probably correlated with a high degradation of flavonols that are accumulated in orange tomatoes compared with the more stable anthocyanins accumulated in the vacuoles of purple and indigo tomatoes

We also measured Malondialdehyde (MDA), a by-product of lipid peroxidation, and which can be used as a marker of damage resulting from oxidative stress during tissue senescence (Jimenez et al., 2002). MDA levels in WT MicroTom fruits increased during ripening. In purple and indigo tomatoes, however, up to four weeks after breaker, MDA levels were stable but not for orange tomato for which there is a sudden increase in this compound after B+24d suggesting that the antioxidant activity of the high-flavonol fruits is not maintained as well as in purple and indigo fruits to delay ripening.

So these two lines of evidence suggest that a reduction in the antioxidant activity during the ripening could explain the sudden loss of fruit firmness/ shelf life shown by AtMYB12 fruit. These data are in agreement with Mondal and co-workers's data where they found that the increase of oxidative/peroxidative stress can be the cause

of the metabolic changes associated with maturation and ripening of tomato fruits. In their work it was evident that tomato fruits respond to the progressive increase in oxidative stress during earlier stages of maturation by increasing both the activities of scavenging enzymes as well as the concentration of ROS scavenging compounds. Furthermore in this paper they highlighted that a cultivar with short shelf life had higher levels of oxidative stress (ROS) than a cultivar with longer shelf life. Increases in production of lipid hydroperoxides and other reactive oxygen species during development eventually induced higher activities of peroxidase, glutathione reductase, superoxide dismutase, catalase and ascorbate peroxidase, but not until the later stages of ripening. Accordingly, cultivars with short shelf life showed reduced scavenging ability and associated increases in oxidative stress. In addition, increases in polyamines have also been reported to extend shelf life of tomatoes, and may achieve their effects through their activities as antioxidants (Mehta et al., 2002). It is likely that increased antioxidant activity results in the observed reduction in expression of ripening-related genes, including those involved in cell wall modification and responses to oxidative stress similar to what has been observed for SlTBG4.

Furthermore my work highlighted that AtMYB12 fruit have no resistance against Botrytis cinerea infection, either by puncture or spray, showing the same phenotype as observed in WT, as confirmed by quantitative PCR of the cutinase gene to check fungal growth.

Our data, from 3,3'-Diaminobenzidine staining of hydrogen peroxide in fruits after infection with Botrytis cinerea (between 24-48hpi), showed that lesions on AtMYB12 and WT spread quickly while on Del/Ros1 fruits the size of lesions remained small, highlighting that a ROS burst was generated at the infection site during infection with Botrytis and that the ROS spread can determine the tolerance/susceptibility to necrotrophic pathoges. Observing the pictures it is clear that on Del/Ros1 N fruits ROS induction was restricted to the inoculation site and there was no spread. Necrotrophic pathogens, such as B. cinerea, induce an oxidative burst and cell death in infected plant tissues. Govrin and Levine found thatinfection with B. cinerea triggers a hypersensitive response, which facilitates its colonization of plants, and it exploits the host defence mechanism to support its own pathogenicity, utilizing dead tissue killed by the oxidative burst and facilitating the expansion of disease lesions (Govrin, E. M. & Levine, A., 2000). In purple tomato, the existence of anthocyanins may enhance the tolerance of fruit tissues to the ROS burst generated by Botrytis cinerea infection, preventing spread of the fungus through the induced cell death of the fruits. Significant was also to discover that in the Money Maker background, AtMYB12 fruit showed worse resistance to B. cinerea than WT following inoculation by wounding, although more extensive analysis is necessary in both MT and MM backgrounds to confirm the AtMYB12 fruit phenotype following Botrytis cinerea infection. If it is confirmed that orange tomato has less resistance than WT to B. cinerea infection, this could be associated with the large differences in metabolite levels between AtMYB12 and the other genotypes analysed, in particular the enhanced sugar levels suggesting an involvement of sugars in determination of resistance/susceptibility to Botrytis. Indeed from the metabolic analysis is evident the different amount of sugars among the genotypes, in particular the bigger accumulation in AtMYB12 fruit of the hexoses glucose and and mannose which could support production of ROS in the generation of the oxidative burst (glucose oxidase plus Glucose produce •O2– or H2O2), that can trigger hypersensitive cell death in

plant tissues, and that is implicated in the fungal response mechanism (Eri M. Govrin and Alex Levine, 2000).
Interestingly, when we grew Botrytis cinerea on agar plates supplemented with WT Del/Ros and AtMYB12 fruit juices in Money Maker background, neither extract directly inhibited the growth of the fungus. However, when we supplemented Botrytis spores with purple tomato juice during the infection of WT MicroTom fruit and Arabidopsis thaliana leaves, infection symptoms were reduced significantly compared to supplementation of spores with WT and AtMYB12 tomato juices. These data indicate that anthocyanins do not suppress the growth of Botrytis directly, and may require living cells to exploit the activity of these flavonoids.

4. Conclusions

The general objective of this thesis was the study of genetic mechanisms that regulates tomato fruit quality traits under abiotic (water deficit) and biotic (Botrytis cinerea) stress conditions. It was realized through two different ways approaches.

1. The first one, namely identification of candidate genes controlling tomato fruit quality in response to water deficit, was realized by the use of IL9-2-5 having an introgression segment from the wild type *Solanum pennellii* in the cultivated M82 genetic background that gives fruit with high soluble solids.
   Specifically, the objectives were achieved through:

- **Investigation of fruit quality traits in one Introgression Line compared with control genotype (cultivated variety) under water stress.** Phenotipic yield and quality traits data highlighted a lower yield losses under response to water deficit and a major stability in fruit quality trait in IL 9-2-5, compared to M82. In particular, the AsA content showed in M82 a dramatic decrease under water deficit in the first experiment.
- **Selection of candidate genes involved in the control of Ascorbic acid content under water deficiency.** Trascriptomic data allowed the identification of a key gene involved in AsA biosynthesis, the GDP-mannose pyrophosphorylase, and a gene putatively involved in fruit photoassimilate amount, the photoassimilate-responsive protein.
- **Understanding molecular networks activated in the two genotypes to elucidate the basis of phenotypic differences observed.** The networking by the correlation analysis among selected genes, highlighted many interesting interactions among genes involved in AsA biosynthesis, in carbohydrate metabolism, in stress response

Comprehensively, this part of work allowed to identify IL-9-2-5 as an interesting genotype to study QTL for drought tolerance considering the complexity of its genetic variation (quantitative heredity). The data obtained could open the way to obtain fruits with improved quality traits, in particular, soluble solid and vitamin C content, two traits considered particularly important for tomato processing industry at a low water consumption.

2. Regarding the second objective, the study of shelf life and *Botrytis cinerea* resistance of transgenic tomatoes enriched in flavonoids, results were achieved through different points:

- **The Screening of transgenic tomatoes accumulating flavonoids, for exthended shelf life and enhanced Botrytis cinerea resistance.** These

analysis allowed to define only purple and indigo tomatoes with exhibited 2-fold longer shelf life and increased resistance to *Botrytis cinerea,* the opportunistic pathogen tested. By contrast, orange tomatoes showed longer shelf life compared with the control (MicroTom genotype), but less compared with transgenic genotypes enriched in anthocyanins

- **Determination of antioxidant capacity of soluble extracts from transgenic lines during ripening and during fungus infection.** It was possible to identify a specific relation between antioxidant capacity and longer shelf life that is maintained high in lines accumulating anthocyanis during all the ripening process. In adding, it was evidenced that anthocyanins may also enhance the cell tolerance to the ROS burst during necrotrophic pathogen infection, thus increasing the resistance to *Botrytis cinerea* better than flavonols. On the contrary, the enhanced sugar levels in orange tomatoes may increase ROS production or stimulate fungal growth.

  Comprehensively all transgenic lines investigated were very interesting as healthy foods, and longer shelf life compared to the control red tomato, but not for resistance to *Botrytis cinerea*. Furthermore, the peculiar behaviour of orange fruit could help the understanding of the mechanisms involved in tomato resistance to a necrotrophic pathogen like *Botrytis cinerea* with the ultimate aim of developing new commercial genotypes with better fungal resistance. These data highlighted the importance of transgenic approach to study the activity of specific genes involved in many biological mechanisms.

  Summarily this thesis evidenced the importance of two different biotechnological tools studying tomato fruit quality under water stress and *Botrytis cinera* infection. The first approach validates the use of introgression lines to study quantitative traits (water deficit tolerance and AsA content), traits that are difficult to handle because involve a lots of genes, which are affected by environment. The second approach validated the great potential of genetic engineering tool to study complex metabolic pathways and the effects of specific compounds on important fruit quality traits such as shelf life and *Botrytis cinerea* resistance.

5. References

- Abbott J.A. (2004). Textural quality assessment for fresh fruits and vegetables. Quality of Fresh and Processed Foods 542, 265–279.
- Aboul-Enein H.Y., Al-Duraibi I.A., Stefan R.I., Radoi C., Avramescu A. (1999). Analysis of L- and D-ascorbic acid in fruits and fruit drinks by HPLC". Seminars in Food Analysis 4 (1): 31–37.
- Ackland M.L.,Waarsenburg S. and Jones R. (2005).Synergistic Antiproliferative Action of the Flavonols Quercetin and Kaempferol in Cultured Human Cancer Cell Lines. *In Vivo* 19 no. 1: 69-76.
- Agius F., Gonzalez-Lamothe R., Caballero J., Munoz-Blanco J. Botella M., Valpuesta V (2003). Engineering increate Vitamin C levels in plants overexpression of a D-galacturonic acid reductase .Nature Biotechnology Vol 21 177:181.
- Alba R., Payton P., Fei Z., McQuinn R., Debbie P., Martin G.B., Tanksley S.D., Giovannoni J.J. (2005). Transcriptome and selected metabolite analyses reveal multiple points of ethylene control during tomato fruit development. *Plant Cell.* 17 (11): 2954-65.
- Apel K. and Hirt H. (2004). Reactive Oxygen Species: Metabolism, Oxidative Stress, and Signal Transduction. Annual Review of Plant Biology. Vol. 55: 373-399.
- Arima H., Ashida H., Danno G. (2002). Rutin-enhanced antibacterial activities of flavonoids against Bacillus cereus and Salmonella enteritidis. *Biosci Biotechnol Biochem* 66(5):1009-14.
- Armstrong G. A., Weisshaar B. and Hahlbrock K. (1992). Homodimeric and heterodimeric leucine zipper proteins and nuclear factors from parsley recognize diverse promoter elements with ACGT cores. doi: http://dx.doi.org/10.1105/tpc.4.5.525 *The Plant Cell* 4 no. 5: 525-537
- Barone A., A. Di Matteo, D. Carputo and L. Frusciante. High-Throughput Genomics Enhances Tomato Breeding Efficiency (2009). Current Genomics10, 1-9.
- Bartley, G.E., Coomber, S.A., Bartholomew, D.M., and Scolnik, P.A (1991a). Genes and enzymes for carotenoid biosynthesis. In Cell Culture and Somatic Cell Genetics of Plants, eds New York: Academic Press, 78, 331-364.
- Batu A. (1998). Some Factors Affeting on Determination and Measurement of Tomato Firmness. J. of Agriculture and Forestry 22, 411–418.
- Baxter C.J., Carrari F., Bauke A., Overy S., Hill S.A., Quick P.W., Fernie A.R., Sweetlove L.J. (2005). Fruit carbohydrate metabolism in an introgression line of tomato with increased fruit soluble solids. Plant and Cell Physiology 46, 425–437.
- Bianchi G., Gamba A., Murelli C., Salamini F. & Bartels D. (1991). Novel carbohydrate metabolism in the resurrection plant Craterostigma plantagineum. Plant Journal 1, 355–359.
- Blum A. (2005) Drought resistance, water-use efficiency, and yield potential—are they compatible, dissonant, or mutually exclusive?. Australian Journal of Agricultural Research 56, 1159–1168.
- Borevitza J. O., Xiaa Y., Blountb J. Dixonb R. A. and Lamba C. (2000). Activation Tagging Identifies a Conserved MYB Regulator of Phenylpropanoid Biosynthesis. *The Plant Cell* 12 no. 12: 2383-2393.

- Bovy A., Vosa R., Kempera M., Schijlena E., Pertejoa M. A., Muirb S., Collinsb G., Robinsonb S., Verhoeyenb M., Hughesc S., Santos-Buelgad C. and Tunena A. (2002). High-Flavonol Tomatoes Resulting from the Heterologous Expression of the Maize Transcription Factor Genes LC and C1. *The Plant Cell* 14 no. 10: 2509-2526.
- Bowler, C., Vanmontagu, M., and Inze, D. (1992). Superoxide dismutase and stress tolerance. Annu. Rev. Plant Physiol. Plant Mol. Biol. 43, 83–116.
- Brouillard, R., George, F. and Fougerousse, A. (1997) Polyphenol produced during red wine ageing. *Biofactors* 6: 403–410.
- Bray EA, Bailey-Serres J, Weretilnyk E. Responses to abiotic stresses.In W Gruissem, B Buchannan, R Jones (2000) eds, Biochemistry and Molecular Biology of Plants. American Society of Plant Physiologists, Rockville, MD, , 1158–1249.
- Brummell D.A., Harpster M.H. (2001). Cell wall metabolism in fruit softening and quality and its manipulation in transgenic plants. Plant Molecular Biology 47, 311–340.
- Butelli E., Titta L., Giorgio M., Mock H.P., Matros A., Peterek S., Schijlen E.G., Hall R.D., Bovy A.G., Luo J., et al. (2008). Enrichment of tomato fruit with health-promoting anthocyanins by expression of select transcription factors. *Nat Biotechnol* 26: 1301-1308.
- Cantu D., Vicente A. R., Greve L. C., Dewey F. M., Bennett A. B., Labavitch J. M., and Powell A. L. T. (2008). The intersection between cell wall disassembly, ripening, and fruit susceptibility to Botrytis cinerea. *Proc Natl Acad Sci U S A* 105: 859-864, doi: 0709813105 [pii] 10.1073/pnas.0709813105.
- Carrari F., Fernie A.R. (2006) Metabolic regulation underlying tomato fruit development. J Exp Bot 57: 1883–1897.
- Carpenter J.F., Crowe L.M. & Arakawa T. (1990) Comparison of solute-induced protein stabilization in aqueous solution and in the frozen and dried states. Journal of Dairy Science 73, 3627 3636.
- Chaı¨b J., Devaux M.F., Grotte M.G., Robini K., Causse M., Lahaye M., Marty I. (2007). Physiological relationships among physical, sensory, and morphological attributes of texture in tomato fruits. J Exp Bot 58: 1915–1925.
- Chaves M.M., Flexas J., Pinheiro C. (2009) Photosynthesis under drought and salt stress: regulation mechanisms from whole plant to cell. Annals of Botany*103*, 551–560.
- Chen Z., Young T.E., Ling J., Chang S.C., Gallie D.R. (2003). Increasing vitamin C content of plants through enhanced ascorbate recycling. Proceedings of the National Academy of Sciences, 100, 3525-3530.
- Choi J., Park J.K., Lee K.T., Park K.K., Kim W.B., Lee J.H., Jung H.J. and Park H.J. (2005). In vivo antihepatotoxic effects of Ligularia fischeri var. spiciformis and the identification of the active component, 3,4-dicaffeoylquinic acid. *J. Med. Food*, 8, 348–352.
- Clinton S. K. (1998) Lycopene: chemistry, biology and implications for human health and disease. Nutr. Rev., 56, 35-51.
- Conklin P.L., Gatzek S., Wheeler G.L., Dowdle J., Raymond M.J., Rolinski S., IsupovM, Littlechild J.A., Smirnoff N. (2006). Arabidopsis thaliana VTC4 encodes L-galactose-1-P phosphatase, a plant ascorbic acid biosynthetic enzyme. J Biol Chem 281: 15662–15670.

- Conklin P.L., Norris S.R., Wheeler G.L., Williams E.H., Smirnoff N., Last R.L. (1999) Genetic evidence for the role of GDP-mannose in plant ascorbic acid (vitamin C) biosynthesis. Proc Natl Acad Sci USA 96:4198–4203.
- Conklin P.L., Saracco S.A., Norris S.R., Last R.L. (2000) Identification of ascorbic acid-deficient Arabidopsis thaliana mutants. Genetics 154:847–856.
- Corona V., Aracri B., Kosturkova G., Bartely G. E., Pitto L., Giorgetti L., Scolmik P.A. and Giuliano G., (1996). Regulation of a carotenoid biosynthesis gene promoter during plant development. *Plant J*. 9, 505-512.
- Daniel X., Lacomme C., Morel J.-B. and Roby D. (1999). A novel myb oncogene homologue in Arabidopsis thaliana related to hypersensitive cell death. *The plant Journal* 20, 66-57.
- Daood H.G., Al-Qitt M.A., Bshenah K.A., Bouragba M. (1990).Varietal and chemical aspect of tomato processing. Acta Alimentaria19, 347–357.
- Davey M. W., Gilot C., Persiau G., Ostergaard J., Han Y., Bauw G. C., Van Montagu M. C. (1999). Ascorbate Biosynthesis in Arabidopsis Cell Suspension Culture. Plant Physiology, 121, 535-543.
- Deikman J., Kline, R. and Fischer R.L. (1992). Organization of ripening and ethylene regulatory regions in a fruit-specific promoter from tomato (Lycopersicon esculentum). *Plant Physiol*. 100, 2013–2017.
- DellaPenna D., Pogson B.J. Vitamin synthesis in plants: tocopherols and carotenoids. Annu Rev Plant Biol. 2006 57, 711-38.
- Demmig-Adams B., Adams W.W. (2000). Photosynthesis– harvesting sunlight safely. Nature 403, 231.
- Deutsch J.C. (1998). Spontaneus hydrolysis and dehydration of dehydroascorbic acid in aqueous solution. Anal Biochem, 260, 223-229.
- Dhindsa R. S., Plumb-Dhindsa, P. and Thorpe, T. A. (1981). Leaf senescence: correlated with increased levels of membrane permeability and lipid peroxidation, and decreased levels of superoxide dismutase and catalase. *Journal of Experimental Botany* 32, 93-101, doi:10.1093/jxb/32.1.93.
- Dubos C., Stracke R., Grotewold E., Weisshaar B., Martin C. and Lepiniec L. (2010). MYB transcription factors in Arabidopsis. Trends Plant Sci. , 15, 573-58.
- Di Matteo A., Sacco A., Anacleria M., Pezzotti M., Delledonne M., A. Ferrarini, Frusciante L., Barone A. (2010). The ascorbic acid content of tomato fruits is associated with the expression of genes involved in pectin degradation. BMC Plant Biology, 10:163.
- Eltayeb A.E., Kawano N., Badawi G.H., Kaminaka H., Sanekata T., Shibahara T., Inanaga S., Tanaka K. (2007). Overexpression of monodehydroascorbate reductase in transgenic tobacco confers enhanced tolerance to ozone, salt and polyethylene glycol stresses. Planta, 225, 255-1264.
- Estruch R., Martı´nez-Gonza´ lez M.A., Corella D., et al. (2006). Effects of a Mediterranean-style diet on cardiovascular risk factors. Annals of Internal Medicine 145, 1–11.
- Eshed Y., Abu-Abied M., Saranga Y., Zamir D. (1992). Lycopersicon esculentum lines containing small overlapping introgressions from L. pennellii. Theoretical and Applied Genetics 83, 1027–1034.
- Eshed Y., Zamir D. (1994). A genomic library of Lycopersicon pennellii in L. esculentum: a tool for fine mapping of genes. Euphytica 79, 175–179.

- Foolad M.R. (2007). Genome Mapping and Molecular Breeding of Tomato. Int J Plant Genomics, 1–52.
- Feldbrugge M., Sprenger M., Hahlbrock K. and Weisshaar B. (1997). PcMYB1, a novel plant protein containing a DNA-binding domain with one MYB repeat, interacts in vivo with a light-regulatory promoter unit. *Plant J.* 11: 1079–1093.
- Fleschhut, J., F. Kratzer, et al. (2006). Stability and biotransformation of various dietary anthocyanins in vitro. Eur. J. Nutr. 45(1): 7-18.
- Forkmann G., Heller W. (1999). Biosynthesis of flavonoids. *Elsevier* 713-748.
- Foyer, C. (1993). Ascorbic acid. In: Antioxidants in Higher Plants. R.G. Alscher and J.L. Hess (eds) CRC Press, Boca Raton, 31-58.
- Franceschi S., Bidoli E., La Vecchia C., Talamini R., D'Avanzo B., Negri E. (1994). Tomatoes and risk of digestive-tract cancers. Int. J. Cancer, 59, 181-184.
- Fridman E., Liu Y.S., Carmel-Goren L., Gur A., Shoresh M., Pleban T., Eshed Y. and Zamir D. (2002) Two tightly linked QTLs modify tomato sugar content via different physiological pathways. Mol. Genet. Genomics 266: 821–826.
- Fridman E., Zamir D. (2003) Functional divergence of a syntenic invertase gene family in tomato, potato, and Arabidopsis. Plant Physiol 131: 603–609.
- Fry S.C. (2004). Primary cell wall metabolism: Tracking the careers of wall polymers in living plant cells. *New Phytol* 161:641–675.
- Fry S.C. (1998). Oxidative scission of plant cell wall polysaccharides by ascorbate-induced hydroxyl radicals. Biochem J 332: 507–515.
- Gey K. F. (1998). Vitamins E plus C and interacting conutrients required for optimal health. A critical and constructive review of epidemiology and supplementation data regarding cardiovascular disease and cancer. Biofactors, 7, 113-174.
- Gilbert L., Alhagdow M., Nunes-Nesi A., Quemener B., Guillon F., Bouchet B., Faurobert M., Gouble B., Page D., Garcia V., Petit J., Stevens R., Causse M.,Fernie A. R., Lahaye M., Rothan C. and Baldet P. (2009).GDP-D-mannose 3,5-epimerase (GME) plays a key role at the intersection of ascorbate and non-cellulosic cell-wall biosynthesis in tomato. The Plant Journal 60, 499–508
- Gillaspy G., Ben-David H., and Gruissem W. (1993). Fruits: A developmental perspective. *Plant Cell* 5: 1439–1451.
- Giovannoni J., DellaPenna D., Bennett A., and Fischer R. (1989). Expression of a chimeric polygalacturonase gene in transgenic rin (ripening inhibitor) tomato fruit results in polyuronide degradation but not fruit softening. *Plant Cell* 1: 53–63.
- Giovannoni J. (2001). Molecular Biology of fruit maturation and ripening. *Annu. Rev. Plant Physiol. Plant Mol. Biol.* 52:725–49.
- Giovannoni J. (2004). Genetic regulation of fruit development and ripening. *Plant Cell* 16:S170–S180.
- Giovannoni J. (2007). Fruit ripening mutants yield insights into ripening control. *Current Opinion in Plant Biology* 10, Issue 3: 283–289.
- Giovannucci E., Ascherio A., Rimm E. B., Meir J., Stampfer M. I., Colditz C. A., Willer W. C. (1995) Intake of carotenoids and Retinol in relation to risk of prostate cancer. J. Natl. Cancer Inst., 87, 1767-1767.
- Godt D.E., Roitsch T. (1997) Regulation and tissue-specific distribution of mRNAs for three extracellular invertase isoenzymes of tomato suggests an

important function in establishing and maintaining sink metabolism. Plant Physiol 115: 273–282.
- Govrin E.M. & Levine A. (2000). The hypersensitive response facilitates plant infection by the necrotrophic pathogen *Botrytis cinerea*. *Curr Biol* 10, 751-757, doi:S0960-9822(00)00560-1 [pii].
- Green M.A., Fry S.C. (2005). Vitamin C degradation in plant cells via enzymatic hydrolysis of 4-Ooxalyl- L-threonate. Nature, 433, 83-87.
- Grotte M., Cadot Y., Poussier A., Loonis D., Piétri E., Duprat F., Barbeau G. (2001). Détermination du degré de maturité des baies de raisin par des measures physiques: aspects méthodologiques. J. Int. Sci. Vigne Vin 35, 87–98.
- Hannum S.M. (2004). Potential impact of strawberries on human health: a review of the science. *Crit. Rev. Food Sci. Nutr.* 44: 1–17.
- Harker F.R., Redgwell R.J., Hallett I.C., Murray S.H., Carter G. (1997). Texture of fresh fruit. Horticultural Reviews 20, 121–224.
- Hartmann U., Sagasser M., Mehrtens F., Stracke R. and Weisshaar B. (2005). Differential combinatorial interactions of cis-acting elements recognized by R2R3-MYB, BZIP, and BHLH factors control light-responsive and tissue-specific activation of phenylpropanoid biosynthesis genes. *Plant Molecular Biology* 57, Num 2 : 155-171, DOI: 10.1007/s11103-004-6910-0.
- Haupt-Herting S., Klug K. and Fock H. P. (2001). A New Approach to Measure Gross CO2 Fluxes in Leaves. Gross CO2 Assimilation, Photorespiration, and Mitochondrial Respiration in the Light in Tomato under Drought Stress. Plant Physiology vol. 126 no. 1 388-396.
- van der Hoeven R.S., Ronning, Giovannoni J. J., Martin G., and Tanksley S. D. (2002). Deductions about the number, C. organization, and evolution of genes in the tomato genome based on analysis of a large expressed sequence tag collection and selective genomic sequencing. The Plant Cell, vol. 14, no. 7, pp. 1441–1456.
- Hertog M.G.L., Hollman P.C.H., Putte B. (1993). Content of potentially anticarcinogenic flavonoids of tea infusions, wines, and fruit juices. *J. Agric. Food Chem.* 41 (8): 1242–1246.
- Hirayama T. and Shinozaki K. (1996). A cdc51 homolog of a higher plant, Arabidopsis thaliana. *Plant Biology* 93: 13371–13376.
- Holiman P.C.H., Hertog M.G.L. and Katan M.B. (1996). Analysis and health effects of flavonoids. *Food chemistry* 57 (1): 43–46.
- Holton T.A., Cornish E.C. (1995). Genetics and biochemistry of anthocyanin biosynthesis. *Plant Cell* 7: 1071–1083.
- Horemans N, Foyer CH, Asard H (2000).Transport and action of ascorbate at the plant plasma membrane. Trends in Plant Science 5, 263-267.
- Hou D., Fujii M.,1 Terahara N., and Yoshimoto M. (2004). Molecular mechanisms behind the chemopreventive effects of anthocyanidins. *J. of Biom. and Biotech.* 5: 321–325.
- Islam S. (2006). Sweetpotato (Ipomoea batatas L.) leaf: its potential effect on human health and nutrition. *J. Food. Sci.* 71, R13–R21.
- Jang J.C., Sheen J. (1994). Sugar sensing in higher plants. Plant Cell 6:1665-1679.
- Jeandet P., Douillet-Breuil A., Bessis R., Debord S., Sbaghi M., and Adrian M (2002). Phytoalexins from the vitaceae: biosynthesis, phytoalexin gene

expression in transgenic plants, antifungal activity, and metabolism *J. Agric. Food Chem.*, 50 (10): 2731–2741 DOI: 10.1021/jf011429s.
- Jimenez A., Creissen G., Kular B., Firmin J., Robinson S., Verhoeyen M. and Mullineaux P. (2002). Changes in oxidative processes and components of the antioxidant system during tomato fruit ripening. *Planta* 214, 751-758, doi:10.1007/s004250100667.
- van Kan J. (2006). Licensed to kill: the lifestyle of a necrotrophic plant pathogen. *Trends in Plant Sciences* 11: 247-253.
- Kars I., Krooshof C.A., Wagemakers M., Joosten R., Benen J.A.E. and van Kan J.A.L. (2005). Necrotizing activity of five Botrytis cinerea endopolygalacturonases produced in Pichia pastoris. *Plant J.* 43:213-225.
- Koes R.E., Quattrocchio F., Mol J.N.M. (1994). The flavonoid biosynthetic pathway in plants: function and evolution. Bioessays 16:123–132.
- Kuo S.M. (1997). Dietary flavonoid and cancer prevention: evidence and potential mechanism. Critical Reviews in Oncogenesis 8(1): 47-69.
- Levin I., Lalazar A., Bar M., Schaffer A.A. (2004). Non GMO fruit factories strategies for modulating metabolic pathways in the tomato fruit. Industrial Crops and Products 20, pp. 29–36.
- Le Gall G., Dupont M. S., Mellon F. A., Davis A. L., Collins G. J., Verhoeyen M. E., and Colquhoun I. J (2003). Characterization and content of flavonoid glycosides in genetically modified tomato (Lycopersicon esculentum) fruits. *J. Agric. Food Chem*., 51, 2438-2446.
- Levy J., Bosin E., Feldman B., Giat Y., Miinste A., Danilenko M., Sharoni Y. (1995). Lycopene is a potent inhibitor of human cancer cell proliferation than either alfa-carotene or beta-carotene. Nutr. Cancer, 24, 257-266.
- Leung J., and Giraudat J. (1998). Abscisic acid signal transduction. Annu. Rev. Plant Physiol. Plant Mol. Biol. 49, 199–222.
- Linnaeus C., Species Planatarium, Holmiae, Stockholm, Sweden, 1st edition, 1753.
- Livak K.J., Schmittgen T.D. (2001). Analysis of relative gene expression data using realtime quantitative PCR and the 2-DDCT method. Methods, 25:402-408.
- Luo J., Butelli E., Hill L., Parr A., Niggeweg R., Bailey P., Weisshaar B., and Martin C. (2008). AtMYB12 regulates caffeoyl quinic acid and flavonol synthesis in tomato: expression in fruit results in very high levels of both types of polyphenol. *Plant J* 56: 316-326.
- Marri L., Trost P., Pupillo P., and Sparla F.. Glyceraldehyde-3-Phosphate Dehydrogenase/CP12/Phosphoribulokinase Supramolecular Complex of Arabidopsis. Plant Physiology (2005) Vol. 139, 1433–1443.
- Martin C., Butelli E., Petroni K., and Tonelli C. (2011). How Can Research on Plants Contribute to Promoting Human Health? *The Plant Cell Preview* 1-15.
- Martin C. and Paz-Ares J. (1997). Myb transcription factors in plant. Rev. *TIG* 13 No 2: 67-73.
- Mehrtens F., Kranz H., Bednarek P., and Weisshaar B. (2005). The Arabidopsis transcription factor MYB12 Is a flavonol-specific regulator of phenylpropanoid biosynthesis *Plant Physiology*, 138: 1083–1096.
- MehtaR.A., Cassol T., Li N., Ali N., Handa A. K., and Mattoo A. K. (2002). Engineered polyamine accumulation in tomato enhances phytonutrient content,

juice quality, and vine life. *Nat Biotechnol* 20: 613-618, doi:10.1038/nbt0602-613 nbt0602-613 [pii].

- Miller P., The Gardeners Dictionary, John and Francis Rivington, London, UK, 4th edition, 1754.
- Mintz-Oron S., Mandel T., Rogachev I., Feldberg L., Lotan O., Yativ M.,Wang Z., Jetter R., Venger I., Adato A., et al (2008). Gene expression and metabolism in tomato fruit surface tissues. Plant Physiol 147: 823–851Mondal K., Sharman S., Malhotra S.P., Dhawan K. and Singh R. (2004). Antioxidant systems in ripening tomato fruits. *Biologia Plantarum* 48: 49-53.
- Muir S.R., Collins G.J., Robinson S, Hughes S., Bovy A., De Vos C.H.R., van Tunen A.J., Verhoeyen M.E. (2001). Overexpression of petunia chalcone isomerase in tomato results in fruit containing increased levels of avonols. *Nature Biotechnology* 19: 470-474.
- Nijveldt R. J., Nood E., Hoorn D. EC, Boelens P. G., Norren K. and Leeuwen P. A.M. (2001). Flavonoids: a review of probable mechanisms of action and potential applications. *Am J Clin Nutr* 74 no. 4: 418-425.
- Nakajima Y., Shimazawa M., Mishima S. and Hara H. (2007). Water extract of propolis and its main constituents, caffeoylquinic acid derivatives, exert neuroprotective effects via antioxidant actions. Life Sci. 80, 370–377.
- Najib E. Amer J. and Hmoud A. (2009). Technical and Economical Evaluation of Traditional vs. Advanced Handling of Tomatoes in Jordan. Journal of Agronomy, 8: 39-44.
- Ohashi Y., Matsuoka M. (1985). Synthesis of stress proteins in tobacco leaves. Plant Cell Physiol 26:473-480.
- Oppenheimer D. G., Herman P. L., Sivakumaran S., Esch J., and Marks M. D. (1991). A myb gene required for leaf trichome differentiation in Arabidopsis is expressed in stipules. Cell 67 (3): 483–493.
- Padayatty S. J., Katz, A., Wang Y., Eck P., Kwon O., Lee J. H., Chen S., Corpe C., Dutta A., Dutta S. K., Levine M. (2003). Vitamin C as an antioxidant: evaluation of its role in disease prevention. J. Am. Coll. Nutr., 22(1):18-35.
- Padh H. (1990). Cellular functions of ascorbic acid. Biochemistry and cell Biology, 68, 1166-1173.
- Pastori G.M., and Foyer C.H. (2002). Common components, networks, and pathways of cross-tolerance to stress. The central role of ‘‘redox’’ and abscisic acid-mediated controls. Plant Physiol. 129, 460–468.
- Pastori GM, Kiddle G, Antoniw J, Bernard S, Veljovic-Jovanovic S, Verrier PJ, Noctor G, Foyer CH (2003). Leaf vitamin C contents modulate plant defense transcripts and regulate genes that control development through hormone signaling. Plant Cell 15: 939–951.
- Pierpoint W.S., Robinson N.P, Leason M.B. (1981).The pathogenesis-related proteins in tobacco: Their induction by viruses in intact plants and their induction by chemicals in detached leaves. Physiol Plant Path 19:85-97.
- Pignocchi C., Fletcher J. M., Wilkinson J. E., Barnes J. D. and Foyer C.H. (2003). The Function of Ascorbate Oxidase in Tobacco. Plant Physiology vol. 132 no. 3 1631-1641.
- Potters G., de Gara L., Asard H., Horemans N. (2002). Ascorbate and glutathione: guardians of the cell cycle, partners in crime? Plant Physiol Biochem 40: 537–548.

- Powell A.L.T., Kan J., Have A., Visser J., Greve L.C., Bennett A.B., Labavitch J.M. (2000). Transgenic expression of pear PGIP in tomato limits fungal colonization. *Mol Plant Microbe Interact* 13: 942–950.
- Proteggente A.R., Pannala A.S., Paganga G., Van Buren L., Wagner E., Wiseman S., Van De Put F., Dacombe C., Rice-Evans C.A. (2002). The antioxidant activity of regularly consumed fruit and vegetables reflects their phenolic and vitamin C composition. FreeRadical Research 36, 217–233.
- Prusky D., McEvoy J. L., Leverentz B. and Conway W. S. (2001). Local Modulation of Host pH by Colletotrichum Species as a Mechanism to Increase Virulence. *Molecular Plant-Microbe Interactions* 14, No. 9: 1105–1113.
- Rawls W.J., and Brakensiek D.L.. (1985). Prediction of soil water properties for hydrologic modeling. p. 293–299. In E.B. Jones and T.J.Ward (ed.) Proc. Symp.Watershed Management. in the Eighties, Denver, CO. 30 Apr.–1 May 1985. Am. Soc. Civil Eng., New York.
- Redgwell R.J., Fischer M. Fruit texture, cell wall metabolism and consumer perceptions. In Knee M (Ed.). Fruit quality and its biological basis Oxford Blackwell 2002 46–88.
- Renaud S.C., Gueguen R., Schenker J., d'Houtaud A. (1998). Alcohol and mortality in middle-aged men from eastern France. Epidemiology, 9, 184-188.
- Rick C.M. (1973). Potential genetic resources in tomato species: clues from observation in native habitats. In: Srb AM, ed. Handbook of genetics, Vol. 2. FL: Plenum Press, 255–269.
- Roessner-Tunali U., Hegemann B., Lytovchenko A., Carrari F., Bruedigam C., Granot D. and Fernie, A. (2003). Metabolic profiling of transgenic tomato plants overexpressing hexokinase reveals that the influence of hexose phosphorylation diminishes during fruit development. Plant Physiol. 133: 84–99.
- Roitsch T. (1999). Source-sink regulation by sugar and stress. Curr. Opin. Plant Biol. 2: 198–206.
- Ross J. A. and Kasum M. (2002). DIETARY FLAVONOIDS: Bioavailability, Metabolic Effects, and Safety. *Annual Review of Nutrition* 22: 19-34 DOI: 10.1146/annurev.nutr.22.111401.144957.
- Rowan D. D., Cao M., Lin-Wang K., Cooney J. M., Jensen D. J., Austin P. T., Hunt M. B., Norling C., Hellens R. P., Schaffer R. J. and Allan A. C. (2009). Environmental regulation of leaf colour in red 35S:PAP1 Arabidopsis thaliana. *New Phytologist*182:102–115doi: 10.1111/j.1469-8137.2008.02737.x
- Rui Hai Liu. (2003). Health benefits of fruit and vegetables are from additive and synergistic combinations of phytochemicals. *Am J Clin Nutr*; 78 (suppl): 517S–20S.
- Saladie M., Matas A.J., Isaacson T., Jenks M.A., Goodwin S.M., Niklas K.J., Xiaolin R., Lavavitch J.M., Shackel K.A., Fernie A.R., Lytovchenko A., O'Neil M.A., Watkins C.B., Rose J.KC (2007). A reevaluation of the key factors that influence tomato fruit softening and integrity. *Plant Physiol* 144: 1012–1028.
- Sapir M., Oren-Shamir M., Ovadia R., Reuveni M., Evenor D., Tadmor Y., Nahon S., Shlomo H., Chen L., Meir A. and Levin I. (2008). Molecular aspects of Anthocyanin fruit tomato in relation to high pigment-1. J. Hered. 99, 292–303.
- Sato P., Udenfriends S. (1978). Scurvy-prone animals, including man, monkey and guinea pig do not express the gene for gulonolactone oxidase. Arch

Biochem Biophys, 71, 293-299Sévenier R., Van der Meer I.M., Bino R., Koops A.J. (2002). Increased production of nutriments by genetically engineered crops. J. American College Nutrition 21, 199S-204S.

- Smirnoff N. and. Wheeler G. L. (2000). Ascorbic Acid in Plants: Biosynthesis and Function. Critical Reviews in Biochemistry and Molecular Biology 35(4) :291-314.
- Smirnoff N., Conklin P.L., Loewus F.A. (2001). Biosynthesis of ascorbic acid in plants: a renaissance. Annual Review of Plant Physiology and Plant Molecular Biology, 52,437-467.
- Smith D.L., Abbott J.A. and Gross K.C. (2002). Down-regulation of tomato beta-galactosidase 4 results in decreased fruit softening. Plant Physiol 129, 1755-1762, doi:10.1104/pp.011025.
- Soobrattee M.A, Bahorun T., Aruoma O.I (2006). Chemopreventive actions of polyphenolic compounds in cancer. BioFactors 27, Issue 1-4: 19–35.
- Stracke R., Werber M., Weisshaar B. (2001). The R2R3-MYB gene family in Arabidopsis thaliana. Curr Opin 4(5): 447-56.
- Stevens R., Buret M., Duffé P., Garchery C., Baldet P., Rothan C. and Causse M. (2007). Candidate Genes and Quantitative Trait Loci Affecting Fruit Ascorbic Acid Content in Three Tomato Populations. Plant Physiology vol. 143 no. 4 1943-1953.
- Sturm A. and Chrispeels M.J. (1990). cDNA cloning of carrot extracellular fl-fructosidase and its expression in response to wounding and bacterial infection. Plant Cell 2:1107-1119.
- Szczesniak A.S. (2002). Texture is a sensory property. Food Quality and Preference 13, 215–225.
- Tamura, H., Akioka, T., Ueno, K., Chujyo, T., Okazaki, K., King, P.J. and Robinson, W.E. Jr (2006). Anti-human immunodeficiency virus activity of 3,4,5-tricaffeoylquinic acid in cultured cells of lettuce leaves. Mol. *Nutr. Food Res.* 50, 396–400.
- Temple N. J. (2000). Antioxidants and disease: more questions than answers. Nutrition Research, 20, 449-459.
- Ten Have R., Hartmans S., Teunissen P.J.M. and Field J.M. (1998). Purification and characterization of two lignin peroxidase isozymes produced by Bjerkandera sp. strain BOS55. FEBS Letters 422: 391-394
- Thomasset SC, Berry DP, Garcea G, Marczylo T, Steward WP, Gescher AJ. (2007). Dietary polyphenolic phytochemicals--promising cancer chemopreventive agents in humans? A review of their clinical properties. Int J Cancer. 120(3), 451-8.
- Tieman D.M., Harriman R.W., Ramamohan G., Handa A.K. (1992). An antisense pectin methylesterase gene alters pectin chemistry and soluble solids in tomato fruit. Plant Cell 4: 667–679.
- Toor RK, Savage GP, Lister CE (2006) Seasonal variations in the antioxidant composition of greenhouse grown tomatoes. J Food Compos Anal 19: 1–10.
- Trichopoulou A., Naska A., Antoniou A., Friel S., Trygg K., Turrini A. (2003). Vegetable and fruit: the evidence in their favour and the public health perspective. International Journal for Vitamin and Nutrition Research 73, 63–69.
- Tuberosa R. and Salvi S. (2006). Genomics-based approaches to improve drought tolerance of crops. TRENDS in Plant Science Vol.11 :405-412 No.8.

- Valpuesta V., Botella M.A. (2004). Biosynthesis of L-ascorbic acid in plants: new pathways for an old antioxidant. Trends Plant Sci 9: 573–577
- Vicente A.R., Saladie M., Rose J.K.C., Labavitch J.M. (2007). The linkage between cell wall metabolism and fruit softening: looking to the future. J Sci Food Agric 87: 1435–1448.
- Vina J., Gomez-Cabrera M.C. and Borras C. (2007). Fostering antioxidant defences: up-regulation of antioxidant genes or antioxidant supplementation? *Br. J. Nutr.* 98, S36–S40.
- Visioli F., Grande S., Bogani P., Galli C. (2004). The role of antioxidants in the Mediterranean diets: focus on cancer. European Journal of Cancer Prevention 13, 337–343.
- Xiao W., Sheen J. and.Jang J. (2000). The role of hexokinase in plant sugar signal transduction and growth and Development. Plant Molecular Biology 44: 451–461.
- Warnock S. J. (1988). A review of taxonomy and phylogeny of the genus Lycopersicon. HortScience, vol. 23, no. 4, pp. 669–673,
- Weisshaar B. and I. Jenkins G. (1998). Phenylpropanoid biosynthesis and its regulation. Curr Opinion in Plant Biol 1 (3): 251–257.
- Welsch R., Beyer P., Hugueney P., Kleinig H., von Lintig J. (2000). Regulation and activation of phytoene synthase, a key enzyme in carotenoid biosynthesis, during photomorphogenesis. Planta 211, 846–854.
- Wheeler G. L., Jones M. A., Smirnoff N. (1998). The biosynthetic pathway of Vitamin C in higher plants. Nature, 393, 365-369.
- Yang B., Kotani A., Arai K., Kusu F. (2001). Estimation of the antioxidant activities of flavonoids from their oxidation potentials. Analytical Sciences 17 No. 5: 599-604.
- Yeum, K.J., Russella R.M., Krinsky N.I., Aldini G. (2004). Biomarkers of antioxidant capacity in the hydrophilic and lipophilic compartments of human plasma. Arch. Biochem. Biophys. 430: 97–103 Physiol 38: 1095-1102.
- Yoshiba Y., Kiyosue T., Nakashima K., Yamaguchi-Shinozaki K., Shinozaki K. (1997). Regulation of levels of proline as an osmolyte in plants under water stress. Plant Cell 38(10):1095-102.

Supplementary table 1 – Categorization of selected TCs showing significant interaction *genotype x treatment*.

Probe name	Annotation	Adj p value interacton	FC M82 50% vs. M82 100%	FC IL9-2-5 50% vs. IL9-2-5 100%
id_9217	---NA---	0.0001	-3.94	-0.15
id_1219	---NA---	0.0041	-3.57	1.35
id_11656	chloroplast protein cp12	0.0010	-3.42	-0.17
id_18167	---NA---	0.0029	-3.35	-0.31
id_17952	---NA---	0.0040	-3.23	0.58
id_9437	peptidyl-prolyl cis-trans isomerase-like 3	0.0013	-3.19	-0.18
id_8551	myb transcription factor	0.0098	-3.17	-0.42
id_17891	24 kda seed maturation protein	0.0067	-3.17	0.57
id_18324	40s ribosomal protein s30	0.0001	-3.07	0.35
id_4468	protein	0.0049	-3.03	0.14
id_7320	aspartyl protease family protein	0.0022	-3.02	-0.09
id_2161	ppgpp synthetase	0.0084	-3.00	-0.52
id_13760	acyltransferase-like protein	0.0062	-2.98	-0.46
id_11580	cdk5 activator-binding	0.0002	-2.89	0.12
id_1314	yth domain containing 2	0.0019	-2.85	0.40
id_18973	---NA---	0.0008	-2.83	0.12
id_6417	3-ketoacyl-thiolase acetyl-acyltransferase	0.0045	-2.82	0.83
id_8706	zinc finger (an1-like) family protein	0.0058	-2.82	-0.23
id_2850	peptidase s1 andchymotrypsin hap:pdz dhr glgf	0.0025	-2.77	0.51
id_12347	---NA---	0.0056	-2.75	-0.06
id_16343	plas_sollcame: full=chloroplastic flags: precursor	0.0071	-2.69	-0.53
id_5962	fcly prenylcysteine oxidase	0.0055	-2.68	-0.09
id_14044	---NA---	0.0074	-2.67	-1.14
id_10752	r2r3-myb transcription factor	0.0005	-2.66	-0.11
id_4569	serine carboxypeptidase	0.0041	-2.60	0.20
id_12018	DnaJ-class molecular chaperone	0.0015	-2.60	-0.02
id_16240	phosphosulfolactate synthase-related protein	0.0031	-2.57	0.05
id_1251	at5g25460 f18g18_200	0.0023	-2.55	0.00
id_314	brix domain-containing protein 2 - biogenesis of ribosome	0.0036	-2.54	0.09
id_16702	fiber protein fb15	0.0012	-2.53	0.26
id_6192	histone deacetylase	0.0025	-2.53	-0.13
id_11907	---NA---	0.0010	-2.50	0.41
id_1148	---NA---	0.0076	-2.48	-0.09
id_7532	receptor-like protein kinase	0.0000	-2.48	-0.30
id_540	heat- and acid-stable phosphoprotein	0.0048	-2.47	0.25
id_10413	---NA---	0.0039	-2.47	-0.37
id_1781	udp-glucose dehydrogenase	0.0033	-2.46	-0.65
id_8223	protein binding zinc ion binding	0.0047	-2.45	-0.17
id_6639	nbs-lrr type disease resistance protein	0.0046	-2.44	-0.57
id_12248	protein kinase c inhibitor	0.0039	-2.44	0.48

id_3375	ble1 protein	0.0084	-2.43	-0.26
id_4116	---NA---	0.0029	-2.42	0.14
id_16035	p2a13_arathame: full=f-box protein pp2-a13ame	0.0046	-2.40	0.34
id_14442	response regulator receiver cct	0.0057	-2.40	-0.02
id_1769	at5g10910 t30n20_180	0.0014	-2.35	0.24
id_12822	steroid sulfotransferase	0.0004	-2.33	-0.44
id_4539	60s ribosomal protein l34	0.0044	-2.32	0.04
id_7401	short-chain dehydrogenase reductasefamily protein	0.0092	-2.31	-0.15
id_12383	retinoblastoma-related protein	0.0023	-2.30	-0.18
id_13216	transmembrane and coiled-coil domain-containing protein 1	0.0010	-2.30	0.70
id_12071	drought-induced protein rdi	0.0020	-2.29	0.87
id_399	cytochrome b561	0.0002	-2.29	0.44
id_15561	cyc07-like protein	0.0074	-2.28	-0.10
id_1127	---NA---	0.0026	-2.26	0.33
id_4436	ubiquitin-conjugating enzyme	0.0009	-2.25	0.11
id_6643	ribosomal protein l10a	0.0072	-2.25	-0.12
id_16804	protein	0.0098	-2.24	0.24
id_1324	short chain alcohol dehydrogenase	0.0088	-2.24	-0.17
id_8260	seven transmembrane protein mlo8	0.0002	-2.24	0.23
id_6835	mevalonate diphosphate decarboxylase	0.0047	-2.23	0.25
id_14502	---NA---	0.0027	-2.22	0.05
id_3714	---NA---	0.0054	-2.22	-0.06
id_4922	---NA---	0.0021	-2.22	0.33
id_14287	aspartate aminotransferase	0.0027	-2.22	0.58
id_18763	chloroplast srp receptor cpprecursor	0.0071	-2.21	0.32
id_19341	nicotianamine synthase 1	0.0081	-2.21	-0.36
id_7187	---NA---	0.0006	-2.20	0.01
id_5542	---NA---	0.0063	-2.18	-0.29
id_1090	photoassimilate-responsive protein par-1b-like protein	0.0002	-2.17	0.33
id_19359	protein	0.0024	-2.15	1.03
id_1111	---NA---	0.0021	-2.14	-0.04
id_3770	---NA---	0.0057	-2.14	0.14
id_11690	---NA---	0.0059	-2.13	0.33
id_6150	---NA---	0.0037	-2.13	-0.04
id_9529	---NA---	0.0020	-2.12	-0.34
id_14788	pointed first leaf	0.0034	-2.12	0.17
id_13114	tpl wsip1 (wus-interacting protein 1)	0.0012	-2.12	-0.39
id_19787	ric10 (rop-interactive crib motif-containing protein 10)	0.0089	-2.12	0.05
id_5561	glutamate receptor	0.0052	-2.11	0.16
id_15504	dehydration responsive element-binding protein 1	0.0040	-2.11	0.02
id_8576	---NA---	0.0012	-2.11	0.04
id_9980	dna-binding protein	0.0018	-2.11	0.03
id_9645	40s ribosomal protein s25	0.0051	-2.10	0.41
id_10478	ring zinc finger	0.0055	-2.10	-0.32

id_20010	importin alpha	0.0037	-2.09	-0.04
id_16522	40s ribosomal protein s19	0.0064	-2.08	-0.06
id_17500	polyubiquitin	0.0056	-2.07	0.33
id_14830	ump6_arathame: full=uncharacterized proteinmitochondrial flags: precursor	0.0060	-2.07	0.21
id_17746	splicingarginine serine-rich 4	0.0012	-2.06	0.90
id_283	at3g61870 f21f14_40	0.0081	-2.06	0.01
id_11379	glutamate decarboxylase	0.0015	-2.06	0.17
id_2761	rwd domain containing 1	0.0087	-2.05	0.26
id_14933	---NA---	0.0014	-2.05	0.00
id_13588	ssxt protein containingexpressed	0.0010	-2.04	0.53
id_2990	protein	0.0001	-2.04	0.24
id_11676	Putative nucleotide repair protein	0.0008	-2.04	0.13
id_13540	mago nashi	0.0003	-2.03	0.45
id_17712	---NA---	0.0039	-2.02	-0.19
id_6503	rac protein	0.0029	-2.01	0.28
id_19906	chitinase	0.0014	-2.01	0.05
id_4356	atcel5 atgh9b4	0.0003	-2.00	-0.05
id_15356	---NA---	0.0023	-2.00	0.70
id_12631	protein	0.0062	-1.99	0.22
id_14226	acid phosphatase	0.0008	-1.99	0.16
id_14716	protein disulfide isomerase	0.0001	-1.98	-0.09
id_14260	---NA---	0.0002	-1.98	0.20
id_17242	20s proteasome beta subunit pbb2	0.0063	-1.97	-0.16
id_303	translational inhibitor protein	0.0037	-1.97	0.00
id_773	40s ribosomal protein s4	0.0047	-1.96	0.13
id_16155	---NA---	0.0011	-1.96	0.11
id_2873	rna polymerase ii transcriptional	0.0021	-1.96	-0.10
id_3144	rna binding protein	0.0075	-1.94	0.12
id_1183	protein	0.0005	-1.94	-0.31
id_3845	eukaryotic translation initiation factor 6	0.0068	-1.93	0.37
id_17779	protein - similar to self prouning 2 of tomato (FASTA33)	0.0000	-1.92	0.02
id_160	rna-binding protein	0.0000	-1.91	0.08
id_4406	oligopeptidase a	0.0000	-1.91	0.18
id_315	nicalin precursor	0.0004	-1.91	0.19
id_7450	water channel protein	0.0061	-1.91	0.97
id_16317	repressor protein	0.0008	-1.91	-0.06
id_11353	phytocyanin	0.0045	-1.91	0.04
id_6908	skp1-like protein 1	0.0065	-1.91	0.29
id_2199	anaphase promoting complex subunit 11 homolog	0.0081	-1.90	0.09
id_5713	mucin-like protein	0.0093	-1.89	0.35
id_11393	eif4eiso protein	0.0031	-1.89	-0.16
id_693	wd repeat domain 5	0.0064	-1.88	0.34
id_18970	---NA---	0.0041	-1.88	0.35
id_11547	glycyl-trna synthetase	0.0045	-1.88	0.49
id_917	at5g19150 t24g5_50	0.0046	-1.88	-0.05

id_9131	---NA---	0.0047	-1.88	-0.06
id_997	---NA---	0.0056	-1.87	0.16
id_1176	protein kinase family protein	0.0026	-1.87	0.09
id_15037	splicing factor u2af 38 kda subunit	0.0098	-1.87	0.10
id_4557	23kda polypeptide of the oxygen evolving complex of photosystem ii	0.0021	-1.86	0.22
id_9676	cyclin dependent kinase inhibitor	0.0080	-1.86	-0.55
id_9071	---NA---	0.0057	-1.86	-0.24
id_14206	aspartyl protease family protein	0.0042	-1.86	-0.23
id_12982	peptidylprolyl isomerase	0.0010	-1.85	-0.11
id_13052	---NA---	0.0057	-1.85	0.00
id_3977	chloroplast chlorophyll a b-binding protein	0.0005	-1.84	0.25
id_1525	40s ribosomal protein s16	0.0033	-1.84	-0.02
id_11506	---NA---	0.0035	-1.84	0.02
id_12274	neurogenic locus notch protein precursor-like	0.0092	-1.82	-0.20
id_412	prolyl 4-hydroxylase alpha subunit-like protein	0.0078	-1.82	0.22
id_9530	agamous-like protein	0.0021	-1.81	0.42
id_3020	---NA---	0.0001	-1.81	0.65
id_6619	er degradation-enhancing alpha-mannosidase-like 1	0.0009	-1.81	0.32
id_15208	adp atp translocase-like protein	0.0063	-1.81	0.33
id_10501	40s ribosomal protein s25	0.0054	-1.81	-0.02
id_2107	---NA---	0.0001	-1.80	0.36
id_8230	40s ribosomal protein s10	0.0009	-1.80	0.55
id_16729	multiple stress-responsive zinc-finger protein isap1	0.0068	-1.80	0.17
id_3643	glycine rich	0.0021	-1.80	0.22
id_5787	sec8 (secretion 8)	0.0053	-1.80	0.26
id_14672	nadh dehydrogenase subunit 1	0.0059	-1.80	0.29
id_18362	af218765_1 177 protein	0.0007	-1.80	0.04
id_16596	40s ribosomal protein s12	0.0035	-1.79	-0.08
id_16124	zinc transporter protein zip1	0.0060	-1.79	0.38
id_7354	dof zinc finger protein	0.0066	-1.78	-0.07
id_15577	eukaryotic translation initiation factor 3 delta subunit	0.0065	-1.78	0.15
id_14378	receptor-like kinase	0.0047	-1.78	-0.22
id_10950	cinnamoylreductase	0.0043	-1.78	0.59
id_13194	protein translocase	0.0009	-1.77	-0.02
id_1621	annat4 calcium ion binding calcium-dependent phospholipid binding	0.0010	-1.77	0.19
id_3029	pepidyl-trna hydrolase family protein	0.0037	-1.76	0.15
id_18584	gibberellin 2-oxidase	0.0009	-1.75	-0.02
id_16351	serine carboxypeptidase i	0.0069	-1.75	0.17
id_4787	harpin-induced hin1-related harpin-responsive	0.0012	-1.73	0.90
id_15558	---NA---	0.0015	-1.72	0.00
id_8945	---NA---	0.0013	-1.72	0.80
id_8639	threonyl-trna synthetase	0.0055	-1.72	0.20
id_7865	tf-like protein	0.0006	-1.72	0.04
id_16921	dcp1-like decapping family protein	0.0094	-1.71	0.14

id_4160	40s ribosomal protein s4	0.0056	-1.70	-0.05
id_16120	inorganic pyrophosphatase	0.0026	-1.70	0.54
id_500	mandelonitrile lyase	0.0094	-1.69	0.34
id_12800	lipase-like protein	0.0038	-1.69	0.01
id_797	---NA---	0.0005	-1.68	0.38
id_6833	rna recognition motif familyexpressed	0.0076	-1.68	-0.07
id_5231	calcineurin b-like protein 2	0.0030	-1.68	0.53
id_19560	bhlh transcription factor	0.0034	-1.67	0.16
id_6955	transducin familyexpressed	0.0010	-1.67	0.43
id_6229	at3g01470 f4p13_2	0.0019	-1.66	0.36
id_17851	fiber protein fb11	0.0003	-1.66	0.45
id_13347	3-deoxy-d-arabino-heptulosonate 7-phosphate synthase	0.0010	-1.65	1.31
id_17489	gtp binding protein	0.0045	-1.65	-0.09
id_11041	wd-40 repeat protein	0.0095	-1.65	0.12
id_10584	alpha- alpha-d-galactoside	0.0091	-1.65	0.41
id_7568	50s ribosomal protein l13	0.0074	-1.65	0.44
id_18284	delta 9 desaturase	0.0017	-1.64	0.13
id_4782	calmodulin	0.0068	-1.64	0.29
id_11128	gpi-anchored protein	0.0047	-1.63	0.21
id_6981	rna recognition motif-containing protein	0.0005	-1.63	0.35
id_7018	---NA---	0.0061	-1.63	0.21
id_11655	---NA---	0.0050	-1.63	-0.08
id_1728	---NA---	0.0098	-1.63	0.29
id_11014	---NA---	0.0089	-1.62	0.53
id_986	fiber protein fb2	0.0086	-1.62	0.48
id_19814	elicitor-inducible cytochrome p450	0.0074	-1.62	0.11
id_15921	cytochrome c1 precursor	0.0018	-1.62	0.29
id_2485	pearli 1-like protein	0.0085	-1.61	0.17
id_19147	heat shock protein 70	0.0096	-1.61	-0.22
id_7293	---NA---	0.0093	-1.61	0.21
id_7277	---NA---	0.0011	-1.61	0.10
id_17088	vtc2-like protein	0.0098	-1.60	-0.13
id_16064	40s ribosomal protein s19	0.0008	-1.60	0.05
id_16359	nhl3	0.0028	-1.60	0.44
id_14927	s haplotype-specific f-box	0.0000	-1.59	0.19
id_1660	Glucan endo-1 3-beta-glucosidase B precursor	0.0012	-1.58	0.31
id_12633	7-dehydrocholesterol reductase - consuma AsA	0.0065	-1.58	0.59
id_12097	seed maturation protein lea 4	0.0080	-1.57	0.18
id_6635	---NA---	0.0064	-1.57	0.52
id_7351	qc-plant sft1-family	0.0084	-1.56	0.10
id_7251	glycosyl transferase	0.0026	-1.55	0.43
id_8184	lysyl-trna synthetase	0.0074	-1.55	0.27
id_6759	patatin-like protein	0.0012	-1.55	0.39
id_8593	gene product	0.0061	-1.55	-0.04
id_7612	---NA---	0.0021	-1.55	0.42
id_8434	---NA---	0.0016	-1.54	0.19

id_10318	histone deacetylase	0.0014	-1.54	0.19
id_17277	adp-ribosylation factor	0.0004	-1.54	0.33
id_6178	ids4-like protein	0.0008	-1.53	0.29
id_12815	ring zinc finger protein	0.0081	-1.52	0.18
id_14902	---NA---	0.0046	-1.51	0.03
id_4751	catalytic cation binding hydrolyzing o-glycosyl compounds	0.0030	-1.50	0.49
id_13242	protein phosphatase	0.0032	-1.50	0.42
id_3583	adp ribosylation factor 1 gtpase activating protein	0.0034	-1.50	1.00
id_4614	aaa-type atpase family protein	0.0067	-1.50	0.04
id_8597	rwp-rk domain-containing protein	0.0100	-1.49	0.14
id_6394	dna rna binding protein	0.0003	-1.49	0.14
id_12334	splicing factorsubunit66kda	0.0017	-1.49	0.22
id_7106	small heat shock protein	0.0053	-1.48	0.09
id_16566	atm (ataxia-telangiectasia mutated)	0.0012	-1.48	0.20
id_9937	vesicle-associated membranesynaptobrevin 7b	0.0093	-1.48	0.21
id_3151	atnudt23 (arabidopsis thaliana nudix hydrolase homolog 23) hydrolase	0.0092	-1.47	0.14
id_10371	msp1 intramitochondrial sorting	0.0051	-1.47	0.16
id_4603	snrnp protein	0.0035	-1.46	0.20
id_5202	chloroplast unusual positioning 1a	0.0066	-1.46	0.37
id_6364	pol protein serine threonine phosphatase	0.0007	-1.45	0.22
id_15086	ring-h2 finger proteinexpressed	0.0041	-1.45	0.13
id_19867	cytochrome p450	0.0090	-1.45	0.29
id_17911	ring-h2 finger proteinexpressed	0.0001	-1.45	0.22
id_14447	ubiquitin related modifier 1 homolog	0.0094	-1.45	0.18
id_14083	p-hydroxybenzoate polyprenyltransferase	0.0077	-1.44	0.44
id_14846	dihydrolipoamide dehydrogenase precursor	0.0069	-1.44	-0.28
id_20019	gdsl-motif lipase hydrolase family protein	0.0083	-1.43	0.23
id_19157	cellulose synthase-like proteinsle1	0.0055	-1.43	0.29
id_4473	catalase	0.0069	-1.43	-0.09
id_15580	---NA---	0.0051	-1.42	0.25
id_8319	MtN3 protein precursor	0.0024	-1.42	0.26
id_1288	---NA---	0.0052	-1.42	0.17
id_7996	boron transporter	0.0093	-1.41	-0.01
id_2788	protein phosphatase type 1	0.0041	-1.41	0.19
id_6950	cytochrome c oxidase subunit	0.0020	-1.41	0.22
id_8694	erwinia induced protein 2	0.0073	-1.40	-0.05
id_17233	protein	0.0083	-1.40	0.01
id_5872	membrane receptor-like protein 1	0.0058	-1.39	-0.30
id_19630	photosystem ii phosphoprotein	0.0001	-1.39	0.27
id_6193	---NA---	0.0041	-1.39	0.37
id_3858	---NA---	0.0091	-1.38	0.06
id_4000	adp-ribosylation factor	0.0096	-1.37	0.32
id_15667	vhs and gat domain protein	0.0022	-1.37	0.12
id_1087	succinyl--ligase alpha subunit	0.0019	-1.37	0.51
id_4346	---NA---	0.0022	-1.37	0.27

id_16332	dna repair protein rad23	0.0060	-1.36	0.52
id_11702	cdc2 protein kinases-like	0.0100	-1.36	0.68
id_9206	voltage-dependent anion channel	0.0038	-1.35	0.17
id_14033	mannose-1-phosphate guanyltransferase	0.0084	-1.35	0.30
id_12028	---NA---	0.0065	-1.35	-0.01
id_11940	polyphenol oxidase	0.0054	-1.35	0.25
id_18805	---NA---	0.0069	-1.34	-0.25
id_6709	beta-galactosidase	0.0006	-1.34	-0.03
id_18724	cytochrome p450	0.0027	-1.33	0.03
id_9522	disease resistance protein r3a-like protein	0.0047	-1.33	0.19
id_3790	cysteine synthase	0.0052	-1.32	0.39
id_11794	smc2 protein	0.0048	-1.32	-0.24
id_10965	glutamyl-trna synthetase	0.0035	-1.32	0.49
id_16095	---NA---	0.0071	-1.31	0.18
id_19008	---NA---	0.0046	-1.31	0.19
id_19944	60s ribosomal protein l22-2	0.0049	-1.30	0.26
id_16550	acch1_arathame: full=1-aminocyclopropane-1-carboxylate oxidase homolog 1	0.0050	-1.29	0.43
id_8398	histone h2b	0.0033	-1.29	-0.03
id_13457	allyl alcohol dehydrogenase-like protein	0.0061	-1.28	0.65
id_12317	peptidylprolyl isomerase	0.0048	-1.27	0.05
id_13494	auxin response factor 3	0.0050	-1.27	0.29
id_1049	---NA---	0.0099	-1.27	0.48
id_18451	---NA---	0.0061	-1.27	0.11
id_12526	nod26-like major intrinsic protein	0.0020	-1.27	-0.18
id_3486	squalene epoxidase	0.0078	-1.27	0.02
id_19879	---NA---	0.0045	-1.27	0.40
id_2126	mitochondrial import receptor subunit tom20	0.0052	-1.26	0.51
id_7849	---NA---	0.0095	-1.26	0.21
id_12725	mate efflux familyexpressed	0.0048	-1.25	-0.02
id_9314	at1g15070 f9l1_1	0.0006	-1.24	0.09
id_5608	rna-binding protein	0.0098	-1.24	0.12
id_15339	40s ribosomal protein s28	0.0001	-1.23	0.25
id_1331	---NA---	0.0061	-1.22	0.12
id_11056	nucleosome chromatin assembly factor a	0.0013	-1.22	0.35
id_9586	---NA---	0.0076	-1.22	0.08
id_11368	wd repeat domain 46	0.0011	-1.22	0.44
id_2104	transcription factor btf3 - modulated by Pto and ERF genes	0.0052	-1.21	0.25
id_20002	40s ribosomal protein s9	0.0064	-1.21	-0.05
id_3012	6-phosphogluconolactonase-like protein	0.0015	-1.21	0.01
id_9029	acetylglutamate kinase	0.0002	-1.20	-0.08
id_5807	cyp	0.0004	-1.20	0.29
id_12607	---NA---	0.0096	-1.20	0.09
id_13453	btb poz domain-containing protein	0.0030	-1.20	0.66
id_3904	c-x8-c-x5-c-x3-h type zn-finger	0.0002	-1.18	0.45
id_5543	---NA---	0.0068	-1.18	0.04
id_6084	spla ryanodine receptordomain-containing	0.0096	-1.18	0.32

	protein			
id_14311	cyclophilin	0.0063	-1.17	-0.11
id_8878	luminal binding protein	0.0025	-1.17	0.04
id_2998	gns1 sur4 membrane family protein	0.0018	-1.17	0.18
id_10841	---NA---	0.0028	-1.17	-0.09
id_16038	annexin-like protein	0.0082	-1.15	0.31
id_16218	rna polymerase beta subunit	0.0098	-1.15	0.06
id_7770	abc transporter-like	0.0068	-1.15	0.24
id_6321	adp-ribosylation factor	0.0099	-1.14	0.24
id_2605	src2 homolog	0.0053	-1.14	0.33
id_17797	---NA---	0.0049	-1.14	0.52
id_3887	tpl wsip1 (wus-interacting protein 1)	0.0093	-1.14	-0.09
id_16453	shikimate kinase family protein	0.0059	-1.13	-0.19
id_9662	burp domain-containing protein	0.0044	-1.13	0.36
id_18800	dnaj heat shock n-terminal domain-containing protein	0.0018	-1.13	0.01
id_3934	membrane steroid-binding protein 1	0.0043	-1.13	0.35
id_3277	---NA---	0.0077	-1.12	0.47
id_12685	---NA---	0.0060	-1.12	0.23
id_1754	---NA---	0.0031	-1.12	0.35
id_9259	---NA---	0.0085	-1.12	0.65
id_8026	catalase	0.0071	-1.11	0.51
id_18740	gaga-binding transcriptional activator	0.0046	-1.11	0.01
id_11097	protein kinase-like protein	0.0047	-1.09	0.16
id_15648	---NA---	0.0099	-1.08	0.01
id_7885	gh3 like protein	0.0060	-1.08	0.59
id_4243	axr1 (auxin resistant 1) small protein activating enzyme	0.0093	-1.08	0.26
id_9788	elongation factor 1-alpha	0.0075	-1.07	0.17
id_4320	glycosyl hydrolase family 17 protein	0.0072	-1.07	0.28
id_6121	---NA---	0.0027	-1.06	0.35
id_19561	---NA---	0.0041	-1.06	0.13
id_6940	zinc finger transcription factor-like protein	0.0003	-1.05	1.42
id_3768	---NA---	0.0059	-1.05	0.42
id_12897	---NA---	0.0070	-1.05	0.13
id_16148	zinc finger (ccch-type) family protein	0.0030	-1.03	0.16
id_18447	sugar transporter family protein	0.0038	-1.03	0.00
id_2862	cellulose synthase-likeglycosyltransferase family 2	0.0047	-1.03	0.46
id_15771	sialyltransferase-like protein	0.0007	-1.01	0.18
id_12850	secondary cell wall-related glycosyltransferase family 47	0.0052	-1.00	0.24
id_9260	---NA---	0.0076	-0.99	0.18
id_5607	---NA---	0.0040	-0.99	0.39
id_19516	---NA---	0.0057	-0.99	0.06
id_172	pyruvate kinase	0.0088	-0.98	0.10
id_1773	tetratricopeptide-like helical	0.0064	-0.97	0.45
id_9177	adenylate kinase	0.0059	-0.97	0.24
id_4949	at5g37360 mnj8_150	0.0024	-0.96	-0.09

id_19497	---NA---	0.0082	-0.95	0.46
id_2202	ccr4-associated factor	0.0029	-0.95	0.73
id_6529	cytidine deaminase	0.0029	-0.94	0.65
id_5520	heat shock protein	0.0097	-0.93	0.09
id_16110	s-domain receptor-like protein kinase	0.0078	-0.93	0.52
id_10977	ssy2_soltuame: full=granule-bound starch synthase chloroplastic amyloplasticame	0.0038	-0.92	0.19
id_6953	---NA---	0.0062	-0.86	0.28
id_13562	u2 snrnp auxiliary factor	0.0005	-0.86	-0.07
id_18072	---NA---	0.0053	-0.85	-0.03
id_19208	---NA---	0.0092	-0.82	0.03
id_19353	calcium-binding ef hand family protein	0.0080	-0.82	0.20
id_12699	---NA---	0.0055	-0.81	0.24
id_10605	zinc finger (ran-binding) family protein	0.0055	-0.81	0.17
id_9861	cp protein	0.0006	-0.75	0.56
id_4309	af462857_1at1g29350 f15d2_27	0.0011	-0.70	0.28
id_1972	pentatricopeptiderepeat-containing protein	0.0013	-0.68	0.37
id_9618	---NA---	0.0082	-0.62	0.23
id_15553	casein kinase	0.0044	-0.62	0.96
id_2933	transcription factor	0.0045	-0.62	0.48
id_5240	nodulin-like protein 5ng4	0.0079	-0.58	0.39
id_18735	xs domain containingexpressed	0.0085	-0.52	0.14
id_2056	f-box familyexpressed	0.0032	-0.47	0.25
id_11333	mitogen-activated protein kinase kinase	0.0042	-0.04	1.44
id_13631	aminoacyl-trna synthetase	0.0068	0.38	-0.37
id_15061	40s ribosomal protein s20	0.0076	0.46	-0.68
id_8564	---NA---	0.0082	0.61	-0.53
id_7224	ubiquitin conjugating enzyme	0.0085	0.62	-0.45
id_12880	elongation factor 1 gamma-like protein	0.0037	0.66	-0.41
id_3821	---NA---	0.0056	0.67	0.05
id_326	peroxidase 1	0.0050	0.69	-0.12
id_4358	far-red impaired responseprotein	0.0055	0.74	0.09
id_12983	---NA---	0.0028	0.75	-0.46
id_8089	protein kinase	0.0078	0.76	-0.25
id_16245	tyramine hydroxycinnamoyltransferase	0.0045	0.78	-0.02
id_4875	potyviral helper component protease-interacting protein 2	0.0084	0.83	-0.42
id_18756	cellulose synthase	0.0023	0.85	0.00
id_18154	vacuolar sorting receptor	0.0089	0.85	-0.53
id_19776	subtilisin-like protease	0.0087	0.88	-0.21
id_12835	major latex-like protein	0.0092	0.88	-0.54
id_16225	mycorrhiza-inducible inorganic phosphate transporter	0.0032	0.90	-0.24
id_8970	filamentation temperature-sensitive h 2b	0.0056	0.90	0.07
id_14738	ankyrin repeat family protein	0.0009	0.91	0.23
id_10591	cullin 3b	0.0045	0.93	-0.56
id_15103	nua (nuclear pore anchor)	0.0032	1.00	-0.21
id_12366	auxin-induced saur-like protein	0.0061	1.01	-1.04

id_17015	udp-galactose 4-epimerase-like protein	0.0040	1.01	-0.53
id_19246	c-4 sterol methyl oxidase	0.0022	1.02	0.08
id_11299	---NA---	0.0009	1.02	-0.15
id_6089	2-oxoglutarate-dependent dioxygenase	0.0035	1.03	-0.35
id_1763	tata-binding protein	0.0010	1.03	0.21
id_12820	gdsl-motif lipase hydrolase family protein	0.0045	1.05	-0.42
id_1349	kelch motif family protein	0.0075	1.06	-0.16
id_18701	---NA---	0.0096	1.07	0.06
id_2150	hipl1 proteinexpressed	0.0060	1.07	-0.10
id_9157	alcohol dehydrogenase	0.0008	1.08	-0.32
id_15140	3-hydroxy-3-methylglutaryl coenzyme a synthase	0.0037	1.09	0.25
id_13742	---NA---	0.0053	1.09	-0.17
id_19648	ypjb_ecoliame: full=uncharacterized protein ypjb	0.0066	1.11	-0.23
id_7587	acyl-oxidase acx3	0.0065	1.12	-0.53
id_11952	aldehyde dehydrogenase	0.0052	1.12	-0.30
id_6726	auxin-responsive protein	0.0036	1.13	-0.06
id_4177	ubiquitin	0.0030	1.13	-0.23
id_8675	---NA---	0.0008	1.14	-0.25
id_18821	microtubule-associated protein	0.0039	1.15	0.16
id_12986	---NA---	0.0079	1.15	-0.23
id_17483	peroxidase familyexpressed	0.0047	1.16	-0.36
id_12454	serine-threonine kinase	0.0089	1.17	0.06
id_6961	---NA---	0.0054	1.17	0.03
id_7658	---NA---	0.0079	1.18	0.18
id_6248	protein kinase-like protein	0.0030	1.18	-0.27
id_11350	glycosylphosphatidylinositol anchor biosynthesis protein 11	0.0035	1.20	0.11
id_647	arf8	0.0047	1.21	0.06
id_13021	acyl-acp thioesterase	0.0083	1.21	-0.37
id_4506	non-specific lipid transfer protein	0.0019	1.21	0.15
id_2263	---NA---	0.0054	1.22	0.25
id_9787	chloroplastic quinone-oxidoreductase	0.0059	1.22	-0.53
id_3148	mfs family transporter: sugar (sialic acid)	0.0000	1.22	0.18
id_19170	cyclase dehydrase	0.0033	1.23	0.06
id_8	acid phosphatase	0.0097	1.23	-0.22
id_1509	tetratricopeptide repeat-containing protein	0.0019	1.24	0.35
id_10774	mynd finger familyexpressed	0.0082	1.24	-0.08
id_8074	protein kinase family protein	0.0053	1.25	0.00
id_8932	mrp-like abc transporter	0.0005	1.25	0.04
id_11408	---NA---	0.0075	1.26	-0.11
id_14082	orcinol o-methyltransferase	0.0086	1.27	-0.34
id_6296	---NA---	0.0018	1.29	-0.09
id_7433	nitrate transporter	0.0073	1.30	0.10
id_17351	---NA---	0.0097	1.30	-0.34
id_2449	protein - similar to sigma factorb di ricinus (FASTA33)	0.0019	1.31	0.00
id_14395	---NA---	0.0079	1.31	-0.14

id_4873	fringe-related protein	0.0041	1.32	0.18
id_18350	---NA---	0.0060	1.33	0.06
id_20018	glycine-rich rna-binding protein	0.0060	1.33	0.05
id_7706	---NA---	0.0094	1.33	0.16
id_3564	dna-directed rna polymerase ii largest subunit	0.0092	1.34	0.40
id_16137	---NA---	0.0028	1.34	-0.10
id_19329	---NA---	0.0072	1.34	0.11
id_14114	---NA---	0.0022	1.35	-0.35
id_8495	plas_sollcame: full=chloroplastic flags: precursor	0.0061	1.36	-0.47
id_8420	anthranilate phosphoribosyltransferase	0.0082	1.36	-0.23
id_2059	galactose kinase	0.0021	1.36	-0.22
id_8283	dcl2 (dicer-like 2) atp-dependent helicase ribonuclease iii	0.0059	1.38	0.11
id_15832	at4g01050 f2n1_31	0.0032	1.38	0.20
id_16956	at5g03870 - shows some alignment with b3 TF	0.0064	1.38	-0.11
id_8524	proteinase inhibitorserpin emp24 gp25l p24	0.0077	1.39	-0.01
id_17225	---NA---	0.0053	1.39	-0.01
id_19007	rubisco subunit binding-protein alpha subunit	0.0076	1.39	-0.50
id_15397	chloroplastic quinone-oxidoreductase	0.0084	1.39	0.09
id_97	rna recognition motif-containing protein	0.0065	1.39	-0.12
id_18536	proline transporter	0.0027	1.39	-0.03
id_13169	hexokinase 2	0.0034	1.40	-0.17
id_11902	fructose-bisphosphatase precursor	0.0009	1.43	-0.01
id_19468	---NA---	0.0034	1.44	0.08
id_8273	dna methyltransferase zmet4	0.0025	1.44	-0.11
id_7705	---NA---	0.0039	1.44	-0.01
id_12100	purine permease	0.0000	1.45	0.01
id_2026	---NA---	0.0038	1.46	0.02
id_8330	wrky dna-binding protein	0.0079	1.46	-0.31
id_3418	---NA---	0.0085	1.46	-0.47
id_9049	pentatricopeptiderepeat-containing protein	0.0056	1.46	0.24
id_17030	---NA---	0.0070	1.47	0.28
id_831	aspartic protease	0.0007	1.47	-0.05
id_15291	plastid alpha-amylase	0.0054	1.48	-0.33
id_6565	lipid transfer protein	0.0082	1.49	-0.17
id_19375	phd-finger family homeodomain protein	0.0060	1.50	-0.22
id_15785	by genscan and genefinder	0.0017	1.50	0.07
id_724	en spm-like transposon protein	0.0015	1.51	-0.33
id_12682	---NA---	0.0047	1.51	-0.45
id_9630	atp-dependent clp protease atp-binding subunit1	0.0049	1.51	0.04
id_18565	atp-dependent helicase	0.0070	1.52	-0.17
id_4302	domain containingexpressed	0.0032	1.52	-0.02
id_7514	---NA---	0.0057	1.53	-0.22
id_15943	2-oxoglutarate-dependent dioxygenase	0.0002	1.53	0.07
id_1067	high-affinity potassium transporter	0.0055	1.55	-0.02
id_8115	pglr_sollcame: full=polygalacturonase-2	0.0059	1.55	-0.20
id_19904	photosystem ii reaction center w protein	0.0094	1.57	0.18

id_16989	dna-binding related protein	0.0022	1.58	0.25
id_9476	transferring glycosyl groups	0.0008	1.58	-0.63
id_2487	inositol polyphosphate 5-phosphatase i	0.0018	1.58	0.46
id_9556	kpya_tobacame: full=pyruvate kinase isozymechloroplastic flags: precursor	0.0084	1.60	-0.58
id_5933	---NA---	0.0048	1.60	-0.29
id_8791	nadh-ubiquinone oxireductase	0.0089	1.61	-0.49
id_3552	jasmonate zim-domain protein 1	0.0083	1.61	-0.02
id_9719	cbs domain containingexpressed - cystathionine beta synthase domain	0.0089	1.66	-0.01
id_15682	---NA---	0.0011	1.66	-0.10
id_5379	myb transcription factor-like	0.0088	1.66	0.17
id_6261	p-p-bond-hydrolysis-driven protein transmembrane transporter	0.0018	1.68	-0.01
id_9799	transformer-sr ribonucleoprotein	0.0032	1.68	-0.11
id_7894	protein kinase	0.0028	1.69	0.12
id_1935	at4g30400 f17i23_260	0.0029	1.69	0.18
id_8614	branched-chain-amino-acid aminotransferasechloroplastexpressed	0.0063	1.69	-0.15
id_13625	rad23-like protein	0.0009	1.71	0.17
id_7806	retrotransposonty3-gypsy subclass	0.0071	1.71	-0.57
id_16984	ras-related gtp-binding protein	0.0052	1.72	-0.01
id_9214	elicitor-inducible cytochrome p450	0.0011	1.72	0.25
id_2789	2 family protein	0.0039	1.73	0.17
id_10909	---NA---	0.0066	1.74	0.22
id_14926	at3g58640 f14p22_230	0.0068	1.75	0.24
id_14976	f-box domain-containing protein	0.0041	1.78	-0.20
id_8583	aldo keto reductase	0.0030	1.78	-0.16
id_11500	ac069473_15ras-related gtp-binding 1694-2636	0.0014	1.81	0.26
id_5237	esterase precursor	0.0063	1.83	0.15
id_19252	n-acylethanolamine amidohydrolase	0.0036	1.84	0.08
id_15139	lem3 (ligand-effect modulator 3) family protein cdc50 family protein	0.0061	1.85	-0.12
id_18217	pectin methylesterase	0.0065	1.86	0.34
id_17155	---NA---	0.0077	1.87	-0.32
id_6491	k+ channel protein	0.0083	1.87	0.03
id_8334	fructose-bisphosphatase precursor -indotto da fattori Pti assieme a btf3	0.0044	1.87	0.00
id_11086	snf7-like protein	0.0070	1.88	-0.10
id_2893	vatg2_tobacame: full=v-type proton atpase subunit g 2	0.0088	1.88	-0.04
id_4096	two-component response regulator-likeexpressed	0.0046	1.89	-0.05
id_19332	protein prenyltransferase alpha subunit-like	0.0069	1.89	-0.49
id_14997	protein kinase-like protein	0.0069	1.90	-0.10
id_6710	plasma membrane h+-atpase	0.0097	1.90	-0.28
id_14267	coatomer delta subunit (delta-coat protein) (delta-cop)	0.0058	1.91	0.21
id_12388	auxin-regulated protein	0.0036	1.96	-0.13
id_17939	---NA---	0.0018	1.97	-0.49

id_1739	---NA---	0.0055	1.97	-0.03
id_15058	phosphate transporter	0.0057	1.98	0.03
id_8151	elongation factor 1-alpha	0.0027	2.04	-0.20
id_17261	agenet domain-containing protein bromo-adjacent homologydomain	0.0007	2.04	-0.29
id_11625	elongation factor 2	0.0091	2.04	-0.05
id_5134	pleckstrin homologydomain-containing protein domain-containing protein	0.0029	2.05	0.07
id_18879	pollen specific protein	0.0037	2.13	0.22
id_8311	glycyl-trna synthetase	0.0014	2.29	0.09
id_2678	tropinone reductase	0.0048	2.31	0.36
id_4162	abortive infection protein	0.0012	2.31	0.37
id_18608	1-deoxy-d-xylulose 5-phosphate synthase	0.0002	2.33	0.04
id_7519	---NA---	0.0029	2.49	0.04
id_16354	fatty acid elongase-like protein (cer2-like)	0.0038	2.96	-0.29

Pubblicazioni e poster presentati

- Autori: Yang Zhang, Eugenio Butelli, Rosalba De Stefano, Henk-Jan Schoonbeek, Andreas Magusin, Chiara Pagliarani, Nikolaus Wellner, Lionel Hill, Diego Orzaez, Antonio Granell, Jonathan Jones & Cathie Martin.
  Titolo: Anthocyanins double the shelf life of tomatoes by inhibiting processes late in ripening and increasing resistance to grey mould. In submission.

- Autori: Antonio Di Matteo, Adriana Sacco, Rosalba De Stefano, Luigi Frusciante, and Amalia Barone (2011). Comparative transcriptomic profiling of two tomato lines with different ascorbate content in the fruit. Biochemical Genetics, 50:908-921
  DOI 10.1007/s10528-012-9531-3

- Autori: R. De Stefano, B. Greco, A. Di Matteo and A. Barone (2010).
  Titolo: Genetic and physiological characterization of tomato genotypes for drought tolerance.Minerva Biotecnologica (2010), *22 (2 suppl. 1): 27-9*

- Poster presentato al 55th Annual Congress (AGI-SIBV-SIGA), tenutosi in data: 19 – 22 settembre 2011
  Autori: Vasco M., De Stefano R., Di Matteo A., Punzo B., Lotti C., Ricciardi L., Barone A.
  Titolo: Candidate genes controlling fruit quality in a tomato introgression line tolerant to water deficit.
  Codice identificativo: ISBN 978-88-904570-2-9

- Comunicazione orale presentato a “The 7th Solanaceae Conference Dundee”, tenutosi in data: 5 - 9 settembre 2010
  Autori: Antonio Di Matteo, Vasco Maria, Rosalba De Stefano, Concetta Lotti, Luigi Ricciardi, Amalia Barone
  Titolo: Genetic control of fruit quality traits in tomato plants under water deficiency

- Poster presentato alle XV Giornate Scientifiche organizzate dal Polo della Scienza, tenutesi in data 24 - 26 novembre 2010
  Autori: Rosalba De Stefano, Barbara Greco, Valentino Ruggieri, Adriana Sacco, Amalia Barone, Antonio Di Matteo
  Titolo: Identificazione di geni coinvolti nell’accumulo di antiossidanti nel frutto di pomodoro usando risorse genetiche e genomiche

- Poster presentato al 1er Workshop y 4to Tecnologia de Recursos Naturales, Universidad de La Frontera, Sede Pucòn, tenutosi in data 23 november 2009
  Autori: Greco B, De Stefano R., Reyes-Diaz M., Wulf-Zottele C., Di Matteo A., Mora Gil M. L. and Barone A.
  Titolo del poster: Genetic and Physiological Characterization of the Drought response in tomato.

- Poster presentati al 54th Annual Congress SIGA, tenutosi in data 27 - 30 settembre 2010

  1. Autori: Greco B; De Stefano R; Di Matteo A; Lombardi N; Guida G.; Giorio P.; Albrizio R; Barone A.

  Titolo: Drought Response in tomato: Molecular and Physiological Analysis

  Codice identificativo: (4.19) ISBN 978-88-904570-0-5

  2. Autori: Di Matteo A; Vasco M; De Stefano R.;Trotta N; Lotti C; Ricciardi L; Barone A.

  Titolo: Transcriptomic Analysis of High Quality Fruit from an introgression line tolerant to water deficit

  Codice identificativo: (4.20) ISBN 978-88-904570-0-5

Anthocyanins double the shelf life of tomatoes by inhibiting processes late in ripening and increasing resistance to grey mould

Yang Zhang[1], Eugenio Butelli[1], Rosalba De Stefano[2], Henk-Jan Schoonbeek[1], Andreas Magusin[1], Chiara Pagliarani[3], Nikolaus Wellner[4], Lionel Hill[1], Diego Orzaez[5], Antonio Granell[5], Jonathan DG Jones[6]& Cathie Martin[1]*

[1]John Innes Centre, Norwich Research Park, Norwich, NR4 7UH, UK

[2]Department of Soil, Plant, Environmental and Animal Sciences, University of Naples "Federico II", Italy.

[3]Department of Agricultural, Forestry, and Food Sciences, University of Turin, via Leonardo da Vinci, 44 10095 Grugliasco (TO), Italy

[4]Institute of Food Research, Norwich Research Park, Colney, Norwich, NR4 7UA, UK

[5]Instituto de Biologı´a Molecular y Celular de Plantas (Consejo Superior de Investigaciones Científicas-Universidad Politécnica de Valencia), 46022 Valencia, Spain

[6]The Sainsbury Laboratory, Norwich Research Park, Colney, Norwich, NR4 7UH, UK

* Correspondence should be addressed to C.M. (cathie.martin@jic.ac.uk).

Anthocyanins double the shelf life of tomatoes by inhibiting processes late in ripening and increasing resistance to grey mould

Shelf life is a very important quality trait for many fruit, including tomatoes. We report that enrichment of anthocyanin, a natural pigment, in tomato can significantly extend shelf life. Processes late in ripening are suppressed by anthocyanin accumulation and resistance to *Botrytis cinerea*, one of the most important postharvest pathogens, is increased in purple tomato fruit. We show that resistance to *B.cinerea* is dependent specifically on the accumulation of anthocyanins which effectively quench the ROS burst during necotrophic pathogen infection. The increased antioxidant capacity of purple fruit slows the processes of over-ripening. Enhancing the levels of natural antioxidants in tomato provides a novel strategy for extending shelf life by genetic engineering or conventional breeding.

Important challenges for the cultivation of tomato include postharvest losses and reduced quality due to fruit senescence and pathogen infection. Most tomatoes grown for fresh consumption are picked when still firm and green, stored at low temperature and exposed to exogenous ethylene to induce colour and ripeness before reaching the supermarket shelf. Although effective in limiting postharvest losses, these procedures negatively affect tomato flavour, aroma and texture (*1*).The common use of mutants affected in ripening has similar negative impacts on flavour. Over the last two decades genetic engineering has been used to extend tomato shelf life, by modulating the activity of cell wall degrading enzymes (*2-5*) and enhancing metabolic pathways (*6, 7*).

Anthocyanins are water-soluble pigments responsible for the red, purple, and blue colours of many flowers and fruit (*8, 9*). They are produced by plants to attract pollinators and seed dispersers (*10*). Anthocyanin production is also induced under stress conditions *(11)* and infection by pathogens (*12*). Besides their physiological

roles in plants, dietary anthocyanins are associated with protection against certain cancers (*13*), cardiovascular diseases (*14*) and other chronic human disorders (*14*).

We have shown that, in tomato, ectopic expression of two transcription factors, *Delila* (*Del*) and *Rosea1* (*Ros1*), from snapdragon, under the control of the fruit-specific E8 promoter, results in increased expression of all the genes committed to anthocyanin biosynthesis to create intensely purple fruit (*15*). While growing the purple tomatoes, we observed that they had improved shelf life compared to wild type, red fruit. The shelf life of food is defined as the period during which a stored product remains suitable for consumption. Both fruit softening late during ripening and pathogen infection determine the shelf life of tomato. Purple fruit from *Del/Ros1* tomato plants have normal size, shape and number of seeds. However, purple fruit exhibit delayed ripening after breaker compared to red fruit. This was evident from the appearance of the fruit both on the vine and during postharvest storage and a reduced level of fungal infection of fruit under either condition **(Fig. 1A and 1B)**.

Both WT and purple tomatoes were harvested at the ripe stage and stored under sterile conditions. For purple fruit, ten weeks of storage were required to observe the levels of softening and shrivelling observed in red fruit at five weeks, indicating that expression of *Del* and *Ros1* can double the shelf life of tomato fruit (**Fig. 1C-D and fig. S1A-B**). These differences were accompanied by a smaller reduction in fresh weight during storage **(fig.S1E)** and a greater ability to resist tensile forces **(fig.S1F)** in purple tomatoes.

Production of ethylene, required for full ripening in climacteric fruit such as tomato, increased just after breaker and was 2-fold greater in purple fruit than controls (**fig. S2A**). Measurements of cuticle thickness showed no difference between WT and purple tomato (**fig.S2B-D**). In addition, Fourier Transformed Infra-Red (FT-IR) spectroscopy indicated there were no significant cell wall compositional changes in purple tomato peel compared to normal peel (**fig. S2E**). These observations implied that the extended shelf life of purple fruit was due neither to impaired ethylene production nor altered cuticle/peel composition.

The susceptibility of purple fruit to pathogens was investigated by infecting intact or

wounded tomatoes with *B.cinerea*, the causal agent of grey mould disease, one of the most important post-harvest pathogens of tomato. When intact fruit were sprayed with a *B.cinerea* spore suspension without wounding, the proportion of purple fruit showing severe symptoms of infection was substantially lower than for red fruit **(fig. S3)**. When wounded fruit were inoculated with the *B.cinerea* spore suspension, the size of the lesions did not increase one day post-inoculation (1dpi) in either fruit type, indicating that the fungus needs about 24 hours to establish following inoculation. From 2dpi, however, there was greater spread of infection in red fruit than in purple fruit. At 3dpi, the average size of the lesions in purple tomatoes was significantly smaller than in red fruit, indicating greater resistance to *B.cinerea* infection **(Fig. 1E)**. Quantitative PCR using DNA extracted from infected tomatoes confirmed that there was significantly more *Botrytis* growing on red fruit than on purple fruit at 3dpi **(Fig. 1F).** Enhanced pathogen resistance was also observed in purple fruit introgressed into the MoneyMaker genetic background **(fig. S4),** indicating that the greater resistance of purple tomatoes to *B.cinerea* is not dependent on a specific genetic background.

The susceptibility of tomato fruit to necrotrophic pathogens increases during ripening (*16, 17*). A correlation between late fruit ripening and increased susceptibility was observed in red fruit. However, in purple fruit, susceptibility to *B.cinerea* did not increase from the breaker stage when anthocyanin production was induced **(Fig. 1g)**. This observation suggested a direct role for anthocyanins in limiting the spread of fungal infection, as supported by the intermediate resistance displayed by two different *Del/Ros1* lines (C and Y) which produce lower levels of anthocyanins than line N (used for the initial tests) (*15*) (**fig. S5**).

To ensure that the effects on delayed ripening and pathogen resistance were compared at exactly the same developmental stage, virus-induced gene silencing (VIGS) was used to silence the expression of *Del* and *Ros1* in purple fruit in the MoneyMaker background (where large fruit size allows dissection of tissue sectors relatively easily). Agro-infiltrated *Del/Ros1* fruit showed a phenotype of purple and red sectors, the latter defining those parts of the fruit where *Del* and *Ros1* had been silenced (*18*) and hydrophilic antioxidant capacity was reduced **(Fig. 2A, B)**. In older fruit, the red sectors were clearly softer and the tissues were more collapsed than

purple sectors, indicating a shorter storage life of red sectors compared to purple sectors **(Fig. 2A)**. Red sectors showed no resistance to *B.cinerea* compared to purple sectors **(Fig. 2A)**.

Microarray analysis was used to compare gene expression profiles of red and purple sectors of VIGS-*Del/Ros1* fruit. Samples were harvested at 8, 30 and 45 days after breaker. A 3-fold difference in expression levels (purple vs red) was set as the threshold for significant changes detected using the TOM2 microarray. We identified 241 genes showing significant differences in expression between purple and red sectors in at least two stages **(Fig. 2C**). Functional annotation revealed that many of these genes are involved in primary and secondary metabolism, cell wall modification, oxidative stress and pathogen resistance **(fig. S6A and data S1)**. Reduced expression of many genes active in ripe fruit was observed in purple sectors **(Fig. 2D and fig. S6B-C)**, indicating that the suppression of expression of ripening-related genes in purple tomatoes contributes to the extended shelf life of the fruit.

The suppression of genes expressed late in ripening of purple fruit was confirmed by qRT-PCR. Two ripening related genes involved in cell wall softening, encoding polygalacturonase (*SlPG2a*) (*4*) and β-galactosidase (*SlTBG4*) (*5*), showed substantially lower expression in purple fruit during ripening **(fig. S7)**. The lower levels of gene expression resulted in lower total activities of polygalacturonase and β-galactosidase in purple tomatoes compared to red tomatoes **(Fig. 2E, F)**.

To identify the specific effects of anthocyanins on extension of shelf life, we silenced dihydroflavonol 4-reductase (*SlDFR*), a key gene in anthocyanin biosynthesis, by VIGS using purple tomatoes. On the same fruit, VIGS-*SlDFR* silenced, orange sectors showed similar *Del/Ros1* expression levels to non-silenced, purple sectors whereas *SlDFR* expression was significantly reduced **(Fig. 3A)**. Anthocyanin levels were reduced by 80% although other flavonoids accumulated in the silenced sectors giving silenced sectors their orange colour **(fig. S8).** *SlDFR*-silenced sectors were sensitive to *B.cinerea* whereas the purple sectors on the same fruit remained resistant (**Fig. 3B**). Compared to non-slienced sectors, *SlDFR*-silenced sectors had reduced hydrophilic antioxidant capacity (**Fig. 3C**) although this was higher than the

antioxidant capacity of WT red fruit, due to the accumulation of flavonols (**Fig. 2B**). Storage tests indicated *VIGS-DFR*-silenced fruit could be kept longer than WT fruit but not as long as purple tomatoes (**Fig. 3D**). We confirmed these observations by crossing *Del/Ros1* plants with the *aw* mutant of tomato, which lacks DFR activity and cannot make anthocyanins (*19*). In the F2, the plants that contained *Del/Ros1* but lacked DFR activity ($aw^{-/-}$) produced orange fruit due to high levels of flavonols. Like the *VIGS-SlDFR*-silenced sectors, the $aw^{-/-}$ *Del/Ros1* fruit had no greater resistance to *B.cinerea* than red tomatoes (**Fig. 3E**). The orange fruit had two-fold higher hydrophilic antioxidant capacity than the parental $aw^{-/-}$ line (**Fig. 3F**) and they could be kept longer, post-harvest, although not as long as purple tomatoes (**Fig. 3G**). Consequently, the delay in over ripening and the enhanced pathogen resistance of purple tomatoes are not due to off-targets of the Del and Ros1 transcription factors. Resistance to *B.cinerea* is specifically the result of the accumulation of anthocyanins whereas the delay in over-ripening is associated with the increased hydrophilic antioxidant capacity of fruit.

Levels of oxidative stress increase markedly in the later stages of ripening and may facilitate many of the metabolic changes associated with maturation of tomato fruit (*20*). Cultivars with short shelf life show reduced scavenging ability and increased levels of reactive oxygen species (ROS) (*21*). Accordingly, increasing antioxidant capacity or reducing levels of ROS using different antioxidants, can extend shelf life (*6, 22, 23*). Elevation of the levels of antioxidants in fruit may reduce the tissue-damaging activity of oxidative stress and is likely responsible for the delay in over-ripening observed in purple (*Del/Ros1*) and orange (*VIGS-SlDFR* and *Del/Ros1,*$aw^{-/-}$) tomatoes.

Malondialdehyde (MDA) is a by-product of lipid peroxidation and can be used to measure damage resulting from oxidative stress during tissue senescence (*21, 24*). MDA levels in red MicroTom fruit increase late in ripening. In purple tomatoes, however, MDA levels do not increase significantly up to four weeks after breaker (**Fig.4A**). Lower oxidative damage in purple tomato was associated closely with increased total antioxidant capacity during ripening, which resulted principally from the accumulation of anthocyanins (**Fig.4B**). The higher antioxidant capacity/ lower ROS levels were associated with suppression of ripening related enzyme activities,

an effect likely to be of importance in extending shelf life, since down-regulation of some of the corresponding genes by antisense results in fruit that are significantly firmer for longer than controls (*3, 5*). Induced expression of these genes, late in ripening, may be involve increases in ROS signalling. Our data suggest that ROS signalling is an important determinant of the rate of ripening, late in fruit development. High hydrophilic antioxidant capacity can suppress ROS signalling and activity, and delay the processes of over-ripening.

Resistance to *B.cinerea* is associated specifically with anthocyanin accumulation. Anthocyanin levels have been associated with resistance to *Botrytis* in grape (*25*), and may reduce post-harvest spoilage of fruits in general by *Botrytis*. When we grew *B.cinerea* on agar plates supplemented with red and purple fruit juice, neither extract inhibited the growth of the fungus **(Fig. 4C).** This indicates that anthocyanins do not suppress the growth of *B.cinrea* directly, and that the resistance requires living host cells. Between 24-48h post infection with *B.cinerea*, lesions on red fruit spread quickly, while on purple fruit their size remained small **(Fig.1E)**. 3,3'-Diaminobenzidine staining of infected red and purple fruits during this period showed that a ROS burst was generated at the infection site. However, the ROS burst on red fruit spread widely, whereas on purple fruit, strong ROS induction was restricted to the inoculation site (**Fig.4D**). The oxidative burst is thought to potentiate infection by necrotrophic pathogens that feed on dead tissue, facilitating the expansion of disease lesions (*26-28*). Vacuum infiltration of diphenyleneiodonium chloride (DPI), an NADPH oxidase inhibitor, into red fruit prior to *B.cinerea* inoculation, reduced the development of lesions, while infiltrating purple tomatoes with glucose and glucose oxidase, (which induce ROS, through the generation of H_2O_2), increased their susceptibility (**fig. S9**). In purple tomatoes, anthocyanins reduce the spreading of the ROS burst generated by *B.cinerea* infection, and limit the induction of cell death necessary for growth of the necrotroph.

In addition to their high nutritional value (*15*), anthocyanin-rich purple tomatoes have two-fold longer shelf life, the combined result of increased resistance to opportunistic pathogens and slower ripening at late stages. These traits are associated with the accumulation of anthocyanins in tomatoes. Anthocyanins specifically enhance the tolerance of fruit to the ROS burst generated as part of necrotrophic infection, and so

increase resistance to *B.cinerea.* Accumulation of anthocyanins resulting in high hydrophilic antioxidant capacity reduces the increase in ROS levels, that occurs late in fruit development, and so suppresses the later stages of ripening (**Fig. 3F**). The association of slower ripening with elevated antioxidant capacity of fruit offers novel yet broad targets for breeders to extend the post-harvest shelf-life of fruit. Additionally, anthocyanins can be used to enhance the resistance of ripe fruit specifically to necrotrophic pathogens.

References:

1. E. Baldwin, A. Plotto, J. Narciso, J. Bai, Effect of 1-methylcyclopropene on tomato flavour components, shelf life and decay as influenced by harvest maturity and storage temperature. *J Sci Food Agric* **91**, 969 (Apr, 2011).
2. V. S. Meli *et al.*, Enhancement of fruit shelf life by suppressing N-glycan processing enzymes. *Proc Natl Acad Sci U S A* **107**, 2413 (Feb 9, 2010).
3. A. L. Powell, M. S. Kalamaki, P. A. Kurien, S. Gurrieri, A. B. Bennett, Simultaneous transgenic suppression of LePG and LeExp1 influences fruit texture and juice viscosity in a fresh market tomato variety. *J Agric Food Chem* **51**, 7450 (Dec 3, 2003).
4. C. J. S. Smith *et al.*, Antisense RNA inhibition of polygalacturonase gene expression in transgenic tomatoes. *Nature* **334**, 724 (1988).
5. D. L. Smith, J. A. Abbott, K. C. Gross, Down-regulation of tomato beta-galactosidase 4 results in decreased fruit softening. *Plant Physiol* **129**, 1755 (Aug, 2002).
6. S. Nambeesan *et al.*, Overexpression of yeast spermidine synthase impacts ripening, senescence and decay symptoms in tomato. *Plant J*, (Jun 24, 2010).
7. D. C. Centeno *et al.*, Malate Plays a Crucial Role in Starch Metabolism, Ripening, and Soluble Solid Content of Tomato Fruit and Affects Postharvest Softening. *Plant Cell*, (Jan 14, 2011).
8. E. Grotewold, The genetics and biochemistry of floral pigments. *Annu Rev Plant Biol* **57**, 761 (2006).
9. A. Lytovchenko *et al.*, Tomato fruit photosynthesis is seemingly unimportant in primary metabolism and ripening but plays a considerable role in seed development. *Plant Physiol* **157**, 1650 (Dec, 2011).
10. Y. Shang *et al.*, The molecular basis for venation patterning of pigmentation and its effect on pollinator attraction in flowers of Antirrhinum. *New Phytologist*, no (2010).
11. K. S. Gould, Nature's Swiss Army Knife: The Diverse Protective Roles of Anthocyanins in Leaves. *J Biomed Biotechnol* **2004**, 314 (2004).
12. K. Lorenc-Kukula, S. Jafra, J. Oszmianski, J. Szopa, Ectopic expression of anthocyanin 5-o-glucosyltransferase in potato tuber causes increased resistance to bacteria. *J Agric Food Chem* **53**, 272 (Jan 26, 2005).
13. L. S. Wang, G. D. Stoner, Anthocyanins and their role in cancer prevention. *Cancer Lett* **269**, 281 (Oct 8, 2008).
14. T. Tsuda, F. Horio, K. Uchida, H. Aoki, T. Osawa, Dietary cyanidin 3-O-beta-D-glucoside-rich purple corn color prevents obesity and ameliorates hyperglycemia in mice. *J Nutr* **133**, 2125 (Jul, 2003).
15. E. Butelli *et al.*, Enrichment of tomato fruit with health-promoting anthocyanins by expression of select transcription factors. *Nat Biotechnol* **26**, 1301 (Nov, 2008).
16. D. Cantu *et al.*, Ripening-regulated susceptibility of tomato fruit to Botrytis cinerea requires NOR but not RIN or ethylene. *Plant Physiol* **150**, 1434 (Jul, 2009).
17. D. Cantu *et al.*, The intersection between cell wall disassembly, ripening, and fruit susceptibility to Botrytis cinerea. *Proc Natl Acad Sci U S A* **105**, 859 (Jan 22, 2008).
18. D. Orzaez *et al.*, A visual reporter system for virus-induced gene silencing in tomato fruit based on anthocyanin accumulation. *Plant Physiol* **150**, 1122 (Jul, 2009).
19. A. Goldsbrough, F. Belzile, J. I. Yoder, Complementation of the Tomato anthocyanin without (aw) Mutant Using the Dihydroflavonol 4-Reductase Gene. *Plant Physiol* **105**, 491 (Jun, 1994).
20. A. Jimenez *et al.*, Changes in oxidative processes and components of the antioxidant system during tomato fruit ripening. *Planta* **214**, 751 (2002).
21. K. Mondal, N. S. Sharma, S. P. Malhotra, K. Dhawan, R. Singh, Antioxidant Systems in Ripening Tomato Fruits. *Biologia Plantarum* **48**, 49 (2004).

22. T. Zidenga, E. Leyva-Guerrero, H. Moon, D. Siritunga, R. Sayre, Extending Cassava Root Shelf Life via Reduction of Reactive Oxygen Species Production. *Plant Physiol* **159**, 1396 (Aug, 2012).
23. A. Bhagwan, Y. N. Reddy, P. V. Rao, K. C. Mohankumar, Shelf life extension of tomato fruits by postharvest antioxidant application. *Journal of Applied Horticulture* **2**, 88 (2000).
24. R. S. Dhindsa, P. PLUMB-DHINDSA, T. A. THORPE, Leaf Senescence: Correlated with Increased Levels of Membrane Permeability and Lipid Peroxidation, and Decreased Levels of Superoxide Dismutase and Catalase. *Journal of Experimental Botany* **32**, 93 (February 1, 1981, 1981).
25. M. Iriti, M. Rossoni, M. Borgo, F. Faoro, Benzothiadiazole enhances resveratrol and anthocyanin biosynthesis in grapevine, meanwhile improving resistance to Botrytis cinerea. *J Agric Food Chem* **52**, 4406 (Jul 14, 2004).
26. J. Glazebrook, Contrasting mechanisms of defense against biotrophic and necrotrophic pathogens. *Annu Rev Phytopathol* **43**, 205 (2005).
27. E. M. Govrin, A. Levine, The hypersensitive response facilitates plant infection by the necrotrophic pathogen Botrytis cinerea. *Curr Biol* **10**, 751 (Jun 29, 2000).
28. N. Segmuller *et al.*, NADPH oxidases are involved in differentiation and pathogenicity in Botrytis cinerea. *Mol Plant Microbe Interact* **21**, 808 (Jun, 2008).
29. T. H. Yeats *et al.*, The fruit cuticles of wild tomato species exhibit architectural and chemical diversity, providing a new model for studying the evolution of cuticle function. *Plant J* **69**, 655 (Feb, 2012).
30. F. L. Stefanato *et al.*, The ABC transporter BcatrB from Botrytis cinerea exports camalexin and is a virulence factor on Arabidopsis thaliana. *Plant J* **58**, 499 (May, 2009).
31. R. C. Bugos *et al.*, RNA isolation from plant tissues recalcitrant to extraction in guanidine. *Biotechniques* **19**, 734 (Nov, 1995).
32. G. K. Smyth, Linear models and empirical bayes methods for assessing differential expression in microarray experiments. *Statistical applications in genetics and molecular biology* **3**, Article3 (2004).
33. J. Luo *et al.*, AtMYB12 regulates caffeoyl quinic acid and flavonol synthesis in tomato: expression in fruit results in very high levels of both types of polyphenol. *Plant J* **56**, 316 (Oct, 2008).

Online Methods:

Storage tests

WT (red) and *Del/Ros1* (purple) MicroTom fruits were harvested at 14 days post breaker (d0=14dpb). All fruits were sterilized in 10% bleach for 10 minutes, followed by rinsing three times in sterilized water and air-drying. Ten fruits were placed in one sterilized glass jar and kept at 18°C in the dark. Every week, the total weight of 10 fruits was measured and softening (**fig. 1A** and **B**) and shrivelling of fruit (**fig. 1C** and **D**) were calculated. After each measurement, fruits were transferred to a new sterilized jar.

Texture analysis

Mechanical tests were carried out with a Stable Microsystems TaXT2 texture analyzer (. A 0.5 mm diameter probe with a 45° conical tip was attached to the crosshead of the test machine. Skin penetration tests were carried out with a test speed of 0.1 mm/sec and a maximum penetration depth of 3 mm. Fruits were held in a small cup between two metal plates on the sample table.

The force-distance plots show typically two distinct regions. At the beginning there was an approximately linear increase of the force up to the bioyield point. At this point the skin was penetrated and the force reading suddenly dropped from its local maximum (fmax). After that, a second gradient was observed, which represented the penetration of the probe into the flesh.

The bioyield force (MPa) = $f_{max}/ (\pi R^2)$

R equals the radius of probe (0.25 mm)

To obtain the firmness of the fruit skin, the slope= $(f_{max}-f_0)/d_{max}$, (with: initial force (f_0), the bioyield force at the local maximum (fmax) and at distance (d_{max})) was divided by the area of the flat end of the probe tip.

$$\text{The firmness of fruits (MPa/mm)} = (f_{max}-f_0)/(d_{max}\times \pi R^2)$$

Scanning electron microscopy of tomato cuticle

Blocks of fruit pericarp tissue including peel were frozen in nitrogen slush at –190°C. Frozen samples were warmed to -100°C prior to fracture, and the specimens were then sputter-coated with platinum and examined in a Philips XL 30 FEG scanning electron microscope (SEM) fitted with a cold stage.

Measurement of cuticle thickness

Light microscope cuticle thickness measurements were modified from methods described previously(*29*). WT and purple fruit were sliced into 10-30 µm thick sections using sections were stained with Sudan red and thickness was determined by Leica DM6000 microscope, taking the average of 8-10 measurements(**fig. 2D**). The average and standard error of the mean of three to five biological replicates is reported.

FT-IR (Fourier Transform Infra-Red) spectroscopy of tomato peel

Tomato peel was obtained from ripe wild type and *Del/Ros1* tomato fruit carefully removing any attached flesh material. The material was washed sequentially with 1% (w/v) SDS in 50 mMTris-HCL pH 7.2, water, 50% ethanol, acetone and then air dried at room temperature. FT-IR spectra were recorded on a BioRad FTS175C (BioRad, now Varian) spectrometer equipped with a MCT detector and a Golden Gate single-reflection diamond ATR sampling accessory (Specac). Both the outer and inner sides of the peel were measured. The dry samples were gently pressed onto the ATR crystal, with either the inside or outside in contact with the crystal. For each spectrum, 128 scans at 2 cm^{-1} resolution were averaged and referenced against the empty crystal.

***Botrytis cinerea* infection**

B.cinerea (B05.10) was collected as described previously (*30*). Red and purple tomatoes were harvested 14 days after breaker and surface sterilized. Intact red and purple fruits were sprayed thoroughly with spores (2.5×10^5 spores/mL) three times in the fume cabinet and kept at 20°C, in high humidity. Infection symptoms were observed at 3dpi, 4dpi and 5dpi.

For wounding inoculation, the fungal culture was diluted with medium to 5×10^4 spores/mL (for MicroTom fruit) or 1×10^5 spores/mL (for MoneyMaker fruit) and inoculated for 1.5 h to stimulate germination. Fungal culture (5µL) was added to each wound. Lesion diameter was measured 24, 48 and 72 hours after inoculation. To quantify *Botrytis* growth using qPCR, half infected MicroTom fruits were harvested three days after inoculation. Seeds were removed from fruit samples which were then freeze dried. Tissues were homogenised with aTissueLyser and total DNA was extracted using Qiagen DNeasy Plant Mini Kit. DNA (50ng) was used for qPCR and the ratio of *B.cinerea Cutinase A*gDNA to tomato *ACTIN* gDNA was measured. The primers designed for genomic DNA were *SlACT*-q-F (ACAACTTTCCAACAAGGGAAGAT), *SlACT*-q-F (TGTATGTTGCTATTCAG GCTGTG), *BcCutA*-q-F (ATTCCACAATATGGCATGAAATC) and *BcCutA*-q-R (ATGTTATCTC ATGTTATCTC).

Growth tests of *B.cinerea* were performed on PDA plates. PDA medium was made up with 50% red or purple tomato juice. As a negative control, 15mg/mL Triademinol was added to PDA medium. Blocks of B05.10 mycelium (5mm diameter) were cut from a *B.cinerea* plate and placed in the cente of the test plates. Mycelial growth was measured daily. Streptomycin and ampicillin (100mg/L) were added to all the plates to prevent infection by other fungi or bacteria, respectively.

Virus Induced Gene Silencing (VIGS)

TRV-based silencing vectors pTRV1, pTRV2 and pTRV2-*Del/Ros1* were prepared as recorded previously (*18*).271bp of *SlDFR* cDNA was inserted into a pTRV2 gateway vector. Primers for gateway cloning are:

SlDFR-attB1
(GGGGACAAGTTTGTACAAAAAAGCAGGCTTAATTGATTTCATTAGCATCA) and

SlDFR-attB2
(GGGGACCACTTTGTACAAGAAAGCTGGGTACTGGCCATTTCTGTCGCAC).
Agroinfiltration of *Del/Ros1*MoneyMaker fruit was performed by syringe (*18*).

Microarrays

The TOM2 array was used to monitor changes in transcript levels. Total RNA was extracted from the red and purple sectors on *Del/Ros1* VIGS fruits, 8, 30 and 45 days after breaker (*31*). RNA amplification and aminoallyl labeling were performed by using the Message Amp™ aRNA kit (Ambion # AM1750). Microarray hybridisation, scanning and data analyses were performed as described previously(*9*): Telechem Hybridization Chambers (Corning) were employed for the manual hybridisation of labelled samples to the TOM2 long-oligo, 11,862 - gene, microarray. The GenePix 4000B scanner was used for scanning the microarray slides at 532 nm and 635 nm; with a resolution of 10 µm and 100% power. Images were quantified using the GenePix Pro 4.1 image analysis software (Axon Instruments/Molecular Devices). Valid spots were defined as having intensity values ≥2-fold the mean background intensity in ≥1 channel.

Normalisation and calculation of differential expression were performed in R (http://cran.r-project.org) using the Bioconductor libraries (http://www.bioconductor.org). Within-array normalisation was performed with the aim of making the background-subtracted log-ratios average to zero within each microarray. This was achieved by fitting a LOESS curve to each print tip (with the parameters smoothing filter = 0.4, iterations = 3; and δ = 0.01). The resulting data were then subject to a between-array normalisation step where the average

intensity values for each array were transformed such that they followed the same empirical distribution; while leaving the log-ratios unaffected. Differential expression was calculated by fitting a linear model for each gene across the microarrays(*32*) (where the contrasts were parameterised as differential gene expression between purple and red sectors, at 8, 30 and 45 days post-breaker respectively); the estimated coefficients were, in turn, computed from the fit; followed by computation of moderated *t*-scores and log-odds by empirical Bayes shrinkage of the standard errors towards a common constant. Genes exhibiting a fold-change of ≥3 and Benjamini Hochberg-adjusted *p*-values ≤ 0.05 were selected for further scrutiny.

RT-qPCR

RNA extraction and cDNA synthesis were conducted as described previously (*33*). Primers for RT-qPCR are listed in **table S1**.

Cell wall degrading enzyme activities

Red and purple tomatoes were washed, deprived of seeds and homogenized in liquid nitrogen. Homogenized sample (1g) was extracted with 3 mL of sodium acetate buffer (50 mM, pH 5.5, 1 M NaCl, 10 g/L polyvinyl-polypyrrolidone; PVPP) under agitation for 2h at 4°C, centrifuged at 1000 x g for 10 min and the supernatant collected. The supernatant then was dialyzed against sodium acetate buffer (50 mM, pH 5.0) overnight at 4°C.PG activity was measured[38] in a mixture containing 50 mM sodium acetate buffer pH 5.0, 0.15% (w/v) polygalacturonic acid, and 1 mL of enzyme extract, in a total volume of 3mL. The mixture was incubated at 37°C, aliquots of 300 µL were taken at different times, mixed with 1mL Borate buffer pH9 and 200µL 1% 2-cyanoacetamide (Sigma-Aldrich). To stop the reaction, the mixture was immersed in a boiling bath for 10 mins. Samples were cooled to room temperature and the OD 276 nm was measured. Results were expressed as delta OD in 1s under the assay conditions per kilogram of fresh fruit.β-Galactosidase (TBG) reaction mixture[38] consisted of 0.5 mL of 0.1 M citrate (pH 4.0), 0.4 mL of 0.1% BSA, 0.1 mL of enzyme extract, and 0.5 ml of 10 mM p-nitrophenyl-,B-galactoside. After 15 min at 37°C, the reactions were terminated by the addition of 2 mL of 0.4 M sodium carbonate, and the liberated p-nitrophenol was measured at 420 nm. Results were expressed as delta OD in 1s under the assay conditions per kilogram of fresh fruit.

Malondialdehyde measurements

Fruit pericarp (2.5g) was ground in 10 mL of 10 mM sodium phosphate buffer, pH 7.2 and then centrifuged at 2000g for 10 min. A sample of supernatant (100µL) was added to a 2mL

tube containing 0.4mL of distilled water, 0.25 mL of 20% (w/w) trichloroacetic acid, and 0.5 mL of 10 mM thiobarbituric acid. A control was run for each sample in which thiobarbituric acid was replaced by an equal volume of distilled water. The mixture was heated in a boiling water bath for 30 min and then centrifuged for 10 min at 2000g to remove haziness. The cleared samples were allowed to equilibrate to room temperature before the absorption at 532 nm was measured. The concentration of malondialdehyde (MDA) was calculated using its molar extinction coefficient of 156 mM^{-1} cm^{-1}.

Analysis and identification of anthocyanins and other phenylpropanoids

Freeze-dried tomato tissue (1g) was extracted with 50mL 80% MeOH overnight. Extracts were cleared by filtration through paper and then through a 0.22 mm membrane filter (Millipore). 30µL of the original sample were then diluted with 270µL 20% MeOH and centrifuged. Finally 20µL of the diluted sample were added to 180µL 20% MeOH in flat-bottomed inserts.

All samples were analysed on a Surveyor HPLC system attached to a DecaXPplus ion trap MS (both Thermo), using 10µL injections. Phenolics were separated on a 100×2mm 3µ Luna C18(2) column (Phenomenex) using the following gradient of acetonitrile versus 0.1% formic acid in water, run at 300µL.min^{-1} and 30°C: 0 min, 1% ACN; 4 min, 1% ACN; 23 min, 30% ACN; 30 min, 70% ACN; 30.5 min, 1% ACN; 37 min, 1% ACN.

Phenolics were detected by light absorbance collecting full spectra from 200-600 nm, and chromatograms at 280 nm and 500-550 nm both with 19nm band width. For positive electrospray detection, spectra from *m/z* 100-2000 and data-dependent MS2 of the most abundant precursor ions at collision energy of 35% and an isolation width of *m/z* 4.0 were collected. Dynamic exclusion was used to ensure that after two spectra had been collected for a precursor ion, it would be ignored for 0.5min in favour of the next most abundant ion. Spray chamber conditions were 50 units sheath gas, 5 units aux gas, 350°C capillary temperature, and 3.8kV spray voltage using a steel needle kit.

Acknowledgements

EB and CM were supported by the European Union FP6 FLORA project (FOOD-CT-01730), and YZ, EBand CM are supported by the European Union FP7 ATHENA collaborative project (Grant Agreement 245121). YZ is also supported by a Rotation Studentship from the John Innes Foundation. CM and EB were supported by the core strategic grant of the Biological and Biotechnological Science Research Council (BBSRC) to the John Innes Centre, and are currently supported by the Institute Strategic Program *Understanding and Exploiting Plant and Microbial Secondary Metabolism* (BB/J004596/1)from the BBSRC. EB was supported by a short-term EMBO fellowship for undertaking part of the research reported in this paper. H-JS was supported by grant BB/G042960/1 from BBSRC and the John Innes Foundation, AG and DO are supported by the FundaciónGenoma (Calitom project) and the Spanish Ministry of Science and Education (project BIO2010-15384).

Figure Legends

Figure 1.Accumulation of anthocyanins in tomato fruit delays late ripening process and enhances pathogen resistance.

(**A**) Wild type, red (i and ii) and transgenic, purple (iii and iv) tomato fruit were tagged during the initial stages of development and harvested and photographed at the end of the green stage (i and iii). The same fruit, stored at room temperature, were re-photographed after two months (ii and iv). Scale bar represents 2cm.

(**B**)Severe symptoms of opportunistic infection normally associated with over-ripe red wild type tomato fruit (left) were not observed in purple, *Del/Ros1* tomato fruit of the same age grown under identical greenhouse conditions (right). Scale bar shows 2cm.

(**C and D**) The purple fruits showed slower softening(**C**) and delayed drying (**D**)compared to wild type fruits. Error bars show the standard error of the mean (n=4). Fruits were harvested at 14 days post breaker (d0=14dpb).

(**E**) Symptoms of wounded red and purple fruits after inoculation with *B.cinerea* B05.10. White dots represent the lesion margin.

(**F**) Quantitative PCR revealed more *Botrytis* growing on the WT tomatoes than on purple fruit, 3dpi. *Botrytis* growth was calculated by comparing the ratio of *Botrytis* DNA to tomato DNA. Error bars show the standard error of the mean (n=3).

(**G**) The ripening-related increase in susceptibility to *Botrytis* did not occur in purple fruit. Lesion diameter was measured 3dpi. Error bars show the standard error of the mean (n≥3). Scale bar shows 2cm.

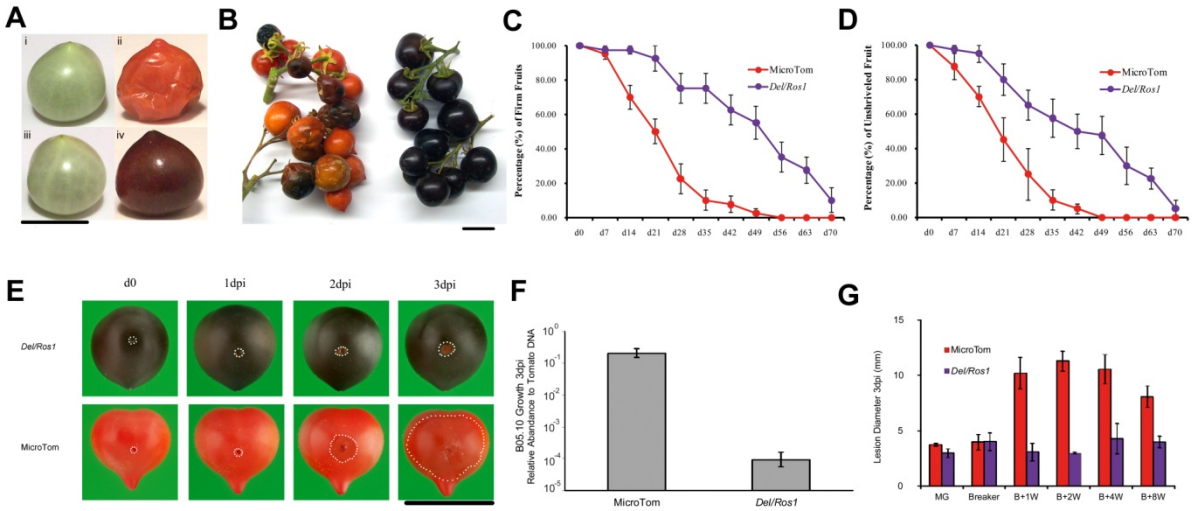

Figure 2. Delayed ripening and enhanced pathogen resistance are associated with the accumulation of anthocyanins.

(**A**) VIGS-*Del/Ros1*tomato fruits showed reduced accumulation of anthocyaninsin silenced areas, pictures were taken at 14 days after breaker (i). The red sectors showed quicker softening than purple sectors, pictures were taken at 42 days after breaker (ii). The purple sectors showed resistance to *B.cinerea* 3dpi(iii). The red sectors of VIGS-silenced tomatoes were susceptible to *B.cinerea*3dpi (iv). All scale bars, 2cm.

(**B**) VIGS-*Del/Ros1* silenced sectors have reduced antioxidant capacity.Error bars show the standard error of the mean (n=3). S = Silenced sectors; NS = Non-silenced sectors. Solid bars show hydrophilic antioxidant capacity, open bars show lipophilic antioxidant capacity.

(**C**) 241 genes were selected by showing>3-fold changes between the purple and red sectors ofVIGS-*Del/Ros1* silenced fruit for at least two time points.

(**D**) Numbers of differentially expressed genes at 8 dpb organised by functionality.

(**E and F**)Total polygalacturonase (**E**) and β-galactosidase (**F**) activities in the red and purple fruit at different stages during ripening. Error bars show the standard error of the mean (n=3).

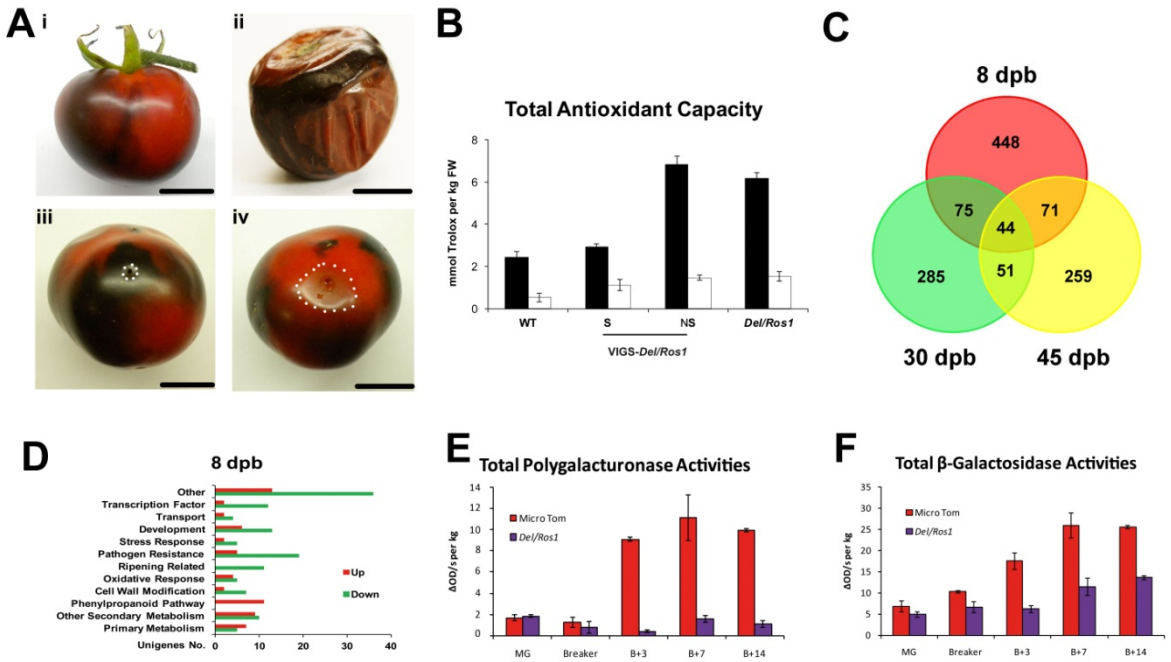

Figure 3.Inhibition of anthocyanin biosynthesis in purple tomatoes alters pathogen resistance and post-harvest storage.

(A) Comparison of gene expression (determined by qRT-PCR) in silenced and non-silenced sectors of VIGS-SlDFR fruit. Red and purple sectors showed similar expression of *Del* and *Ros1*, whereas *SlDFR* expression was significantly reduced in silenced sectors. Error bars show standard error of the mean, n=3.

(B) *SlDFR* silenced sectors lost resistance to *B.cinerea* whereas the non-silenced sectors on the same fruit still showed resistance. Pictures were taken at 3dpi. White dots indicate lesion sizes. Scale bars, 2cm.

(C) The total antioxidant capacity of *SlDFR*-silenced sectors was lower than non-silenced sectors, although still higher than of WT fruit (see Fig.3B) due to the accumulation of flavonols. Error bars show standard error of the mean, n=3. Solid bars show hydrophilic antioxidant capacity, open bars show lipophilic antioxidant capacity.

(D) Storage tests indicate *SlDFR*-silenced fruit can be kept for longer than WT fruit but for less time than non-silenced purple fruit. Fruit were harvested two weeks after breaker, and the times that silenced sectors took to show the symptoms of over-ripening (shrivelling and drying of tissue; **fig. S1**) was recorded. Error bars show standard error of the mean, n=7.

(E) High levels of flavonols accumulate in *Del/Ros1 aw*$^{-/-}$F2 tomato fruit obtained by crossing *Del/Ros1*MicroTom with *aw*$^{-/-}$ (*DFR*$^{-}$) mutants. The orange, flavonol enriched tomato (left) lost resistance to *B.cinerea*. Pictures were taken at 3dpi. White dots represent lesion size. Scale bars, show 2cm.

(F) Comparisons of antioxidant capacities of *aw*$^{-/-}$,*aw*$^{-/-}$*Del/Ros1*and *Del/Ros1*fruit. Error bars show standard error of the mean, n=3.Solid bars show hydrophilic antioxidant capacity, open bars show lipophilic antioxidant capacity.

(G) *aw-/- Del/Ros1* fruit had longer shelf life than parental *aw*$^{-/-}$fruit. Picture was taken four weeks after breaker. Scale bar shows 2cm. Top row shows *aw*$^{-/-}$ tomatoes, bottom row shows *aw*$^{-/-}$ *Del/Ros1* orange tomatoes.

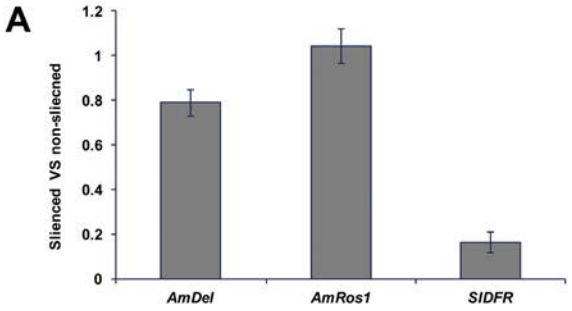
A
Silenced VS non-sliecned
1.2
1
0.8
0.6
0.4
0.2
0
AmDel
AmRos1
SlDFR

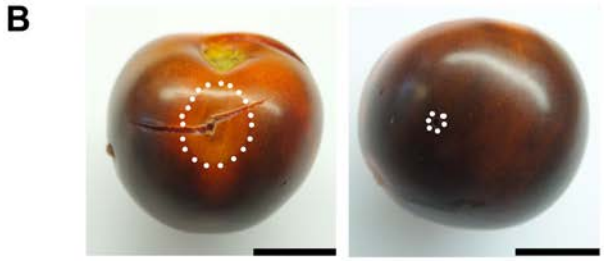
B

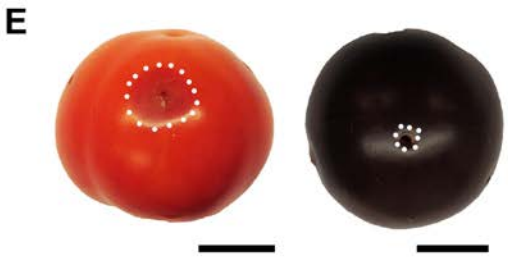
E

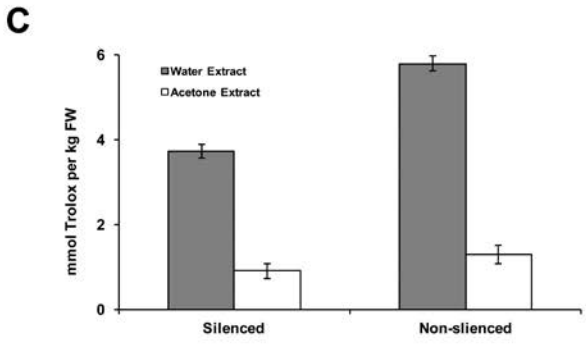
C
mmol Trolox per kg FW
6
4
2
0
Water Extract
Acetone Extract
Silenced
Non-slienced

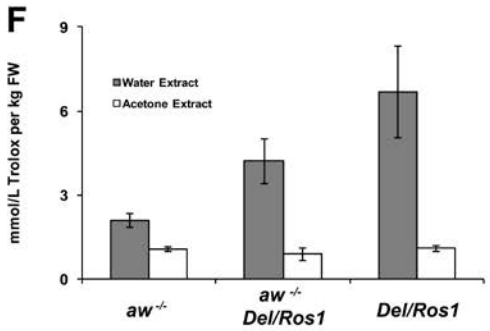
F
mmol/L Trolox per kg FW
9
6
3
0
Water Extract
Acetone Extract
aw -/-
aw -/-
Del/Ros1
Del/Ros1

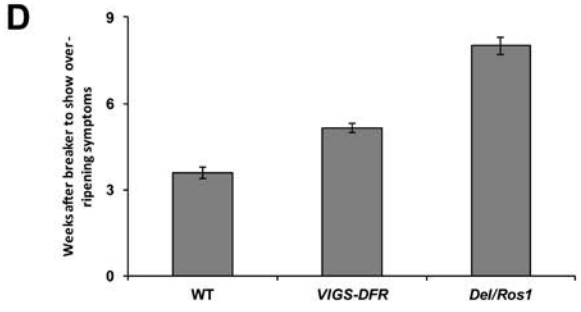
D
Weeks after breaker to show over-ripening symptoms
9
6
3
0
WT
VIGS-DFR
Del/Ros1

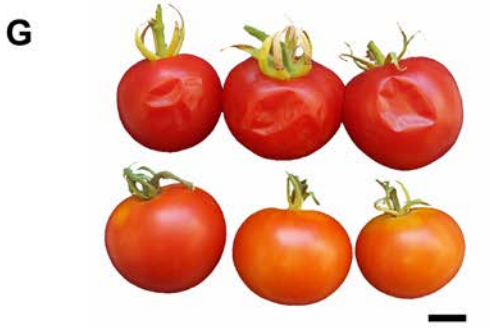
G

Figure 4. Extended shelf life in purple tomatoes is associated with their high antioxidant capacity.

(**A**) Malondialdehyde levels in pericarp of red and purple Microtom fruits during ripening. Error bars show the standard error of the mean (n=3).

(**B**) Trolox equivalent total antioxidant capacity (TEAC) of water extracts from red and purple tomatoes during ripening. Error bars show the standard error of the mean (n=3).

(**C**) Addition of juice from either red or purple tomatoes to the growth medium had no effect on growth of *B.cinerea*. PDA medium (i) and PDA with 15mg/L Triademinol (ii) PDA supplemented with 50% red juice (iii) and with 50% purple juice(iv). Pictures were taken three days after inoculation. Scale bars, 2cm.

(**D**) 3,3'-Diaminobenzidine staining of hydrogen peroxide produced 24 h after inoculation of *B.cinerea*: red (i) and purple (ii) fruits stained with DAB 24 h after inoculation, wound only red (iii) and purple (iv) fruit stained 24 h after wounding. Scale bars, 1mm.

(**E**). Model for the mechanism of shelf life extension in purple, high anthocyanin tomatoes.

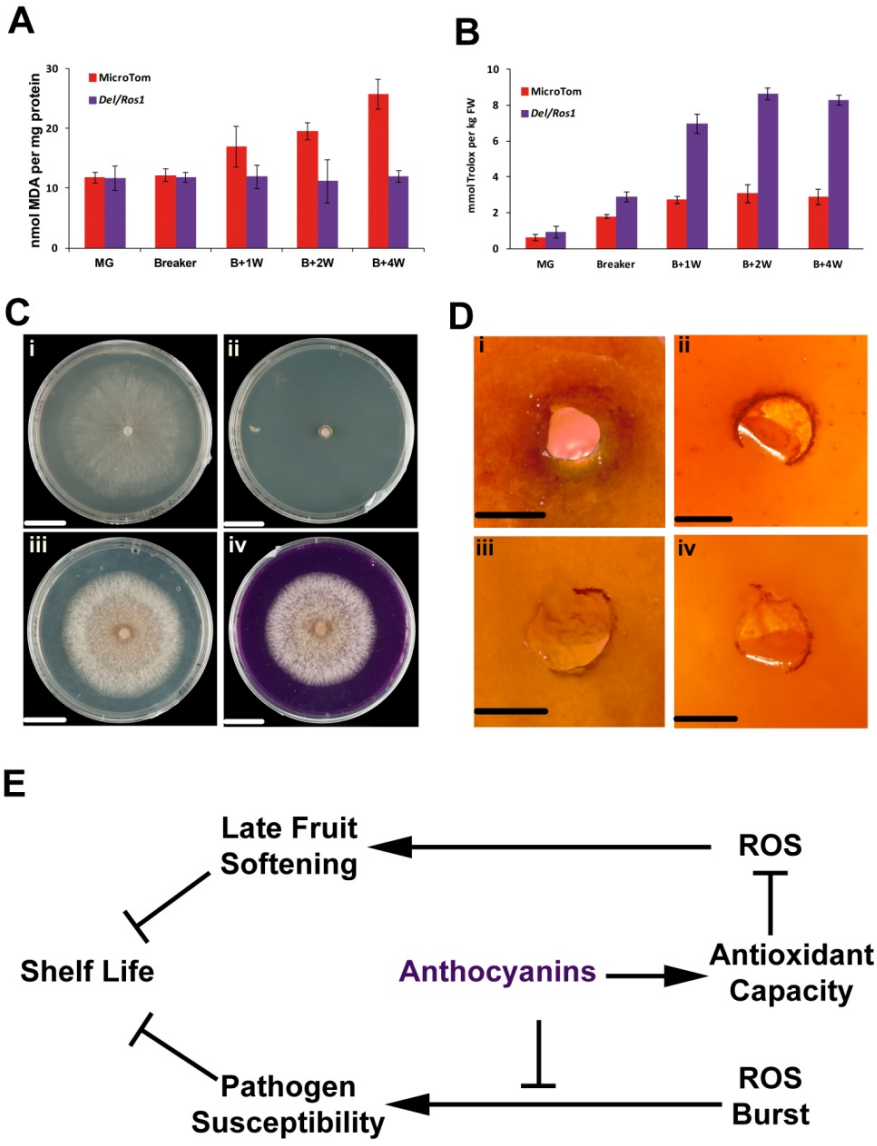

Figure S1.Purple fruit showed extended shelf life compared to red fruits.

(**A**-**D**) Phenotypes of red and purple fruit showing softening (**A** and **B**) and drying (**C** and **D**) during storage. All scale bars represent 2cm.

(**E**) Fresh weight losses during storage tests. Average values were calculated for four individual groups and error bars indicate the standard error of the mean (n=4). Fruits were harvested at 14 days post breaker (d0=14dpb).

(**F**) Texture strength changes in MicroTom and *Del/Ros1* fruits during storage tests. Average values were calculated for at least eight individual fruits and error bars indicate the standard error of the mean. Fruits were harvested at 14 days post breaker (d0=14dpb).

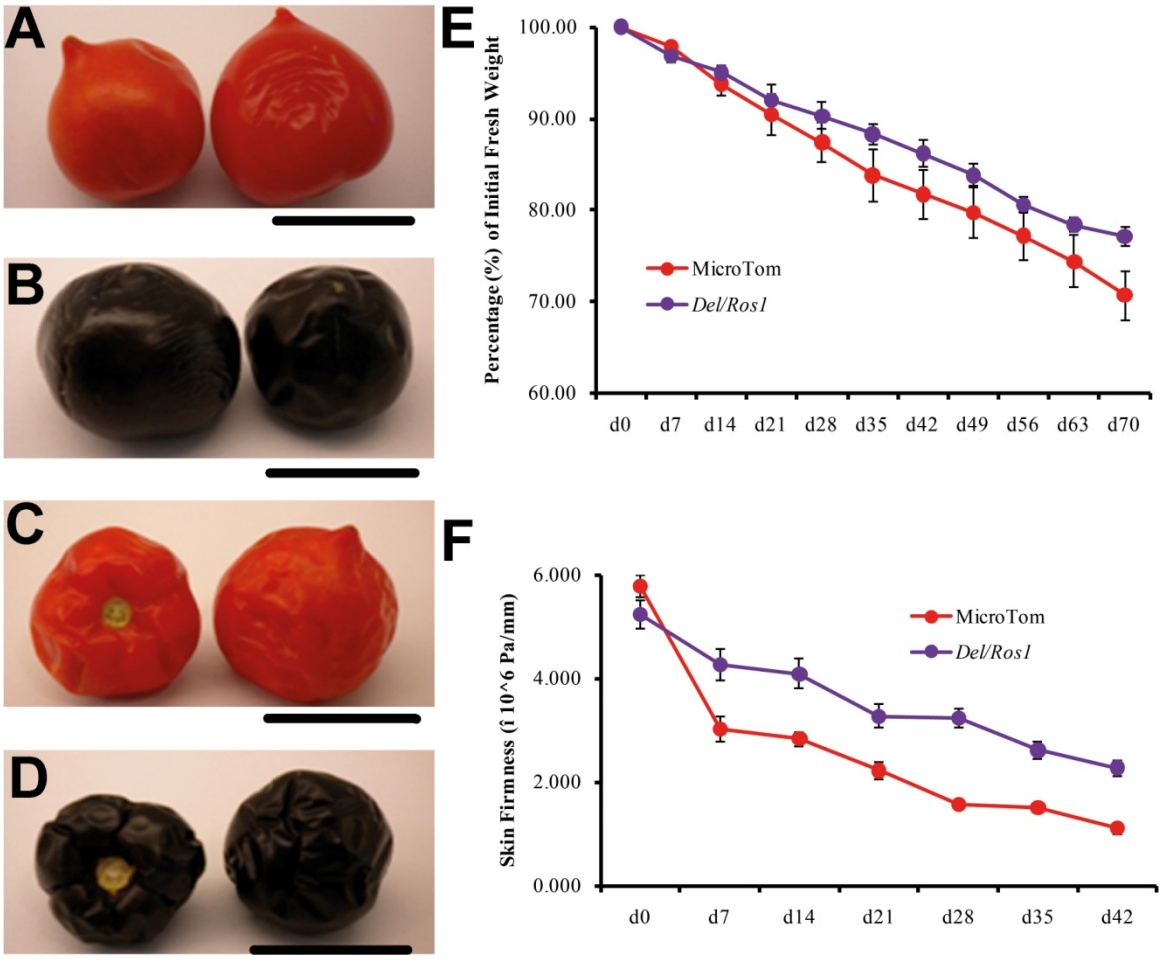

Figure S2. Extended shelf life in purple tomato is not due to impaired ethylene production or changes of cuticle structure.

(**A)** Ethylene production in red (○) and purple (●) tomato fruit during ripening. Data represent mean values ± se of at least ten individual fruits for each genotype.

(B)Freeze-fracture scanning electron microscopy (SEM) indicated no significant morphological changes to the peel of purple fruit. Arrows indicate cuticle. Scale bars represent 50µm.

(**C**) Cuticle thickness of purple and red tomatoes. Measurements were made above the centre of each epidermal cell as indicated by bars in (**D**). Error bars show the standard error of the mean (n≥3).

(**D**) Light micrographs of sections of the fruit surface of tomato stained with Sudan Red.Bars indicate cuticle thickness. Scale bars show 20 µm.

(**E**) FT-IR (Fourier Transformed Infra Red) spectra of wild type (**top**) and *Del/Ros1* (**bottom**) tomato peel. The analysis of the outer (**left**) and inner side (**right**) of the peel is shown.

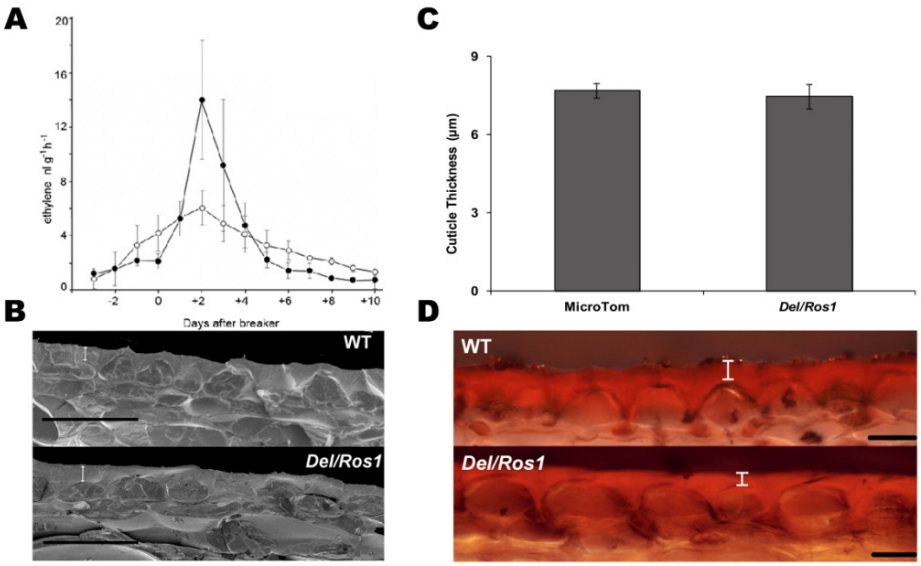

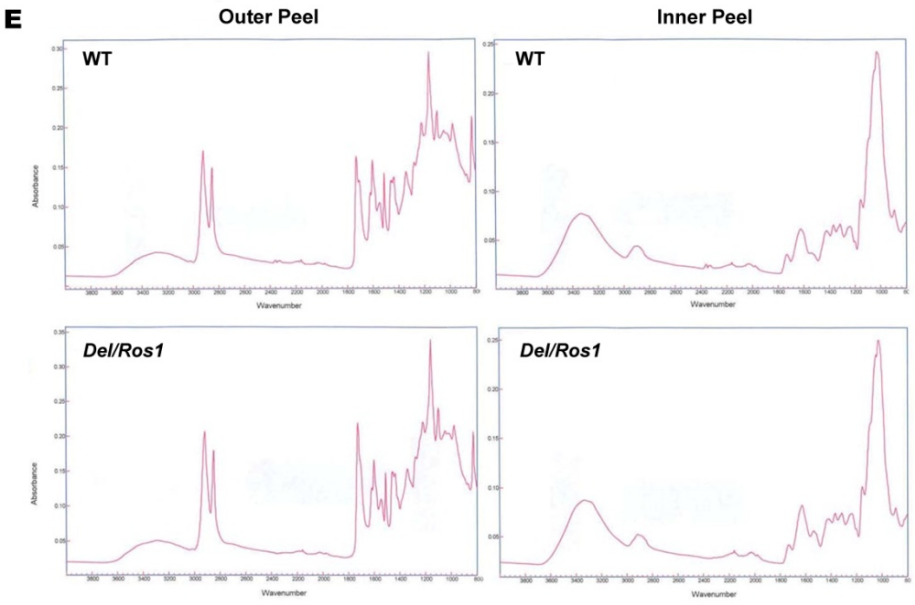

Figure S3. Intact purple fruit showed better resistance to *B.cinerea* than red fruit in spraying tests.

(**A-F**) Phenotypes of fruits showing resistance (**A** and **D**), partial resistance (**B** and **E**) and susceptibility (**C** and **F**) when sprayed with spores of *B.cinerea*, pictures were taken at 5dpi. All scale bars represent 2 cm.

(**G**) Percentages of the different degrees of resistance in red and purple fruit in spraying tests with *B.cinerea*. Fruit were checked 5 days after inoculation.

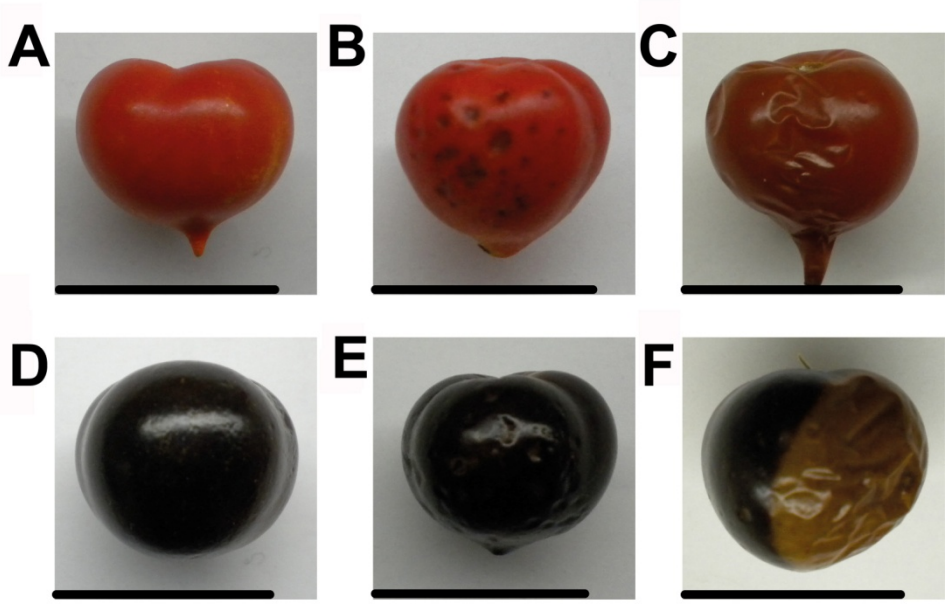

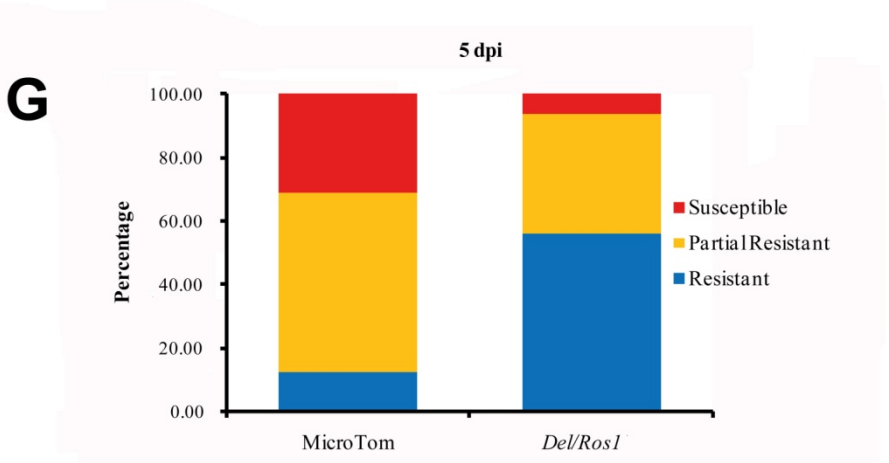

.

Figure S4. Accumulation of anthocyanins in the MoneyMaker genetic background also enhanced pathogen resistance.

(**A**) Phenotype of WT, red MoneyMaker fruit after *Botrytis* inoculation. Picture was taken at 3dpi. Scale bar represents 2cm.

(**B**) *Del/Ros1,* purple MoneyMaker fruit showed resistance to *B.cinerea*. Pictures were taken at 3dpi. Scale bar shows 2cm.

(**D**) Lesion development following *Botrytis* inoculation of red and purple fruits. Error bars indicate the standard error of the mean (n≥3).

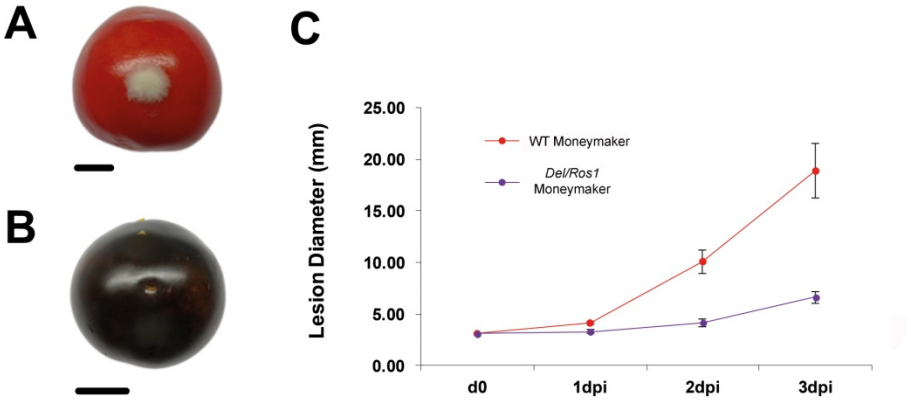

Figure S5. The strength of resistance to *B.cinerea* is associated with the levels of anthocyanins in fruits.

(**A**) Anthocyanin contents in different transgenic lines. Error bars represent the standard error of the mean (n=3).

(**B**) Trolox equivalent total antioxidant capacity of different transgenic lines. Error bars represent the standard error of the mean (n=3)

(**C**) Lesion development following *B.cinerea* inoculation. Error bars show the standard error of the mean (n=3)

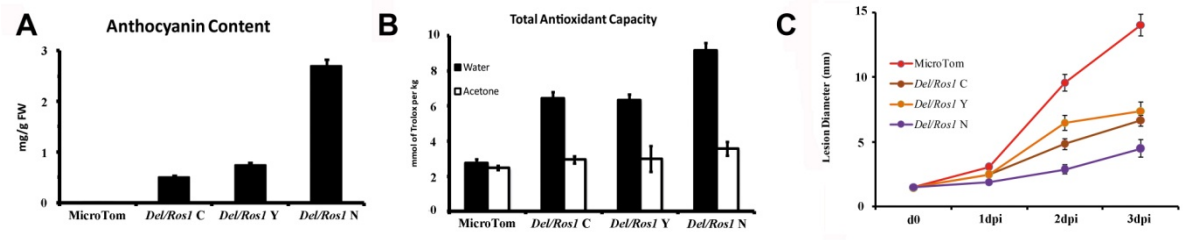

Figure S6.(**A**) Functional annotation of the 241 genes showing >3-fold differences in expression between purple and red sectors over at least two time points.

(**B** and **C**) Functional classification of selected differentially-expressed genes at 30 dpb (**B**) and 45 dpb (**C**).

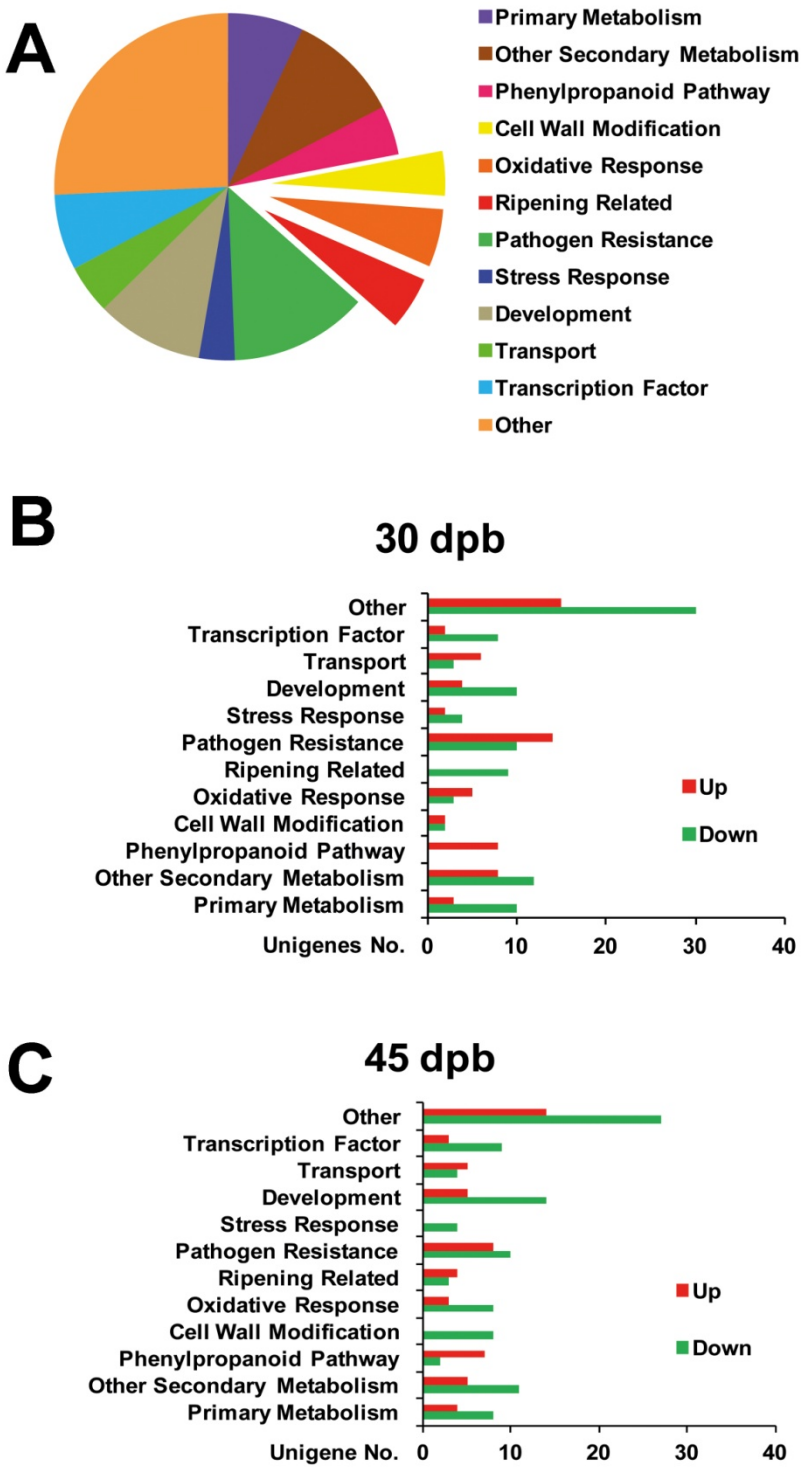

Figure S7. RT-qPCR analysis of ripening-related genes in WT and *Del/Ros1* fruits during ripening stages. (**A**) polygalacturonase 2a (*SlPG2a*), (**B**) β-galactosidase 4 (*SlTBG4*), (**C**) phytoene synthase (*SlPSY*). Error bars show standard error of the mean (n=3).

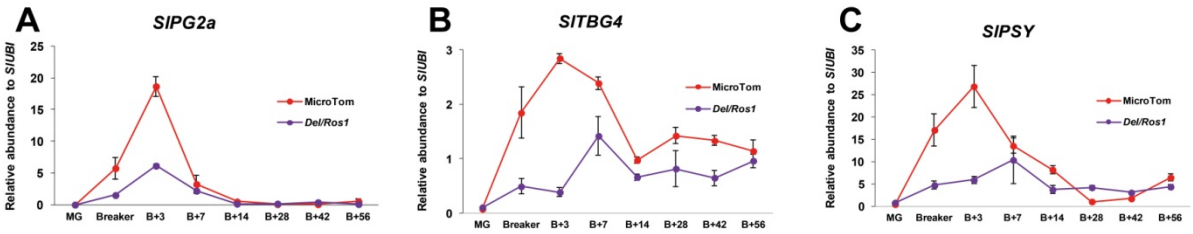

Figure S8.Silencing of *SlDFR* in purple tomato by VIGS substantially reduces anthocyanin accumulation but maintains elevated levels of other phenolic compounds.

(A) Comparative HPLC analysis of methanol extracts of tomato fruit recorded at 500-550 nm showing the accumulation of anthocyanin compounds were reduced in VIGS-DFR-silenced sectors (orange) compared to non-silenced sectors (purple).

(B) Comparative HPLC analysis of methanol extracts of tomato fruit at 280 nm indicates aside from >80% reduction in anthocyanin levels (peaks 1-4, the same as in (A)), there were no significant changes in levels of other phenoilc compounds between VIGS-DFR-silenced and non-silenced sectors.

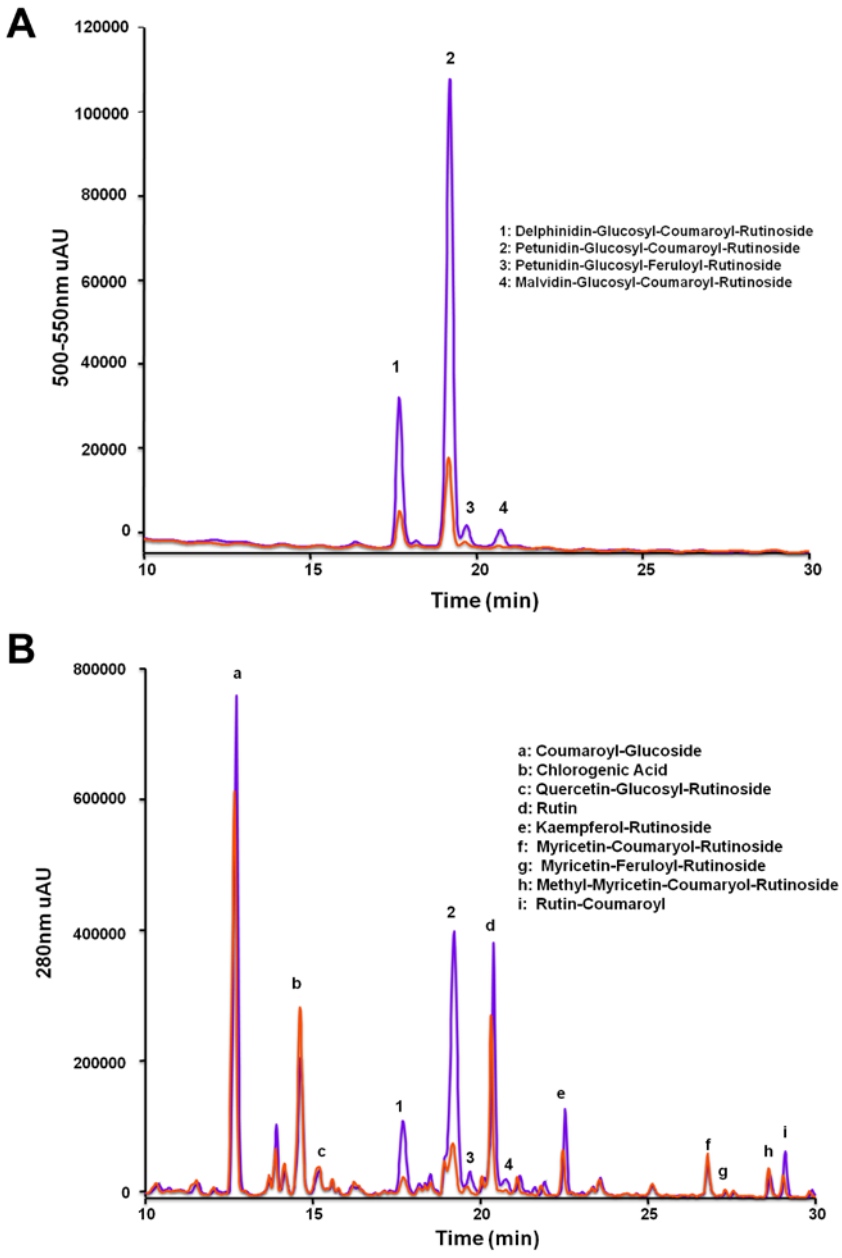

Figure S9. ROS contribute negatively to the resistance of tomato to *B.cinerea*.

The levels of ROS in red and purple tomatoes were altered by infiltration of a water control (**A** and **D** respectively), DPI (10 mM) (**B** and **E**) or glucose oxidase (50 units/mL) plus 1% glucose (**C** and **F**). Fruits were wounded and infiltrated one hour prior to *B.cinerea* inoculation. Pictures were taken 3dpi. White doted lines represent lesion margin. All scale bars represent 2 cm.

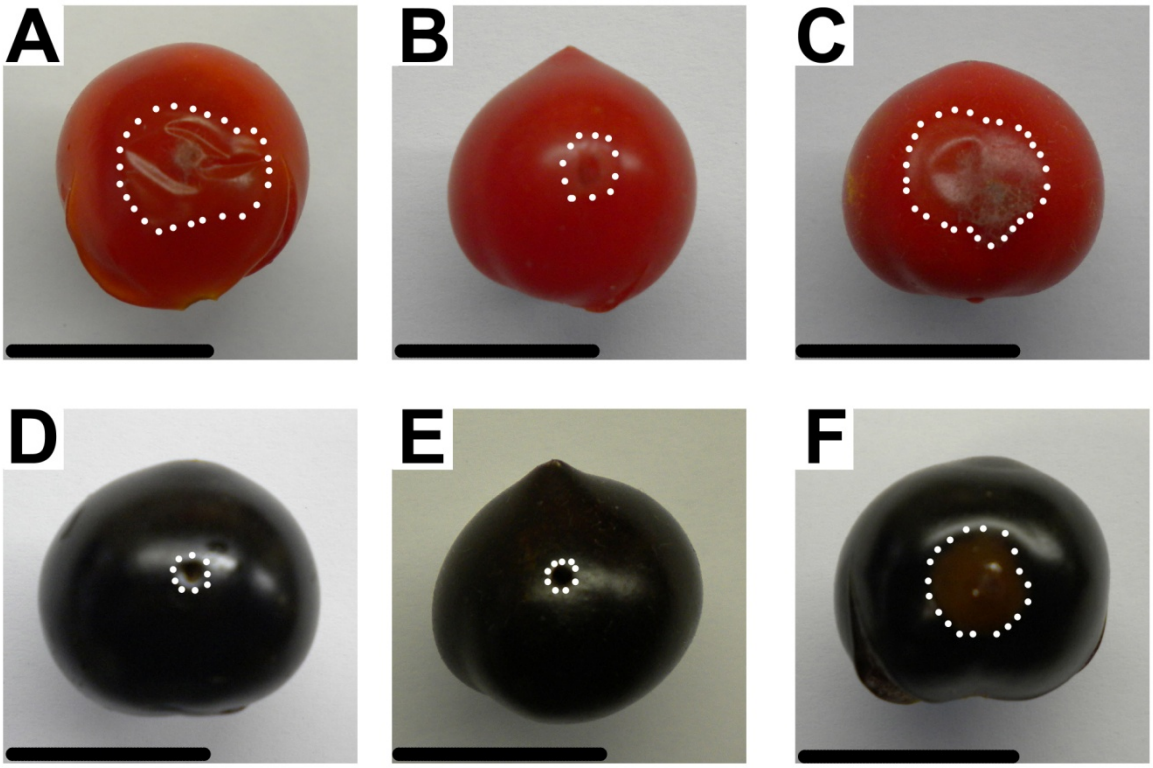

Table S1. Primers used in RT-qPCR

Gene	Locus	Primer sequence (5'-3')
SlUBI	Solyc01g056940	F: GCCAAAGAAGATCAAGCACA R: TCAGCATTAGGGCACTCCTT
SlPG2a	Solyc10g080210	F: ATCTGGACAAGCTAGCAACATCAA R: TATACATGGTTCAACTCGATCACAA
SlTBG4	Solyc12g008840	F: CTTGGCGAAACAGAAATGGT R: ACCTCGAACCCATTCAACAG
SlPSY	Solyc03g031860	F: TGTTGGAGAAGATGCCAGAA R: TTTATCGGTCACCCTTCCAG
AmDel	M84913	F: AGAAAACACGGGTGTCCAAG R: CGTCGACTTTCCTCTCAAGC
AmRos1	DQ275529	F: AAAAGAATTGTCGTGGAGTGAGA R: ATCATTGTAAAATTGCGTTTGCT
SlDFR	Solyc02g085020	F: GACTTGCCGACAGAAGCAAT R: GTGCATTCTCCTTGCCACTT

Comparative Transcriptomic Profiling of Two Tomato Lines with Different Ascorbate Content in the Fruit

Antonio Di Matteo, Adriana Sacco, Rosalba De Stefano, Luigi Frusciante & Amalia Barone

Biochemical Genetics

ISSN 0006-2928

Biochem Genet
DOI 10.1007/s10528-012-9531-3

Springer

Biochem Genet
DOI 10.1007/s10528-012-9531-3

Comparative Transcriptomic Profiling of Two Tomato Lines with Different Ascorbate Content in the Fruit

Antonio Di Matteo · Adriana Sacco · Rosalba De Stefano · Luigi Frusciante · Amalia Barone

Received: 29 December 2011 / Accepted: 30 April 2012

Abstract In recent years, interest in tomato breeding for enhanced antioxidant content has increased as medical research has pointed to human health benefits from antioxidant dietary intake. Ascorbate is one of the major antioxidants present in tomato, and little is known about mechanisms governing ascorbate pool size in this fruit. In order to provide further insights into genetic mechanisms controlling ascorbate biosynthesis and accumulation in tomato, we investigated the fruit transcriptome profile of the *Solanum pennellii* introgression line 10-1 that exhibits a lower fruit ascorbate level than its cultivated parental genotype. Our results showed that this reduced ascorbate level is associated with an increased antioxidant demand arising from an accelerated oxidative metabolism mainly involving mitochondria, peroxisomes, and cytoplasm. Candidate genes for controlling ascorbate level in tomato fruit were identified, highlighting the role of glycolysis, glyoxylate metabolism, and purine breakdown in modulating the ascorbate pool size.

Keywords Antioxidants · Berry quality · Carbohydrate metabolism · *Solanum* spp. · Reactive oxygen species

Antonio Di Matteo and Adriana Sacco contributed equally to this work.

Electronic supplementary material The online version of this article (doi: 10.1007/s10528-012-9531-3) contains supplementary material, which is available to authorized users.

A. Di Matteo · A. Sacco · R. De Stefano · L. Frusciante · A. Barone (✉)
Department of Soil, Plant, Environmental and Animal Sciences, University of Naples "Federico II", Via Università 100, 80055 Portici, Italy
e-mail: ambarone@unina.it

Published online: 22 August 2012

Introduction

In recent years, the compositional quality of crops has received increasing interest, particularly given the results of recent studies highlighting human health benefits brought about by antioxidants (Chu et al. 2002; Naidu 2003; Stanner et al. 2004). The tomato (*Solanum lycopersicum* Mill.) represents a major contribution to dietary nutrition worldwide, and its beneficial effects are generally attributed to its antioxidant content. Its antioxidant compounds include ascorbate (also known as vitamin C), which is an essential nutrient for humans, primates, and a number of other animals that have lost the ability to synthesize it because of inactivation of the last enzyme in the pathway. In plants, ascorbate accumulates at intracellular concentrations of 2–25 mM (Davey et al. 2000) and acts as an antioxidant, as a cofactor for various enzymes, and as a contributor to the regulation of cell division and expansion (Smirnoff and Wheeler 2000). As a signaling agent, ascorbate participates in the interaction with the environment, pathogens and oxidizing agents, and water loss (Pastori et al. 2003; Sanmartin et al. 2003; Fotopoulos et al. 2006). It is essential for plant growth, participates in stress resistance, and seems to control flowering time and senescence (Davey et al. 2000).

Plants synthesize ascorbate through alternative biosynthetic pathways (Valpuesta and Botella 2004). In particular, the Wheeler–Smirnoff pathway operates through L-galactose as a key intermediate. In addition, L-gulose and myo-inositol have been proposed as intermediates in ascorbate biosynthesis, and an L-galactonic acid intermediate has also been reported. The simultaneous operation of these pathways has been demonstrated only in *Arabidopsis*, but their physiological relevance still has to be demonstrated in vivo. Independent of the biosynthetic pathways, the reduced ascorbate is oxidized into an unstable radical, monodehydroascorbate (MDA), which dissociates into ascorbate and dehydroascorbate (DHA). DHA undergoes irreversible hydrolysis to 2,3-diketogulonic acid or is recycled to ascorbate by DHA reductase, which uses glutathione as the reductant, whereas MDA reductase can recycle MDA to ascorbate. This pathway, also called the Foyer–Halliwell–Asada cycle, is an efficient way to control hydrogen peroxide and recycle ascorbate using glutathione as the electron donor (Halliwell and Gutteridge 2000). Overall, the regulation of ascorbate levels in cells is tightly controlled by the level of synthesis, recycling, degradation, and transport of this molecule within the cell or between organs (Hancock and Viola 2005).

Very little is known about the relative contribution of alternative pathways for ascorbate biosynthesis operating in ripening tomato fruit and mechanisms governing the ascorbate pool size in this fruit (Zou et al. 2006; Ioannidi et al. 2009; Di Matteo et al. 2010; Haroldsen et al. 2011). Therefore, understanding such mechanisms will provide an opportunity to breed nutritional quality and enhance postharvest quality. A trait exhibiting quantitative variation, ascorbate content is controlled by several genes and is more or less influenced by the environment (Stevens et al. 2007), and it thus lends itself to quantitative trait loci (QTL) analysis. One approach to identify QTLs controlling ascorbate accumulation in tomato is the use of introgression lines (ILs). These are homozygous lines with single chromosome segment substitutions from one wild relative (Eshed and Zamir 1995). In addition, the combined use of ILs and transcriptomic profiling (Barone

et al. 2009) could be effective in rapidly identifying transcriptional networks and candidate genes involved in fruit antioxidant accumulation.

In order to provide additional insights into genetic mechanisms controlling fruit quality in tomato fruit, in a previous work (Di Matteo et al. 2010) we investigated the fruit transcriptome of a *Solanum pennellii* introgression line (IL12-4) that exhibited a higher ascorbate content than the control variety, M82. This work highlighted the link between genes associated with cell wall catabolism, ethylene, and genes involved in ascorbate pathways. Thus, to explore further mechanisms controlling fruit quality traits in tomato, in the present work we investigated the fruit transcriptome of an additional introgression line (IL10-1) that produces a lower level of ascorbate than the parental cultivated variety M82. In particular, genes and molecular networks mapping to glyoxylate pathways have been involved for the first time in controlling the ascorbate level in tomato fruit. This is discussed according to a model that explains the control of ascorbate level by regulating the steady-state level of specific mRNAs. Indeed, candidate mRNAs in controlling ascorbate level in IL10-1 reported here are expected to drive new strategies of precision breeding aimed at engineering the tomato for quality fruit.

Materials and Methods

Plant Material

The tomato introgression line IL10-1 and its parental genotypes *S. lycopersicum* cv. M82 and *S. pennellii* were cultivated over three consecutive years (2006–2008) in a greenhouse at the Department of Soil, Plant, Environmental, and Animal Production Sciences at the University of Naples (Portici, Italy), as previously described (Di Matteo et al. 2010). IL10-1 (accession LA4102) is a green shoulder red-fruited tomato containing a 43 cM homozygous introgression from *S. pennellii* (acc. LA0716) in an *S. lycopersicum* cv. M82 background (acc. LA3475) (Eshed and Zamir 1995). LA0716 is a homozygous, self-fertile indeterminate accession from Atico, Peru, with green fruits. M82 is a determinate, red-fruited tomato used for processing. All seeds were provided by the C. M. Rick Tomato Genetics Resource Center at the University of California (Davis).

Fruits were collected from IL10-1 and its cultivated parent when 75 % were full sized and red-ripe, softening had increased, and the inside of the columella was completely red. For both lines, three samples were collected within each year. Samples were generated by pooling ripe fruit from the same plant and discarding the seeds, jelly parenchyma, columella, and placenta tissues. Frozen samples under liquid nitrogen were stored at −80 °C prior to homogenization in a Waring blender and processing for the extraction of total RNA and ascorbate.

Phenotypic Evaluation

Ascorbate levels in the pericarp of red-ripe fruit were measured using the procedure described by Di Matteo et al. (2010). Statistical analysis was performed using SPSS

15.0 for Windows (evaluation version release 15.0.0). The significance of genotype with respect to ascorbate level in fruit over three consecutive greenhouse trials was determined by comparing mean levels in IL10-1 and M82 samples using a univariate ANOVA. Because ascorbate revealed a significant interaction between genotype and year ($P < 0.05$), an independent-sample Student's *t*-test was used to compare IL10-1 to the M82 reference within each trial.

Transcriptomic Analysis

A microarray experiment was designed and conducted according to the MIAME guidelines (www.mged.org/miame) on a 90K TomatArray 1.0 microarray synthesized using the CombiMatrix platform at the Plant Functional Genomics Center of the University of Verona (http://ddlab.sci.univr.it/FunctionalGenomics/), as previously described by Di Matteo et al. (2010).

Total RNA used for downstream microarray hybridization and qPCR validation was extracted from frozen, homogenized, and powdered fruit tomato samples of genotypes IL10-1 and M82 using the CTAB (hexadecyltrimethylammonium bromide) method described by Griffiths et al. (1999). Within each line, three samples per trial (2007 and 2008) were assembled and each sample was obtained by pooling 3-5 red-ripe fruit from a single plant. Antisense RNA (aRNA) was obtained using the SuperScript Indirect RNA Amplification System Kit (Invitrogen), and labeling was performed by incorporating Alexa Fluor 647 Reactive Dye. Prehybridization, RNA fragmentation, hybridization with 3 μg labeled and fragmented aRNA, and posthybridization washes were performed according to CombiMatrix protocols (http://www.combimatrix.com/docs/PTL020_00_90K_Hyb_Imaging.pdf).

Imaging of the microarray slides was performed using a Perkin Elmer ScanArray 4000XL and the accompanying acquisition software (ScanArray Express Microarray Analysis System version 4.0). The resulting TIFF images were processed to extract raw data using the CombiMatrix Microarray Imager software version 5.8.0. Signal probe medians and standard deviations were imported into the SPSS software, and normalization was achieved by correcting each probe mean based on the ratio between the median of the array and the average median of arrays. Following data normalization and quality control, all values were log transformed (base 2). Finally, probe signals with a variability coefficient higher than 0.5, as well as spikes and factory probes, were filtered out. Also, probes with signal intensities in the uppermost and lowermost 10 % of values were deleted. The microarray data were deposited in the Gene Expression Omnibus under the series accession GSE26962. Differential signals in the IL10-1 versus M82 fruit transcriptomes were identified using the two-factor ANOVA module in the TIGR MultiExperiment Viewer version 4.5 (MeV, part of the TM4 software suite at http://www.tm4.org/mev/). Because small changes in gene expression might underlie differences in ascorbate accumulation, differentially expressed transcripts were not filtered using a fold-change threshold, and differences were considered irrespective of the intensity of the change. Hierarchical clustering of differentially expressed signals was achieved using the Pearson correlation as a metric to investigate gene expression coregulation. In addition, a relevance network analysis was carried out on

Table 1 Primer pairs used for qPCR validation of genes involved in ascorbate accumulation

TIGR ID	Forward primer	Reverse primer
TC178207	5′-ggatgcaagtggatatgctg-3′	5′-gaaatgaggatggtgttctgg-3′
TC177287	5′-tcccatgctgaggcaacttc-3′	5′-gggcaattccatctccaagag-3′
TC182471	5′-gccatccattggcattcct-3′	5′-tgaaccattagcccagtggg-3′
TC180820	5′-ccaagccattgaattagcatt-3′	5′-caggcctcggtagcaatatg-3′
TC190330	5′-tggcgaaagaggaatctgtt-3′	5′-tccagttcttcaaacccacag-3′
TC190409	5′-cgtttgccaagtaaccaaca-3′	5′-catgactcgtaatggtcgtatca-3′
TC172563	5′-cgtatccccgtgttcctgg-3′	5′-gcccaataaacacgcctgat-3′

microarray normalized data from all 233 probes that previously showed statistically significant variation in their expression, as a result of running the two-factor ANOVA module. The network was generated using the Pearson correlation as the metric and retaining only probes correlated with an R^2 range of 0.92–1.0.

Blast2GO (http://blast2go.bioinfo.cipf.es/) was used to provide automatic high throughput annotation, gene ontology mapping, and categorization of tentative consensus (TC) transcripts showing differential transcription signals. Manually curated annotation was performed for those sequences that were not automatically annotated through similarity matching in the NCBI's nonredundant database. In particular, a number of sequences were processed manually using the similarity search tools BlastX (http://blast.ncbi.nlm.nih.gov/Blast.cgi) and/or SGN Blast (http://sgn.cornell.edu/tools/blast/). In each case, an expectation threshold of 10^{-10} was used. Sequences were also mapped to chromosomes on the tomato genome sequence release 2.40 by performing a multi-Blast search in the Sol Genomics Network Database (http://sgn.cornell.edu/tools/blast).

The expression profiles of a group of TC transcripts considered to be key control points for ascorbate accumulation were validated by real-time quantitative RT-PCR in a 7900HT Fast Real-Time PCR System (Applied Biosystems). Moreover, to assay the reproducibility of the microarray experiment, we performed RT-qPCR on 86 transcripts; 69 of them confirmed the expression pattern shown by microarray analysis. Primer pairs (Table 1) were validated using a standard curve over a dilution range of $1–10^{-3}$ ($R^2 > 0.98$; slope close to -3.32). Amplification was performed in 12.5 µl reaction volumes using a Power SYBR Green PCR Master Mix (Applied Biosystems). Relative quantification was achieved by the $\Delta\Delta C_T$ method (Livak and Schmittgen 2001). The assembly of reactions in a 96-well plate format was automated with a Tecan FreedomEvo 150 liquid handler.

Results

Phenotypic Characterization

Compared with the parental line M82, IL10-1 showed a significantly reduced level of fruit ascorbate content over three consecutive trials (Fig. 1). The average

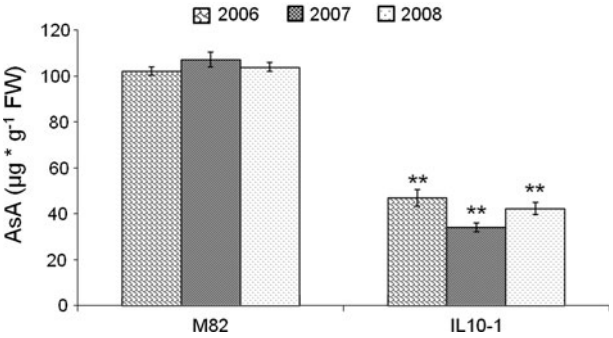

Fig. 1 Ascorbate concentration in red-ripe fruit from the tomato lines M82 and IL10-1. Concentrations are expressed as µg g^{-1} fresh weight (FW); mean values ± SE are reported for three years (2006, 2007, 2008); **statistically significant difference at $P < 0.001$, Student's *t*-test

ascorbate concentration in red-ripe M82 fruit was 122 µg g^{-1} fresh weight, whereas in IL10-1 it was 62 µg g^{-1} fresh weight. This difference was statistically significant (univariate ANOVA procedure; $F_{1,31} = 56.56$; $P < 0.001$). A significant difference among years was also observed ($F_{2,31} = 3.33$; $P < 0.05$), but the interaction genotype × year over the three consecutive trials was not significant ($F_{2,31} = 0.441$; $P > 0.05$). Within each trial, the ascorbate level in the IL10-1 fruit was significantly lower than in M82 (Student's *t*-test, $P < 0.001$). Indeed, the ascorbate content on average was 58 % lower in IL10-1 fruit than in M82 in 2006, 53 % lower in 2007, and 40 % lower in 2008. Therefore, the introgression from the *S. pennellii* genome into IL10-1 contributes to lower fruit ascorbate content at the red-ripe stage, providing evidence that a QTL in this region negatively affects ascorbate concentration in the fruit.

Comparative Microarray Analysis

Transcriptomic analysis revealed 233 mRNA sequences that were differentially expressed between IL10-1 and M82 (Supplementary Table 1). These sequences accounted for 1.15 % of those represented on the TomatArray 1.0 chip; 84 (36 %) of them were upregulated and 149 (63.9 %) were downregulated in IL10-1. Of the differentially expressed sequences, 18 % significantly matched (*e* value $< 1 \times 10^{-10}$) with sequences generically annotated as protein in the NCBI's nonredundant database, whereas 6.9 % showed no matches and were thus reported as nonannotated. They were distributed in GO categories according to biological process, molecular function, and cellular component vocabularies (Supplementary Figs. 1–3).

Even though the TomatArray 1.0 chip contains an exhaustive coverage of expressed sequences related to ascorbate alternative biosynthetic pathways, oxidation, and recycling, including those reported by Zou et al. (2006) and Ioannidi et al. (2009), our experiment did not identify differences in the expression of any of these sequences, as was also confirmed by qPCR validations carried out on a set of

genes belonging to these pathways (data not shown). This suggests that reduced ascorbate level in IL10-1 fruit was not affected by transcriptional mechanisms operating within ascorbate biosynthetic pathways.

To gain additional insights on transcriptional mechanisms controlling ascorbate accumulation, we used hierarchical clustering and relevance networks to investigate the correlation among differentially expressed transcripts. In the cluster analysis, cluster 2 contains upregulated sequences in IL10-1 fruit linking genes involved in carbohydrate (glycolysis and the citric acid cycle) and amino acid catabolism with ethylene and defense responses, whereas cluster 5 mainly includes sequences related to peroxisome metabolism and biogenesis, such as a glycolate oxidase and a peroxisomal biogenesis factor (Supplementary Fig. 4). The relevance networks visually link 22 TC transcripts with strongly correlated transcriptional patterns (Supplementary Fig. 5). In particular, 17 of the sequences mapped to the introgression 10-1, 3 sequences to chromosome 10 outside the introgression 10-1 (TC179505, TC189885, and TC177168), and one each to chromosomes 1 (TC180796) and 12 (TC174331).

Altogether, these transcripts could be relevant key elements in reducing ascorbate content in IL10-1 red-ripe fruit. Indeed, based on functional annotation, gene ontology classification, clustering, and networking, a subset of the 233 differentially expressed TC transcripts (Table 2) was selected to develop a model that could explain the lower ascorbate content in IL10-1. Within this selected group, four transcripts fell in glycolysis, five in fatty acid biosynthesis, five in the tricarboxylic acid cycle, five in glyoxylate metabolism, and six in the antioxidant system. Most transcripts relevant to explaining the IL10-1 fruit phenotype were also validated in their expression pattern by real-time RT-qPCR (Fig. 2). Besides those, 89 more transcripts were analyzed, and 69 of them confirmed their pattern of expression according to microarray analysis, thus revealing 80 % concordance between data obtained from microarray and RT-qPCR analyses.

As for transcripts likely involved in glycolysis (Fig. 3), the microarray experiment revealed the upregulation of a phosphoglycerate mutase (TC186449), two pyruvate decarboxylases (TC172484 and TC178207), and an acetyl-CoA synthetase (TC187142). The four upregulated transcripts belong to cluster 2, and two of them mapped to the introgression 10-1. Their overexpression could reflect an increased supply of acetyl-CoA, which suggests that carbohydrate pool depletion could contribute per se to lower ascorbate accumulation. The extra pool of acetyl-CoA could be channeled toward fatty acid biosynthesis or could increase the tricarboxylic acid flux. The first flux is supported by changes in the expression of transcripts annotated as stearoyl-acp desaturase (TC180054), fatty acid elongase-like protein (TC171885), nonspecific lipid transfer protein (TC172218), and wax synthase (TC177287 and TC182471). The second is supported by the upregulation of an NAD^+-dependent isocitrate dehydrogenase subunit 1 (TC170372), of a glutamate decarboxylase (TC190777), of two tyrosine aminotransferases (TC180820 and TC190330), and an aspartate aminotransferase (TC190409), which comprehensively contribute to increased ROS production.

Regarding glyoxylate metabolism (Fig. 4), the microarray experiment revealed the downregulation of a glycolate oxidase (TC172563) and a gluconokinase

Table 2 Differential expression of transcripts involved in the genetic control of ascorbate content in fruit of tomato lines IL10-1 and M82

TIGR ID	IL10-1 versus M82 expression[a]	Chromosome location[b]	Cluster[c]	Annotation
Glycolysis				
TC172484	+	10[b]	2	Pyruvate decarboxylase
TC178207	+	10[b]	2	Pyruvate decarboxylase
TC186449	+	6	2	Phosphoglycerate mutase
TC187142	+	1	2	Acetyl-CoA synthetase
Fatty acid biosynthesis				
TC171885	−	9	5	Fatty acid elongase-like protein
TC172218	+	10[b]	2	Non-specific lipid transfer protein
TC177287	+	1	2	Wax synthase
TC180054	+	6	2	Stearoyl-acp desaturase
TC182471	+	1	2	Wax synthase
Tricarboxylic acid cycle				
TC170372	+	10[b]	2	NAD^+-dependent isocitrate dehydrogenase subunit 1
TC180820	+	10[b]	2	Tyrosine aminotransferase
TC190330	+	10[b]	2	Tyrosine aminotransferase
TC190409	+	7	2	Aspartate aminotransferase
TC190777	+	1	2	Glutamate decarboxylase
Glyoxylate metabolism and peroxisome-related processes				
TC172563	−	10[b]	5	Glycolate oxidase
TC172641	+	10[b]	2	Endoribonuclease l-psp family protein
TC178654	+	2	2	Allantoate amidinohydrolase
TC187192	−	1	3	ATP-citrate lyase a-3
TC188826	−	10[b]	6	Gluconokinase
Antioxidant system				
TC175968	−	1	1	Glutathione *S*-transferase
TC177168	−	10	5	Thioredoxin m
TC179606	−	10[b]	3	NADH dehydrogenase
TC182153	−	1	3	Glutathione *S*-transferase
TC185135	−	10[b]	6	Thioredoxin m
TC189778	−	1	1	Glutathione *S*-transferase

[a] According to microarray results; + upregulated, − downregulated

[b] Physically mapping on introgression 10-1 of the tomato genome; release 2.40

[c] From hierarchical clustering in Supplementary Fig. 4

(TC188826), both mapping to the introgression 10-1 and probably involved in reducing the peroxisomal supply of glyoxylate. The key role of glycolate oxidase (TC172563) is also evidenced by its node position in the relevance network analysis. In addition, the downregulation of a sequence annotated as ATP-citrate lyase (TC187192) also suggests decreased synthesis of glyoxylate within the

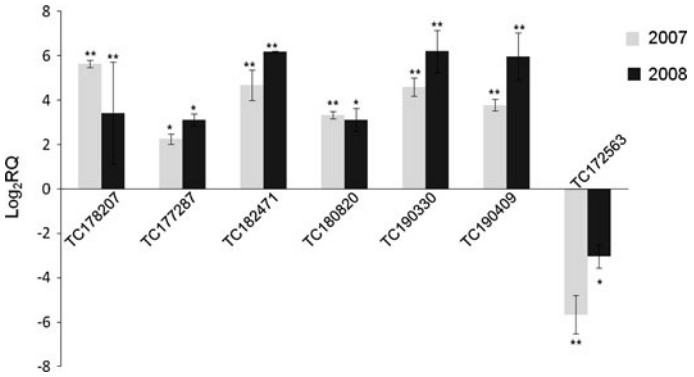

Fig. 2 Validation of differential expression of seven TC transcripts by qRT-PCR. The relative quantification (RQ) of transcripts between tomato lines IL10-1 and M82 was evaluated in years 2007 (*gray bar*) and 2008 (*black bar*). Mean values ± SE are shown. *Asterisks* indicate statistically significant differences: *$0.01 < P < 0.05$; **$P < 0.01$; Student's *t*-test

cytoplasm. On the other hand, our results point out the upregulation of an allantoate amidinohydrolase (TC178654), which is likely to increase the synthesis of glyoxylate from purine precursors, and this is also supported by the upregulation of a sequence annotated as endoribonuclease L-psp family protein (TC172641), mapping to the introgression and likely involved in supplying increasing amounts of purine intermediates to the peroxisomal ROS-producing catabolism. Thus, the reduced glyoxylate pool may be compensated through an increased breakdown of purines that operates through the hydrogen peroxide-producing xanthine oxidase. As a consequence, the increased synthesis of glyoxylate from purines rather than from glycolate would also increase the production of ROS by-products. Also, reduced synthesis of glyoxylate might be compensated via ascorbate catabolism from oxalate (Yu et al. 2010), which could further reduce the ascorbate pool. All these variations could lead to a lower ascorbate level if they occur in an NADH-limiting environment, as is the case in IL10-1 fruit where we observed the downregulation of NADH dehydrogenase (TC179606), suggesting a low NADH/NAD^+ ratio in the cytoplasm. Furthermore, an increased ROS level in IL10-1 is supported by the upregulation of sequences involved in defense response (Supplementary Table 1).

Finally, a reduced ROS-scavenging activity is also suggested by the downregulation of two thioredoxins (TC177168 and TC185135, the latter mapping to the introgression) and three glutathione *S*-transferases (TC175968, TC189778, and TC182153). Therefore, changes in the expression of genes involved in increasing processes producing more ROS and downregulation of ROS-scavenging genes in an NADH-limited environment could lead to higher antioxidant demand that may contribute to lower ascorbate pool size. In addition, the depletion of carbohydrates, which are important ascorbate precursors, may also contribute to lowering the ascorbate pool in IL10-1 fruit.

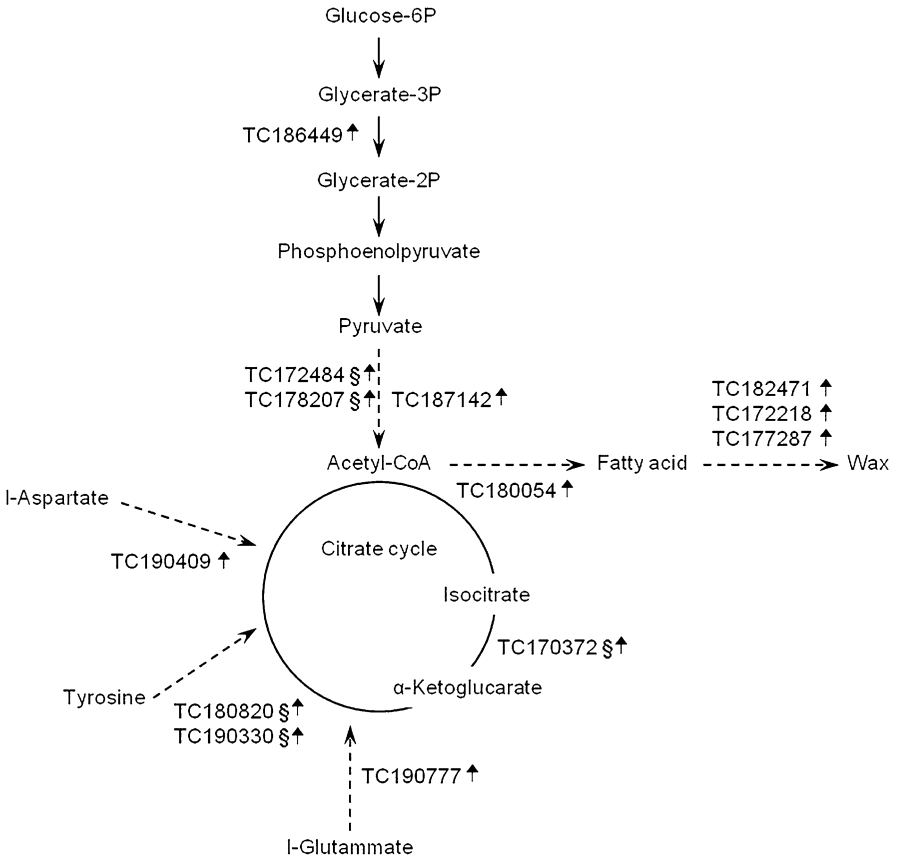

Fig. 3 Network of genes mapping to glycolysis, fatty acid, and citrate cycle metabolism, illustrating changes in their expression between IL10-1 and M82. §, Transcript mapping on the introgression 10-1

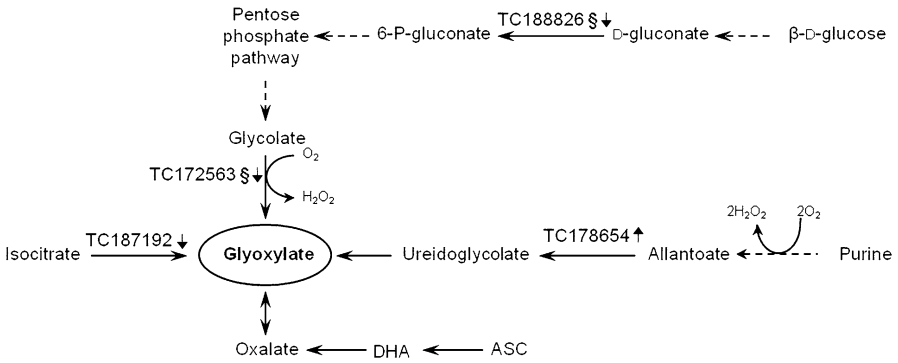

Fig. 4 Network of genes mapping to glyoxylate metabolism, illustrating changes in their expression between IL10-1 and M82. §, Transcript mapping on the introgression 10-1. *DHA* dehydroascorbate, *ASC* ascorbate

Discussion

As the most abundant antioxidant in plant tissues, ascorbate protects cells and organelles from oxidative damage by scavenging reactive oxygen species (Noctor and Foyer 1998) and is important for plant growth, stress resistance, maintenance of redox homeostasis, and as a signaling molecule involved in the regulation of plant response to environmental constraints (Pastori et al. 2003; Conklin and Barth 2004). Little is known about coordination and cross talk between genes and molecular mechanisms within ascorbate metabolism, their interaction with other biological processes, or how they control ascorbate biosynthesis and accumulation in tomato fruit. In a previous study (Di Matteo et al. 2010), we reported the fruit transcriptomic profiling of a tomato plant expressing a QTL for enhanced ascorbate content and highlighted a functional association between genes involved in cell wall catabolism, ethylene biosynthesis, and ascorbate pathways. Here, we report results from transcriptomic profiling of an additional IL (IL10-1) harboring a QTL with decreasing effect on fruit ascorbate content. Our results confirmed those previously reported by Rousseaux et al. (2005) and by Schauer et al. (2006).

Microarray analysis allowed us to identify a subset of genes differentially regulated in IL10-1 fruit and likely involved in reducing the ascorbate level. The model we proposed explains variation in ascorbate pool size in terms of changes in the steady-state level of specific mRNAs mainly occurring within glycolysis, fatty acid biosynthesis, glyoxylate metabolism, and the antioxidant system. Specifically, we propose that the reduced ascorbate concentration in the IL10-1 pericarp may result from depletion in the carbohydrate pool and increase in antioxidant demand. In particular, the upregulation of genes involved in glycolysis could result in decreasing the level of carbohydrate precursors thus limiting ascorbate biosynthesis. In fact, the influence of the carbohydrate pool size on ascorbate biosynthesis has long been established (Grace and Logan 1996). Also, the upregulation of genes involved in fatty acid biosynthesis and the tricarboxylic acid cycle in IL10-1 fruit suggested a competition between these pathways for acetyl-CoA and a decrease in the redox potential due to NADH reoxidization in fatty acid biosynthesis. Moreover, the detected upregulation of an NAD^+-dependent isocitrate dehydrogenase subunit and other genes involved in the tricarboxylic acid cycle could reflect an increased tricarboxylic acid flux being generated from amino acid precursors. Indeed, this was in line with the higher soluble solid concentration in IL10-1 tomato fruit observed in our laboratory (data not shown) and already reported by Causse et al. (2004).

As for the antioxidant demand, our model proposes an increase in ROS levels in the IL10-1 fruit rising from a boost in ROS generation and a fall in the ROS-scavenging system. In particular, regulated processes leading to increased ROS generation in IL10-1 include (1) increased NADH level within the tricarboxylic acid cycle that might enhance electron leakage and ROS generation within the mitochondrion (Lenaz 2001; Hirst et al. 2008), (2) upregulated synthesis of glyoxylate from purines at the expense of the competing photorespiratory synthesis from glycolate in the peroxisome, and (3) reduced activity of antioxidant system components. According to our model, the decreased synthesis of glyoxylate via photorespiration and the glyoxylate cycle is partially compensated by purine via

superoxide-producing xanthine oxidase where the synthesis occurs with a greater gain of ROS.

The increased antioxidant demand generated by ROS overproduction would imply a higher utilization of ascorbate and a possible effect on its overall level. Ascorbate can directly scavenge oxygen free radicals with and without enzyme catalysts (Shirahata et al. 1997; Halliwell and Gutteridge 2000) and can indirectly scavenge them by recycling tocopherol to its reduced form (Shao et al. 2008). Our results suggest that reduced strength of the ROS-scavenging system contributes to increased ROS levels and antioxidant demand in the IL10-1 fruit. Indeed, the reduced redox potential generated by the reoxidation of NADH in fatty acid biosynthesis could limit the efficiency of the Foyer–Halliwell–Asada cycle (Halliwell and Gutteridge 2000), which plays a key role in controlling ROS scavenging and the ascorbate level. Consistent with our hypothesis that the increase in ROS is the main determinant of ascorbate reduction in IL10-1 fruit, comparative profiling allowed us to identify a stress-related response presumably arising from peroxide accumulation, as also evidenced by the modified expression of many stress-related genes.

In conclusion, we propose that the ascorbate level in tomato fruit may be transcriptionally controlled by the expression of genes involved in carbohydrate catabolism, fatty acid biosynthesis, glyoxylate metabolism, and antioxidant system. Overall, the model proposed is intended to give a simplified meaning for molecular mechanisms controlling ascorbate accumulation in tomato fruit that have not been described so far. We report here for the first time that genes and processes operating outside the ascorbate biosynthetic pathways are effective in controlling the final concentration of ascorbate in a fruit system.

Consequently, candidate genes and molecular mechanisms identified may be relevant to biotechnological applications aimed at engineering the tomato for high fruit quality. Further attempts at enhancing ascorbate in tomato fruit could investigate the effectiveness of engineering glyoxylate metabolism, targeting, for instance, the cytoplasmic ATP-citrate lyase and the peroxisomal glycolate oxidase. Also, silencing genes controlling fatty acid synthesis or transmembrane transport, such as the lipid transport protein, may result in enhanced ascorbate levels in tomato fruit. By combining the overexpression of key genes in controlling the tricarboxylic acid cycle and key genes of glyoxylate metabolism, we expect to enhance soluble solid concentrations and ascorbate levels simultaneously.

Acknowledgments The authors thank Dr. Mark Walters for editing the manuscript. This work was funded by the MiPAF Agronanotech and MiUR Genopom programs. Contribution No. 265 from the DISSPAPA.

References

Barone A, Di Matteo A, Carputo D, Frusciante L (2009) High-throughput genomics enhances tomato breeding efficiency. Curr Genomics 10:1–9

Causse M, Duffe P, Gomez MC, Buret M, Damidaux D, Zamir D, Gur A, Chevalier M, Lemaire-Chamley M, Rothan C (2004) A genetic map of candidate genes and QTLs involved in tomato fruit size and composition. J Exp Bot 403:1671–1685

Chu Y-F, Sun J, Wu X, Liu RH (2002) Antioxidant and antiproliferative activities of common vegetables. J Agr Food Chem 50:6910–6916

Conklin PL, Barth C (2004) Ascorbic acid, a familiar small molecule intertwined in the response of plants to ozone, pathogens, and the onset of senescence. Plant Cell Environ 27:959–970

Davey MW, Van Monatgu M, Sanmatin M, Kanellis A, Smirnoff N, Benzie IJJ, Strain JJ, Favell D, Fletcher J (2000) Plant L-ascorbic acid: chemistry, function, metabolism, bioavailability and effects of processing. J Sci Food Agric 80:825–860

Di Matteo A, Sacco A, Anacleria M, Pezzotti M, Delledonne M, Ferrarini A, Frusciante L, Barone A (2010) The ascorbic acid content of tomato fruits is associated with the expression of genes involved in pectin degradation. BMC Plant Biol 10:163

Eshed Y, Zamir D (1995) An introgression line population of *Lycopersicon pennellii* in the cultivated tomato enables the identification and fine mapping of yield-associated QTLs. Genetics 141: 1147–1162

Fotopoulos V, Sanmartin M, Kanellis AK (2006) Effect of ascorbate oxidase over-expression on ascorbate recycling gene expression in response to agents imposing oxidative stress. J Exp Bot 57:3933–3943

Grace SC, Logan BA (1996) Acclimation of foliar antioxidant systems to growth irradiance in three broadleaved evergreen species. Plant Physiol 112:1631–1640

Griffiths A, Barry C, Alpuche-Solis AG, Grierson D (1999) Ethylene and developmental signals regulate expression of lipoxygenase genes during tomato fruit ripening. J Exp Bot 50:793–798

Halliwell B, Gutteridge JMC (2000) Free radicals in biology and medicine. Oxford University Press, Oxford

Hancock RD, Viola R (2005) Improving the nutritional value of crops through enhancement of L-ascorbic acid (vitamin C) content: rationale and biotechnological opportunities. J Agric Food Chem 53: 5248–5257

Haroldsen VM, Chi-Ham CL, Kulkarni S, Lorence A, Bennett AB (2011) Constitutively expressed DHAR and MDHAR influence fruit, but not foliar ascorbate levels in tomato. Plant Physiol Biochem 49:1244–1249

Hirst J, King MS, Pryde KR (2008) The production of reactive oxygen species by complex I. Biochem Soc Trans 36:976–980

Ioannidi E, Kalamaki MS, Engineer C, Pateraki I, Alexandrou D, Mellidou I, Giovannonni J, Kanellis AK (2009) Expression profiling of ascorbic acid-related genes during tomato fruit development and ripening and in response to stress conditions. J Exp Bot 60:663–678

Lenaz G (2001) The mitochondrial production of reactive oxygen species: mechanisms and implications in human pathology. IUBMB Life 52:159–164

Livak KJ, Schmittgen TD (2001) Analysis of relative gene expression data using realtime quantitative PCR and the 2–ΔΔCT method. Methods 25:402–408

Naidu KA (2003) Vitamin C in human health and disease is still a mystery? An ovierview. Nutr J 2:7

Noctor G, Foyer CH (1998) Ascorbate and glutathione: keeping active oxygen under control. Annu Rev Plant Physiol Plant Mol Biol 49:249–279

Pastori GM, Kiddle G, Antoniw J, Bernard S, Veljovic-Jovanovic S, Verrier PJ, Noctor G, Foyer CH (2003) Leaf vitamin C contents modulate plant defense transcripts and regulate genes that control development through hormone signaling. Plant Cell 15:939–951

Rousseaux MC, Jones CM, Adams D (2005) QTL analysis of fruit antioxidants in tomato using *Lycopersicon pennellii* introgression lines. Theor Appl Genet 111:1396–1408

Sanmartin M, Drogoudi PA, Lyons T, Pateraki I, Barnes J, Kanellis AK (2003) Over-expression of ascorbate oxidase in the apoplast of transgenic tobacco results in altered ascorbate and glutathione redox states and increased sensitivity to ozone. Planta 216:918–928

Schauer N, Semel Y, Roessner U, Gur A, Balbo I, Carrari F, Pleban T, Perez-Melis A, Bruedigam C, Kopka J, Willmitzer L, Zamir D, Fernie AR (2006) Comprehensive metabolic profiling and phenotyping of interspecific introgression lines for tomato improvement. Nat Biotechnol 24: 447–454

Shao HB, Chu LY, Lu ZH, Kang CH (2008) Primary antioxidant free radical scavenging and redox signaling pathways in higher plant cells. Int J Biol Sci 4:8–14

Shirahata S, Kabayama S, Nakano M, Miura T, Kusumoto K, Gotoh M, Hayashi H, Otsubo K, Morisawa S, Katakura Y (1997) Electrolyzed-reduced water scavenges active oxygen species and protects DNA from oxidative damage. Biochem Biophys Res Commun 234:269–274

Smirnoff N, Wheeler GL (2000) Ascorbic acid in plants: biosynthesis and function. Crit Rev Biochem Mol Biol 35:291–314

Stanner SA, Hughes J, Kelly CNM, Buttriss J (2004) A review of the epidemiological evidence for the antioxidant hypothesis. Public Health Nutr 7:407–422

Stevens R, Buret M, Duffe P, Garchery C, Baldet P, Rothan C, Causse M (2007) Candidate genes and quantitative trait loci affecting fruit ascorbic acid content in three tomato populations. Plant Physiol 143:1943–1953

Valpuesta V, Botella MA (2004) Biosynthesis of L-ascorbic acid in plants: new pathways for an old antioxidant. Trends Plant Sci 9:573–577

Yu L, Jiang J, Zhang C, Jiang L, Ye N, Lu Y, Yang G, Liu E, Peng C, He Z, Peng X (2010) Glyoxylate rather than ascorbate is an efficient precursor for oxalate biosynthesis in rice. J Exp Bot 61: 1625–1634

Zou L, Ouyang LH, Zhang B, Ye JZ (2006) Cloning and mapping of genes involved in tomato ascorbic acid biosynthesis and metabolism. Plant Sci 170:120–127

MINERVA BIOTEC 2010;22 Suppl. 1 No. 2:27-9

Genetic and physiolocical characterization of tomato genotypes for drought tolerance

R. DE STEFANO, B. GRECO, A. DI MATTEO, A. BARONE

Department of Soil, Plant, Environmental and Animal Production Sciences, University of Naples Federico II, Portici (NA), Italy

Drought stress in plants is consequence of climatic changes in the world due to CO_2 emissions. It causes huge yield losses, since most crop plants are sensitive to drought stress. Variation for drought tolerance exists within the cultivated tomato (*Solanum lycopersicum*) and in related wild species[1]. However, the response to drought stress is not well understood, because it is a quantitative trait (controlled by many genes and highly influenced by environment) and this makes difficult to develop drought-tolerant cultivars.

Aims of this work are: a) to identify polymorphisms in putative stress-related genes in different tomato cultivars and wild species and b) to characterize these genotypes for drought response.

Materials and methods

The tomato genotypes tested are reported in Table I. They belong to different *Solanum* species and to a collection of cultivated varieties and ecotypes. The genes analyzed (Table II) come from a catalog of 76 gene/EST putatively involved in drought stress response and provided by Dr. Grillo of CNR-IGV (Naples, Italy). Three of them were selected and PCR primers were designed on the sequences deposited in GenBank. After amplification, Single Nucleotide Polymorphisms (SNPs) discovery was achieved by re-sequencing PCR products by ABIPRISM 3130 GENETIC ANALYZER.

The phenotypic test was performed in greenhouse on a sample of 10 genotypes using three treatments: A) control plants; B) 50% water reduction and C) 100% water reduction, both starting two weeks after transplant. Drought stress response was estimated by measuring weekly the Relative Water Content (RWC) of leaves.

Table I.—*List of tomato genotypes analyzed.*

Cultivar and ecotypes		Species
ADVF	Al-22/041	*S. lycopersicum* (LA2711)
Casarbore	Al-22/044	*S.lycopersicum* (LA1421)
Già Giù	Al-22/046	*S. pennellii* (LA0716)
M82	Al-22/057	*S. peruvianum* (LA0462)
Momor	Al-22/059	*S. pimpinellifolium* (LA1579)
Parminatella	Al-22/064	*S. chilense* (LA1958)
Pasqua RS	Al-22/070	*S. chilense* (LA1959)
PI15250	Al-22/076	*S. chilense* (LA1972)
Principe Borghese	IT-22/005	*S. sitiens* (LA1974)
Pull	IT-22/030-13	
Selezione 6		
Stevens		
Vesuvio 2001		

Results and discussion

The genes included in the tomato catalog were analysed by BLAST against BAC sequences released

Table II.—*Tomato genes involved into stress response that were analyzed for SNP discovery.*

Name	Description	GeneBank ID	Size	Tomato BAC localization	Note
TSW12	Lipid transfer protein	X56040	675 bp	No	mRNA Induced in stem by NaCl
Asr2	Transcription factor	X74907	821 bp	C04HBa0094K06	Up-regulated in roots and leaves of water or salt stressed plants
MKP1	MAP1 kinase phosphatase	AF312747	522 bp	C05HBa0025A19	Necessary in Arabidopsis for plant recovery after stress

Table III.—*Mutation revealed for three genes analyzed in the 32 genotypes.*

Gene	SNP (n.)	IN/Del (n.)	Polymorphic genotypes (n.)
MKP1	20	4	8
Asr2	5	1	All
TSW12	10	0	6

in SGN database (http://sgn.cornell.edu/). Initially, three genes were selected for SNP discovery. The genes analysed were MKP1 (MAP kinase phosphatase), Asr2 (ABA stress ripening), TSW12 (a lipid transfer protein gene). They were completely re-sequenced in all genotypes analyzed.

MKPs are regulators of MAP kinase signalling[2], that occurs during both biotic and abiotic stresses.

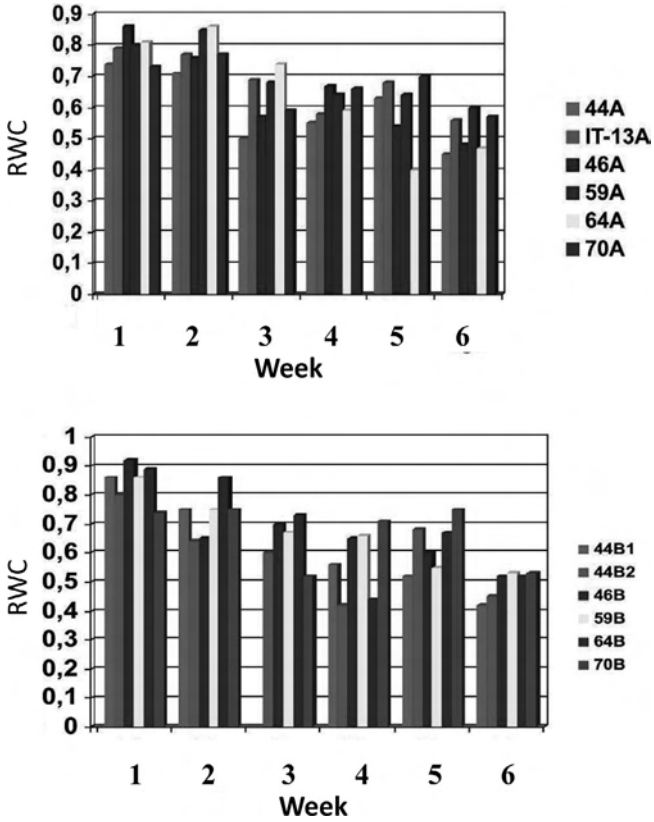

Figure 1.—RWC (FW-DW/SW-DW) values of five plants from treatment A and B. On July 10th and 24th all the plants were watered. FW=fresh weight, DW=drought weight, SW=saturated weight.

The *in silico* analysis showed that the tomato gene MKP1 lacks introns and maps on chromosome 5. A total of 20 SNPs was identified in this gene (Table 3), five of which are silent, three nonsense and 13 missense, whereas out of four deletions, three do not imply codon stop. The wild species showed many mutations and this was predictable because the reference sequence reported in GenBank was from *S. lycopersicum*.

The Asr gene family is involved in transcriptional regulation. Its members are up-regulated in roots and leaves of water- or salt-stressed plants. Asr2 encodes a putative transcription factor likely to be involved in one of the signalling pathways of ABA[3]. The DNA sequence of Asr2 is 821 bp with 2 exons and it is located on chromosome 4. Five SNPs (Table III) were identified in 32 genotypes analyzed and almost all showed the same changes of bases when compared with the same sequence of Ailsa Craig retrieved from the SGN database. Additionally, one deletion that leads no codon stop was also observed.

TSW12 encodes a lipid transfer protein[4] and its mRNA is accumulated during tomato seed germination, its level increases after NaCl treatment or heat shock. In mature plants, TSW12 mRNA is only detected upon treatment with NaCl, mannitol or ABA and its expression mainly occurs in stems. It is a sequence of 675 bp in length, and it doesn't show any significant alignment with sequenced BAC clones. For this gene, 10 SNPs were found only in

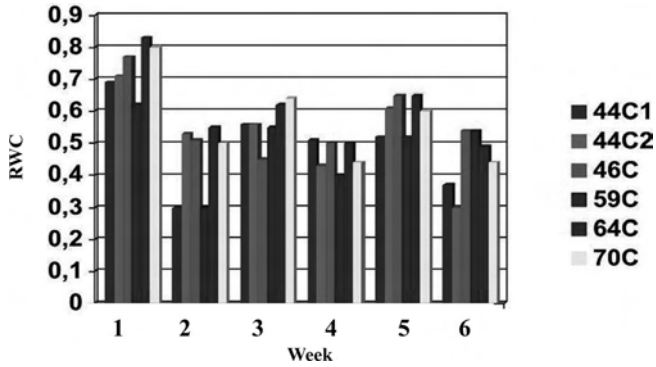

Figure 2.—RWC (FW-DW/SW-DW) values of five plants from treatment C. On July 10th and 24th all the plants were watered. FW=fresh weight, DW=drought weight, SW=saturated weight.

wild species. All showed one change of an asparagine in glycine at the position 56 of the amino acid sequence. This result is confirmed by Trevino and O'Connell[5], who characterized the TSW12 protein in *S. pennellii*. For all three genes a higher coverage will be performed to confirm polymorphisms identified. Moreover, other genes will be characterized using primers specifically designed and SNPs will be searched.

Finally, in order to evaluate drought tolerance a preliminary test was performed on a sample of 10 ecotypes. In our experimental conditions the treatment B (50% water reduction) was not informative, because plants grew similarly to those of treatment A (Figure 1). Figure 2 reports RWC values measured on five genotypes from treatment C. After the first week, RWC values highly decreased for two genotypes (44 and 59). All genotypes were re-watered for two times and at the end of the experiment genotype 44 clearly showed to be more susceptible than the others, whereas genotype 59 showed a good recovery. The same test will be performed for all 32 genotypes, as well as other putative stress-related genes will be analyzed for SNP discovery. These analyses could help to identify polymorphisms in genes that can be associated to the tolerant or susceptible phenotype, leading to the design useful molecular markers for assisted selection programs.

References

1. Wudiri BB, Henderson DW. Effects of water stress on flowering and fruit set in processing tomatoes. Sci. Hortic 1985;27:89-98.
2. Ulm R, Revenkova E, di Sansebastiano GP, Bechtold N, Paszkowski J. Mitogen-activated protein kinase phosphatase is required for genotoxic stress relief in Arabidopsis. Genes Dev 2001;15:699-709.
3. Finkelstein, R. R., S. S. Gampala, and C. D. Rock. Abscisic acid signaling in seeds and seedlings. Plant Cell 2002; 4:15-45.
4. Torres-Schumann S, Godoy JA, Pintor-Toro JA. A probable lipid transfer protein gene is induced by NaCl in stems of tomato plants. Plant Mol 1992;18:749-57.
5. Trevino MB, OConnell MA. Three drought-responsive members of the nonspecific lipid-transfer protein gene family in Lycopersicon pennellii show different developmental patterns of expression. Plant Physiol 1998;116:1461-8.